

University of New Mexico

UNM Digital Repository

Biomedical Engineering ETDs

Engineering ETDs

Summer 8-18-2019

ASSESSMENT OF THE BIOCOMPATIBILITY, STABILITY, AND SUITABILITY OF NATURAL AND SYNTHETIC POLYMERS AND DRUGS IN THE FDA APPROVAL PROCESS

Phuong Anh Hoang Nguyen
University of New Mexico

Follow this and additional works at: https://digitalrepository.unm.edu/bme_etds



Part of the [Biomaterials Commons](#), [Other Biomedical Engineering and Bioengineering Commons](#), [Other Chemicals and Drugs Commons](#), and the [Pharmaceutical Preparations Commons](#)

Recommended Citation

Nguyen, Phuong Anh Hoang. "ASSESSMENT OF THE BIOCOMPATIBILITY, STABILITY, AND SUITABILITY OF NATURAL AND SYNTHETIC POLYMERS AND DRUGS IN THE FDA APPROVAL PROCESS." (2019).
https://digitalrepository.unm.edu/bme_etds/29

This Dissertation is brought to you for free and open access by the Engineering ETDs at UNM Digital Repository. It has been accepted for inclusion in Biomedical Engineering ETDs by an authorized administrator of UNM Digital Repository. For more information, please contact amywinter@unm.edu, lsloane@salud.unm.edu, sarahrk@unm.edu.

Phuong Anh Hoang Nguyen

Candidate

Center for Biomedical Engineering

Department

This dissertation is approved, and it is acceptable in quality and form for publication:

Approved by the Dissertation Committee:

Heather Canavan, Chairwoman

Eva Chi

David Whitten

Christina Salas

Steven Walsh

ASSESSMENT OF THE BIOCOMPATIBILITY, STABILITY, AND SUITABILITY OF
NATURAL AND SYNTHETIC POLYMERS AND DRUGS IN THE FDA APPROVAL
PROCESS

BY

Phuong Anh Hoang Nguyen

MBA, University of New Mexico, 2017

M.S. Biomedical Engineering, University of New Mexico, 2016

B.S Biology, University of New Mexico, 2014

B.S. Psychology, University of New Mexico, 2014

DISSERTATION

Submitted in Partial Fulfillment of the Requirements for the Degree of:

Doctor of Philosophy, Engineering

The University of New Mexico

Albuquerque, New Mexico

December 2019

Acknowledgements

The path towards this work has been difficult, but I would not have overcome these demanding 5 years without the assistance from many individuals. I would like to start by thanking my faculty advisor, mentor, and one of my primary levels of support, Prof. Heather Canavan. She has helped me navigate through many difficult situations and circumstances while teaching me what being a mentor and Professor truly means. She's dedicated to her students, her class, and is always striving to have all her students succeed. She changes the lives of everyone she interacts with, and I'm truly grateful that she is my advisor. Like a previous student has said, Prof. Canavan is the "Michael Phelps of teachers" and without her, I would not be able to accomplish this work.

I would also like to thank my committee members, Profs. Eva Chi, David Whitten, Steve Walsh, and Christina Salas for taking time out of their tremendous workload to be a part of my dissertation committee.

Within the Center for Biomedical Engineering, many individuals – undergraduate students, graduate students and professors alike have helped train me, troubleshoot my experiments, and listened to me talk about my experiments. I would like to thank all of them, including Darnell Cuylear, Sarah Mounho, Lyndsay Stapleton, Adrian Ledesma-Mendoza, Prof. Linnea Ista, Dr. Jamie Reed, Dr. Marta Cooperstein, Dr. Kent Coombs, Dr. Matthew Rush, Ben Matheson, and other members of the HEC lab Group. Special thanks to Dr. Tye Martin and Angelina Malagodi for letting me into your office and being available to listen and act as a sounding board for ideas.

Individuals and staff at CBME have helped made my life so much easier, and much of my work couldn't have been done without their help. Thank you to Linda Stewart who helped me organize all my paperwork, and ensured that I'm on task and schedule to graduate. I would also like to thank Joanna Rex, and Mary Rhodes for helping me order supplies and ensuring that all of the things I order gets delivered. Finally, thank you to Isela Roeder and Elsa Castillo for helping me navigate scholarships, grant submission protocols, etc.

I would also like to thank the I-Corps Site Program and the mentors within who have taught me much about the translational process between the start of an idea to getting it into the market. Thank you Dr. Rob Del Campo and Dr. Elizabeth (Lisa) Kuuttila for starting the program and allowing students to pursue our interests. Thank you, Cara Michalyszyn, for her great organization and assistance. Finally, a thank you mentors Susan Cornelius and John Chavez for helping me find interviewees, introducing me to your friends, and for spending countless hours going through my presentations as I go through the I-Corps process.

The work within this dissertation could not have been completed without the assistance of other individuals outside of UNM with additional instrumentation that was valuable to the project. In particular, I would like to thank NESAC/BIO, specifically Drs. Gerry Hammer, Dan Graham, and Lara Gamble for their assistance in obtaining XPS data and analyzing my pNIPAM substrates (used in **Chapter 3**). I would also like to thank Drs. Karyn Jarvis, and Sally McArthur for their assistance in helping me analyze my data as well as obtain XPS data for my hydrogels (used in **Chapter 7**). From UNM's Health Science Center, I would also like to thank Drs. Michael Paffett, Michael Burnett, and Russell Morton for training me on the use of the confocal microscope, flow cytometer, and the cryotome.

Finally, I must thank family and friends who have helped mentor me, train me, reminded me to work hard, and stood up for me during times where I was about to give up. I wish to thank my mother, Joyce Nguyen, who threatened me with homelessness and picking up cans off the street, so that I would continue my education. I also wish to thank my older sister, Dr. Ngoc Nguyen who listened to me voice all of my issues. Thank you also to my eldest sister, Dr. Anh Nguyen, for her inspirational bubble tea. I would also like to thank my grandparents, Dieu Nguyen and Van Nguyen and my in-laws, Hao Tat and Muoi Truong. I would also like to extend an extra special thank you to those individuals who have become surrogate parents to me as well as deep close personal friends during this time. So, once again, thank you Elena Benton, Mark Sarnowski, Emily Rhoades Clark, and Arniel Ortega who are personal friends that have become my family. None of this would have been possible without the love and support of my husband, Sam Truong.

The following work was supported by these funding sources: the UNM Center of Biomedical Engineering, the UNM Clinical and Translation Science Center (CTSC), the Women in Science Award (NSF ADVANCE @ UNM), the NSF I-Corps Site award to the Lobo Rainforest, the UNM School of Engineering Excellence Award, the AVS Graduate Student Award, the UNM Doctoral Travel Award, and the Gates Millennium Scholars Program. Additional funding to from NIH MARC funded my co-author DLC for experiments in **Chapters 6 and 7.**

ASSESSMENT OF THE BIOCOMPATIBILITY, STABILITY, AND SUITABILITY OF
NATURAL AND SYNTHETIC POLYMERS AND DRUGS IN THE FDA APPROVAL
PROCESS

BY

Phuong Anh Hoang Nguyen

MBA, University of New Mexico, 2017

M.S. Biomedical Engineering, University of New Mexico, 2016

B.S. Biology, University of New Mexico, 2014

B.S. Psychology, University of New Mexico, 2014

DISSERTATION

Submitted in Partial Fulfillment of the Requirements for the Degree of:

Doctor of Philosophy, Engineering

Abstract

Regulation of the development, production, marketing, and sales of medical pharmaceuticals and devices in the United States fall under the regulatory functions of the Food and Drug Administration (FDA). The current FDA approval process takes an average of 10 years from start to completion, and costs over \$100 million. As a result, companies use many different methods to find additional use of their drugs through marketing directly to the physician, or recycling of previously approved drug moieties. In this work, an evaluation of the *in vitro* and *ex vivo* biocompatibility of polymers and drugs in different phases of FDA approval are evaluated. These include polymers and drugs that are 1) being studied for FDA approval (**Chapter 3**), 2) used for purposes other than their initial clinical setting purposes (**Chapter 4 and 5**), and 3) deemed safe from studies in the 1960s-1970s and have been used due to their low “toxicity” (**Chapter 6**). An alternative method of drug delivery is explored to improve the palatability and allow for more precise control of the concentration of drugs delivered for colonoscopy preparations to help alleviate side effects and improve compliance rates is

explored in **Chapter 7**. The cytotoxicity of reagents (NIPAM) used in current experimental protocols prior to FDA approval were investigated as described in **Chapter 3**. Although other forms of polymerized NIPAM are non-toxic to cells, cpNIPAM purchased from retailers should be purified prior to use to prevent unintended cytotoxic effects. Current surgical procedures often encourage the use of antifibrinolytics to prevent excessive bleeding (**Chapter 4**), antibiotics, and antiseptics to prevent infection (**Chapter 5**). This work demonstrated that each of the antibiotics, antiseptics, and antifibrinolytic tested are detrimental to knee joint cells. **Chapter 6** showed that PEG 3350 at current therapeutic concentrations changes the behavior of gut cells. Taken together, these chapters emphasize the need for careful evaluation of the possible cytotoxic effects of antibiotics in surgical applications prior to their use. **Chapter 7** characterizes the ideal concentrations and their effectiveness as a potential delivery vehicle for PEG 3350 and identifies the optimal fabrication of hydrogels using natural polymers to deliver the maximum amount of drug. Studies were completed evaluating the hydrogels' pH responsiveness utilizing simple pH solutions as well as simulated gastrointestinal and small intestinal simulation fluids.

Table of Contents

| | |
|--|------------------------------|
| Acknowledgements | iii |
| Table of Contents | vi |
| Abstract | vi |
| <i>Cytotoxicity of NIPAM</i> | Error! Bookmark not defined. |
| <i>Cytotoxicity of TXA, antibiotics, and antiseptics</i> | Error! Bookmark not defined. |
| <i>Cytotoxicity of PEG despite FDA approval</i> | Error! Bookmark not defined. |
| <i>Biocompatible devices</i> | Error! Bookmark not defined. |
| Chapter 1: Introduction | 1 |
| 1.1 A brief history of the FDA | 1 |
| 1.2 Current FDA approval process | 4 |
| 1.2.1 <i>Preclinical phase in drug development</i> | 4 |
| 1.2.2 <i>Clinical Phase in Drug Development</i> | 5 |
| 1.3 Controversies with the FDA | 7 |
| 1.3.1 <i>Race to Approve: Industry Pressure</i> | 7 |
| 1.3.2 <i>Race to approve: Public displeasure</i> | 9 |
| 1.3.3 <i>Barrier of Entry</i> | 12 |
| 1.4 Exceptions to the FDA approval process | 14 |
| 1.4.1 <i>Unapproved Uses of Approved Drugs</i> | 14 |
| 1.4.2 <i>Classes of NDA and recycling of approved drug moieties</i> | 16 |
| 1.5 Another look: Drugs and polymers of interest | 18 |
| 1.5.1 <i>Pre-Clinical phase of development: Poly(N-isopropyl acrylamide)</i> | 20 |
| 1.5.2 <i>Unapproved use of approved drugs: Tranexamic Acid, Vancomycin, Bacitracin, Chlorhexidine, and Povidone-iodine</i> | 20 |
| 1.5.3 <i>“Low Risk” drugs and polymers and other potential Uses: Poly(ethylene glycol), sodium alginate, and chitosan</i> | 21 |
| Chapter 2: Cytotoxicity Analysis of Mammalian Cells Exposed to Drugs and Polymeric Surfaces and Extracts (Experimental Procedures and Equipment) | 23 |
| 2.1 Introduction | 23 |
| 2.2 X-Ray Photoelectron Spectroscopy (XPS) | 23 |
| 2.3 Contact Angle (Goniometry) | 25 |
| 2.4 Nuclear Magnetic Resonance (NMR) | 26 |
| 2.5 Rheology | 28 |

| | |
|---|-----------|
| 2.6 Cell Morphology | 29 |
| 2.7 Live/Dead Stain (Ethidium homodimer I/III and Calcein AM) | 33 |
| 2.8 XTT | 35 |
| Chapter 3: Exploring the Anomalous Cytotoxicity of Commercially-Available Poly(<i>N</i>-isopropyl Acrylamide) Substrates | 38 |
| Abstract | 38 |
| 3.1 Introduction | 39 |
| 3.2 Materials and Methods | 41 |
| 3.2.1 <i>Materials</i> | 41 |
| 3.2.2 <i>Surface preparation</i> | 42 |
| 3.2.3 <i>CpNIPAM solution preparation</i> | 42 |
| 3.2.4 <i>SpNIPAM solution preparation</i> | 42 |
| 3.2.5 <i>SpNIPAM and cpNIPAM solution deposition</i> | 43 |
| 3.2.6 <i>Surface characterization</i> | 43 |
| 3.2.7 <i>Cell Culture</i> | 44 |
| 3.2.8 <i>Cell culture on NIPAM substrates</i> | 44 |
| 3.2.9 <i>Preparation of pNIPAM extracts for NMR</i> | 45 |
| 3.2.10 <i>Cytotoxicity Testing of NIPAM surfaces</i> | 45 |
| 3.2.11 <i>Characterization of Extract Solution</i> | 46 |
| 3.3 Results and Discussion | 46 |
| 3.3.1 <i>Polymer Thermoresponse</i> | 47 |
| 3.3.2 <i>Surface Chemistry</i> | 49 |
| 3.3.3 <i>Cytotoxicity Testing</i> | 56 |
| 3.3.4 <i>Cell Morphology</i> | 59 |
| 3.3.5 <i>Nuclear Magnetic Resonance to Determine Extent of Polymerization</i> | 63 |
| 3.4 Conclusions | 65 |
| Chapter 4: <i>Ex vivo</i> Human Chondrocyte Toxicity Following Exposure to Tranexamic Acid | 67 |
| Abstract | 67 |
| 4.1 Introduction | 68 |
| 4.2 Materials and Methods | 69 |
| 4.2.1 <i>Materials</i> | 69 |
| 4.2.2 <i>Osteochondral plug harvest and storage</i> | 69 |
| 4.2.3 <i>TXA biocompatibility test</i> | 70 |
| 4.2.4 <i>Live/dead assay</i> | 70 |
| 4.3 Results and Discussion | 72 |

| | |
|---|------------|
| 4.4 Conclusions | 81 |
| Chapter 5: <i>Ex vivo</i> Human Chondrocyte Toxicity Following Exposure to | 83 |
| Abstract | 83 |
| 5.1.1 Antibiotics | 84 |
| 5.1.1 Antiseptics | 85 |
| 5.1.3 Other treatments | 86 |
| 5.1.4 Evidence of antibiotics, antiseptics, and other treatments in the literature | 86 |
| 5.2 Materials and Methods | 87 |
| 5.2.1 Materials | 87 |
| 5.2.2 Osteochondral plug harvest and storage | 87 |
| 5.2.3 Antiseptics/antibiotics biocompatibility test | 88 |
| 5.2.4 Live/dead Assay..... | 88 |
| 5.3 Results and Discussion | 90 |
| 5.4 Conclusions | 103 |
| Chapter 6: Investigation of the in-vitro cytotoxicity of PEG 3350 with human gastrointestinal cells. | 105 |
| Abstract | 105 |
| 6.1 Introduction | 106 |
| 6.1.1 Colorectal Cancer (CRC) and Colonoscopy | 106 |
| 6.1.2 Patient Compliance and User Experience (UX)..... | 107 |
| 6.1.3 History of Colonoscopy | 108 |
| 6.1.4 History of PEG..... | 108 |
| 6.1.5 Incorporation of PEG into Colonoscopy | 109 |
| 6.1.6 Current Work | 109 |
| 6.2 Materials and Methods | 110 |
| 6.2.1 Materials | 110 |
| 6.2.2 Cell culture..... | 111 |
| 6.2.3 Preparation of cell media/PEG 3350 solutions | 111 |
| 6.2.4 PEG 3350 direct contact test | 111 |
| 6.2.5 Cell morphology..... | 112 |
| 6.2.6 Live/dead assay | 112 |
| 6.2.7 XTT metabolic assay..... | 112 |
| 6.2.8 XTT data analysis | 113 |
| 6.3 Results and Discussion | 113 |
| 6.3.1 Cell Morphology | 113 |

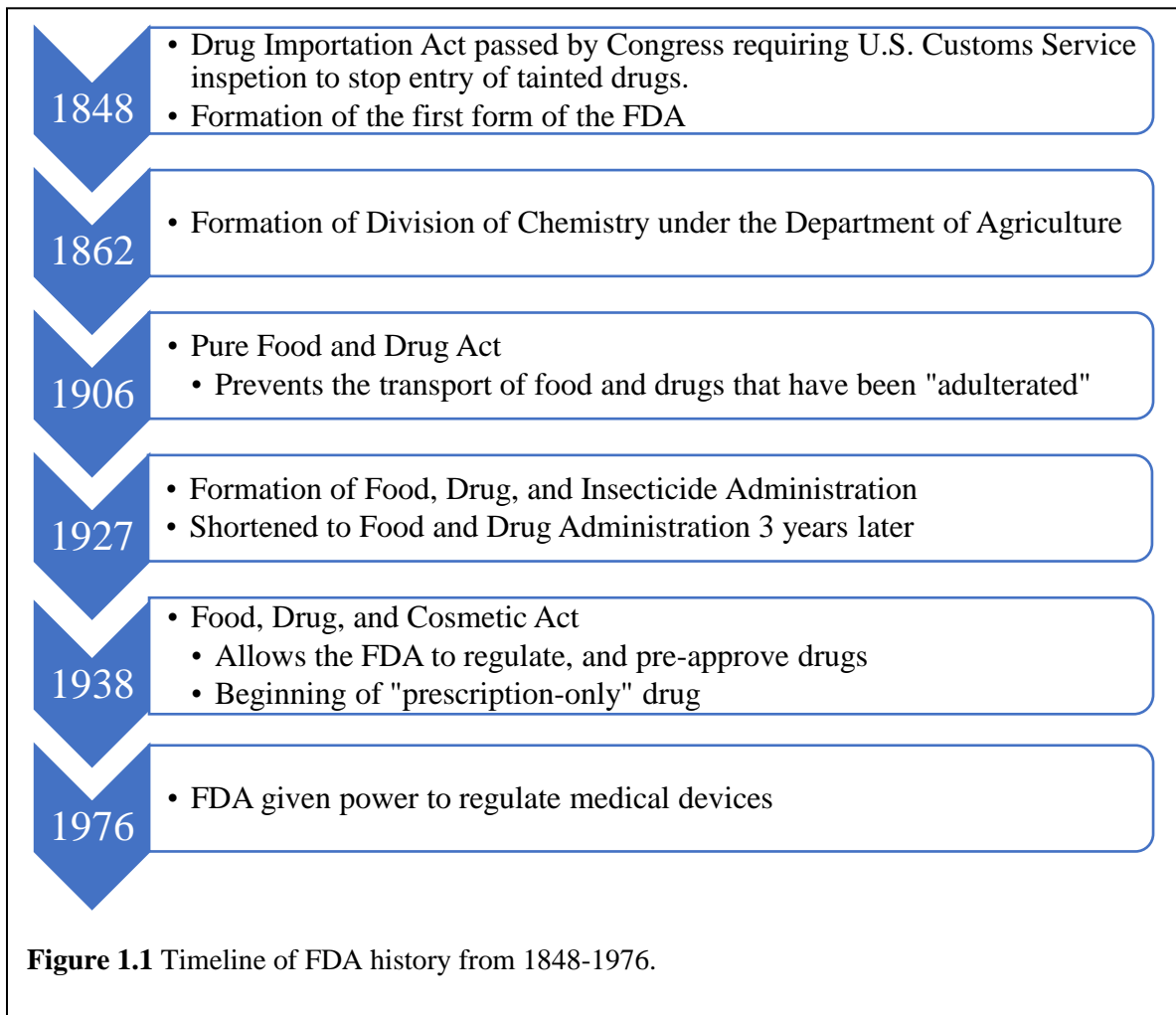
| | |
|--|-----|
| 6.3.2 <i>Live/dead assay</i> | 122 |
| 6.3.3 <i>XTT metabolic assay</i> | 128 |
| 6.4 Conclusions | 137 |
| Chapter 7: Developing a pH responsive hydrogel for the delivery of PEG 3350 within the human gastrointestinal tract | 139 |
| Abstract | 139 |
| 7.1 Introduction | 140 |
| 7.2 Materials and Methods | 144 |
| 7.2.1 <i>Materials</i> | 144 |
| 7.2.2 <i>Chitosan purification</i> | 145 |
| 7.2.3 <i>Hydrogel formation</i> | 145 |
| 7.2.4 <i>X-ray photoelectron spectroscopy (XPS)</i> | 145 |
| 7.2.5 <i>Rheology</i> | 146 |
| 7.2.6 <i>Degradation of hydrogels</i> | 147 |
| 7.2.7 <i>Simulated gastric and small intestine fluids</i> | 147 |
| 7.2.8 <i>Release of PEG functionalized with Rhoadmine</i> | 148 |
| 7.2.9 <i>PEG 3350 release in gastric and small intestine simulation fluid</i> | 148 |
| 7.2.10 <i>NMR characterization of leachate</i> | 148 |
| 7.3 Results and Discussion | 149 |
| 7.3.1 <i>X-ray photoelectron spectroscopy (XPS)</i> | 150 |
| 7.3.2 <i>Rheology</i> | 156 |
| 7.3.3 <i>Weight change of hydrogels in acidic and basic solutions</i> | 161 |
| 7.3.4 <i>Hydrogel weight gain/loss in gastric simulation fluid and small intestine simulation fluid</i> | 164 |
| 7.3.5 <i>Rhodamine-PEG release</i> | 167 |
| 7.3.6 <i>Nuclear Magnetic Resonance of hydrogel leachate</i> | 169 |
| 7.4 Conclusions | 170 |
| Chapter 8: Conclusions and Future Directions | 172 |
| 8.1 Conclusions | 172 |
| 8.1.1 <i>Unanticipated sources of toxicity within existing protocols</i> | 172 |
| 8.1.2 <i>Cytotoxicity despite FDA approval</i> | 173 |
| 8.1.3 <i>Biocompatible devices</i> | 173 |
| 8.2 Future Directions | 174 |
| 8.2.1 <i>Assessing the mechanism of death</i> | 174 |

| | |
|---|-----|
| <i>8.2.2 Search for a potential “safe” and effective concentration of antibiotics and antiseptics</i> | 178 |
| <i>8.2.3 Depth of penetration of antibiotics, antiseptics, and antifibrinolytics and additional techniques to evaluate cytotoxicity</i> | 179 |
| <i>8.2.4 Encapsulation of PEG with electrolytes</i> | 180 |
| <i>8.2.5 Encapsulation of bacteria and other materials using stimulus-responsive polymers for targeted drug delivery</i> | 181 |
| References | 183 |

Chapter 1: Introduction

1.1 A brief history of the FDA

Regulation of the development, production, marketing, and sales of medical pharmaceuticals and devices in the United States fall under the regulatory functions of the U.S. Food and Drug Administration (FDA). The FDA is the oldest consumer agency in the United States, originating in the U.S. Patent office in 1848, and later inherited by the Department of Agriculture's Division of Chemistry (later Bureau of Chemistry) in 1862 under the leadership of Harvey Washington Wiley (see **Figure 1.1** for timeline summary).¹



The FDA had minimal powers of oversight and was unable to oversee drug and medical device marketing until 1906 when President Theodore Roosevelt signed into the law the Pure Food and Drug Act.^{2,3} The act prohibited under penalty of seizure of goods, the interstate transport of food and drugs that had been “adulterated”.^{2,3} The responsibility of examining food and drugs for such “adulteration” or “misbranding” was given to the Bureau of Chemistry.¹ However, the Bureau of Chemistry’s powers were limited by judicial decisions, as they stated that the basis of the law rested on the regulation of product labeling rather than pre-market approval and charges could not be made without proof of “fraudulent intent”.¹ In 1927, the Bureau of Chemistry’s regulatory functions were reorganized under a new USDA body: the Food, Drug, and Insecticide organization. 3 years later, the name was shortened to the Food and Drug Administration.¹

By the 1930s, campaigns for stronger regulatory authority prior to the release of drugs was pushed by regulators, journalists, and the public as a result of several drugs and foods such as false diabetes and cancer cures that was still in the market due to the limitation of the Pure Food and Drug Act.¹ However, it was not until the release of “Elixir Sulfanilamide”, a pediatric drug meant to cure Streptococcal infections that causes cough, that new law was passed through congress. Sulfanilamide have been safely used in powder and tablet form until this time, when a chemist and pharmacist named Harold Watkins experimented and found that he could dissolve it in diethylene glycol (now used as a antifreeze agent).¹ As there were no requirements at that time to test drugs safety on humans or other mammals, the drug was released.⁴ Within one month, several patients had died taking the medication, and by the time the FDA stopped the use of the medication – over 100 children had passed away.¹

This led to the push of Food, Drug, and Cosmetic Act that was signed into law by President Franklin Roosevelt in 1938.² This required FDA regulators to review both pre-clinical and clinical test for new drugs. Although the law did not specify the tests required for approval, the new authority allowed the FDA to block the marketing of new drugs by requiring additional data.² The Act also requires that safe limits be set for unavoidable poisonous matter and allows for factory inspections.⁴ The FDA was now allowed to set certain drugs as “prescription-only” and allowed the FDA to designate certain as safe for use only under the supervision of a medical professional.⁴

The FDA’s regulatory powers strengthened in 1962 by the Kefauver-Harris amendment following Thalidomide’s problems in Europe.⁵ Thalidomide, known by its brand name as Kevadon, applied to market in America in 1960. It was already sold to pregnant women in Europe for morning sickness, but Dr. Frances Kelsey, the new medical officer at the FDA denied the company’s requests, asking for more evidence.⁵ By late 1961, thalidomide was found cause thousands of babies to be born with birth defects in Europe, Britain, Canada, and the Middle East.⁵ The U.S. attributed its success in preventing thalidomide from coming to the U.S. to the FDA, and the Kefauver-Harris amendment now required that drugs be proven “effective” as well as safe, placing stringent controls on the use of investigational drugs that had previously not been regulated.³ Since then, the FDA has lost some powers such as the regulation of consumer products including hazardous toys, but gained many more involving the regulation of drugs and food – including regulation of medical devices in 1976.⁶ Since then, the powers of the FDA have remained relatively constant with primary changes focused on updating the process of obtaining FDA approval for drugs, medical devices, etc. These

changes led to the establishment of laboratory practices and guidelines for clinical trials and pre-clinical trials to ensure the quality and integrity of the safety data filed with the FDA.⁷

The FDA now ensures the safety and effectiveness of over \$2.5 trillion of products used by consumers, representing about \$0.20 of every \$1 spent by U.S. consumers.⁸ **Figure 1.2** shows the highlights of all the products that was regulated by the FDA in 2017, which includes over 19,000 prescription drugs, and 6,000 medical devices.⁸



1.2 Current FDA approval process

1.2.1 Preclinical phase in drug development

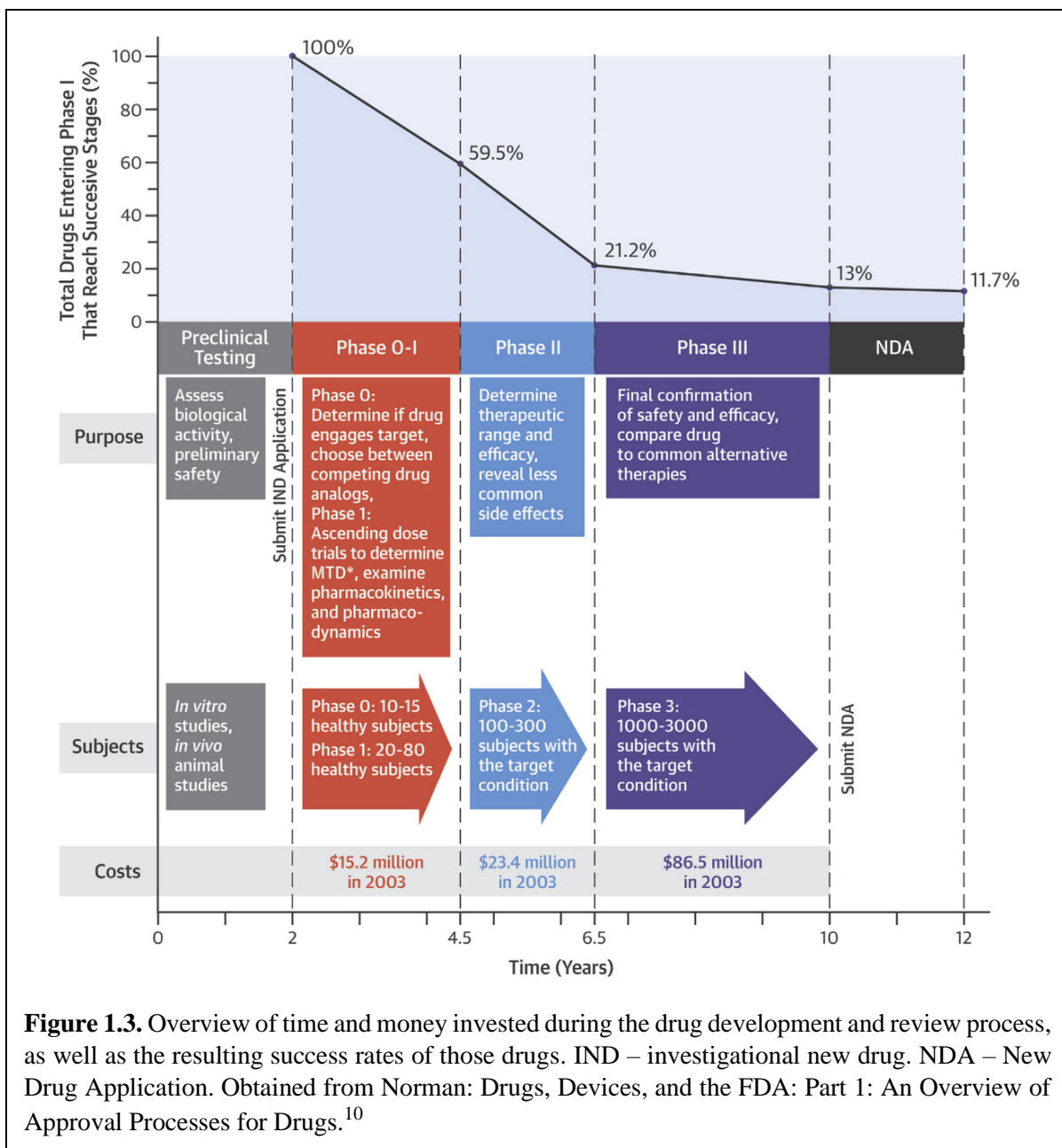
Not every substance taken by patients for their health is considered a drug by the FDA. The FDA defines a drug as: 1) a substance recognized by an official pharmacopoeia or formulary, 2) a substance intended for use in the diagnosis, cure, mitigation, treatment or prevention of disease, 3) a substance (other than food) intended to affect the structure or any function of the body, 4) a substance intended for use as a component of a medicine but not a device or a component, part, or accessory of a device.⁹

Drug development can be divided into 4 phases. The first is the preclinical phase, which usually takes ≤ 2 years to complete. During this time, the drug is tested in the laboratory – assessing its

safety, effectiveness, toxicity and biological activity. Here, drugs are required to undergo chemical and *in vitro/in vivo* testing.⁷ The results of these tests are then used to complete an investigational new drug (IND) application, which is submitted by a physician and the investor and includes potential targets for pharmaceutical action, chemicals that modify the targets, *in vitro* and *in vivo* (animal testing) results to test for the efficacy and cytotoxicity of the drug, initial work to determine pharmaceutical formulations and outline potential manufacturing process, evaluate the drug's purity and stability through the manufacturing process, explain the rationale behind testing a compound in humans, show strategies for protecting human volunteers, and create a plan for clinical testing. If the FDA believes the paperwork to be completed, phase I studies are set to begin (see **Figure 1.3** for the overview of the drug development and review process).^{7,9,10}

1.2.2 Clinical phase in drug development

The clinical trials phase can be split into 4 phases. Phase 1 is often completed with a small group of healthy volunteers to determine acute toxicity and dosage (see **Figure 1.3**). Safe doses can be tested at this time including a single dose, a single ascending dose, or even multiple ascending doses. The escalation of dose ends when “unacceptable” side effects occur – determined by the FDA and the investigator, and the previous dose is considered the maximum tolerated dose. Of all IND applications, ~70% will pass this phase and be found safe enough to progress to phase 2. On average, this process will cost \$4-\$15.2 million and take ~1-2 years to complete.^{7,9-12}



Phase 2 studies the effectiveness of a compound. To avoid unnecessarily exposing a human volunteer to a potentially harmful substance, studies are based on an analysis of the fewest volunteers needed to provide statistical power to determine efficacy. In phase 2, researchers seek to determine the effective dose, the best method of delivery (oral vs intravenous), the dosing interval, and reconfirm product safety. A substantial number of drug trials are discontinued during phase 2 due to ineffectiveness, safety problems, or intolerable side

effects.^{7,9-11} Only ~20%-33% of all INDs will pass phase 2, which costs ~\$13 million on average and take 1-2 years to complete.^{7,9-12}

Following phase 2 testing, the investigator or sponsor must submit updated information to the FDA regarding continuing safety for subjects, incorporating toxicity information found in Phase 2. Phase 3 testing is then allowed to begin. Phase 3 confirms the safety and efficacy of the drug, but in large cohorts. The trials evaluate effectiveness, monitor side effects, and compare the drug with commonly used alternative treatments. These studies can take anywhere from 2-10 years, involving thousands of patients from multiple sites, with an average of 3-5 years, and costing \$20-\$100 million to complete. If a drug survives the clinical trials, an NDA – New Drug Application, is submitted to the FDA containing all the preclinical and clinical information obtained during the testing phase. The FDA will then complete an independent review and make its recommendations, this process is required to take a maximum of 12 months.

If the drug is approved by the FDA, a request for a phase 4 trial may be requested where the users are often the test subjects. This is often to evaluate the longer-term effects of drug exposure, optimize dose, evaluate the effects on pediatric patients, or to examine the effectiveness of the drug for additional indications. At this stage, data of potential drug side effects rely on physicians' reports.^{7,13}

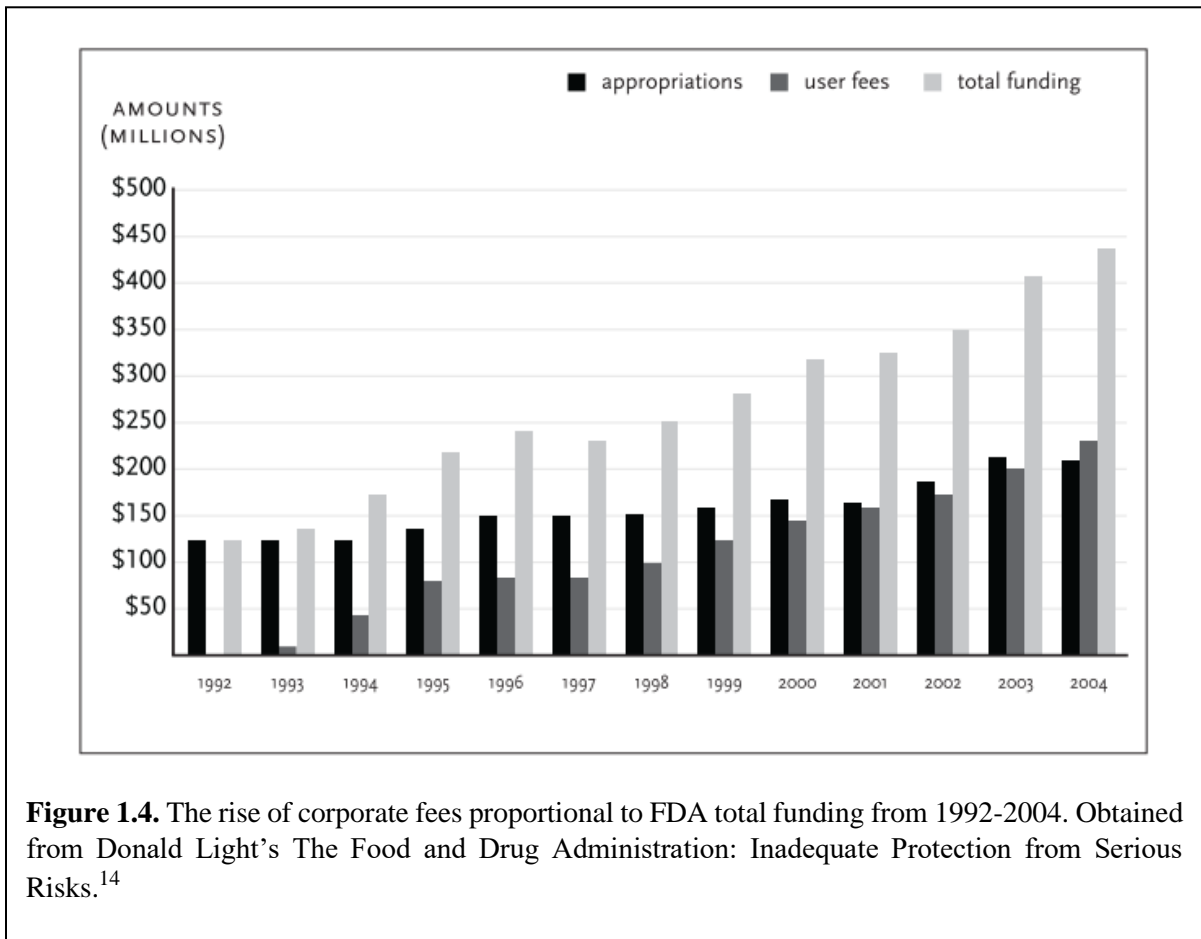
1.3 Controversies with the FDA

1.3.1 Race to Approve: Industry Pressure

Following the Kefauver-Harris amendment to the 1938 Food, Cosmetic and Drug Act, which required the evaluation of old drugs, proof of effectiveness, and safety for all new drugs *prior* to their approval, disclose of contraindications of their labels, overview of advertising, and

reporting of all adverse effects made known to companies, the FDA gained new powers to withdraw approved drugs if they were found to be unsafe or lacking evidence of effectiveness.¹⁴ The review of old drugs found that half were not effective, evidence that companies devoted most of their efforts to developing clinically ineffective new drugs and then marketing them as effective. Hundreds of prescription were removed from use, hundreds more stayed on and continued to be prescribed.¹⁴

Starting in the mid-1970s, the pharmaceutical industry began a backlash against the FDA: they sponsored economists and conferences emphasizing how the heightened standards of safety and efficacy since 1962 were cutting into profits, reducing companies' ability to fund research, leading to the higher costs of drugs, and keeping American patients' from obtaining benefits



of new drugs that were approved quickly. The pressure led the FDA from becoming overburdened with more backlash and cases than they could process quickly. To further push the FDA, the pharmaceutical industry created FDA advocacy council to find ways to improve regulatory operations. They found that a “user fee” system would be the best option: companies would pay for each new drug application, which provide money to the FDA to hire new reviewers. This became law in 1992 in the form of the Prescription Drug User Fee Act.¹⁴

The pharmaceutical industry is now paying large fees to fund its regulators: the FDA (see **Figure 1.4**). The pharmaceutical industry’s funding also comes at a price: the FDA is now required to complete 90% of reviews for all priority drugs and supplements be completed in less than 6 months, and those for standard drugs and supplements in less than 12 months. The accelerated reviews combined with mass marketing of these new medications for uses approved and unapproved, created a dangerous situation where over 20 million Americans were exposed to drugs approved under PDUFA I that were withdrawn soon after for their severe adverse effects.¹⁴ The industry required speed-up has resulted in substantially more risk for patients as the deadline-crunch approvals have resulted in drugs being put on the market that are three times more likely to result in toxic effects leading to severe or serious harm.¹⁴

1.3.2 Race to approve: Public displeasure

The push for rapid FDA approval was not only made by industry. The public, politicians, doctors and even insurance companies were also involved in many instances. Such as a case involving breast cancer in the 1980 when a promising new therapy was developed for women with metastatic breast cancer: high dose chemotherapy followed by bone marrow transplant (HDCT+/BMT). Small, early phase 2 clinical trials of this technique showed a substantial increase in the number of patients with metastatic breast cancer responding to this new therapy

as compared to those treated with standard chemotherapy.¹⁵ While these studies appeared promising, David Eddy published a review in 1992 outlining a number of criticisms that he had found in the studies associated with this therapy. He noted that there were publication bias in favor of positive results, lead-time bias, short follow-up time, small sample sizes, and that there was a markedly increased risk of serious morbidities compared with the risk of standard dose chemotherapy that was not evaluated in these phase 2 studies.¹⁶ Starting in the early 1990s, researchers began doing large, randomized, phase 3 studies to evaluate HDCT+/BMT. Many studies including large multi-centered studies completed by Stadtmauer, Rodenhuis, Peters, Tallman, etc. found no demonstrated advantage of HDCT+/BMT in comparison to standard chemotherapy.¹⁷

Only two other studies completed by Dr. Werner Bezwoda reached a different conclusion and found a significant increase in survival rates of breast cancer patients who received HDCT+/BMT in comparison to standard chemotherapy (See Table 1.1 for summary of findings of randomized studies of HDCT+/BMT).^{18,19} Further investigations into the studies conducted by Dr. Bezwoda showed missing data and paperwork for half of the women he claimed were part of his study. Furthermore, after being confronted by investigators, Dr. Bezwoda admitted to “improving” his results by lying about the drugs given to women in his control group (the chemotherapy dose in his control group was lower than those found in standard controls).^{20,21}

| Study | # Randomized patients | % Survival | Disease-free survival |
|----------------------------------|-----------------------|--|--|
| Bezswana et. al. Metastatic | 154 | 83% 5-year survival with HDCT+/BMT | 100 months with HDCT+/BMT |
| | | 65% 5-year survival with standard chemotherapy | 46.5 months with standard chemotherapy |
| Stadtmauer et. al. Metastatic | 184 | 32% 3-year survival with HDCT+/BMT | 9.6 months with HDCT+/BMT |
| | | 38% 3-year survival control | 9.0 months with standard chemotherapy |
| Rodenhuis et. al. High risk | 885 | 73% 5-year survival with HDCT+/BMT | 65% disease free at 5-years with HDCT+/BMT |
| | | 73% 5-year survival control | 59% disease free at 5-years control |
| Peters et. al. High risk | 783 | 79% 3-year survival with HDCT+/BMT | 71% disease free at 3-years with HDCT+/BMT |
| | | 79% 3-year survival control | 64% disease free at 3-years control |
| Tallman et. al. High risk | 511 | 58% 6-year survival with HDCT+/BMT | 49% disease free at 6-years with HDCT+/BMT |
| | | 62% 6-year survival control | 47% disease free at 6-years control |

Table 1.1. Results of the study by Betswana et. al. and four other randomized clinical trials of HDCT+/BMT for breast cancer.¹⁵⁻¹⁹

As skepticism grew in the research community about HDCT+/BMT's efficacy to treat late stage breast cancer, the perception of the public and oncologists were quite strong and positive. As there were few effective treatments for advanced breast cancer patients, public's demand for this treatment was high even prior to its approval by the FDA. Public outcry greatly increased in 1991 when the television show 60 minutes aired a piece decrying Aetna's decision

to deny insurance coverage for HDCT+/BMT to treat breast cancer.^{15,16} At the same time, Nelene Fox, a 38-year old patient with advanced breast cancer sued her insurance company, HealthNet, for refusing to pay HDCT+/BMT for Fox even though it had recently paid a relative of its CEO to receive the same treatment. Mrs. Fox died of breast cancer before a verdict was reached, but her family was awarded \$89 million dollars. The case received widespread publicity and in 1993, before HDCT+/BMT was ever approved by the FDA or indicated clear positive results, Massachusetts passed a law mandating insurance to pay for HDCT+/BMT.^{15,16} Even in states without mandated benefits laws, the politicization and threat of litigation caused a domino effect in the insurance industry leading to more insurance companies offering HDCT+/BMT although it was an experimental treatment. Furthermore, because coverage was mandated outside the context of randomized clinical trials, only one in ten breast cancer patients who received HDCT+/BMT in the 1990s did so within a clinical trial.^{15,16}

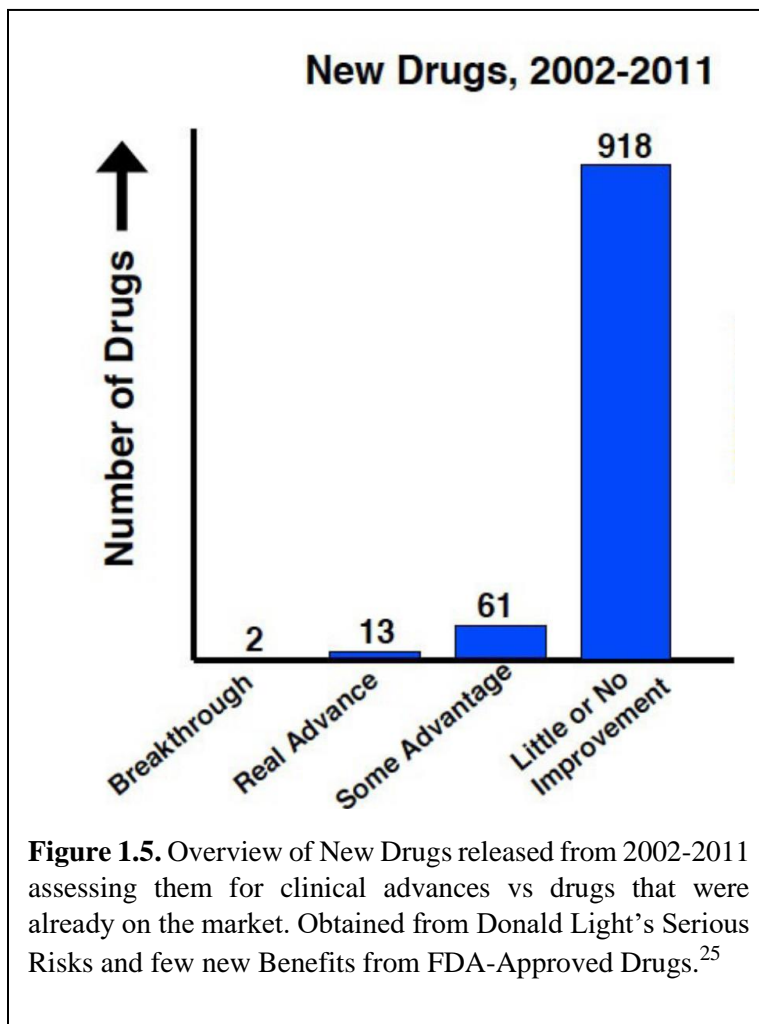
The HDCT+/BMT controversy bears two important lessons about experimental treatments and the FDA. In this case, the FDA was almost entirely bypassed in which more patients were receiving the treatment than those typically found in other standard phase 3 trials and, not only that, many of the patients receiving treatments were not even within a clinical trial context. The political and public pressure caused a domino effect in which the FDA's capabilities and clinical research on safety and effectiveness was hindered. Even so, more cases such as these are being found throughout the United States where the FDA is bypassed due to controversy surrounding access to treatment and care, regardless of effectiveness.

1.3.3 Barriers of entry

Research completed by DiMasi et. al. in 2013, showed that the average cost of new drug and biologicals development, including FDA approval is at ~\$2.6 billion.²² As a result,

pharmaceutical companies often take advantage of the FDA's quick approval process for similar compounds, allowing companies to skip much of phase 1, and even phase 2 trials allowing them to flood the market with hundreds of minor variations.^{23,24} As a result, a review of new drugs released in 2002-2011 showed that only 2 of 994 new drugs released were breakthroughs, with 13 considered real advances, 61 some advantage, and 918 new drugs that offered little to no improvement to their predecessors (see **Figure 1.5**).²⁵

Furthermore, due to the high costs associated with approvals, new smaller companies have difficulties entering the market and undergoing FDA approval even though their product may be novel. Large pharmaceutical companies use this to their advantage. These larger companies, such as Merck reports show that they spend only 1.3% of their sales revenue for basic research



to discover new drugs. Big companies are less interested in discovering new drugs and instead, let thousands of research labs and biotechnology firms try to find promising new products, absorbing the initial costs of FDA approvals, prior to one of these large companies buying in and marketing the products.²³

1.4 Exceptions to the FDA approval process

1.4.1 Unapproved Uses of Approved Drugs

Public regulation to protect patients from unsafe or ineffective drugs rests on the company selecting the indication for which a new drug is to be tested before designing and conducting trials to prove it is more effective than a placebo for that indication.²⁶ After approval, it is illegal for companies to market a drug for any condition or population inconsistent with the evidence of its specific effectiveness against specific conditions summarized in its labels.²³

However, this does not prevent company-sponsored studies and trials in which clinicians are funded to try out a drug for other uses in small trials that do not meet full FDA scientific standards. These clinicians then publish the results in journals that the company supports. Furthermore, the clinicians are also paid to give sponsored grand rounds, talks, educational courses, conference presentation at which these publications are shown as scientific evidence for unapproved (off-label) uses or extensions of approved uses.²³

This push in unapproved use research have led to unapproved prescriptions becoming more common over time. In fact, estimates show that about one in every five prescriptions being written is for unapproved use (see **Figure 1.6** for estimated number of prescriptions for off and on-label uses in 2011).^{23,27} The highest rates of unapproved use were for anticonvulsants (74%), antipsychotics (60%), and antibiotics (41%).²⁷

Companies are very interested in subtly pushing unapproved (or what Stafford calls “off-label use”). A study shows that unapproved prescriptions of 160 common drugs accounted for 21% of all prescriptions and most unapproved uses (73%) had little to no scientific support.²⁷ Even when unapproved uses become the norm, companies are under no obligation to conduct scientifically rigorous studies to assess benefits and risks.²³

According to the FDA, the FDA perspective is that once the FDA approves a drug, healthcare providers may prescribe and utilize the drug for an unapproved use when they judge that it is medically appropriate for their patient.²⁸ Furthermore, there are no laws regulating or preventing the use of approved drugs in unapproved cases. The only limitation is that the FDA policy prohibits direct promotion of products for unapproved use.^{14,27} The drug industry, however, may facilitate unapproved use by having their representatives bring physicians research studies that show unapproved uses. Thus, patients are not being protected by

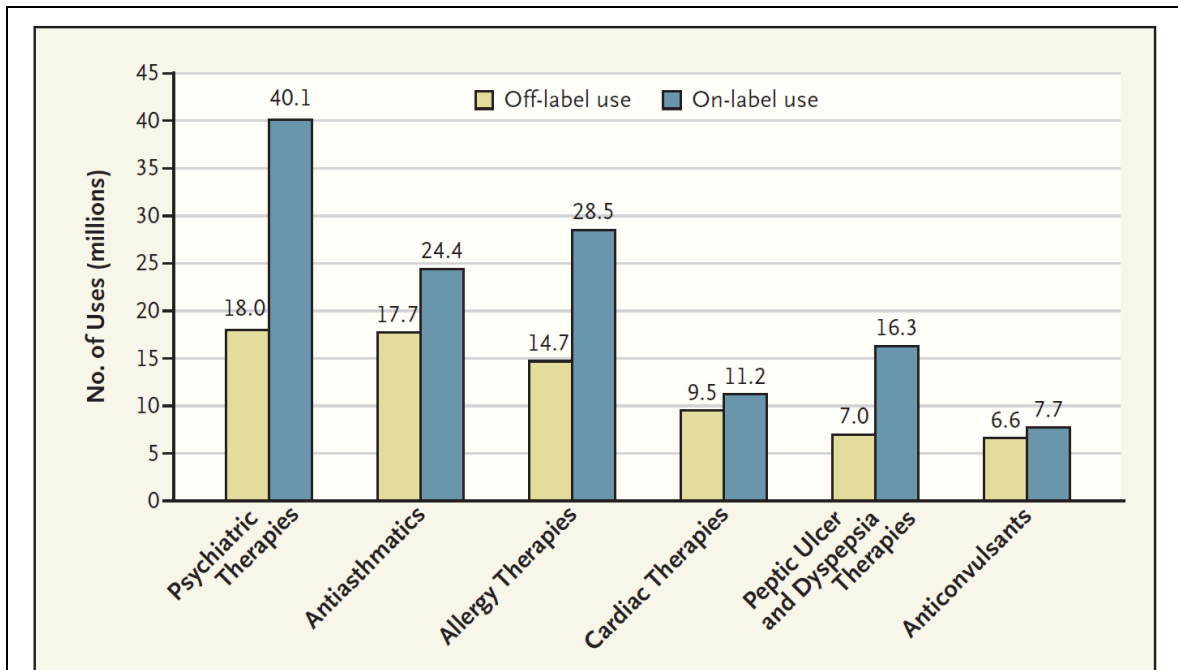


Figure 1.6. Stafford et. al’s estimation of prescription on-label (approved) and off-label (unapproved) uses in a number of functional drug class in 2011.²³

regulators and this puts a growing risk back on patients for uses that have no proven benefit/risk assessment.^{14,27}

1.4.2 Classes of NDA and recycling of approved drug moieties

Within an IND application for an investigation new drug, pharmaceutical companies must identify the type/class of new drug application (NDA) they are submitting (see **Table 1.2**).²⁹ It is possible for one NDA to contain >1 classification, although, as mentioned previously, companies have avoided extensive costs associated with clinical trials by utilizing similar drugs in different concentrations and combinations.

As such, there are few drugs that are classified as Class 1, or new molecular entities (NMEs). NMEs are drugs that contain an active moiety that has not been approved previously or used before and require clinical trials as well as *in vivo* work prior to approval. However, non-class I drugs can skip these clinical trial requirements. This push makes companies more interested in investing in formulations that have previously been used and established, requiring little innovation as formulary changes require little additional clinical trials of these “new” and “improved” drugs on their effectiveness in comparison to previously marketed concentrations. To further their ease of submission, moieties that are deemed low risk, i.e.. When the benefits outweigh the “risks” (side effects) and the “risks” are reversible or minimal, then they can continue to be used over and over again with few trials to no trials or additional work needed by the FDA for approval.

One example of this is seen with poly(ethylene glycol) (PEG) 3350 which are manufactured by many different companies with different names and in different concentrations. In fact, PEG 3350 is the basis for a number of osmotic laxatives and is used to treat constipation and as a bowel irrigation tool in bowel preparation therapy (such as before a colonoscopy). As the drug

| <i>Classification Code #</i> | <i>Name</i> | <i>Summary</i> |
|------------------------------|--|---|
| 1 | New Molecular Entity (NME) | A type 1 NDA is for a drug that contains a NME which is an active ingredient that contains no active compounds/moiety that has previously been approved by the FDA. |
| 2 | New Active Ingredient | A type 2 NDA is for a drug product that contains a new active ingredient, but not an NME. A new active ingredient includes those products whose active moiety has been previously approved or marketed in the U.S. |
| 3 | New Dosage Form | A type 3 NDA is for a new dosage form of an active ingredient that has been approved or marketed in the US by the same or another applicant but in a different dosage form. |
| 4 | New Combination | A type 4 NDA is for a new drug-drug combination with >2 ingredients. This may be >2 active ingredients in a single dosage or >2 ingredients combined together in a label |
| 5 | New formulation or other differences | New Formulation or Other differences (e.g., new indication, new applicant, new manufacturer |
| 6 | New indication or claim | New indication or claim, same applicant NOTE: this classification is no longer used as it has been replaced by type/class 9 and 10 |
| 7 | Previously marketed but not approved NDA | Previously marketed but without an approved NDA |
| 8 | Rx to OTC | Rx to OTC, this is specifically for a drug product intended to for over the counter marketing that contains an active ingredient that has been approved previously or marketed in the United States only for dispensing by prescription |
| 9 | New indication or claim | A type 9 NDA is for a new indication or claim for a drug product that is currently being reviewed under a different name and the applicant <u>does not</u> intend to market this drug product under the Type 9 NDA after approval |
| 10 | New indication or claim | This is for a new indication or claim for a drug product that is reviewed or recently approved and the applicant <u>intends</u> to market this drug product under the type 10 NDA following approval |

Table 1.2. New Drug Application Classification Codes.²⁹

has previously been deemed “safe” by the FDA in the 1970s, it is deemed low risk. Companies that place applications into the FDA are therefore not required to undergo additional studies

on its safety, and are only required to prove that their dosage forms are similar and effective to previous dosages used for constipation and/or bowel preparation.³⁰ Subsequently, PEG 3350 is a part of 8 different patents and there are >220 approved products by the FDA for use under different companies and different concentrations as a prescription product, generic prescription product, over the counter product, mixture product, etc.

1.5 Another look: Drugs and polymers of interest

In this work, an evaluation of the *in vitro* and *ex vivo* biocompatibility of polymers and drugs in different phases of FDA approval are evaluated. These include polymers and drugs that are 1) being studied for FDA approval (**Chapter 3**), 2) used for purposes other than their initial clinical setting purposes (**Chapter 4 and 5**), and 3) deemed safe from studies in the 1960s-1970s and have been used due to their low “toxicity” (**Chapter 6**). Furthermore, an alternative method of drug delivery is explored to improve the palatability and allow for more precise control of the concentration of drugs delivered for colonoscopy preparations to help alleviate side effects and improve compliance rates. A summary of the chemical structures of the drugs and polymers of interest can be found in **Table 1.3**.

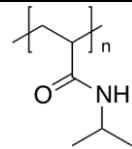
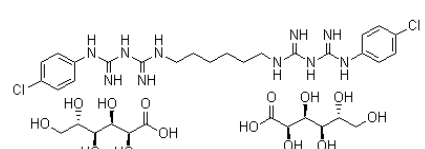
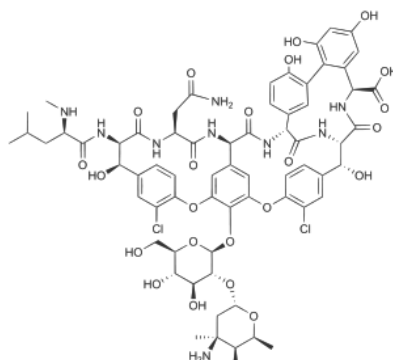
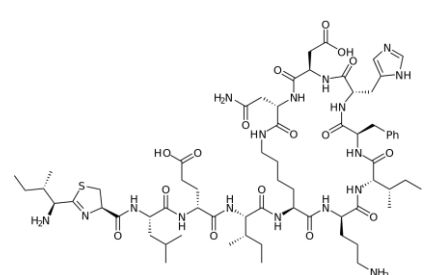
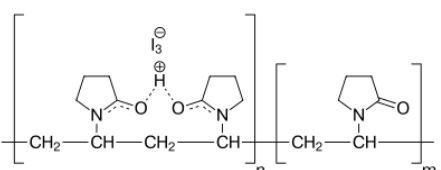
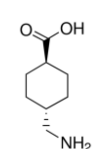
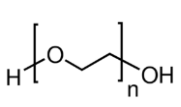
| <i>FDA approval status</i> | <i>Name</i> | <i>Chemical structure</i> | <i>Discussed in Chapter #</i> |
|----------------------------|---------------------------------------|--|-------------------------------|
| Pre-approval | Poly(N-isopropyl acrylamide) (pNIPAM) |  | 3 |
| Approved, Non-approved use | Chlorhexidine Gluconate |  | 4 |
| Approved, Non-approved use | Vancomycin |  | 4 |
| Approved, Non-approved use | Bacitracin |  | 4 |
| Approved, Non-approved use | Povidone-Iodine |  | 4 |
| Approved, Non-approved use | Tranexamic Acid |  | 5 |
| Approved | Poly(ethylene glycol) 3350 (PEG 3350) |  | 6 |

Table 1.3. Chemical structures of drugs and polymers of interest.

1.5.1 Pre-Clinical phase of development: Poly(*N*-isopropyl acrylamide)

Poly(*N*-isopropyl acrylamide) (pNIPAM) is a thermoresponsive polymer that is widely used in bioengineering applications due to its ability to undergo phase changes at physiologically relevant temperatures of around 32°C.^{31,32} As such, pNIPAM has been used in many different works including tissue engineering,^{33–35} drug delivery systems,^{36–38} wound healing,^{39,40} thermo-responsive multifunctional membrane,⁴¹ and ocular adhesives.^{40,42} However, prior to being used in patients and to obtain FDA approval, pNIPAM's *in vitro* cytotoxicity needs to be thoroughly evaluated. Previous work has shown that although many mechanisms of polymerizing NIPAM is non-toxic, our group found that commercially polymerized NIPAM exhibit signs of toxicity similar to those found in monomeric NIPAM. **Chapter 3** further evaluates the biocompatibility of commercially polymerized NIPAM on three cell lines and attempts to answer the reasons behind its toxic effects.

1.5.2 Unapproved use of approved drugs: Tranexamic Acid, Vancomycin, Bacitracin, Chlorhexidine, and Povidone-iodine

Antibiotics and antiseptics are often used in orthopedic surgeries to prevent infections.^{43–46} These include vancomycin, bacitracin, chlorhexidine gluconate (chlorhexidine), and povidone-iodine all of which were originally FDA approved for non-orthopedic surgery uses. Prior to being commonly used in orthopedic surgeries such as total knee arthroplasties, studies were conducted evaluating their effectiveness in preventing infections following surgery which showed great promise.^{43–46} However, all of these studies only evaluate their effectiveness with only one study focusing on biocompatibility. In fact, this study only tested chlorhexidine's biocompatibility on knee chondrocytes using a live/dead assay and found that it was cytotoxic at concentrations currently used in orthopedic surgeries.⁴⁷ To follow up on this study, **Chapter**

4 evaluates the biocompatibility of tranexamic acid towards *ex vivo* chondrocytes using live/dead assays.

Tranexamic acid is a synthetic derivative of the amino acid lysine that functions as a reversible competitive inhibitor to the lysin receptor found on plasminogen, preventing plasmin (activated form of plasminogen) from binding to and stabilizing the fibrin matrix, thereby reducing blood loss. The only FDA-approved usage for TXA is for heavy menstrual bleeding and short-term prevention of excessive blood loss in patients with hemophilia. Since its approval, oral, topical, and intravenous TXA have been used in many different situations including tooth extractions, surgical operations including total knee arthroplasties. However, the cytotoxicity of TXA towards knee chondrocytes not been evaluated prior to its adaptation into the surgical setting. As such, **Chapter 5** evaluates the biocompatibility of tranexamic acid towards *ex vivo* chondrocytes using live/dead assays.

1.5.3 “Low Risk” drugs and polymers and other potential Uses: Poly(ethylene glycol), sodium alginate, and chitosan

As mentioned previously, PEG 3350 is considered a “low risk” drug/polymer used as an osmotic laxative. There are many iterations and forms of PEG 3350 in the market, and it is the go-to drug for colonoscopy preparations. However, few studies have evaluated its biocompatibility in the human gastrointestinal tract as use in humans have shown “minimal”, reversible side effects including: nausea, vomiting, dehydration, severe and worsening stomach cramping and bloating, dizziness, rectal bleeding, etc. In **Chapter 6**, we test PEG 3350 at multiple concentrations for its biocompatibility *in vitro* on human gastrointestinal cells. It appears that although current concentrations are technically biocompatible, assumptions are made about the uniformity of drug concentration in the delivery method. However, this is not

true as patients who undergo colonoscopies receive a drug packet along with a 1 gallon bottle and told to shake the PEG 3350 into the solution. Patients often describe the solution as “clumpy” which is indicative that the current delivery method is non-uniform which could be a reason why patients of smaller stature can experience more side effects than those found in the study in 1970. In **Chapter 7**, we encapsulate PEG 3350 using sodium alginate and chitosan to create a pH responsive hydrogel system that allows for greater control of the delivery process of PEG 3350 as a colonoscopy preparation solution.

Chapter 2: Cytotoxicity Analysis of Mammalian Cells Exposed to Drugs and Polymeric Surfaces and Extracts (Experimental Procedures and Equipment)

Invited tutorial article in preparation for a publication in *Biointerphases* by Nguyen, P.A.H.; Lenz, K; and Canavan, H.E.

2.1 Introduction

Many tests can be used to describe a polymer/drug, some of those that have been used in this work include X-ray photoelectron spectroscopy (XPS), goniometry, rheology, and nuclear magnetic resonance (NMR). Additional techniques used to analyze polymer/drug interactions with cells *in vitro* include cell morphology tests, live/dead assays, and XTT assays. A description of these techniques are presented below.

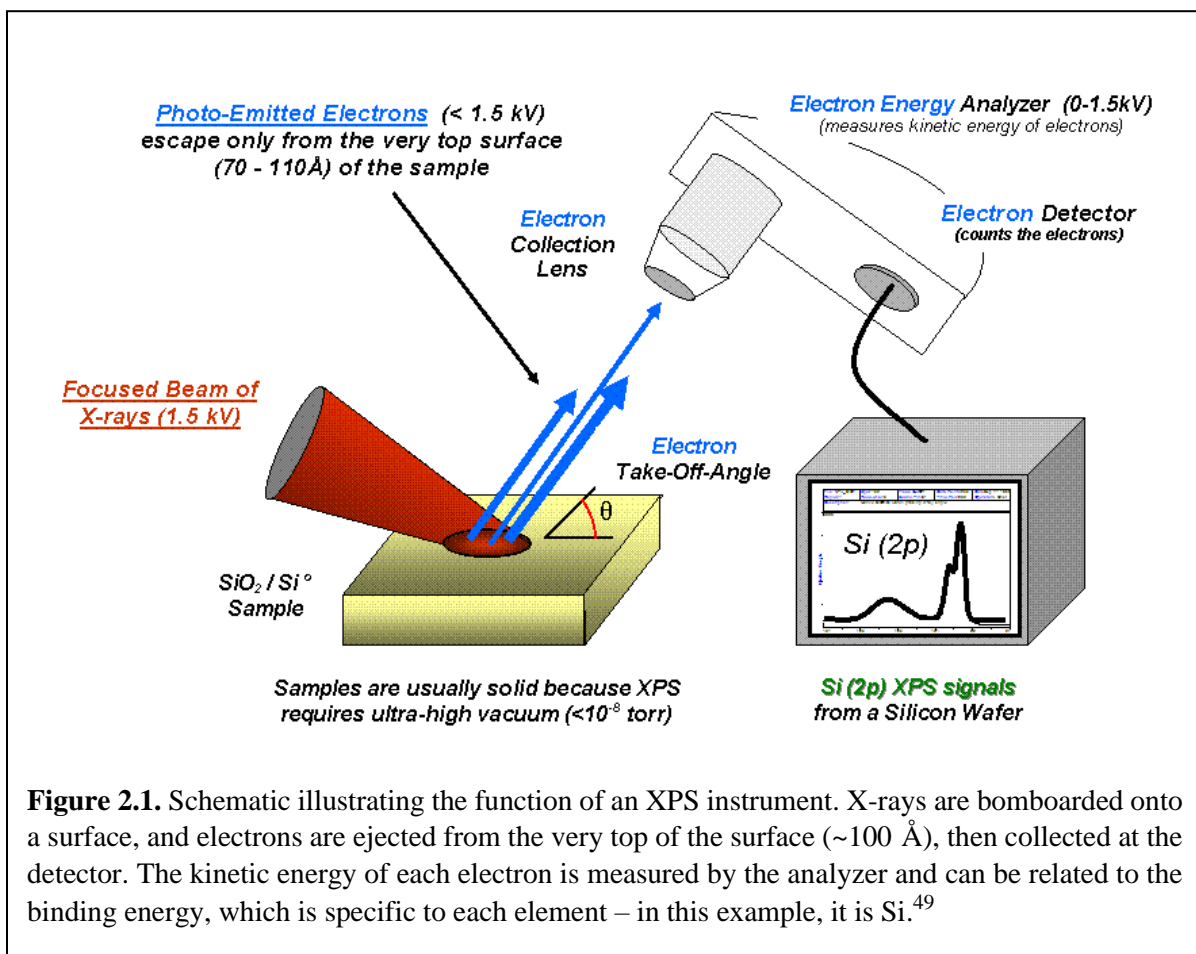
2.2 X-Ray Photoelectron Spectroscopy (XPS)

X-ray photoelectron spectroscopy is a quantitative technique that can be used to determine the elemental composition, bonding environments, and often times, the relative thickness of a surface. Surfaces are irradiated with monoenergetic X-rays (photons) causing photoelectrons to be emitted (See **Figure 2.1**).⁴⁸

The process corresponds to Equation 2.1 where KE is the kinetic energy of the emitted photoelectrons, $h\nu$ is the energy of the photon, BE is the binding energy of the emitted photoelectron and ϕ is the work function of the device.⁴⁸

$$KE = h\nu - BE - \phi \text{ (Equation 2.1)}$$

The kinetic energy is measured using an electron energy analyzer, which allows for the calculation of the binding energy:^{48,49}



Electrons can escape from the top ~100 Å of the surface. From the binding energy and the intensity of the photoelectron peak (based on the number of photoelectrons detected), the identity of the elements on the surface, the chemical state of each element, and the quantity of each element may be determined.⁵⁰⁻⁵³ [Note: In regards to quantity, there is an error of ~5-10% that could be determined]⁵⁰⁻⁵³ The survey spectrum will allow for the determination of elements that are present as well as the elemental composition (atomic %) while a high resolution spectrum will allow for the determination of the elemental binding elements. [It should also be noted the error of estimation is often higher when evaluating the elemental

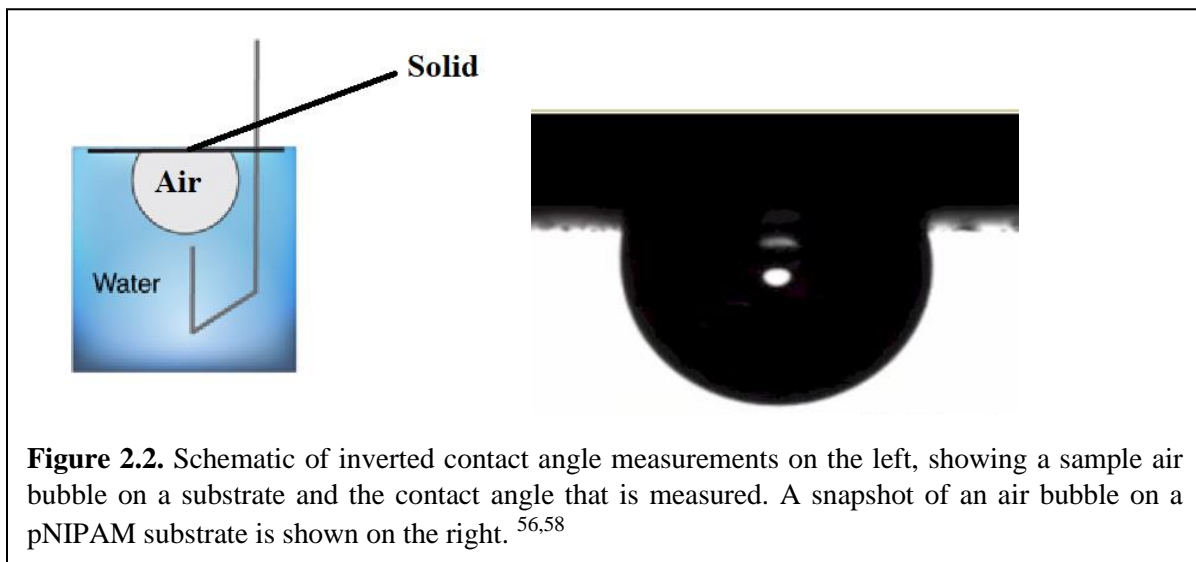
binding elements.] As a result, XPS is often used to measure the elemental composition of surfaces, empirical formulas of pure materials, elements that may contaminate a surface, the chemical or electronic state of each element in the surface, and the uniformity of the elemental composition across the top surface.

Some disadvantages are associated with the use of XPS. XPS is run under high vacuum (10^{-8} to 10^{-11} Torr) meaning that XPS is only ideal for solid samples and focuses on examining surfaces of semi-conductors, thin films and coatings (metal/metal oxide/ DNA films), biosensors, and dry powder pharmaceutical materials.⁵⁴ Biological samples, as well as nanoparticles often fracture under high vacuum and are not always ideal as this can change regions exposed for characterization.⁵⁵

2.3 Contact Angle (Goniometry)

A contact angle goniometer is an instrument used to measure the static contact angle of a surface.⁵⁶ It is a measuring device that uses the angle of interactions with water (or other solutions) on a surface to characterize the relative wettability of surfaces.⁵⁶ This is especially important when depositing materials onto a surface that greatly changes its properties, or in the use of polymers such as poly(*N*-isopropyl acrylamide). In **Chapter 3**, poly(*N*-isopropyl acrylamide) is studied, and its relative wettability is highly dependent on temperature.⁵⁷ Below its lower critical solution temperature (LCST), pNIPAM is hydrophilic, and above its LCST, pNIPAM is hydrophobic. Contact angles using goniometry can be taken to determine surface wettability of pNIPAM on Si as well as on a Si control chip to test the surface properties following deposition of pNIPAM onto the surface. If deposition was successful, exposure to different temperatures will lead to relative wettability changes below and above the LCST. If

not, pNIPAM deposited surfaces will behave similar to Si control chips where no changes are seen.^{56,58}

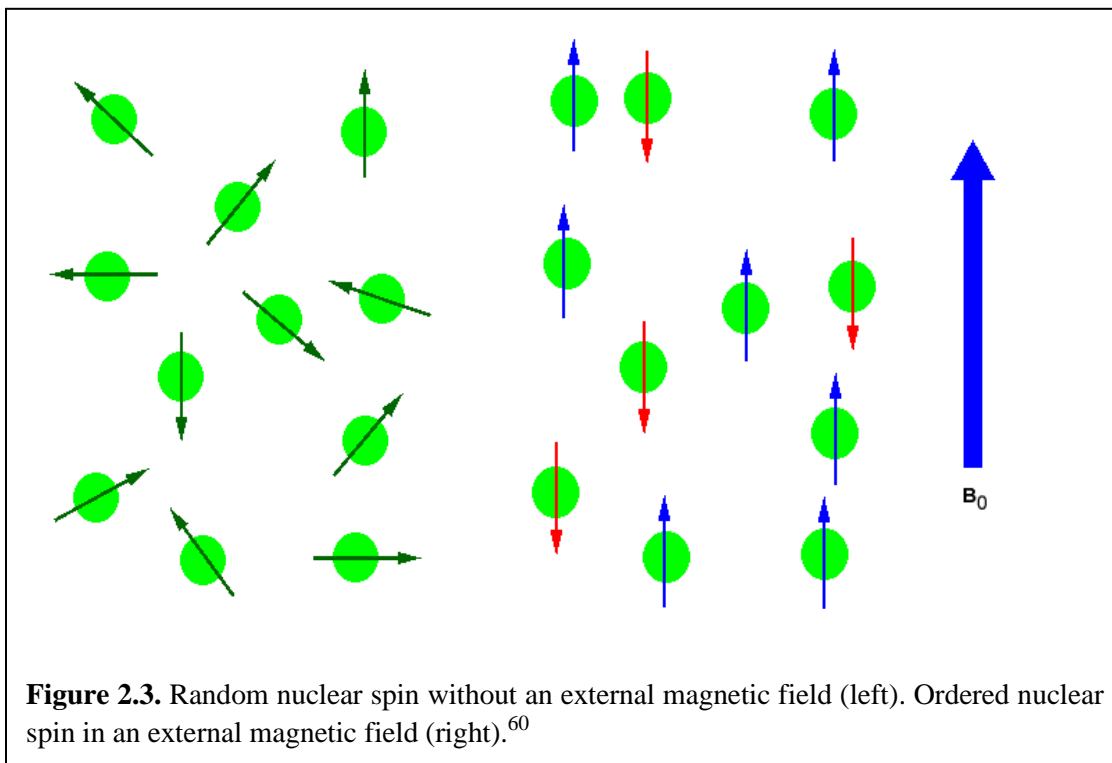


These experiments rely on the use of a technique known as captive (or inverted) bubble. The surface is placed upside down in a quart cell filled with Millipore water. Using a syringe with an inverted needle, an air bubble is placed on the surface and the angle between the drop and the surface is measured (see **Figure 2.2**). This procedure is repeated at different temperatures to evaluate the surfaces' relative hydrophobicity and hydrophilicity in a quick and affordable manner.^{56,58}

2.4 Nuclear Magnetic Resonance (NMR)

Nuclear magnetic resonance (NMR) spectroscopy is an analytical chemistry technique used in quality control and research for determining the content and purity of a sample as well as its molecular structure.⁵⁹ For NMR, the spin and electrical charge of nuclei are used to identify them. In the absence of an external magnetic field, the direction of the spin of the nuclei will be randomly oriented (see **Figure 2.3**).⁶⁰ An external magnetic field is applied, the direction of the field will cause the nuclei to align with it, leading to two possible orientations (parallel to

the magnetic field or antiparallel magnetic field). an energy transfer is possible between the base energy to a higher energy level (usually within a single energy gap). If the ordered nuclei are then subjected to electromagnetic radiation of the proper frequency the nuclei aligned with the field will absorb energy and “spin-flip” to align themselves against the field, at a higher energy state. When this spin-flip occurs, the nuclei are said to be in resonance. The amount of energy, and the exact frequency of electromagnetic radiation required for resonance to occur is dependent on both the strength of the magnetic field applied and the type of nuclei being studied. As the strength of the magnetic field increases, the energy difference between the two spin states increases and a higher frequency (more energy) need to be achieved for a spin-flip. The amount of energy it takes, and the signal that matches this transfer is measured and processed to yield an NMR spectrum which displays the plot of applied radio frequency vs the absorption.⁵⁹ In general, all nuclei with an odd number of protons or nuclei with an odd number of neutrons are required for NMR.⁵⁹



The most common use of NMR spectroscopy is in the study of liquids, including samples dissolved in solvent to characterize for contaminants. This process is used in **Chapter 3 and 7** to detect for possible contaminants in leachates from surfaces and hydrogels.

2.5 Rheology

Rheology is used to describe and assess the deformation and flow behavior of materials.⁶¹ Fluids are often subjected to rheology to study their viscosities, and dispersion behavior. Another process that is often studied is the viscoelastic behavior of fluids, hydrogels, and even solids. An ideally elastic solid, or fluid is a material that has the ability to resist a distorting influence (force) and return to its original size and shape when that force is removed.⁶¹ To determine viscoelastic behavior, a two-plate model is often used (see **Figure 2.4**). Here, the sample is subjected to shear while sandwiched between two plates, with the upper plate moving and the lower plate being stationary. By understanding the shear stress and shear strain applied, and using the shear stress and shear modulus equations (Equations 2.2, and 2.3), the storage modulus (G') and the loss modulus (G'') can be found. [Note: In equations 2.2 and 2.3, F denotes force, A denotes area, s is the deflection path (in m) and h describes the shear gap.] The storage modulus (G' , described in Pascal units) represents the elastic portion of the viscoelastic behavior which describes the solid-state behavior of the sample. The loss modulus (G'' , described in Pascal units) characterizes the viscous portion of the viscoelastic behavior, or the liquid-state behavior of the sample.

$$\tau = \frac{F}{A} \text{ (Equation 2.2, shear stress)}$$

$$\gamma = \frac{s}{h} \text{ (Equation 2.3, shear strain)}$$

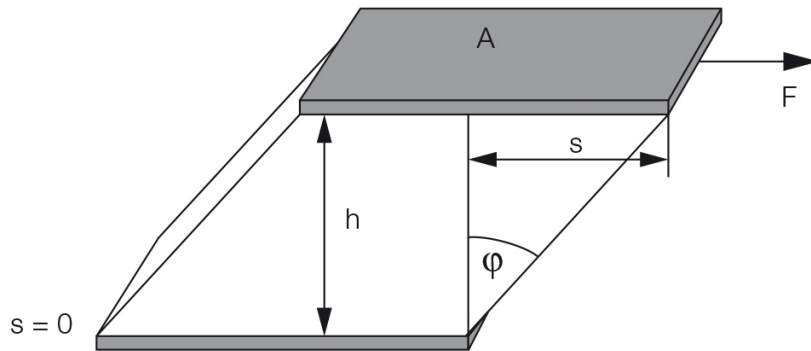


Figure 2.4. Schematic of the two plate model to determine the viscoelastic behavior of a hydrogel, liquid, or other test material. ⁶¹

Due to its ability to describe the viscoelastic behavior of hydrogels, rheology is often used with hydrogels to determine gelling point, and chemical stability. The loss tangent or $\tan \delta = G''/G'$ is the measure of damping of a material and can give information about the change in chemical properties of hydrogels. Gels are considered “stronger” or more solid-like when $G' < G''$, in contrast gels are considered “weaker” or softer and more liquid-like when $G' > G''$. At $G' = G''$, gels are considered stoichiometrically balanced. This is essential when characterizing gels to understand their response to outside stimuli.

2.6 Cell Morphology

Cell cultures take one of two forms: suspension (as single cells, or small free floating clumps in medium) or monolayers that are attached to the tissue culture flask (see **Figure 2.5**).^{62,63}

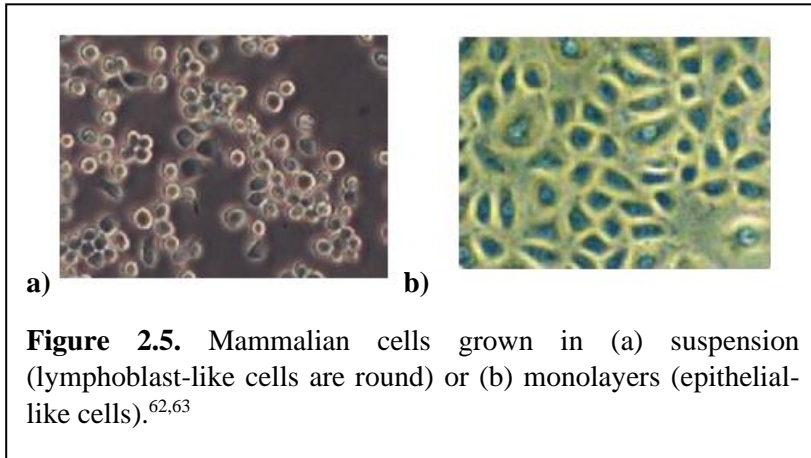


Figure 2.5. Mammalian cells grown in (a) suspension (lymphoblast-like cells are round) or (b) monolayers (epithelial-like cells).^{62,63}

Monolayered cells can come from many different cell types including endothelial (such as bovine aortic endothelial cells (BAECs)),^{64,65} epithelial (such as HeLa cells),⁶³

neuronal (such as SH-SY5Y),⁶³ or fibroblasts (such as 3T3s)⁶⁶ (see **Figure 2.6**).

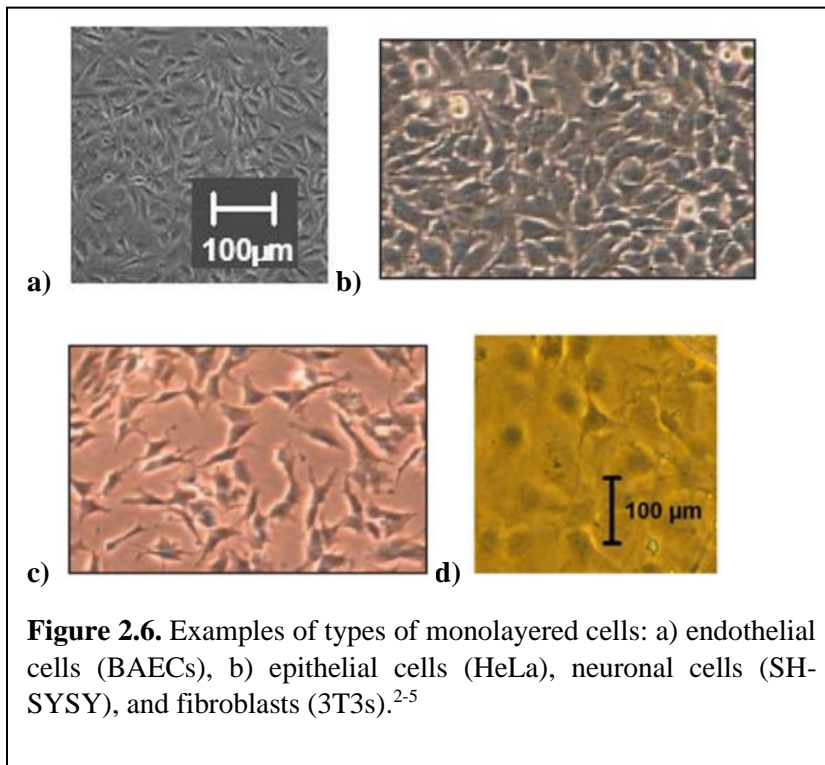


Figure 2.6. Examples of types of monolayered cells: a) endothelial cells (BAECs), b) epithelial cells (HeLa), neuronal cells (SH-SY5Y), and fibroblasts (3T3s).²⁻⁵

Cells grown in culture can be evaluated over time to examine their health by comparing their size, shape, structure and form (morphology) with controls (previously published images of healthy cells).⁶² You can determine the cytotoxicity of novel biomaterials by

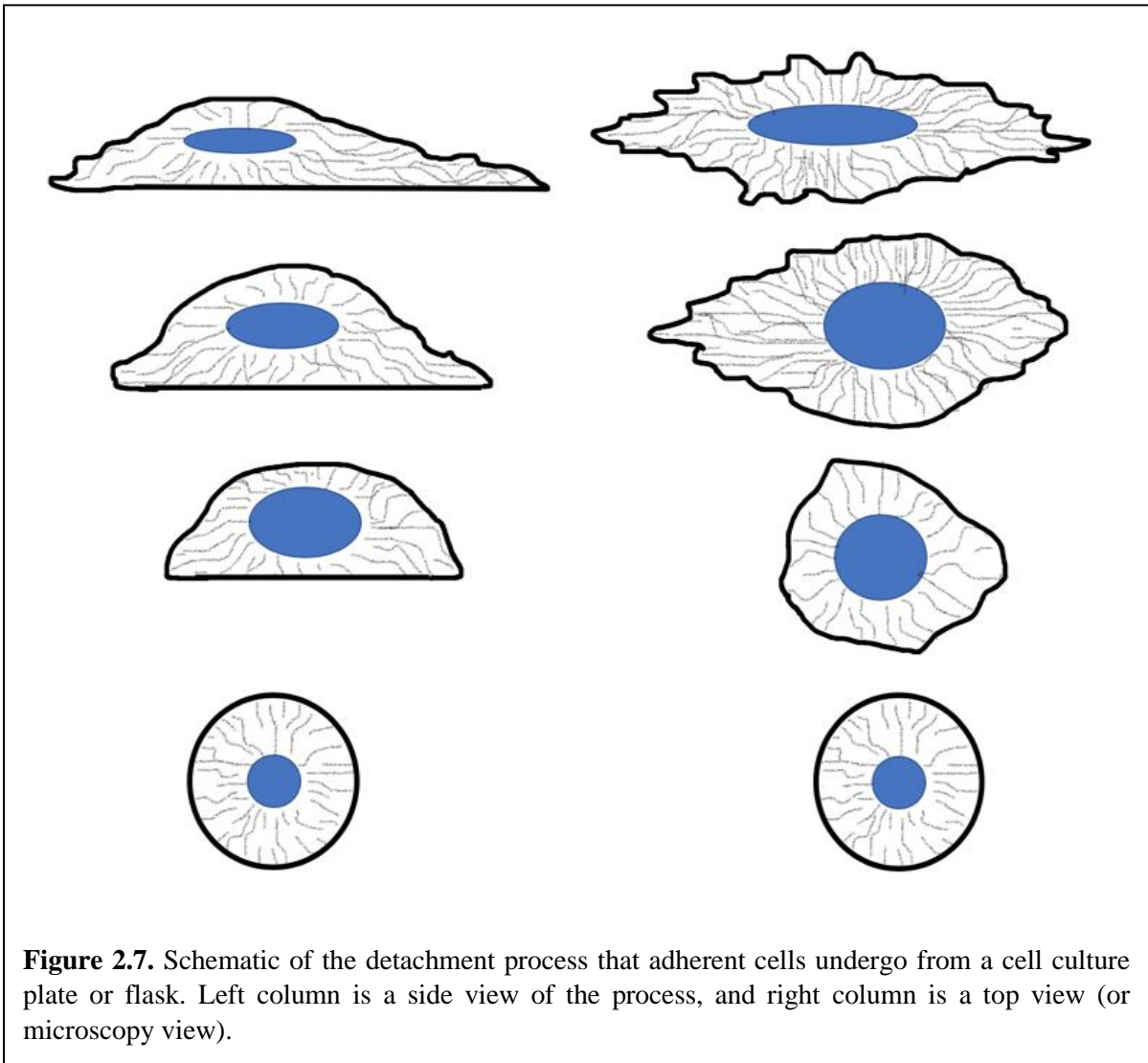
examining the changes in morphology of cells after short-term and long-term exposure. In the presence of cytotoxic materials, adherent cell lines can detach, shrink in size, have a decrease in culture density (decrease in confluence), and experience condensation of nuclear chromatin due to apoptosis or cell lysis.⁶⁵⁻⁷⁰ Considering the high prevalence of morphology testing to

confirm cell health, almost every cell type, that can be purchased, has published images of healthy cells, which can then be used as experimental controls. As a result, cell morphology is often used in cytotoxicity experiments of novel biomaterials *in vitro*.⁷⁰

Protocols for cell culture and observation of morphology are detailed in **Chapters 3 and 6**. Briefly, cells are deposited into tissue culture flasks and grown to ~80% confluence. Cells are then exposed to the biomaterial through direct contact, indirect contact, or elution tests. Following exposure, cells are observed/imaged over time using a light microscope, phase-contrast microscope, scanning electron microscope (SEM), video microscope, or confocal microscope. The duration of the experiment and type of microscope used will depend on the focus of the experiment itself. For most applications with short-term cytotoxicity testing, images should be taken every 12-24 hours over a 48-hour period; for mid-term cytotoxicity testing, it can be every 24-48 hours over a 96 hour period.

While this is a relatively simple technique, the results must be observed over a relatively short time frame. In previous studies where cell are observed over a 24 hour period using video microscopy, morphological changes begin to take place in less than 2 hours.^{71,72} However, the point of irreversible cell injury has been shown to take place several hours before the appearance of morphologic changes.^{71,72} *In vivo*, apoptotic cell death has been estimated to be 6-24 hours.⁷¹ Due to the short time frame of apoptosis *in vitro*, only a few cells are undergoing apoptosis at a single time point, and so that quantitative value of cytotoxicity may be underestimated.⁷¹ Furthermore, cells undergoing apoptosis or cell lysis have already reached irreversible cell injuries, so biomaterials that are mildly cytotoxic or cause reversible cell injuries, may not be seen in cell morphology experiments.⁷²

This technique is dependent upon the experience of the user to be standardized and knowing how their cells generally behave. In **Chapters 3 and 6**, cells are adherent cell lines that are generally elongated and will attach to the surface. As they are detaching or experiencing cytotoxicity, cells will begin to round over time, and detach from the flask they are adhered to. (see **Figure 2.7**). Left of **Figure 2.7** shows the side view of this process, while right of **Figure 2.7** shows the top view of this process.



2.7 Live/Dead Stain (Ethidium homodimer I/III and Calcein AM)

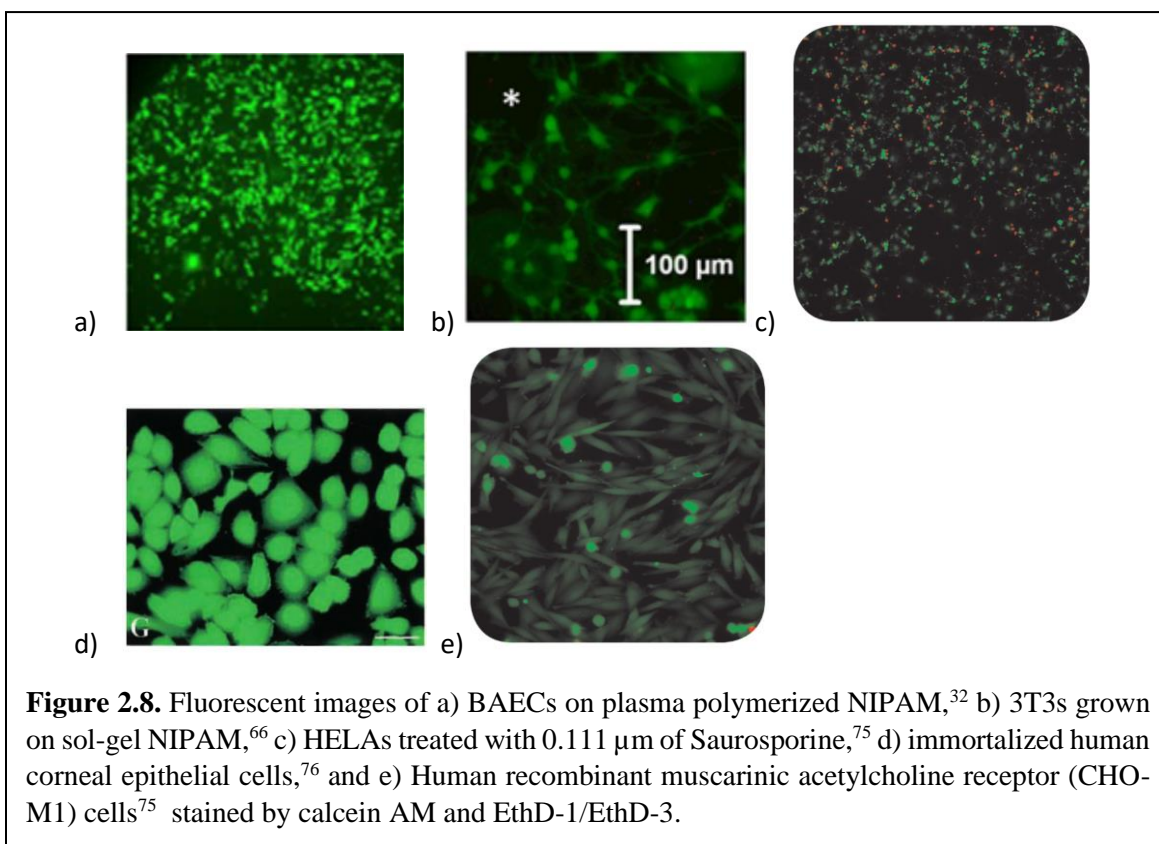
The Live/Dead™ stain is a two-color fluorescence cell viability assay that simultaneously determines live and dead cells with two different probes that measure two parameters of cell viability: intracellular esterase activity and plasma membrane integrity.⁷³ Live cells are distinguished by the presence of intracellular esterase activity, which is determined by the conversion of the non-fluorescent cell-permeant calcein AM to the green fluorescent calcein (ex/em ~495 nm/~515nm).⁷³ Ethidium homodimer I (EthD-1) and Ethidium homodimer III (EthD-3O) enter cells with damaged membranes and undergo a conformational change upon binding to nucleic acids, producing a bright red fluorescence in dead cells (ex/em ~495 nm/~635nm).⁷³ EthD-1 and EthD-3 are both incapable of permeating intact cell membranes, and are therefore, excluded from live cells. EthD-3 is an improved/alternative form EthD-1 developed by Biotium, as it is able to stain DNA 45% brighter than EthD-1.⁷⁴ See **Figure 2.8** for fluorescent images of BAECs on plasma polymerized NIPAM,³² 3T3s grown on sol-gel NIPAM,⁶⁶ HELAs treated with 0.111 μm of Saurosporine,⁷⁵ immortalized human corneal epithelial cells,⁷⁶ and Human recombinant muscarinic acetylcholine receptor (CHO-M1) cells⁷⁵

Calcein AM and EthD can be purchased individually to create a generic form of the Live/Dead™ kit and are often used in place of trypan blue to determine cell viability⁷⁷ and cytotoxicity.^{66,73,78} [Note: it is the generic version used in this dissertation, hence the trademarked name is not listed.] Previous studies have used calcein AM and EthD to measure the cytotoxic effects of tumor necrosis factor (TNF),⁷⁹ β -amyloid protein,⁸⁰ adenovirus protein,⁸¹ polymers such as poly(N-isopropyl acrylamide) (pNIPAM),⁶⁶ etc. Furthermore, the assay has also been used to quantify apoptotic cell death⁸² and cell-mediated cytotoxicity⁸³. As

seen from **Figure 2.8**, calcein AM and Eth-D are compatible with many mammalian cell types, including adherent and non-adherent cell lines.

For all techniques, cells are cultured to confluence. Then, to perform viability assays, cells are exposed to calcein AM and EthD and incubated for 30-45 minutes at room temperature (less time is needed if at 37°C). After exposure, the labeled cells are viewed and the level of cytotoxicity is evaluated qualitatively by using fluorescent microscopy, or quantitatively by using fluorescent microplating or flow cytometry.⁸⁴ All protocols have been described in detail in **Chapters 3-6**.

Assays such as live/dead determine the viability of individual cells by counting point signals



rather than a homogenous signal that represents a population of cells. As a result, this makes it highly difficult for high throughput screening of cell viability in 96 well plates.⁷⁸ Furthermore, users should take into consideration the materials they are testing for cell cytotoxicity.

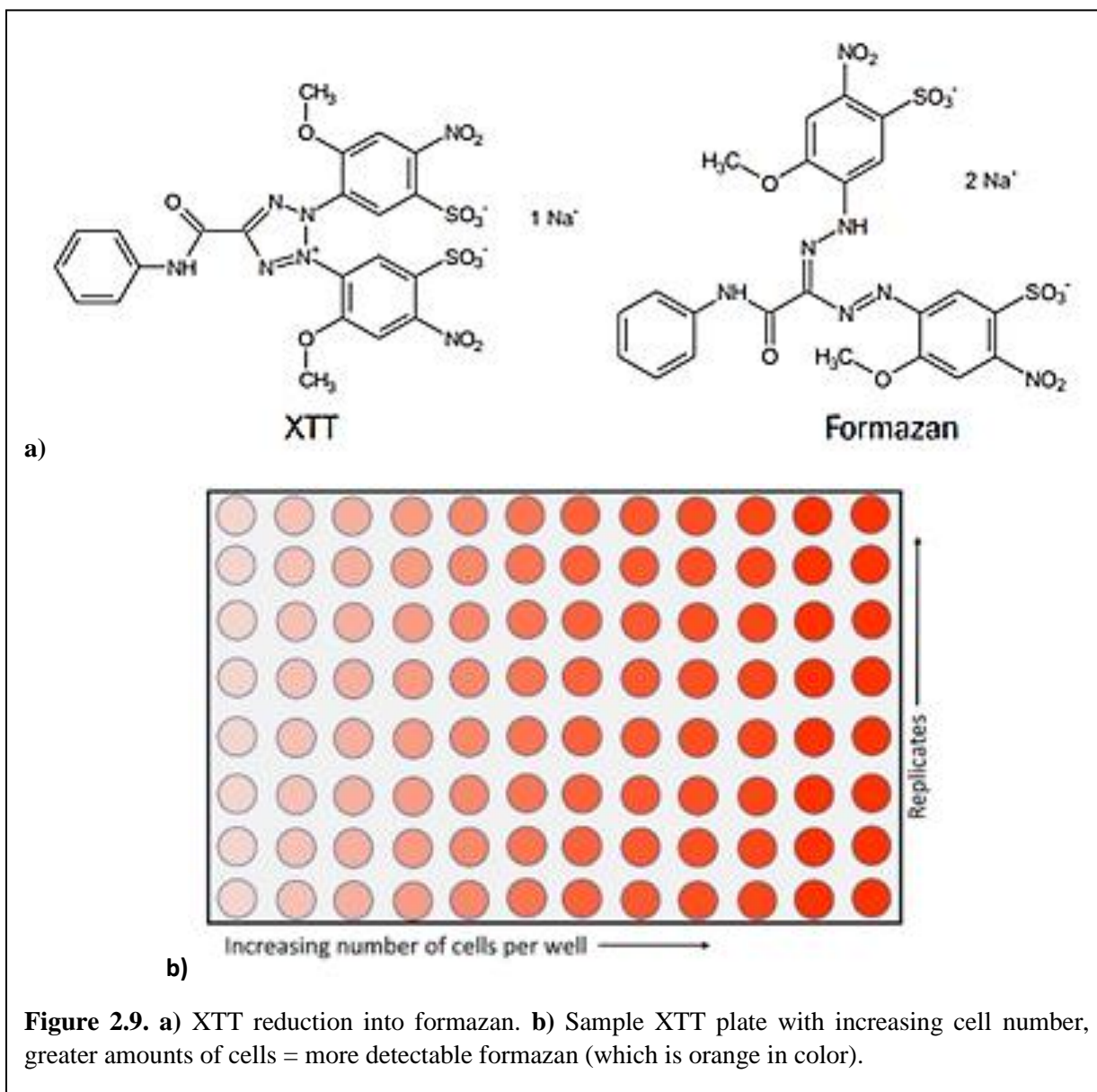
Nanomaterials have been found to settle on top of cell monolayers, which are attached to the bottom of wells causing point signal interference within the cells, and can obliterate cells and make it difficult to quantify individual cells by a live/dead assay.⁷⁸

Although highly used and successful in informing the user if cells are dead – the assay lacks the capability to differentiate between mechanisms of death. Cell death typically occur by necrosis, or apoptosis.⁸⁵ *In vivo*, necrotic cell death typically induces inflammation while apoptotic cell death does not.⁸⁶ As a result, it is important to understand the mechanism of cytotoxicity as well as whether the material is cytotoxic through biological implications. In addition, use of this technique requires access to more advanced equipment such as a fluorescence microscope, a microplate reader/spectrometer, and/or a flow cytometer and user experience is required.

2.8 XTT

XTT is a colorimetric assay that assesses cell metabolic activity by reducing tetrazolium compounds to an insoluble colored product called formazan.⁸⁷ XTT is negatively charged and do not readily penetrate cells.⁸⁸ XTT is often used with an intermediate electron acceptor that can transfer electrons from the cytoplasm or plasma membrane to assist the reduction of tetrazolium into formazan (see **Figure 2.9**).⁸⁸

This set of assays is often used as a measurement of cell viability, proliferation, and testing drug cytotoxicity.⁸⁹⁻⁹² Viable cells with active metabolisms will convert these tetrazolium salts into a colored formazan product. Whereas, when cells die, they lose the ability to convert tetrazolium salts into formazan. As a result, the quantity of formazan is presumed to be directly proportional to the number of viable cells.⁸⁸



Several studies have compared the XTT viability assay against LDH leakage assays, trypan blue assays, etc. and have found XTT to be a more useful and sensitive test for the determination of acute toxicity.^{78,90,93} However, XTT and its related compounds and assays (MTT, and others) have been found to interact with a number of inhibitors, proteins, compounds, and even chemotherapy drugs leading to significant over/underestimation of cell viability by the assay.^{89,94-96} For example, honey's reducing sugars and phenolic compounds interacted with the MTT assay, reducing MTT into formazan although no cells were present.⁸⁹

XTT and its related assays can also not be used with nanomaterials as nanomaterials have been shown to interact with the dye through dye absorption.⁷⁸

2.9 Conclusions

From the descriptions of the techniques, it is clear that one technique is not sufficient in detailing cytotoxic effects of treatments towards cells. As a result, a combination of multiple techniques is preferred to truly determine the biocompatibility/cytotoxicity of polymers and other treatments.

Chapter 3: Exploring the Anomalous Cytotoxicity of Commercially-Available Poly(*N*-isopropyl Acrylamide) Substrates

Published by Nguyen, P.A.H.; Stapleton, L.; Ledesma-Mendoza, A.; Cuylear, D.L.; Cooperstein, M.A.; and Canavan, H.E. in *Biointerphases Volume 13, Issue 6, September 2018*

Abstract

Poly(*N*-isopropyl acrylamide) (pNIPAM) is a stimulus-responsive polymer (SRP) that has been of great interest to the bioengineering community. When the temperature is lowered below its lower critical solution temperature (LCST, ~32 °C), pNIPAM rapidly hydrates, and adherent cells detach as intact cell sheets. This cell-releasing behavior in a physiologically relevant temperature range has led to NIPAM's use for engineered tissues and other devices. In a previous study, however, we found that although most techniques used to polymerize NIPAM yield biocompatible films, some formulations from commercially available NIPAM (cpNIPAM) can be cytotoxic. In this work, we investigate the reasons underlying this anomaly. We evaluated the response of a variety of cell types (e.g., bovine aortic endothelial cells, BAECs; monkey kidney epithelial cells, Vero cells; and mouse embryonic fibroblasts, 3T3s) after culture on substrates spin-coated with sol-gel (spNIPAM) and commercially prepared (cpNIPAM). The relative biocompatibility of each cell type was evaluated using observations of their cell morphology and function (e.g., XTT and Live/Dead assays) after 48 and 96 hours in culture. In addition, the substrates themselves were analyzed using NMR, goniometry, and XPS. We find that all the cell types were compromised by 96 hours in culture with cpNIPAM, although the manner in which the cells are compromised differ; in particular, while Vero and 3T3 cells appear to be undergoing cytotoxic death, BAECs appear to be undergoing apoptotic death. We believe that this result is due to a combination of factors, including the presence of

short chain oligomers of NIPAM in the commercially available preparation. This work provides valuable insights into the cytotoxicity of commercially prepared polymer substrates for this type of bioengineering work, and therefore into the applicability of use of such surfaces for human subjects.

3.1 Introduction

Poly(*N*-isopropyl acrylamide) (pNIPAM or pNIPAAM) is a thermoresponsive polymer that experiences a phase change when exposed to its lower critical solution temperature (LCST) of ~32°C.¹ Above the LCST, pNIPAM is relatively hydrophobic, and the chains of the polymer are collapsed; below the LCST, pNIPAM is relatively hydrophilic, and its chains are extended.² Although the magnitude of the change to the polymer's thickness and wettability is relatively small, it has great impact on adherent mammalian cells: while cell sheets normally require enzymatic digestion or mechanical scraping to remove them from the substrates to which they adhere, they will spontaneously “pop off” from NIPAM substrates as contiguous sheets—similar to a Post-It™ note—capable of adhering and proliferating elsewhere.³ Due to this property occurring at relevant physiological temperatures, pNIPAM has attracted a great deal of attention in cell sheet engineering,^{4–9} drug delivery,^{10–12} formation of gold nanoparticles,¹³ and the development of a thermo-responsive membrane.¹⁴

However, before pNIPAM can be extensively used for human applications, it must be demonstrated that pNIPAM is benign, especially considering that the NIPAM monomer itself is known to be toxic.¹⁵ Although hundreds of papers describe the use of pNIPAM with mammalian cells, few papers assess its cytotoxicity.^{16–19} In a recent study, we performed the first, comprehensive study of NIPAM cytotoxicity.²⁰ In that work, NIPAM monomer, and the most commonly used NIPAM-derivatized substrates were created using a variety of

techniques, including free radical polymerization, sol-gels spin coated onto glass, plasma polymerization, and atom transfer radical polymerization. Using the NIPAM substrates, endothelial cells, epithelial cells, smooth muscle cells, and fibroblasts were cultured. The effects of direct contact with monomeric and pNIPAM substrates were evaluated. Monomeric and commercially available pNIPAM (cpNIPAM) was demonstrated to be the only formulations cytotoxic toward cell types, with as little as 18% viability for MTS assay concentration gradient results.²⁰

In this work, the reason behind this anomaly was explored. The pNIPAM-coated surfaces were first evaluated for their thermoresponse and surface chemistry using contact angle measurements, cell detachment, and XPS. Having observed that different cell types experienced slightly different levels of cytotoxicity by Cooperstein, et al., we evaluated the relative biocompatibility of the substrates toward several cell types: bovine aortic endothelial cells (BAECs), monkey kidney epithelial cells (Veros), and mouse embryonic fibroblasts (3T3s). Cellular response was evaluated by observing their cell morphology, as well as through live/dead and XTT assays. Finally, the leachate (or extract) from the polymerized NIPAM surfaces was evaluated using NMR. We found that 3T3 (fibroblast) cells exposed to cpNIPAM substrates had the lowest viability, indicating that the surfaces were cytotoxic and resulted in more lytic death. However, we also found that BAECs—which appeared to have reasonable viability using live/dead assays—had unusual cell morphology indicative of apoptotic death. We hypothesize that the diminished cell viability is caused by a combination of factors, including the inclusion of short chain length oligomers/NIPAM monomer that disrupts cellular behavior. Given the interest of researchers in this field, this work provides valuable insights into the appropriateness of using as-is commercially-prepared polymer substrates without any

post or pre-processing for this type of bioengineering work, and therefore into the applicability of this type of NIPAM-derived engineered tissues for human use.

3.2 Materials and Methods

3.2.1 Materials

PNIPAM, with a molecular weight of ~40,000 grams/mol, was purchased from Polysciences, Inc. (Warrington, PA). *N*-isopropyl acrylamide (99%) was purchased from Acros Organics (Geel, Belgium). Tetraethyl orthosilicate (TEOS) and isopropanol were purchased from Sigma Aldrich (St. Louis, MO). HPLC-grade methanol, HPLC-grade dichloromethane, HPLC-grade acetone, 200 proof ethanol, and hydrochloric acid (1 Normal) were purchased from Honeywell Burdick and Jackson (Deer Park, TX).

Square glass cover slips were purchased from Fisher Scientific (Pittsburg, PA). Round glass cover slips were purchased from Ted Pella (Redding, CA). The silicon chips were obtained from Silitec (Salem, OR).

Dulbecco's modified eagle's medium (DMEM), minimum essential medium with alpha modification (α MEM), and Dulbecco's phosphate buffered saline without calcium or magnesium were purchased from HyCLone (Logan, UT). Bovine aortic endothelial cells (BAECs) were from Genlantis (San Diego, CA). Fibroblasts (MC3T3-E1, 3T3s) and Vero cells (CCL-81) were purchased from ATCC (Manassas, VA). Fetal bovine serum (FBS), fungizone and penicillin/streptomycin were from HyCLone (Logan, UT). Minimum Essential Medium Non-Essential Amino Acids solution (MEM NEAA) and 0.25% trypsin/EDTA were purchased from Gibco (Grand Island, NY). Ethidium Homodimer I was purchased from Invitrogen (Grand Island, NY). Calcein am was purchased from Biotium (Fremont, CA).

3.2.2 Surface preparation

For surface analysis, silicon chips were cut into .8 cm x 3 cm rectangles for goniometry, and 1 cm x 1 cm squares for X-ray photoelectron spectroscopy (XPS). The surfaces were cleaned using an ultrasonic cleaner from Magnasonic ultrasonic cleaner (Toronto, Canada), for 15 minutes: dichloromethane, acetone, methanol (sequentially). The chips were then rinsed with deionized water, dried with Nitrogen, placed in a Petri dish, wrapped in Parafilm, and stored in a desiccator until used for deposition or goniometry.

Glass cover slides were cleaned for 30 minutes in an acid wash (1:1 solution by volume of methanol: hydrochloric acid), rinsed with deionized water, dried with nitrogen, placed in a Petri dish, sealed with Parafilm under nitrogen, and stored in a desiccator until used for cell culture or solution deposition.

3.2.3 CpNIPAM solution preparation

Isopropanol was poured into a 15 mL centrifuge and its weight was determined. The amount of cpNIPAM to be dissolved into the isopropanol was calculated based of the weight of the isopropanol to achieve 1% of pNIPAM by weight or 2% of pNIPAM by weight.⁶⁶

3.2.4 SpNIPAM solution preparation

Solution preparation using sol-gel (spNIPAM) was performed following a method previously described.¹ 35 mg of pNIPAM, 5 mL of deionized water, and 200 uL of hydrochloric acid were mixed in a 15 mL centrifuge tube and a weight percentage of pNIPAM was determined. In a separate 15 mL centrifuge tube, 250 µL of TEOS solution (1 TEOS: 3.8 ethanol: 1.1 water: 0.0005 HCl), 43 µL of deionized water, and 600 µL of ethanol were mixed and weighed. The appropriate amount of the pNIPAM solution was added to achieve the final weight percentage of pNIPAM of .35%.³¹

3.2.5 SpNIPAM and cpNIPAM solution deposition

To spin coat surfaces with pNIPAM, 100 μL of either the spNIPAM or cpNIPAM solution was evenly distributed onto clean glass slides and Si chips placed on the spin coater, a H6-23 spin coater from Laurell Technologies (North Wales, Pennsylvania). The surfaces were spun at 2000 rpm for 60 seconds. The surfaces were placed in a Petri dish, sealed with Parafilm under nitrogen, and stored in a desiccator until used for cell culture or surface analysis.

3.2.6 Surface characterization

Goniometry

Contact angle measurements were performed with an Advanced Goniometer model 300-UPG from ramè-Hart Instrument Co. (Mountain Lakes, NJ) with an environment chamber and the DROPimage Standard program. Inverted bubble contact angles were taken in Millipore water (18M Ω). Angles were obtained at room temperature (21°C) and at body temperature (37°C) using the Temp Controller model 100 – 500 connected to the environmental chamber.

X-ray photoelectron spectroscopy (XPS)

Survey spectra of the pNIPAM surfaces were taken at NESAC/BIO at the University of Washington on a Surface Science Instruments S-probe spectrometer. This instrument has a monochromatized Al X-ray source and a low energy electron flood gun for charge neutralization. X-ray spot size for these acquisitions was 800 x 800 μm . All samples were run as insulators meaning the electron flood gun was used. Pressure in the analytical chamber during spectral acquisition was about 5×10^{-9} Torr. Pass energy for survey spectra (composition) was 150 eV. The pass energy for high-resolution C1s spectra taken at 0 degree was 50 eV. For the high-resolution C1s spectra all binding energies were referenced to the C1s C-C bonds at 285.0 eV. A detail scan was run for N and Si to improve quantification. Data

analysis was carried out using the Service Physics ESCA Analysis A program (Service Physics, Bend OR).

3.2.7 Cell Culture

For cell culture, BAECs and Vero cells were cultured according to previously established protocols³ in DMEM supplemented with 10% FBS, 1% penicillin/streptomycin, and 1% fungizone. For BAECs, 1% MEM NEAA was also added. 3T3s were cultured in α MEM supplemented with 10% FBS, 1% penicillin/streptomycin, and 1% fungizone. Cells were incubated at 37°C in a humid atmosphere with 5% CO₂. When confluent, the cells were lifted from the cell culture flasks with 0.25% trypsin/EDTA and passaged into new flasks from passage 2 up to 10.

3.2.8 Cell culture on NIPAM substrates

PNIPAM surfaces prepared via plasma polymerization, commercial polymerization and sol-gel were used for culture of mammalian cell lines according to previously established protocols in our group.^{31,32,65,66} These glass slides were placed into 6 well plates and the cells at passage 6 through 9 were seeded at 1.0×10^5 cells directly onto the substrates in regular cell culture media. The time to confluence was about 2 days. From these substrates, cell detachment was performed in cold, 4°C media without added supplements. To initiate the detachment, the regular cell culture media was replaced with cold non-supplemented media. The well plates with cells in the cold media were placed on a shaker table. The detachment was allowed to proceed for the desired amount of time (up to 3 hours) at 4°C. Images were obtained using 20X objective on a Nikon Eclipse TS200F inverted microscope with an epi-fluorescence attachment (Nikon Instruments, Melville, NY) and a SPOT Insight color mosaic digital camera (Diagnostic Instruments, Sterling Heights, MI), before cell detachment began and at 60 minute

intervals during cell detachment. The cells were counted from beginning of detachment to the end of detachment using Image J software.

3.2.9 Preparation of pNIPAM extracts for NMR

Extracts from cpNIPAM, and spNIPAM were obtained at room temperature (20°C) and body temperature (37°C) according to a previously described protocol.⁶⁶ Briefly, to make extracts, the previously mentioned pNIPAM surfaces were incubated in deuterated (surface to liquid volume ratio of 2.16 cm²/mL) for 24 hours at room temperature and body temperature. After 24 hours, the resulting extracts were transferred to centrifuge tube and used for NMR.

3.2.10 Cytotoxicity Testing of NIPAM surfaces

XTT assay

XTT cell viability assay was purchased from Biotium (Fremont, CA). The procedure for XTT assay was adapted from the procedures provided by the manufacturer.⁹⁷ A working of XTT solution was prepared by adding 50uL of activated XTT (Biotium XTT solution + activation reagent) to 100 uL of cell media. After 48 hours, and 96 hours of incubation on pNIPAM and control glass substrates, BAECs, 3T3s, and VEROs were removed from the incubator, and cell media was replaced with working XTT solutions. Cells were incubated for 6 hours then removed for absorbance measurements at 475 nm, and 660 nm (background) with a SpectraMax M5 microplate reader (Molecular Device, San Jose, CA). A blank control was included in empty wells in every plate, in which XTT working solution was added to empty well plates and incubated for 6 hours.

Viability of all cell lines were calculated utilizing this equation:

% Viable Cells

$$= \frac{\text{Sample Absorbance (475nm)} - \text{Sample background (660nm)} - \text{blank absorbance (475nm)}}{\text{Control absorbance (475nm)} - \text{Control background(660nm)} - \text{blank absorbance (475nm)}}$$

Live/Dead Assay

The procedure for live/dead assay follows those previously completed by Cooperstein, et al.⁶⁶ Briefly, a combined solution such as those sold by ThermoScientific was created by combining 1 μ L of 2mM calcein AM and 1 μ L of 2mM ethidium homodimer to every 1mL of DPBS. Cells grown on pNIPAM substrates and control glass were removed from incubation at 48 hours, and 96 hours and cell media were replaced with working live/dead solution. Cells were incubated at 37°C and 5% CO₂ with live/dead solution for 45 minutes, then rinsed with sterile DPBS prior to imaging. Fluorescent images were taken on a Nikon Eclipse TS200F inverted microscope at 10X with an epi-fluorescence attachment (Nikon Instruments, Melville, NY) and a SPOT Insight color mosaic digital camera (Diagnostic Instruments, Sterling Heights, MI).

3.2.11 Characterization of Extract Solution

Nuclear Magnetic Resonance (NMR)

NMR was used to confirm successful polymerization of the cpNIPAM, and spNIPAM. The NMR spectra of cpNIPAM, and spNIPAM were taken at the University of New Mexico (UNM) Nuclear Magnetic Resonance facility with an Advance III NMR spectrometer (Bruker, Billerica, MA). It is a 300 MHz, standard bore, nanobay instrument. Spectra were obtained on a 5 mm broadband/proton probe, at room temperature, using CDC1₃ as a solvent.

3.3 Results and Discussion

In a previous study, our group demonstrated that although the cell types, surface deposition methods, and ultimate utility of cellular/NIPAM constructs differs between laboratories, the vast majority of those preparations are biocompatible, and therefore suitable for use in bioengineering. An anomalous result was that commercially-prepared NIPAM (cpNIPAM)

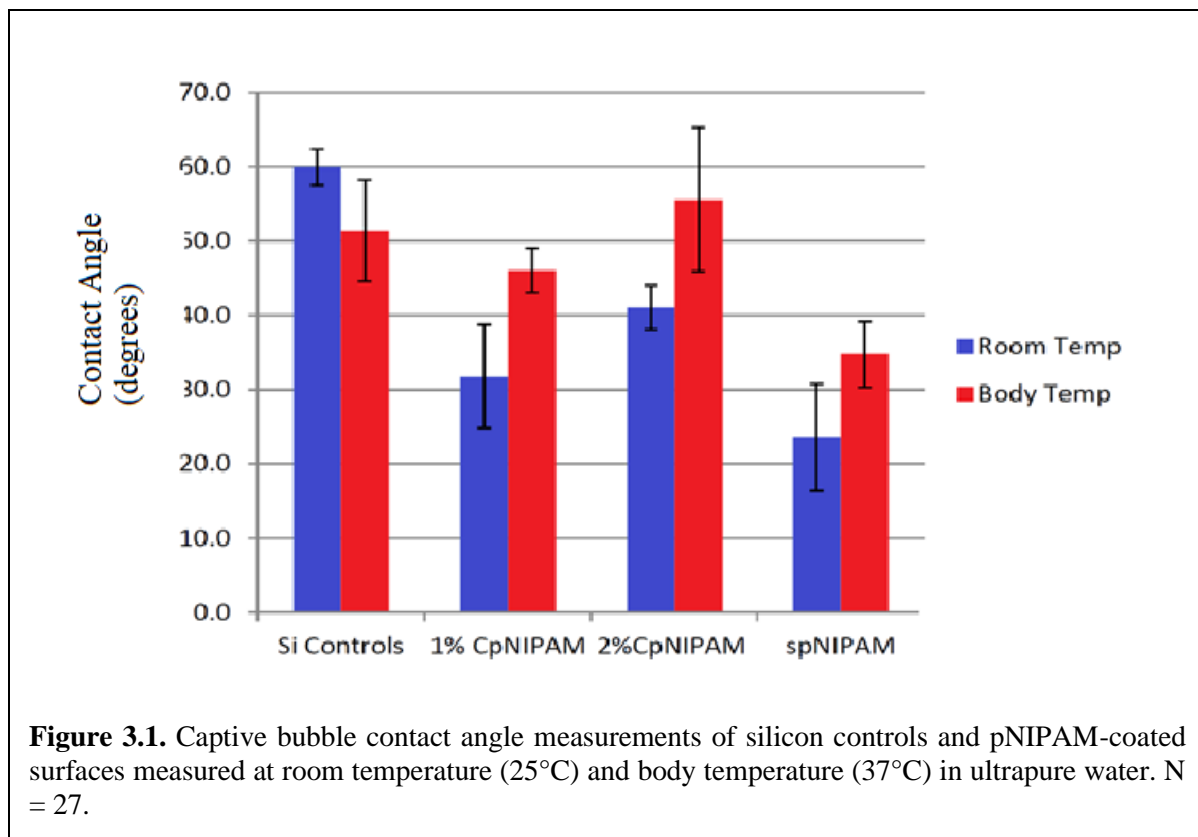
used as-is from its manufacturer was relatively more cytotoxic than all other polymerized forms in our lab (~20%).¹⁶ In addition, we found that endothelial cells (BAECs) had increased sensitivity to commercially-prepared NIPAM after 48 hours. These results were consistent with other research in our laboratory indicating that cellular sensitivity varies with cell type, as endothelial cells were more sensitive to polymers than epithelial cells.⁹⁸

In this work, we further explored these anomalous results. The stimulus-response, chemistry, and biocompatibility of commercially available NIPAM at two concentrations (1% and 2%) were evaluated alongside silicon controls, as well as spin-coated sol-gel NIPAM (spNIPAM). Using contact angle goniometry, cpNIPAM-coated surfaces were first evaluated to demonstrate their thermoresponse. The surface chemistry (and presence or absence of any potentially harmful contaminants) was assessed using XPS. The relative biocompatibility of the substrates toward several cell types was then assessed using endothelial cells (bovine aortic endothelial cells, BAECs), epithelial cells (monkey kidney epithelial cells, Veros), and fibroblasts (mouse embryonic fibroblasts, 3T3s). Cellular response was evaluated via live/dead and XTT assays, as well as observations of cellular morphology. Finally, the leachate (or extract) from the polymerized NIPAM surfaces was evaluated using NMR.

3.3.1 Polymer Thermoresponse

Contact angle measurements were obtained for each of the substrates prepared to determine their thermoresponse. The contact angle of a captive air bubble was measured for each substrate in ultrapure water at either room temperature (~25°C) or body temperature (37°C). Three samples were analyzed on three spots per sample. Three replicates were performed for each type of pNIPAM coated substrates, resulting in n= 27.

Figure 3.1 shows the results of these measurements. Each of the pNIPAM-coated substrates tested yield higher contact angles at body temperature than at room temperature. On average there is a 13° change between contact angles at body temperature and room temperature (46.6° vs. 31.5° for 1% cpNIPAM, 55° vs. 41.6° for 2% cpNIPAM, and 34.6° vs. 23.7° for spNIPAM).



Although the contact angles differ depending on the surface characterization technique, previous studies have shown that the *specific* values at each temperature are not critical to determine the thermoresponse of the substrate—it is the *relative* change in wettability that is crucial to their thermoresponse.⁶ The relative change in contact angles across the LCST indicates the desired result: each of the prepared pNIPAM surfaces are thermoresponsive.

Although the standard deviations are greater (up to 12°) than other preparation methods (e.g., plasma polymerized NIPAM, ±2),⁶⁶ this analysis confirms that the films are stimulus-responsive, and of sufficient quality for later cell response assays. The silicon (negative)

controls showed minimal variation between body temperature and room temperature, which is also consistent with expected results.

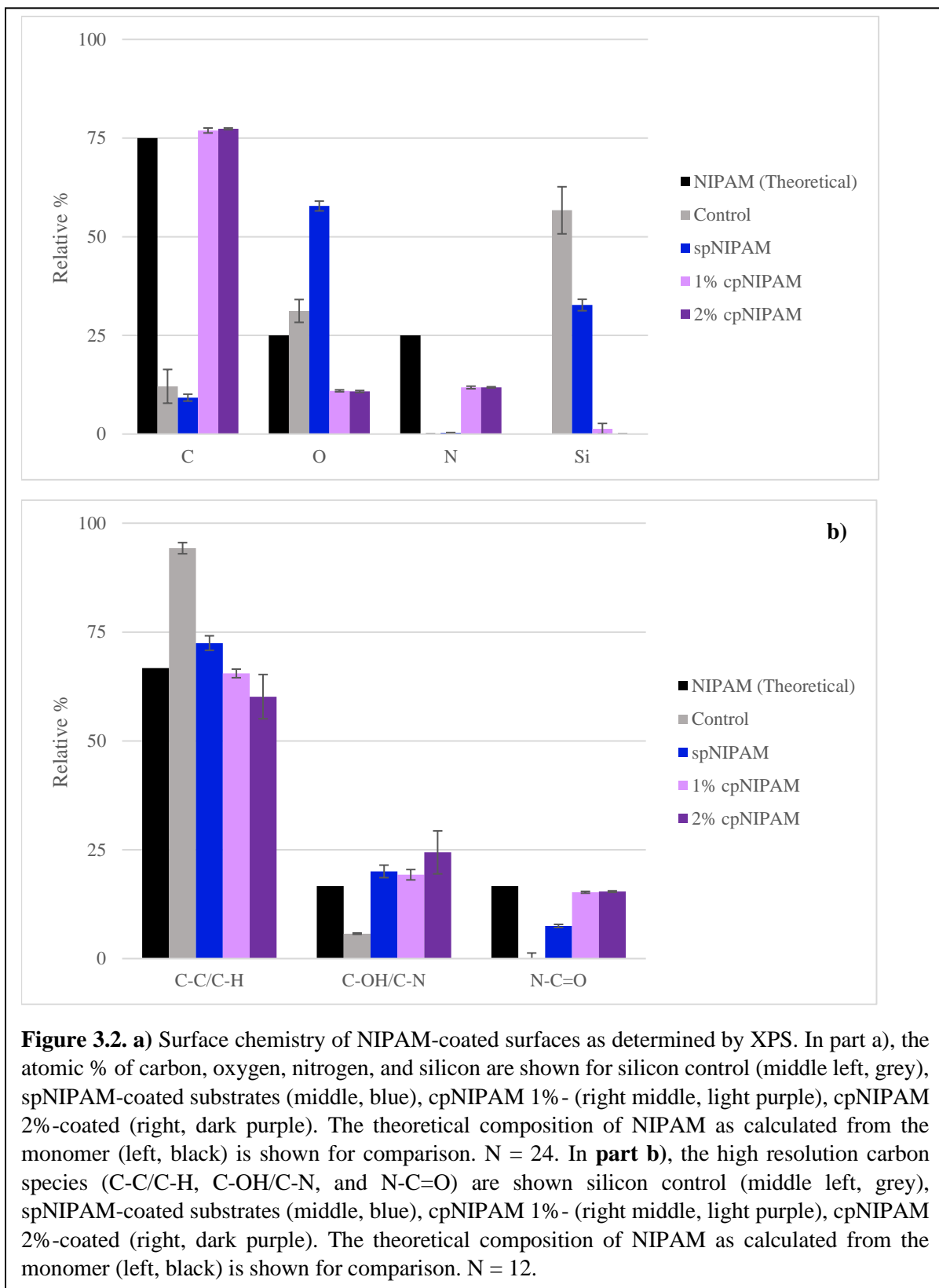
3.3.2 Surface Chemistry

The surface chemistry of these pNIPAM coated substrates was assessed by XPS. **Figure 3.2a and 3.2b** show the results of survey and high resolution C1s spectra for all four types of pNIPAM coated surfaces, as well as the composition of NIPAM as predicted from the stoichiometry of the monomer.

In **Figure 3.2a**, it is shown that spNIPAM contains far less C (and far more Si), which is expected, as the TEOS solution used to create the sol-gel contains organosilanes. In comparison, the presence of silicon in cpNIPAM films is detected at low concentrations/ not detected, indicating that the films are sufficiently thin (i.e., <~50-100 nm thick). The cpNIPAM surfaces have an elemental composition (76.9% C, 11.8% N, 11.0% O, and 1.4% Si; and 77.3% C, 11.9% N, and 10.8% O, respectively for 1% and 2% cpNIPAM) that is consistent with the predicted composition of the monomer (~75% C, 12.5% O, and 12.5% N). No other elements were detected on the cpNIPAM substrates, ruling out the presence of any potentially cytotoxic contaminants (such as catalysts used to polymerize cpNIPAM).

The spNIPAM composition differs significantly from the theoretical composition (8.8% C, 0% N, 36.6% O, and 54.6% Si). As previously stated, the increased concentration of silicon and oxygen are consistent with the presence of TEOS to create the sol-gel (indicating that the NIPAM and TEOS components have phase separated) but could also arise from the underlying silicon surface (glass, indicating patchy coverage of the film). The trace amounts of nitrogen indicates a very small amount of NIPAM. Previous studies done by Bluestein, et al. have

shown that storage conditions such as time after deposition, temperature and humidity all



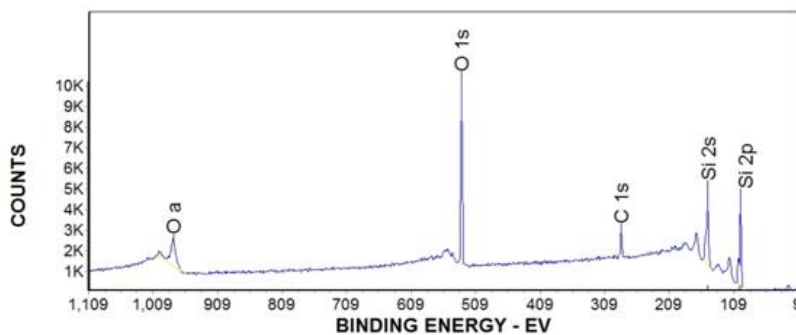
significantly affect spNIPAM film stability.³²

Specifically, over time, regardless of storage conditions, spNIPAM surfaces begin to lose thermoresponsive characteristics and delaminate as spNIPAM is physisorbed and not chemisorbed onto surfaces.³² Furthermore, storage temperatures **a)** y affects this delamination effect, spNIPAM stored at 25°C in low humidity experiences the smallest amount of delamination while spNIPAM stored at 37°C in low humidity experiences the largest amount of delamination. As our samples are sent from the University of New Mexico to the University of Washington, and often awaits one week prior to XPS, it is likely that our XPS results of spNIPAM are associated with delamination. It is important to note that other than XPS, all other experiments utilizing spNIPAM is completed immediately after fabrication.

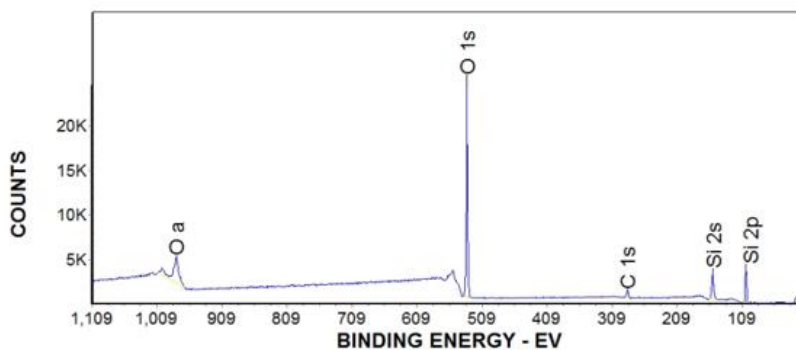
Figure 3.2b shows the high resolution C1s spectra for spNIPAM, 1%cpNIPAM, and 2%cpNIPAM, as well as the silicon control and the theoretical composition of the monomer. The high resolution analysis shows that the spNIPAM films have a thin amount of NIPAM as the expected carbon species is present at appropriate concentrations (72.5% C-C/C-H, 20.0% C-OH/C-N, and 7.5% % N-C=O), consistent with those found with spNIPAM.^{31,32,66,99} CpNIPAM films have the expected carbon species at appropriate concentrations (65.5% C-C/C-H, 19.3% C-OH/C-N, and 15.2% N-C=O), consistent with the predicted composition of the monomer (~66.7%C, 16.7% O, and 16.7%N).

Together, these data indicate that the cpNIPAM-coated surfaces consist of NIPAM that is of sufficient quality to achieve cellular adhesion and popoff, and no contaminants are present that would affect its biocompatibility. Representative survey spectra and high resolution C1s spectra of silicon controls, spNIPAM, 1% cpNIPAM and 2% cpNIPAM can be found in **Figures 3.3 and 3.4.**

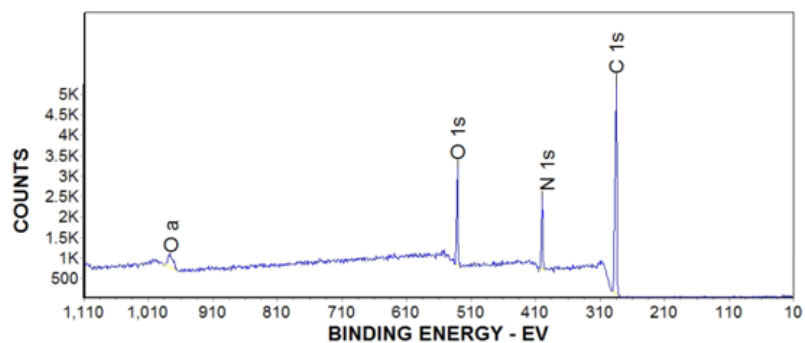
Silicon control



spNIPAM



1% cpNIPAM



2% cpNIPAM

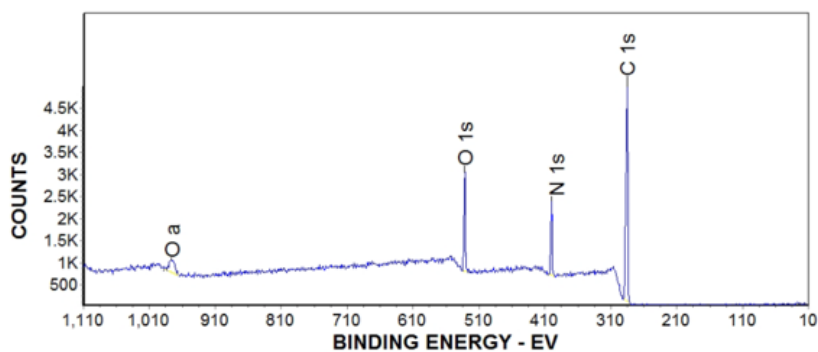
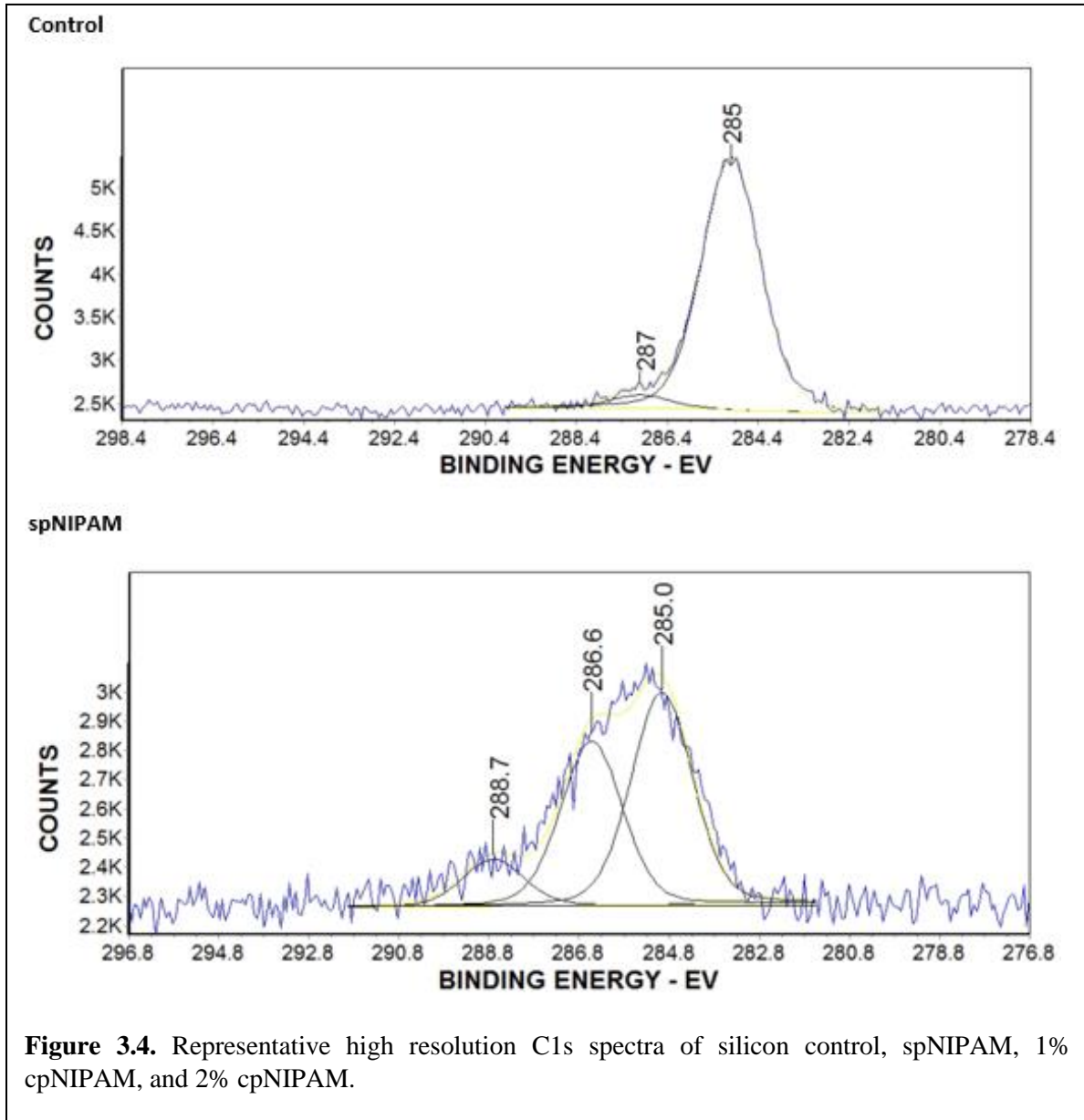


Figure 3.3. Representative XPS spectra of silicon controls, spNIPAM, 1% cpNIPAM, and 2% cpNIPAM.



SpNIPAM coated surfaces warranted further testing, as such, spNIPAM, 1% cpNIPAM and 2% cpNIPAM and glass controls all underwent cell detachment experiments (results found in **Figure 3.5**) utilizing BAECs. After incubation for 48 hours, pNIPAM-derivatized substrates and glass control substrates underwent detachment studies at 4°C, utilizing serum-free media. Cells were observed and imaged every 60 minutes over 3 hours, then analyzed with Image J cell counter. Control glass substrates had difficulties detaching cells as expected (detachment

occurred -3%, -0.4%, and 5.6% at 60 minutes, 120 minutes, and 180 minutes respectively). spNIPAM detached 30.5% of cells, 32.3% of cells and 34.7% of cells at 60 minutes, 120 minutes, and 180 minutes respectively. 1% cpNIPAM detached 12.2% of cells, 13.4% of cells and 14.7% of cells at 60 minutes, 120 minutes, and 180 minutes respectively. 2% cpNIPAM detached 9.4% of cells, 14.3% of cells and 19.1% of cells at 60 minutes, 120 minutes, and 180 minutes respectively.

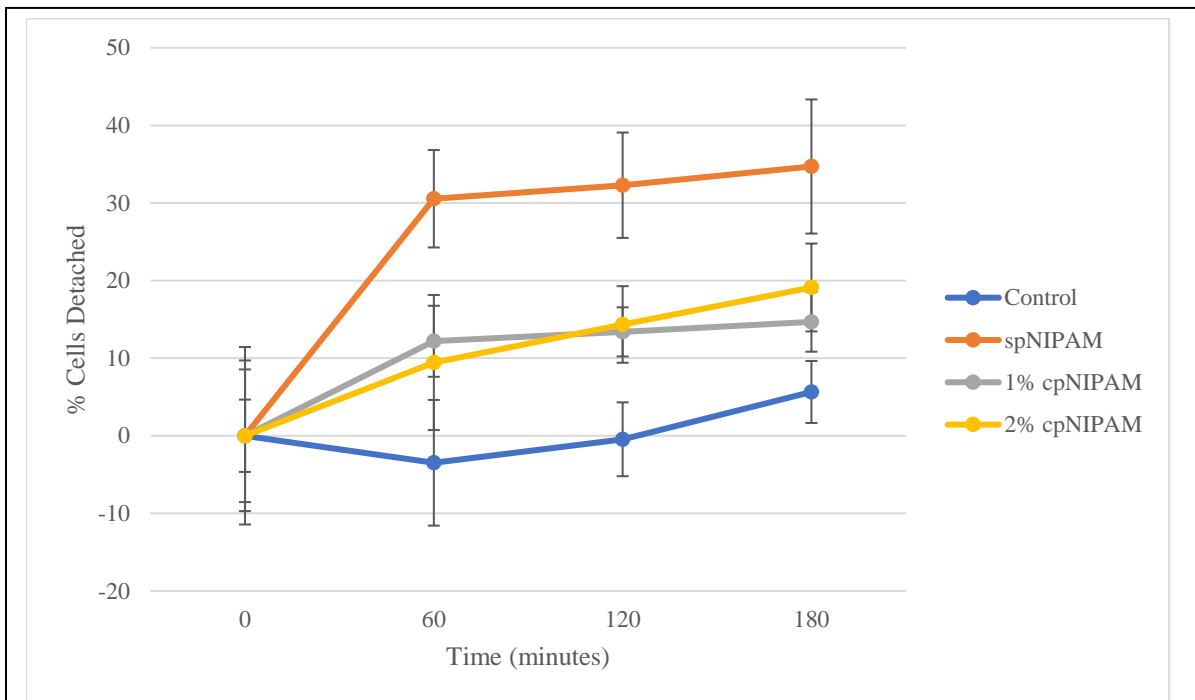
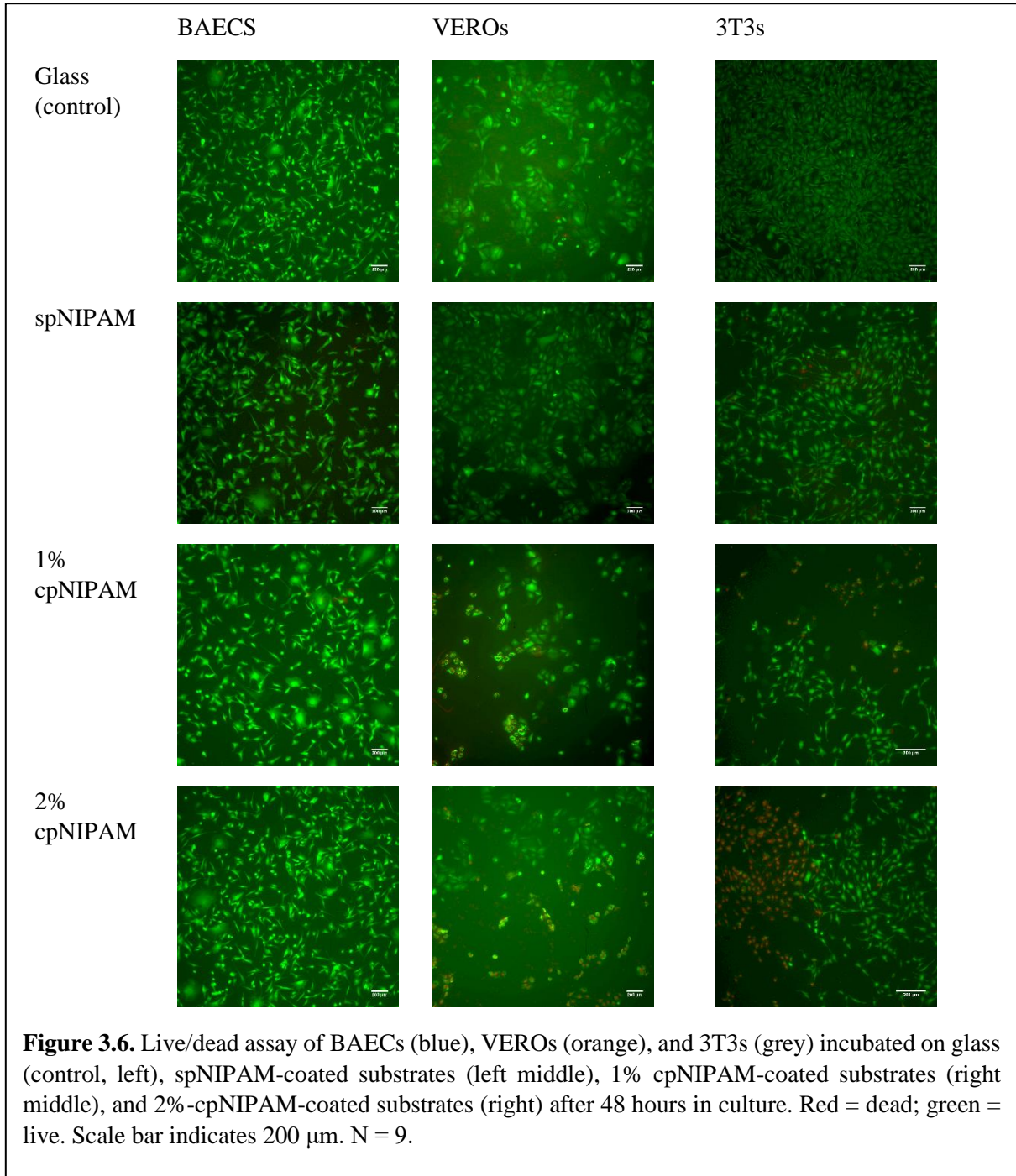


Figure 3.5. BAECs detachment from pNIPAM surfaces. After 48 hours in culture, BAECs are exposed to serum free media at 4°C and observed over 180 minutes. Control (blue) are cells grown on clean glass.

Although many articles have been published using pNIPAM substrates to achieve cell detachment, rarely do the authors publish the yields they achieved using their method. We previously showed that spNIPAM yields detachment of ~35%, and cells would detach in islands instead of a sheet.³¹ In this work, we find that the detachment of cells from spNIPAM and cpNIPAM are consistent with previous results found in our group, which is far greater than

those achieved by controls such as glass (5%). As such, we conclude that all surfaces contain a thin layer of NIPAM, enough for cell adherence and detachment and that there are no contaminants in our NIPAM films that could lead to cytotoxicity effects.

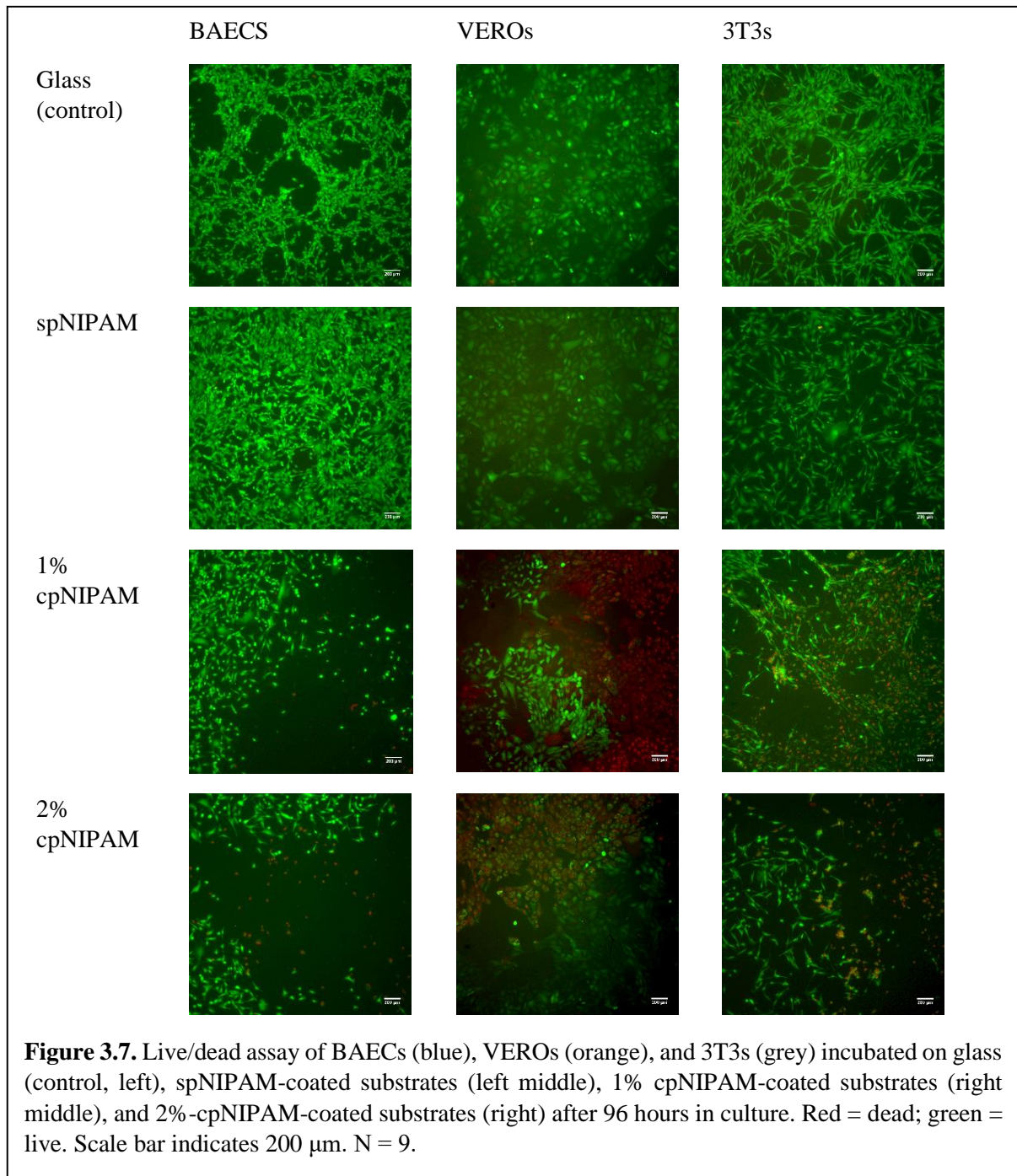


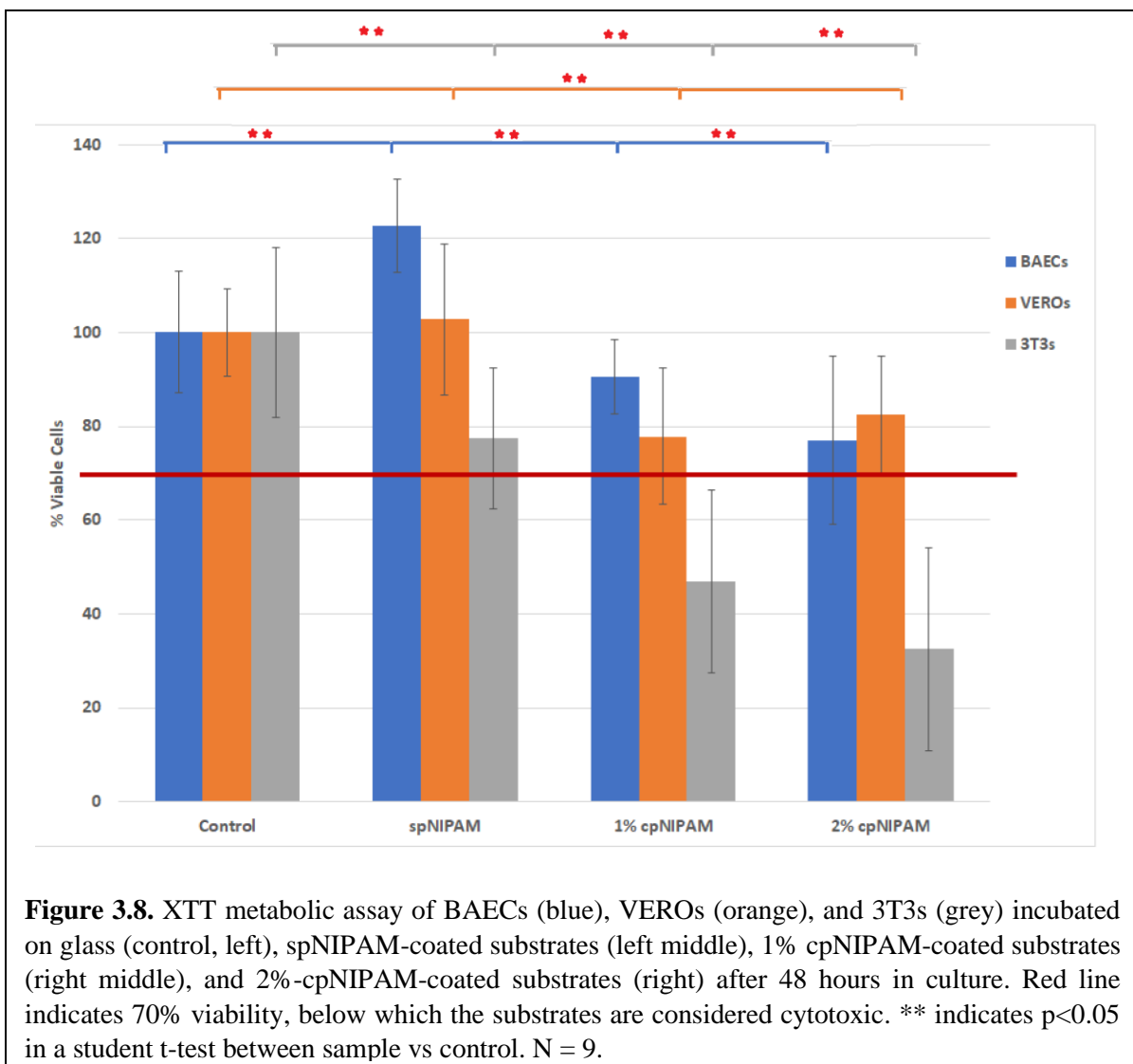
3.3.3 Cytotoxicity Testing

In order to determine the relative biocompatibility of the substrates, live/dead and XTT assays were performed on endothelial cells (BAECs), epithelial cells (Vero cells), and fibroblasts (3T3s) that were cultured on NIPAM substrates for either 48 hours or 96 hours. (See **Figures 3.6 and 3.7**). Live/dead assays are considered a semi-quantitative assay that stain the cell membrane of live cells green, whereas non-viable cells are dyed red due to the breakdown of their membrane.

Figures 3.6 and 3.7 shows representative images of those cells cultured in normal media on glass (control, top row), on spNIPAM (top middle), 1% cpNIPAM (bottom middle), and 2% cpNIPAM (bottom). At 48 hours (**Figure 3.6**), BAEC cells grown on each substrate appear to be viable and identical to those grown on the glass coverslip controls. In comparison, the Vero cells and 3T3s grown on cpNIPAM appear to have some cell death (indicated by red). By 96 hours (**Figure 3.7**), approximately half of the Vero cells grown on cpNIPAM (1 and 2%) are dead. There is also evidence of cell death in the 3T3s grown on these substrates. In contrast, there is relatively little evidence of cell death from BAECs grown on sp- and cpNIPAM

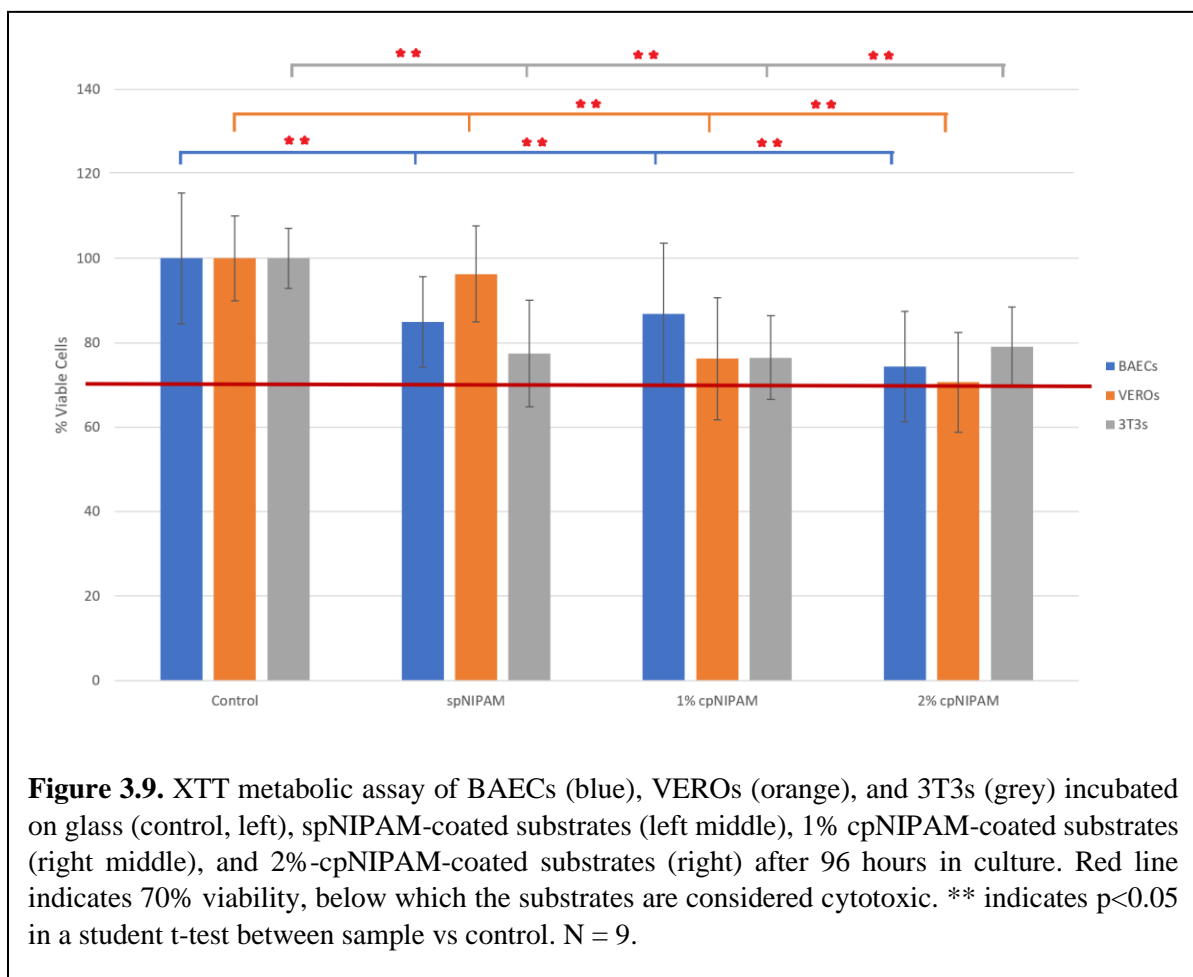
substrates; however, where there is cell death (as evidenced by red spots), there is a large zone of inhibition toward growth.





XTT assays are quantitative metabolic assays that determine the percentage of cells that are viable as determined by their ability to reduce tetrazolium salt and produce formazan derivatives. **Figures 3.8 and 3.9** shows the results of XTT assays of all cell types toward the spNIPAM and cpNIPAM films. The red line on **Figures 3.8 and 3.9** is set to 70% viability, which is the level below which surfaces are considered to be cytotoxic toward cells. At 48 hours (**Figure 3.8**), all three cell types grown on spNIPAM-coated surfaces have >70% viability, indicating that spNIPAM would be considered nontoxic. At the same time point, 3T3 cells grown on cpNIPAM-coated surfaces have 47% and 32% viability (for 1% and 2%

cpNIPAM, respectively), indicating that this substrate is cytotoxic toward 3T3 cells. Interestingly, by 96 hours (**Figure 3.9**), it would appear that all of the NIPAM substrates, as well as the glass control, are biocompatible towards all three cell types (as evidenced by viability >70%). However, this could be an artifact of the XTT assay, which is unable to accurately assess cell viability of highly confluent cells, and even some dead cells are capable of reduction.¹⁰⁰



3.3.4 Cell Morphology

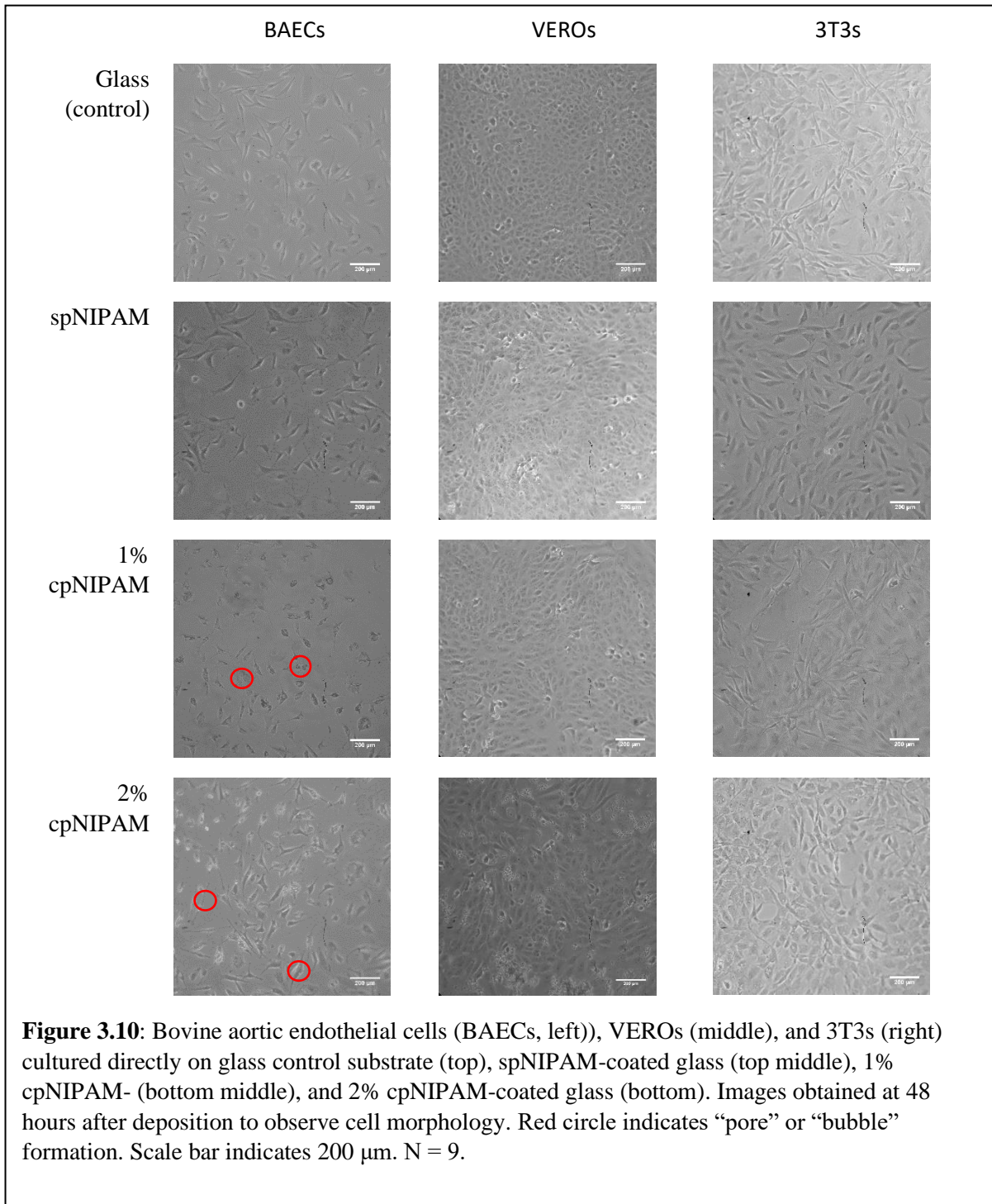
In parallel with the cytotoxicity assays, the morphology of the BAEC, Vero, and 3T3 cells grown on the sp- and cpNIPAM substrates were assessed using brightfield microscopy after 48 hours (**Figure 3.10**) and 96 hours (**Figure 3.11**). The observations of cell morphology

results, when considered alongside the differences in cytotoxicity, are particularly striking: from the live/dead and XTT assays, it would appear that cpNIPAM is most cytotoxic to 3T3 cells, and that BAECs and Vero cells are relatively unaffected. However, close inspection of the morphology of the cells tells a different story.

The cells grown on control samples (glass coverslips) are shown in the top row for both figures. It can be observed that the Vero cells grow to confluence the most rapidly (center column) on each substrate. Also of interest is that the morphology of the Vero and 3T3 cells grown on spNIPAM and cpNIPAM surfaces are consistent with that of controls (especially at the shorter time frame).

By 96 hours, however, distinct abnormalities appear in the cells grown on cpNIPAM substrates (1% and more so on 2%). Close inspection of the BAEC cells shows that distinct “bubbles” or “holes” have formed within the cell bodies (**See Figure 3.10 and 3.11**). In an unrelated set of experiments exploring cellular death after exposure to oligomers, our group showed that cells entering apoptotic death—rather than lytic death—will first form these “bubbles.” (We hypothesize that they are neither bubbles nor holes, but are vacuoles containing cellular material).⁹⁸ Furthermore, other groups have demonstrated similar results from HeLa cells that are undergoing lysis by lysosomes, which appear remarkably similar to those found in our live/dead images of Vero cells and 3T3s.¹⁰¹ Apoptosis may explain why the XTT and live/dead

assays underestimate the cytotoxicity, as those techniques are better suited toward detecting death by cell lysis.



Furthermore, although the results from XTT at 96 hours indicate high cell viability (in **Figure 3.9**), it is clear from observation of the live/dead images in **Figure 3.7** and the morphology images at the same time point in **Figure 3.11** that there are large areas on cpNIPAM substrates

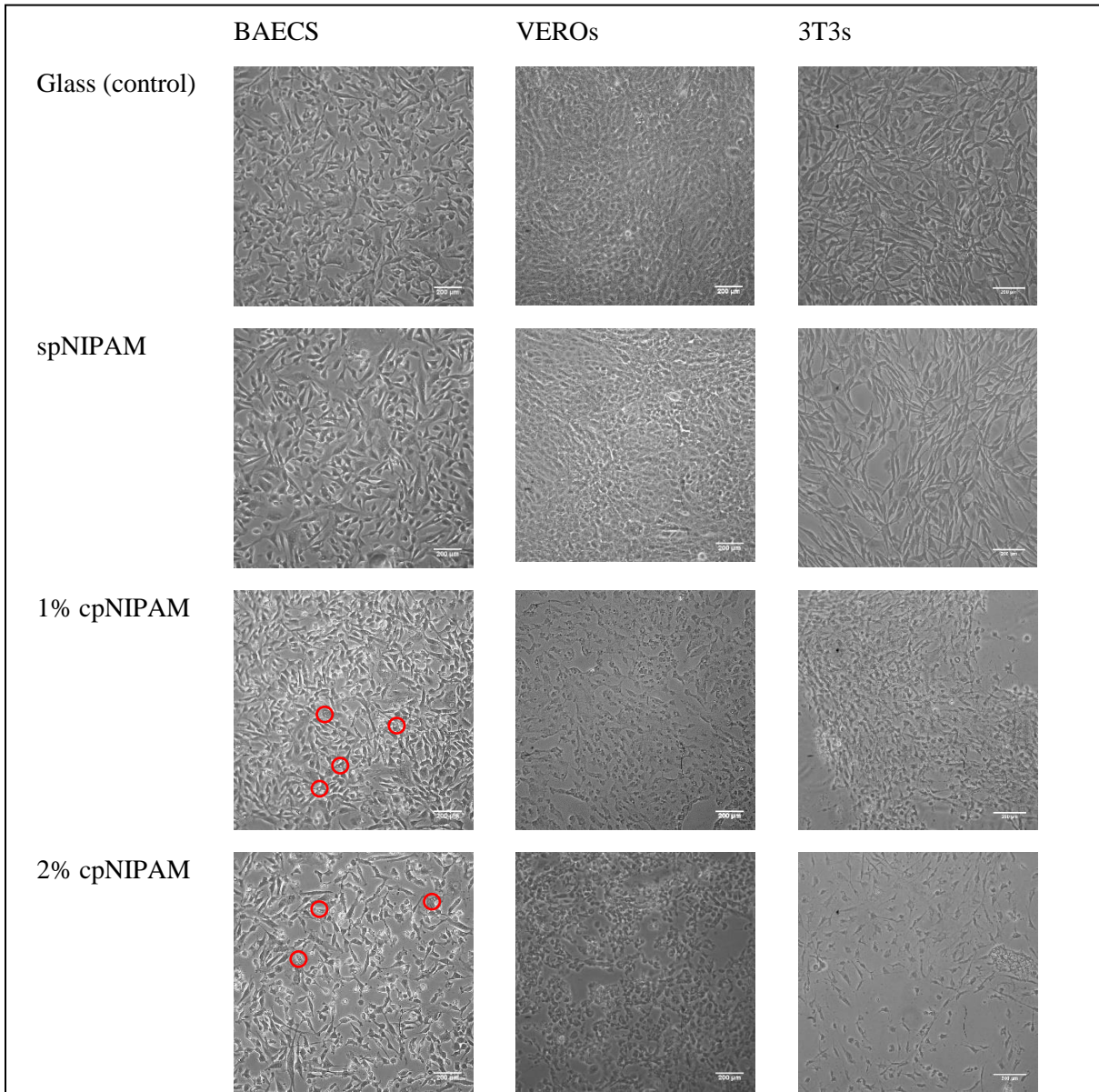


Figure 3.11. Bovine aortic endothelial cells (BAECs, left), VEROs (middle), and 3T3s (right) cultured directly on glass control substrate (top), spNIPAM-coated glass (top middle), 1% cpNIPAM- (bottom middle), and 2% cpNIPAM-coated glass (bottom). Images obtained at 96 hours after deposition to observe cell morphology. Red circle indicates “pore” or “bubble” formation. Scale bar indicates 200 μm . N = 9.

that either have dead cells (such as Vero cells on 1% cpNIPAM) or have no confluence (BAECs on 1% and 2% cpNIPAM).

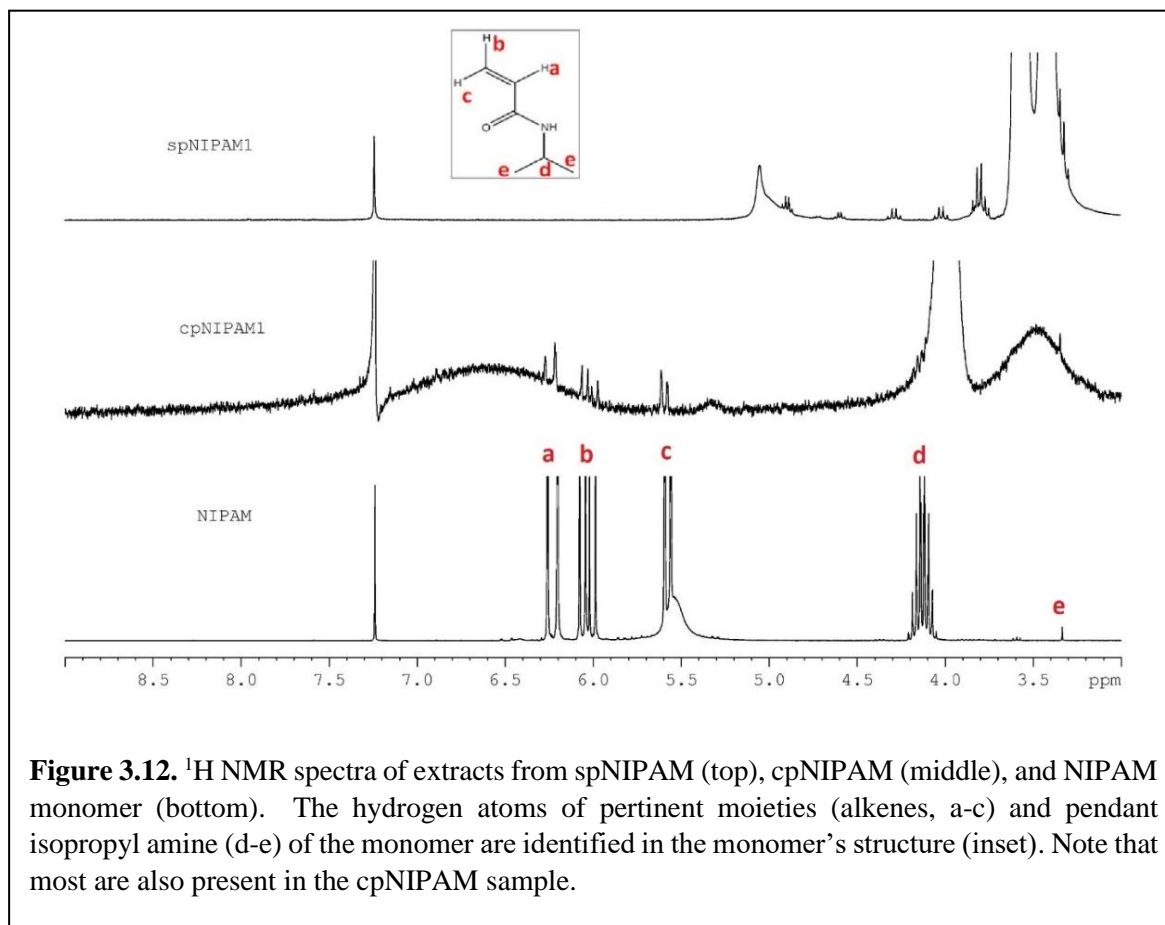
Conversely, the 3T3 cells grown on cpNIPAM substrates do not appear to have a “bubbled” appearance, although their morphology is also quite abnormal. For example, many of the 3T3s in **Figures 3.10 and 3.11** on 1% and 2% cpNIPAM substrates are no longer stellate in appearance, but are rounded and without projections. As the 3T3 cells are the ones found to be least viable by XTT assay at 48 hours, this may indicate that the 3T3 cells are dying via lysis (rather than apoptosis).

From the collected morphology and viability assays, we conclude that exposure to cpNIPAM affects cell viability for all cell types at shorter time periods (48 hours). While some cell types obviously show diminished viability (i.e., 3T3 cells), other cell types undergo changes that will ultimately result in death, potentially by apoptosis. Furthermore, although XTT analysis indicates that cell viability recovers at longer time frames, such results should be viewed with some skepticism, as the appearance of the cells appears compromised (potentially entering apoptosis).

3.3.5 Nuclear Magnetic Resonance to Determine Extent of Polymerization

Given that the cpNIPAM-coated substrates appeared to lack any kind of contaminant that would explain the cell death and abnormal morphology results explained above, extracts from the films themselves were analyzed to determine if there was anything leaching from the films that explained diminished cell viability. NMR was used to determine the structure of cpNIPAM and spNIPAM, including the determination of whether any (potentially toxic) NIPAM monomer was present in the films.

Figure 3.12 shows three NMR spectra: the spNIPAM polymer (top), 1% cpNIPAM extract (middle), and the NIPAM monomer (bottom). The structure of the NIPAM monomer is inset, with the pertinent moieties labeled (alkenes and isopropyl amines). The peaks labeled a, b, and c in the region from 5.5 to 6.5 ppm indicates the location where the hydrogen adjacent to double-bonded carbons appears in the NIPAM monomer. These peaks are unique to the NIPAM monomer.⁶⁶



All three peaks are clearly visible in the NIPAM monomer spectrum, but are missing from the NMR spectrum of spNIPAM; the disappearance of these peaks indicates successful polymerization of the polymer. In contrast, the NMR spectrum of cpNIPAM contains the 3 peaks unique to the NIPAM monomer. Although these 3 peaks are not of the same intensity in cpNIPAM's spectrum as they are in the spectrum for the NIPAM monomer, they are present.

These results indicate that polymerization of cpNIPAM was incomplete, and some unreacted monomer still exists in the leachate. Given the known cytotoxicity of the NIPAM monomer, this may explain to the increased cytotoxicity of cpNIPAM. These results are consistent with previous results that have demonstrated that short oligomers and monomers of otherwise benign polymers can be quite cytotoxic, as their shorter chains allow the polymer to penetrate into the cell membrane, and disrupt cellular processes.

3.4 Conclusions

Ever since it was demonstrated that intact cell sheets could be harvested from pNIPAM substrates in the mid-1990's, there has been interest in the polymer's use for applications such as tissue engineering, biological sensors, and drug delivery systems. One of the factors limiting the development of tissues and devices engineered for use with the human body has been the question of whether polymerized NIPAM had the same cytotoxic effects as the monomer itself. The limited number and haphazard comparison studies that had previously been performed using pNIPAM formulations were not sufficient to answer the question of whether pNIPAM was sufficiently benign for human use. Recently, our group published the first, comprehensive study of NIPAM polymerized using a variety of different techniques, exposed to multiple cell types, and assayed with a variety of tests intended to determine biocompatibility (or cytotoxicity). In that study, we identified one anomalous result: commercially available NIPAM (cpNIPAM) appeared to be cytotoxic.

In this work, we performed a study to determine the source behind the cytotoxicity of cpNIPAM in comparison to other commonly-used techniques. Having confirmed that all pNIPAM-derivatized surfaces had the correct thermoresponse (by contact angle goniometry and cell release statistics), and the correct surface chemistry (by elemental analysis via XPS),

the pNIPAM substrates were used for cell culture up to 96 hours. Using live/dead assays, we demonstrated that the cpNIPAM is statistically more cytotoxic than the other polymerized forms studied. Furthermore, we found that although 3T3 cells appear to be the most sensitive to cpNIPAM toxicity as per live/dead and XTT assays, each of the cell types are actually compromised by the substrate, and experience decreased viability. Finally, the absence of contaminants in the pNIPAM leachates (and the presence of unreacted monomer in the commercially available powder used to coat the surfaces with cpNIPAM) indicates that the source of the cpNIPAM toxicity is the presence of short, mobile chains of NIPAM monomer interfering with cellular function.

These results suggest that the anomalous result previously observed regarding the cytotoxicity of cpNIPAM is due to the presence of unreacted monomer. Therefore, for researchers using NIPAM-derivatized substrates, we recommended that they synthesize their own substrates using the methods (e.g. plasma polymerization, sol-gel polymerization, electrospun pNIPAM) proven to be non-toxic here and in our previous studies. Further studies should evaluate whether additional post-processing of surfaces (e.g., washing commercial coatings) would improve cell viabilities. Additionally, these results suggest that cell viability assays such as XTT or live/dead should always be accompanied by careful observation of the cellular morphology itself, as the assays may underestimate the cytotoxicity of the substrates if apoptotic death has been triggered.

Chapter 4: *Ex vivo* Human Chondrocyte Toxicity Following Exposure to Tranexamic Acid

Manuscript in preparation for publication in *Journal of Arthroplasty* by Nguyen, P.A.H.; Garbrecht, E.; Elghazali, N.; Canavan, H.E.; Salas, C.; and Decker, M.

Abstract

Tranexamic acid (TXA) is an agent used to reduce blood loss by inhibiting the breakdown of fibrin clots. Originally, TXA was approved for use in humans in extreme situations such as prevention of bleeding in hemophiliacs, as well as to treat extremely heavy menstrual bleeding. Over time, however, TXA has been adapted for use in other settings including orthopedic procedures to prevent excess blood loss in arthroplasties, spine, and trauma surgeries. Within total and revision hip and knee arthroplasty literature, it is well established that TXA has reduced operative blood loss and post-operative transfusion requirements. However, topical or intra-articular TXA in the setting of a partial arthroplasty would expose native cartilage to TXA. The impact of topical TXA on human chondrocyte viability has not been well established. In this study, we investigate the effect of a range of commonly utilized concentrations of topical or intra-articular TXA on human chondrocytes *ex vivo*. We evaluated chondrocyte viability qualitatively and quantitatively using live/dead assay and cell counts. Chondrocytes from osteochondral plugs were exposed to TXA for 48 hours, with viability evaluated from 0 days after treatment to 6 days following treatment. We found that up to 2 days following TXA exposure, the osteochondral plugs were viable (no cytotoxicity was found). However, 4 days after treatment, all concentrations of TXA (even the lowest dose of 20g/L led to extensive cell death in osteochondral plugs. As a result, TXA should be considered cytotoxic at all of the levels tested in this study (20⁺g/L). Extreme caution should be used prior

to using TXA at these doses in orthopedic procedures until further studies can be performed to determine the safest dose.

4.1 Introduction

Tranexamic acid (TXA) was originally approved for use in humans for extreme situations such as prevention of bleeding in hemophiliacs, as well as to treat extremely heavy menstrual bleeding.¹⁰² TXA acts to reduce blood loss by inhibiting the breakdown of fibrin clots. Specifically, TXA reversibly binds plasminogen, therefore inhibiting fibrinolysis, and stabilizing fibrin clots. Since its approval as a synthetic agent, TXA has found additional uses during surgeries, and in instances of spontaneous or trauma induced hemorrhage.¹⁰³

The use of TXA in orthopedic procedures has been shown to prevent excessive blood loss in surgical subspecialties including arthroplasty, spine and trauma surgeries.^{104–106} Within primary total knee and hip arthroplasty literature, it is well established that TXA has reduced operative blood loss and post-operative transfusion requirements.^{107–115} Similar advantages have been seen in revision hip and knee arthroplasty surgeries.^{116–118} Although studies showed similar results regarding decreased intra-operative blood loss and decreased post-operative transfusion, dosing and delivery methods vary widely. Currently there is no consensus regarding the dose or delivery method of TXA in total joint arthroplasty. In patients with average risk for venous thromboembolism (VTE), increase in the rate of VTE has not been observed with the administration of TXA.¹¹⁹ Patients with history of VTE, stroke, and cardiac stents have been considered high risk for VTE and systemic or intravenous TXA has been avoided. In these high-risk patients, some have advocated for the use of topical or intra-articular TXA as a safe alternative.¹²⁰

With the clear benefits of TXA demonstrated in primary total joint replacement procedures, its use in partial joint replacement would seem beneficial. However, topical or intra-articular TXA in the setting of a partial arthroplasty would expose native cartilage to TXA. The impact of topical TXA on human chondrocyte viability has not been well established. In this study, we investigate the effect of a range of commonly utilized concentrations of topical or intra-articular TXA on human chondrocytes *ex vivo*. We hypothesized that TXA would be chondrotoxic and demonstrate both a concentration and time-dependent effect on chondrotoxicity.

4.2 Materials and Methods

4.2.1 Materials

Test specimens were obtained through the New Mexico Donor Services for this study.¹²¹ Dulbecco's Modification of Eagle's Medium/F-12 (DMEM/F12) 1:1 media was purchased from Sigma-Aldrich (St. Louis, MO). Fetal Bovine Serum (FBS), fungizone, and penicillin/streptomycin (P/S) were purchased from HyCLone (Logan, UT). Dulbecco's Phosphate Buffer Saline (DPBS) was purchased from VWR Life Sciences (Sanburn, NY). Calcein AM and ethidium homodimer was obtained from a viability assay kit from Biotium (Fremont, CA). Pharmaceutical grade tranexamic acid was obtained from Sigma Aldrich (St. Louis, Missouri).

4.2.2 Osteochondral plug harvest and storage

Human osteochondral plugs were harvested from decedent procured through the local Donor Services. The decedent was a middle-aged male, with plugs harvested within 48 hours after passing using the osteoarticular allograft transfer system (OATS) (Arthrex, Naples, FL). Osteochondral plugs were sterilely obtained from the knee joint (to include distal femur and

proximal tibia). Osteochondral plugs were visually confirmed to have intact healthy-appearing articular cartilage. Any plugs that were obtained from areas devoid of intact articular cartilage were discarded. We obtained 24 osteochondral plugs which were sterilely collected and transferred into FBS solution and then taken to the lab for PBS wash and rescue period.

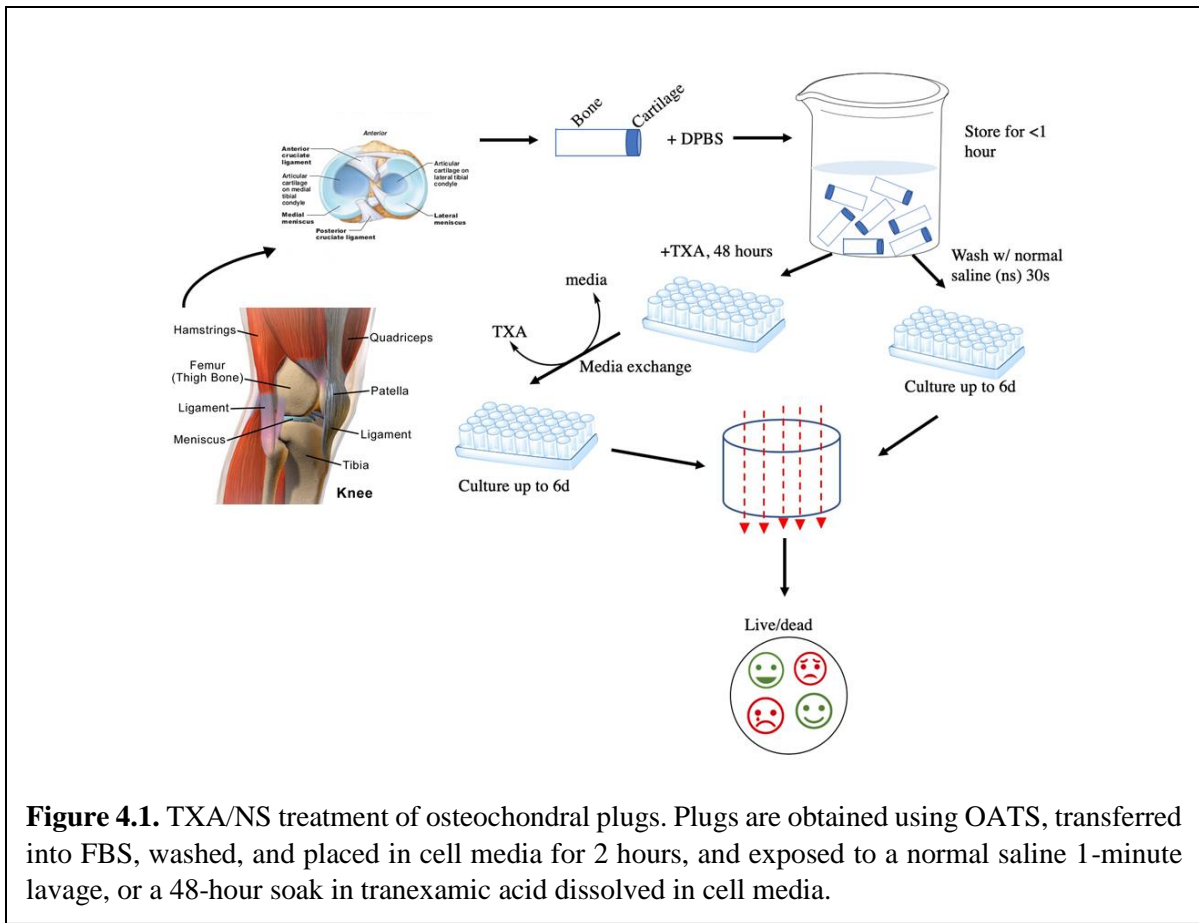
Osteochondral plugs were washed with DPBS before being stored in standard 50/50 Dulbecco's Modified Eagle's Medium/F12 nutrient mixture with 10% fetal bovine serum (FBS), 1% penicillin/streptomycin (P/S), and 1% fungizone at 37° C for 2 hours prior to treatment.

4.2.3 TXA biocompatibility test

Osteochondral plugs were exposed to 0.9% normal saline (NS) or exposure to tranexamic acid at 20g/L, 30g/L, and 40g/L (500 mg, 750mg, and 1000mg diluted in 25mL cell media). Osteochondral plugs were exposed either to: 1) treatment utilizing a 1-minute lavage with NS, or 2) a 48-hour soak of TXA (see **Figure 4.1**). The choice between option 1 vs. 2 was dependent on the thickness of the cartilage; plugs had signs of early arthritis (i.e., thinner cartilage) were used for TXA exposure, as these were the instances where TXA were most likely used in surgery.^{106,114} Day 0 was defined as the time point after completion of exposure.

4.2.4 Live/dead assay

The procedure for performing a live/dead assay followed those previously completed by Cooperstein, et al.⁶⁶ To create the live/dead assay, a combined solution such as those sold by ThermoScientific was mixed by combining by adding 1µL of calcein AM (1mM stock



solution), and 1 μL of ethidium homodimer-1 (2mM) to 1 mL of DPBS. Osteochondral plugs were maintained in cell media and removed for viability tests at specified times after exposure completion: day 0 (immediately after exposure), day 2 (2 days after exposure), day 4 (4 days after exposure), and day 6 (6 days after exposure). Plugs were then rinsed, dissected, and cell media was replaced with working live/dead solution. Cells were incubated at 37° C and 5% CO₂ with live/dead solution for 60 minutes and then rinsed with sterile DPBS prior to imaging. Fluorescent images were taken on a Nikon Eclipse TS200F inverted microscope at 10X with an epifluorescence attachment (Nikon Instruments, Melville, NY) and a SPOT Insight color mosaic digital camera (Diagnostic Instruments, Sterling Heights, MI). Acquired images were then enhanced using Fiji (Image J Software). Images of dead cells (red) were enhanced to increase its' brightness and contrast. This allows dead cells to show in merged images where

otherwise the green stained live cells would be brighter. As a result, several merged images contain red hues.

After imaging, cells were analyzed and counted using Fiji (Image J Software), following a previously established protocol.¹²² Briefly, all images were converted from color to an 8-bit grayscale image. Then, the “Find Maxima” function was used, and “noise tolerance” was set to 15. The formulas used for quantification were:

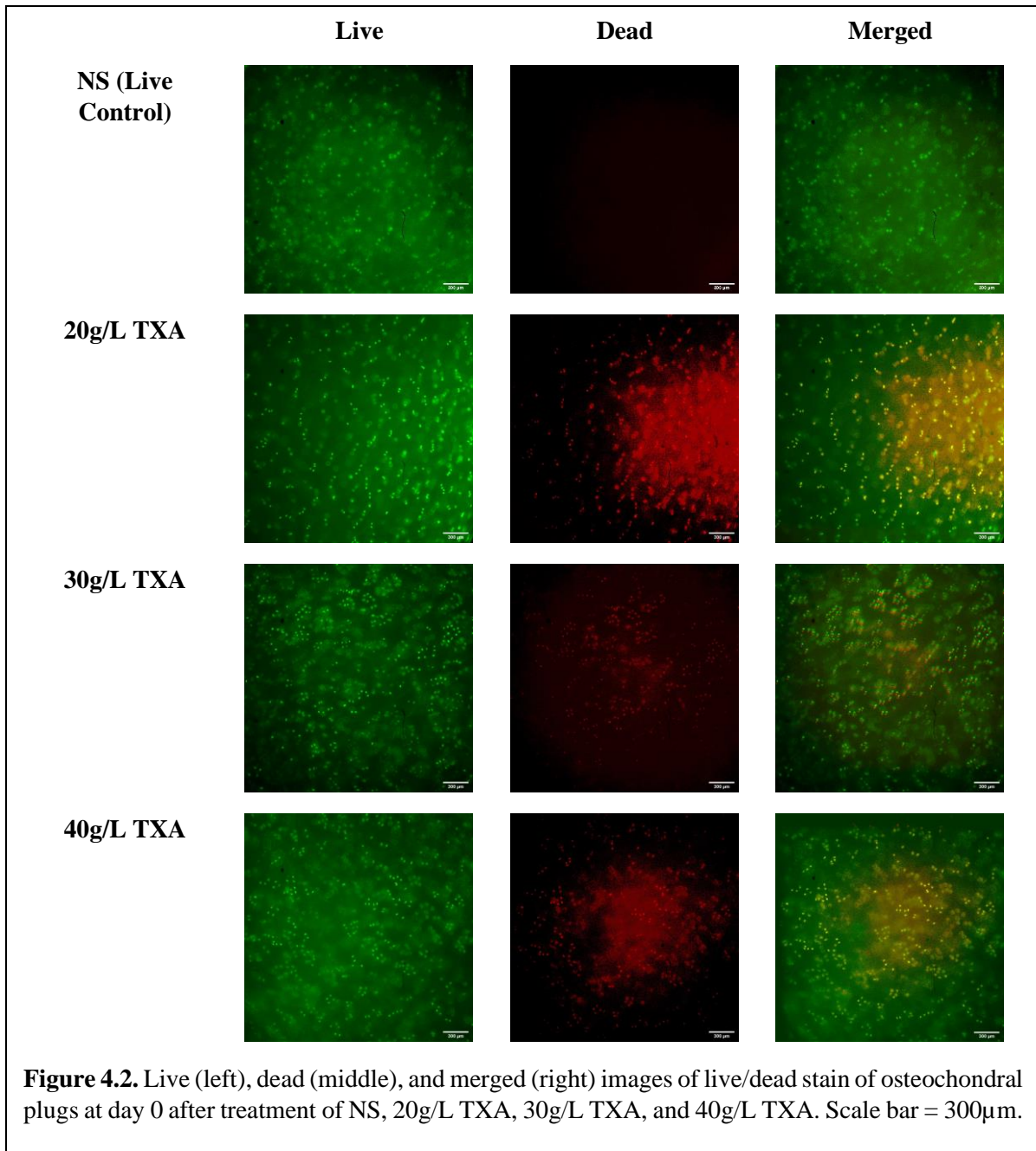
$$1. \text{Total cells} = \# \text{ of Live cells} + \# \text{ of Dead Cells}$$

$$2. \% \text{ Live cells} = \frac{\# \text{ of Live cells}}{\text{Total Cell Number}} * 100$$

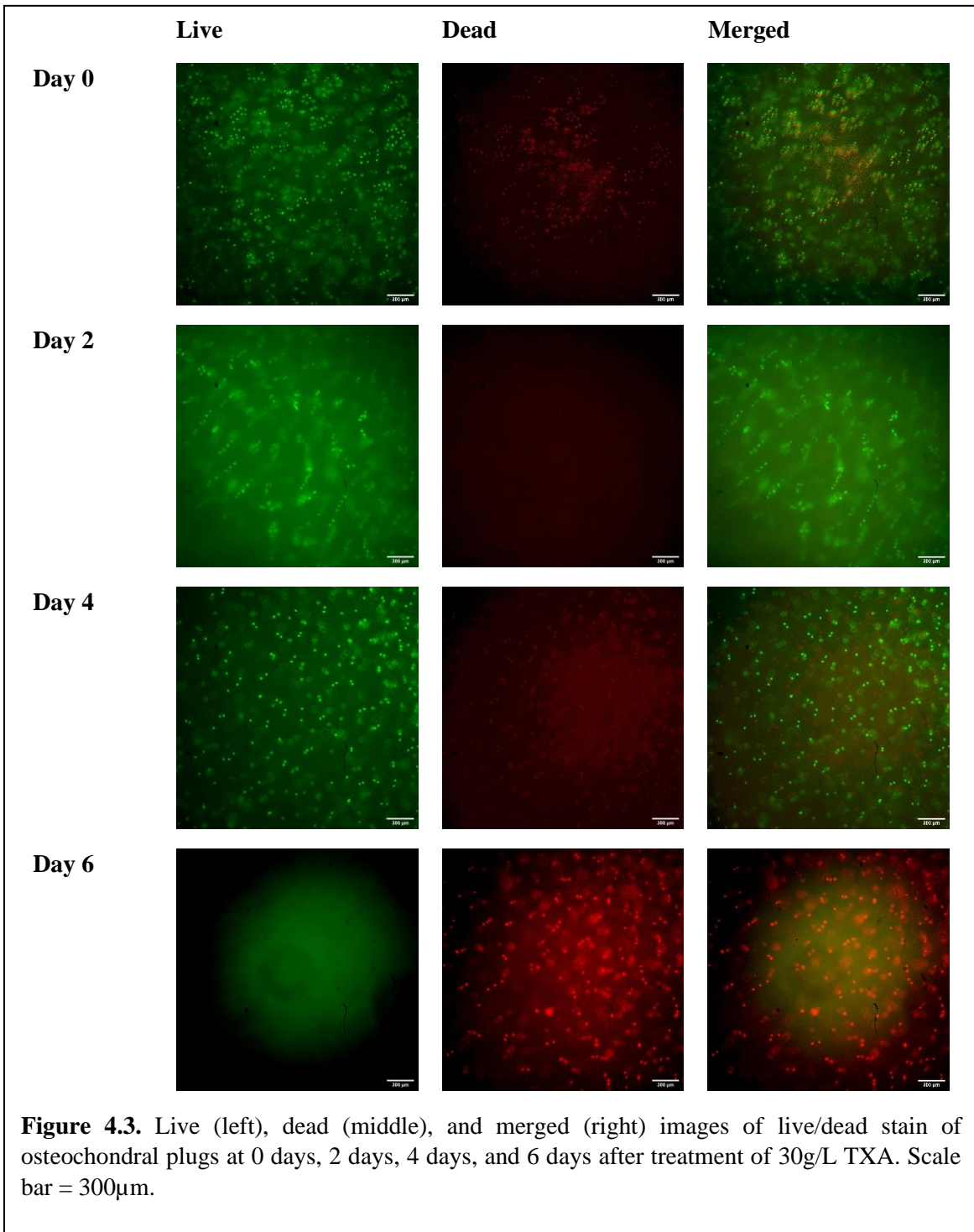
Following live/dead counts and evaluation of % live cells, ANOVA was completed at each day across all treatments. If ANOVA was found to be significant, a post-hoc test of Tukey’s HSD was used to evaluate which treatments were significantly different. Furthermore, an ANOVA was completed within each treatment comparing the differences over time, with a post-hoc test of Tukey’s HSD to evaluate which days, in comparison to day 0, were statistically different.

4.3 Results and Discussion

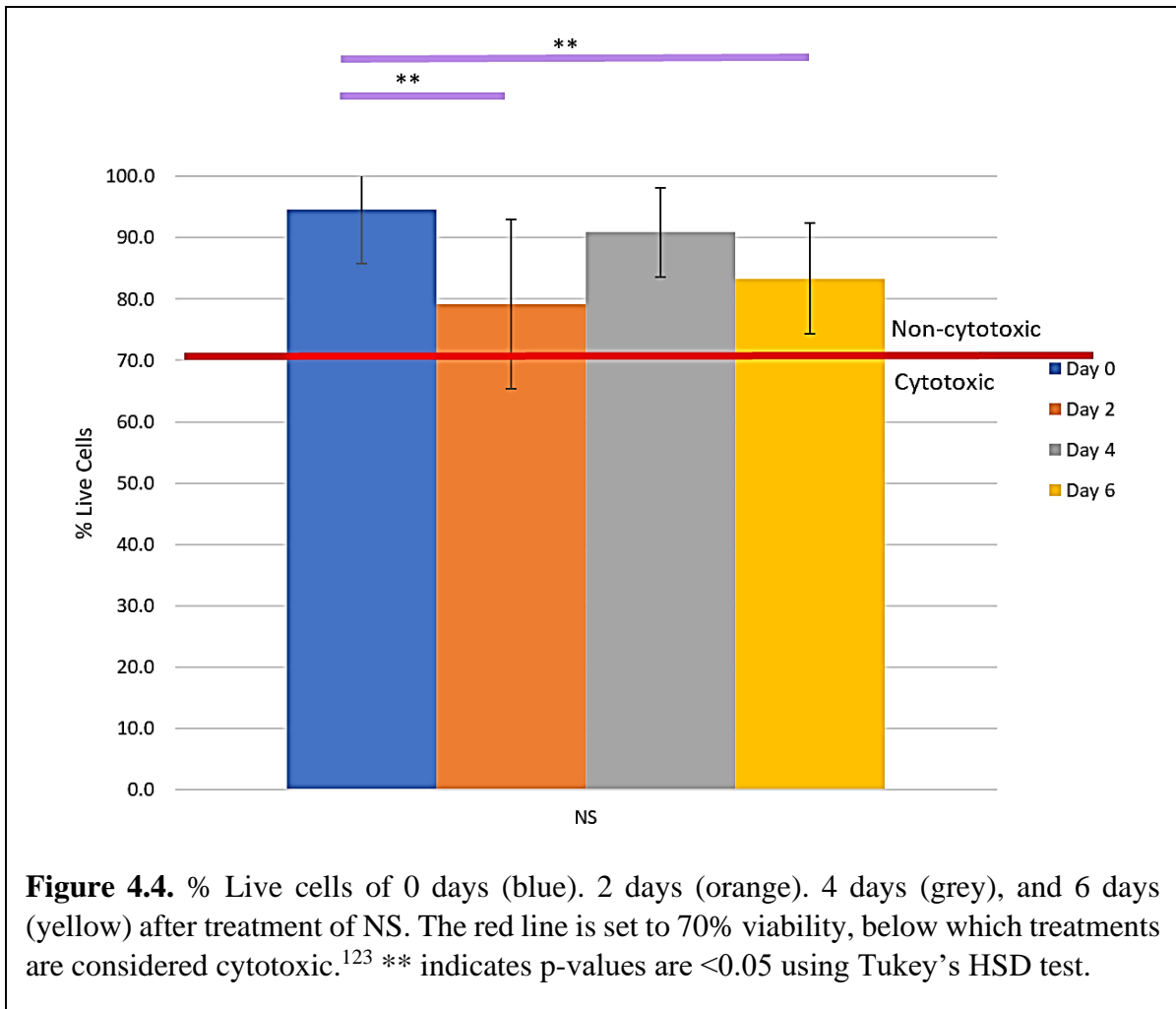
Live/dead viability assays were performed on days 0, 2, 4, and 6 following osteochondral plug harvest and treatment of NS, and TXA. **Figure 4.2** shows representative images of live (left, green), dead (middle, red), and merged images (right) of osteochondral plugs at day 0. In **Figure 4.2**, chondrocytes exposed to NS appear to remain viable, with little cell death. In comparison, chondrocytes exposed to all concentrations of TXA demonstrate some level of cell death, although viability remains high at day 0.



Representative images of live/dead images of osteochondral plugs exposed to 30g/L of TXA over time can be seen in **Figure 4.3**. At day 0 and day 2, little cell death can be seen. However, beginning day 4, a large number of cells were dead. By day 6, the majority of cells were dead. The indiscriminate green staining is likely a result of calcein AM's interaction with cytosolic esterases' within the cells that can leak out as cells die.⁸³



A quantitative evaluation of the live/dead data was completed for all experimental conditions over days 0, 2, 4, and 6 using Fiji's capability to count cells. **Figure 4.4 and 4.5** shows the results of our live/dead counts over all time periods of NS and TXA treatments respectively. The red line on **Figure 4.4 and 4.5** is set to 70% viability, which is the level below which



treatments are considered to be cytotoxic toward cells by ISO-10993.¹²³ **Figure 4.4** shows that chondrocytes are viable *ex vivo* following NS wash treatment even at 6 days after exposure (cell viability >70% for all time points, 94.6% ± 8.9% (day 0), 79.2% ± 13.8% (day 2), 90.9% ± 7.3% (day 4), and 83.3% ± 9.0% (day 6)). **Figure 4.5** shows that TXA is borderline toxic at day 0 for all TXA concentrations (cell viabilities of 70.2% ± 5.6% at 20g/L, 79.0% ± 13.6% at 30g/L, and 78.6% ± 11.6% at 40g/L). 2 days after exposure, chondrocyte viability continues to be borderline toxic at 69.2% ± 15.0% at 20g/L TXA, 67.4% ± 14.1% at 30g/L TXA, and 67.5% ± 17.3% at 40g/L of TXA. However, beginning at 4 days after exposure to treatment, viability decreases to 14.9% ± 12.1% at 20g/L TXA, 21.4% ± 16.3% at 30g/L TXA, and 24.8%

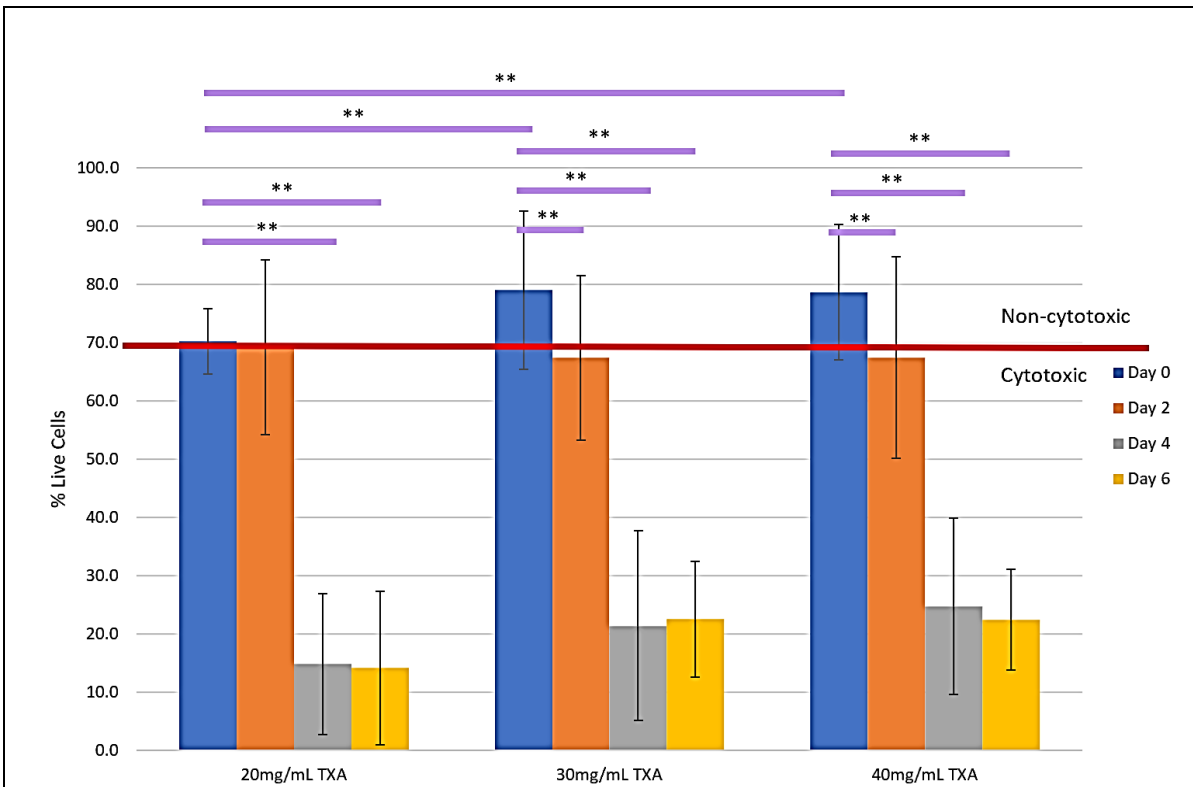


Figure 4.5. % Live cells of 0 days (blue). 2 days (orange). 4 days (grey), and 6 days (yellow) after treatment of 20 g/L TXA, 30g/L TXA, and 40g/L TXA to osteochondral plugs. The red line is set to 70% viability, below which treatments are considered cytotoxic.¹²³ ** indicates p-values are <0.05 using Tukey’s HSD test.

± 15.2% at 40g/L of TXA. This trend continues 6 days after exposure, with viabilities of 14.2% ± 13.2% at 20g/L TXA, 22.5% ± 9.9% at 30g/L TXA, and 22.4% ± 8.6% at 40g/L of TXA.

Based on ANOVA comparing the average % of live cells over time within each treatment group, all treatment groups were statistically significant. As a result, a Tukey’s HSD post-hoc test was used to compare average % live cells between time points to determine which time points are statistically different.

ANOVA of day 0, comparing the different treatments were statistically significant with a p-value of 1.87×10^{-8} , indicates that some of our treatments were significantly different from each other. Further analysis using Tukey's HSD test (as seen in **Table 4.1**) shows that in comparison to normal saline, all treatment conditions of TXA were statistically significant.

| <i>group 1</i> | <i>group 2</i> | <i>mean</i> | <i>q-stat</i> | <i>lower</i> | <i>upper</i> | <i>p-value</i> |
|----------------|----------------|-------------|---------------|--------------|--------------|----------------|
| Normal Saline | TXA 20 g/L | 24.36 | 9.98 | 15.27 | 33.46 | 6.78E-09** |
| Normal Saline | TXA 30 g/L | 15.58 | 6.38 | 6.48 | 24.67 | 1.52E-04** |
| Normal Saline | TXA 40 g/L | 15.96 | 6.53 | 6.86 | 25.05 | 1.02E-04** |
| TXA 20 g/L | TXA 30 g/L | 8.79 | 3.60 | -0.31 | 17.88 | 0.06 |
| TXA 20 g/L | TXA 40 g/L | 8.41 | 3.44 | -0.69 | 17.50 | 0.08 |
| TXA 30 g/L | TXA 40 g/L | 0.38 | 0.16 | -8.71 | 9.48 | 0.99 |

Table 4.1. Tukey's HSD test comparing treatment conditions at day 0. Standard error = 2.44. ** indicates p-values are <0.05 using a Tukey's HSD test.

Continued analysis on day 2 using ANOVA comparing the different treatments showed a statistically insignificant p-value of 0.07. No post-hoc test was followed as this indicates that although there are some differences between NS and the treatment groups on day 2, they were not statistically significant. The following days, day 4 and day 6, after treatment ANOVA showed p-values of 3.39×10^{-28} , and 2.71×10^{-32} , respectively. The post-hoc tests of days 4 and

| <i>group 1</i> | <i>group 2</i> | <i>mean</i> | <i>q-stat</i> | <i>lower</i> | <i>upper</i> | <i>p-value</i> |
|----------------|----------------|-------------|---------------|--------------|--------------|----------------|
| Normal Saline | TXA 20 g/L | 76.07 | 24.50 | 64.50 | 87.64 | 2.55E-14** |
| Normal Saline | TXA 30 g/L | 69.55 | 22.40 | 57.98 | 81.11 | 2.55E-14** |
| Normal Saline | TXA 40 g/L | 66.17 | 21.31 | 54.60 | 77.73 | 2.55E-14** |
| TXA 20 g/L | TXA 30 g/L | 6.52 | 2.10 | -5.05 | 18.08 | 0.45 |
| TXA 20 g/L | TXA 40 g/L | 9.90 | 3.19 | -1.66 | 21.47 | 0.12 |
| TXA 30 g/L | TXA 40 g/L | 3.38 | 1.09 | -8.18 | 14.95 | 0.87 |

Table 4.2. Tukey's HSD test comparing treatment conditions at day 4. Standard error = 3.10. ** indicates p-values are <0.05 using a Tukey's HSD test.

6 can be seen in **Tables 4.2 and 4.3**. At both time points, our results indicate the TXA treated samples are significantly different from our negative control of normal saline.

| <i>group 1</i> | <i>group 2</i> | <i>mean</i> | <i>q-stat</i> | <i>lower</i> | <i>upper</i> | <i>p-value</i> |
|----------------|----------------|-------------|---------------|--------------|--------------|----------------|
| Normal Saline | TXA 20 g/L | 69.95 | 28.95 | 60.95 | 78.95 | 2.55E-14** |
| Normal Saline | TXA 30 g/L | 61.60 | 25.49 | 52.60 | 70.59 | 2.55E-14** |
| Normal Saline | TXA 40 g/L | 61.66 | 25.52 | 52.66 | 70.66 | 2.55E-14** |
| TXA 20 g/L | TXA 30 g/L | 8.35 | 3.46 | -0.65 | 17.35 | 0.078274 |
| TXA 20 g/L | TXA 40 g/L | 8.29 | 3.43 | -0.71 | 17.29 | 0.081869 |
| TXA 30 g/L | TXA 40 g/L | 0.07 | 0.03 | -8.93 | 9.07 | 0.999997 |

Table 4.3. Tukey’s HSD test comparing treatment conditions at day 6. Standard error = 2.42. ** indicates p-values are <0.05 using a Tukey’s HSD test.

Qualitative results during dissection showed degradation of osteochondral plugs over time with exposure to TXA. By day 4 and day 6 after treatment, osteochondral plugs were increasingly difficult to dissect following the same protocols as established by previous experiments. Furthermore, initial exposure to TXA rapidly dropped the cell media’s pH, as indicated by a color change in the cell media from red to yellow (due to the presence of phenol red in the cell media). Although osteochondral plugs were rinsed between every cell media change for plugs exposed to tranexamic acid due to pH changes, cell media was changed every 24 hours due to a change in cell media color (red=>yellow) every 24 hours throughout the experiment. This acidity is likely the cause of the decline in cell viability found in osteochondral plugs exposed to tranexamic acid. These observations were not found in samples exposed to NS treatment.

The principle finding of our study is that human chondrocytes exposed to common concentrations of topical TXA demonstrated marked cell death when compared to controls. Other authors have investigated chondrocyte viability after exposure to TXA. Tuttle et al.,

investigated murine and bovine chondrocyte viability after exposure to TXA. Their work showed bovine and murine chondrocyte viability after exposure to TXA at 25g/L for 48 hours similar to that of controls.¹²⁴ The viability of the murine and bovine chondrocytes was tested immediately after completion of 48 hour exposure.

We hypothesized that there could be delayed cell death after TXA exposure, so our cells were followed up to 6 days after completion of 48-hour exposure. We observed significant decline in human chondrocyte viability at 4 days and 6 days, suggesting delayed cell death after exposure to TXA. Parker et al. investigated human chondrocyte viability after exposure to TXA and found that exposure of TXA concentrations of 10-20g/L for 3 hours on a 3D human chondrocyte laden gelatin-methacryloyl hydrogel model did not show any significant differences in cell viability compared to controls.¹²⁵ The basis for 3-hour exposure was established in a study evaluating the diffusion of TXA from the knee joint by Ahlbery, et al.¹²⁶ The pharmacokinetics of TXA were found to be similar to that of serum in their study. The TXA was administered and concentration was measured prior to any surgical insult of the knee joint, therefore the TXA was likely acting in its solute, or unbound, form. We believe that once TXA binds to plasminogen in the joint it behaves differently from its unbound state. Literature shows that protein, or protein bound solutes, diffuse from a joint at a much slower rate. Wallis et al. demonstrated that the effusion times of radiolabel protein (albumin) had an average elimination half-life of ~32 hours in non-rheumatoid patients.¹²⁷ After surgical insult, it would be presumed that plasminogen would be present for binding of TXA and retard its diffusion from the joint. This was also shown in a clinical study by Sa-ngasoongsong, et al.¹²⁸ After total knee arthroplasty, dilute concentrations of TXA were placed in the joint along with a drain which was clamped. The drains were unclamped at varying time points post-operatively

and concentrations of TXA measured. The concentrations were variable throughout patients, but similar concentrations were seen at 0 hours to 12 hours. If the half-life within the joint was 3 hours, one would expect that concentration at 12 hours would very low. However, this was not observed in their study. Given these findings, we believe protein bound TXA, which would be expected in the setting of postoperative hemarthrosis, has a half-life in the joint around 36-48 hours. We exposed human chondrocytes to TXA for 48 hours, which demonstrated a delayed but significant chondrotoxicity at all concentration of TXA.

Topical TXA concentrations also varied widely in studies assessing the impact of TXA. Protocols in total knee arthroplasty for intra-articular or topical administration of TXA use a wide variety of doses (250 mg to 3 g), but actual intra-articular concentrations are variable and inconsistent and appear to fall between 15-100g/L.¹²³ Picetti et al., has found that 10-15 g/L of TXA result in substantial inhibition of fibrinolysis, but effectiveness regarding operative blood loss or post-operative transfusion was not evaluated in the review study.¹²⁹ We feel obtaining such a specific concentration in an operative setting within the joint would be very difficult, given the differences of joint volume in the setting of postoperative hemarthrosis among patients. In a metanalysis, Panteli et al. found that a dose of more than 2 grams of TXA trended toward decreased post-operative transfusion rates.¹⁰⁹ This suggests that a higher concentration may be needed for clinical effectiveness. Although when topical or intra-articular TXA is used in the setting of post-operative hemarthrosis, it is difficult to predict final concentration which would be highly variable among patients.

Based on our results, we believe that commonly used doses of intra-articular and topical TXA in arthroplasty surgery would be toxic to chondrocytes. It is paramount to preserve and protect cartilage in unicompartmental or partial joint arthroplasties. At this time, we would recommend

against using standard protocols for topical or intra-articular TXA in the setting of native cartilage.

4.4 Conclusions

The original FDA-approved use for TXA is for heavy menstrual bleeding and short-term prevention of excessive bleeding in patients with hemophilia.¹⁰² Specifically, TXA has been often used in tooth extraction in patients with hemophilia. It has been demonstrated that TXA reduces the amount of blood loss, post-operative bleeding, and need for additional clotting factors.¹⁰²

Unapproved use of oral, topical, and intravenous TXA has become more common. TXA is now frequently used in surgical operations such as total knee arthroplasties, total hip replacement surgeries, and other orthopedic surgeries. As with the results when used for hemophiliacs and other FDA-approved uses, TXA has been shown to decrease the need for blood transfusions and reduce the risk for hemorrhage.^{102,114,128,130} In these surgeries, TXA has been administered via intravenous, topical, and injected methods.

Although TXA is becoming more used in orthopedic surgeries to prevent bleeding, to date, only one study appears to have focused on its effect on native human cartilage, including chondrocytes.¹²⁵ (Another study by Tuttle et. al. focused on effects on murine and bovine cells.) Parker, et al. assessed TXA's toxicity to isolated chondrocytes from anterior cruciate ligaments (ACL) from a donor. The chondrocytes were cultured *in vitro* 2-dimensionally as well as 3-dimensionally within a hydrogel, after which they were exposed to TXA and observed for cytotoxicity. They showed that concentrations above 20 g/L (such as those recommended in intra-articular applications) appear cytotoxic to cells, resulting in atypical morphology, reduced adhesion, and metabolic activity. At 20 g/L and below, the dose is

considered either cytotoxic or borderline toxic (~42-79%) metabolically, though the effect is dose- and time-dependent.

Our study is therefore the first to evaluate the cytotoxicity of TXA *ex vivo*. Chondrocytes from osteochondral plugs were exposed to TXA for 48 hours, with viability evaluated from 0 days after treatment to 6 days after treatment. We found that up to 2 days following TXA exposure, the osteochondral plugs were viable (no cytotoxicity was found). However, beginning at 4 days after treatment, all concentrations of TXA (including 20g/L, the level previously deemed biocompatible by Parker, et al.) led to extensive cell death in osteochondral plugs. As a result, TXA should be considered cytotoxic at all of the levels tested in this study (20+g/L). Extreme caution should be used prior to using TXA at these doses in orthopedic procedures until further studies can be performed to determine the safest dose.

Chapter 5: *Ex vivo* Human Chondrocyte Toxicity Following Exposure to Commonly Used Antibiotics and Antiseptics

Manuscript in preparation for publication in *Journal of Bone & Joint Surgery (JBJS)* by Nguyen, P.A.H.; Garbrecht, E.; Elghazali, N.; Canavan, H.E.; Salas, C; and Decker, M.

Abstract

Nosocomial (hospital-acquired) infections are currently listed as the 4th leading cause of death in the USA.¹³¹ As open wounds are one potential entryway for bacteria, fungi, and other potentially harmful microorganisms to enter into the patient's bloodstream, chlorhexidine, povidone-iodine (PI), bacitracin, and vancomycin have been used in orthopedic procedures as preventative measures against infection and as adjuvant treatments in the setting of existing infection. With the common use of these solutions and topical powders during orthopedic surgeries, articular cartilage is likely to be exposed to these solutions/substances. In this work, we examine the impact that dilute solutions of chlorhexidine, povidone-iodine, bacitracin, and vancomycin have on chondrocytes of the knee using live/dead assay. Our research shows that vancomycin, povidone-iodine, bacitracin, and chlorhexidine are cytotoxic toward human chondrocytes when used under the concentrations currently recommended for surgical use. Therefore, their use under these conditions should be re-evaluated.

5.1 Introduction

Nosocomial (hospital-acquired) infections are currently listed as the 4th leading cause of death in the USA.¹³¹ As open wounds are one potential entryway for bacteria, fungi, and other potentially harmful microorganisms to enter into the patient's bloodstream, antiseptic solutions, antibiotic solutions, and topical antibiotics are commonly used in a variety of

orthopedic procedures as preventative measures against infection and as adjuvant treatments in the setting of existing infection (see **Table 5.1**).

| <i>Name</i> | <i>Treatment Type</i> | <i>Method of Exposure</i> | <i>Purpose of Use</i> |
|----------------------|-----------------------|---------------------------|---|
| Vancomycin | Antibiotic | Intra-articular Injection | Prevents post-operative infection; treats total knee arthroplasty (TKA) infection |
| Bacitracin | Antibiotic | Irrigation | Prophylaxis |
| Chlorhexidine | Antiseptic | Irrigation | Prophylaxis |
| Povidone-Iodine (PI) | Antiseptic | Irrigation | Prophylaxis |
| TXA | Antifibrinolytic | Intra-articular Injection | Reduces bleeding post operation |
| Normal Saline (NS) | N/A | Irrigation | Remove debris |

Table 5.1. Classification and use of commonly used solutions in TKA to prevent infections prophylactically.

5.1.1 Antibiotics

Antibiotics are the antimicrobial-active substance of choice as they can kill and/or prevent the reproduction of bacteria. Vancomycin was approved by the FDA as an oral antibiotic in the 1950s, and bacitracin was approved as a topical antibiotic in the 1940s. Once the FDA approves a drug, healthcare providers are then responsible to judge and evaluate its need in nonapproved use. As a result, many healthcare providers including surgeons began using antibiotics and antiseptics during surgery in the 1990s/2000s despite not being approved by the FDA for this purpose.

Numerous *in vivo* studies of topical vancomycin powder have been performed in the setting of spine surgeries. After review of this literature, Kanj et al.¹³² stated that a patient is 4 times more

likely to experience a deep post-operative infection after orthopedic spine surgery than a counterpart who received prophylactic topical vancomycin. In a pilot study within orthopedic trauma surgery, intra-wound vancomycin powder in periarticular tibia fractures has shown reduction in infection rates from 17 to 10%, although this was not statistically significant.⁷

During orthopedic trauma surgeries, many surgeons use a bacitracin solution for irrigation of open fractures.⁴⁶ However, no large randomized control trials specific to orthopedic surgery have studied the effectiveness of a bacitracin irrigation solution to prevent infection. In fact, some studies have recommended discontinuing use of bacitracin since the benefits are unproven and there are concerns regarding increased antimicrobial resistance.⁴³

In their study of instrumented posterior spinal fusion of the thoracolumbar spine,¹³ Sweet et al. found that application of 2 grams of vancomycin significantly reduced post-operative wound infection. Evaluation of the wound at day 0 showed that the concentration of vancomycin within the wound was an average of 1457mg/L; by day 3, the concentration of vancomycin was 128mg/L on day 3. For this reason, we used similar concentrations (1000mg/L, 400mg/L, and 160mg/L) of vancomycin.

5.1.1 Antiseptics

Similar to the use of antibiotics, antiseptics such as povidone-iodine were initially approved by the FDA for topical application on skin. As with vancomycin and bacitracin, surgeons began to use antiseptics during surgeries in 2010 to prevent hospital-acquired infections. In the arthroplasty literature, a dilute (0.35%) povidone-iodine (PI) lavage has been shown to decrease the risk of infection in primary total joint arthroplasty from 0.97% to 0.15%.¹³³ Dilute PI lavage (1.0%) is also commonly used to treat periprosthetic joint infections.¹³⁴ For this

study, PI was evaluated from 0.25 to 1% to evaluate the potential biocompatibility of this antiseptic.

Chlorhexidine is also commonly used in arthroplasty surgeries as an adjuvant treatment. Campbell et al. found that pulse lavage with 0.002% chlorhexidine did not result in significant chondrocyte cell death for up to 7 days after exposure, although higher concentrations resulted in early (day 1 and 2) chondrocyte cell death.¹¹ Campbell et al. also showed that that 0.002% results in effective decontamination of *Staphylococcus aureus*, which is one of the bacterial strains of most concern. For these reasons, this study includes chlorhexidine as a positive control to evaluate our methodology.

An *in vitro* study has shown that dilute chlorhexidine is able to eradicate *Staphylococcus epidermidis* from biofilms,⁴⁴ although there are no studies showing an *in vivo* advantage or effectiveness of the use of dilute chlorhexidine.

5.1.3 Other treatments

Also listed in **Table 5.1** are the use of normal saline (NS), which is currently used to clean debris and blood from the joint during surgery and is used in this study as a negative control. In addition, TXA (which was addressed in **Chapter 4**) has been used as an antifibrinolytic to prevent bleeding.

5.1.4 Evidence of antibiotics, antiseptics, and other treatments in the literature

There are few large randomized control trials within the orthopedic literature that support the use of these adjuvant treatments even though they are commonly used.^{46,132,135} With the common use of these solutions and topical powders during orthopedic surgeries, articular cartilage is likely to be exposed to these solutions/substances. In this work, we examine the

impact that dilute solutions of chlorhexidine, povidone-iodine, bacitracin, and vancomycin have on chondrocytes of the knee.

5.2 Materials and Methods

5.2.1 Materials

Test specimens for this study were procured through New Mexico Donor Services.¹²¹ Dulbecco's Modification of Eagle's Medium/F-12 (DMEM/F12) 1:1 media was purchased from Sigma-Aldrich (St. Louis, MO). Fetal bovine serum (FBS), fungizone, and penicillin/streptomycin (P/S) were purchased from HyCLone (Logan, UT). Dulbecco's phosphate buffer saline (DPBS) was purchased from VWR Life Sciences (Sanburn, NY). Calcein AM and ethidium homodimer were obtained from a viability assay kit from Biotium (Fremont, CA). Pharmaceutical grade vancomycin and bacitracin was obtained from Sigma-Aldrich (St. Louis, Missouri). Chlorhexidine was obtained from CareFusion (San Diego, CA). Normal saline (NS) was obtained from B.Braun (Melsungen, Germany). Povidone-iodine was obtained from Aplicare (Meriden, CT).

5.2.2 Osteochondral plug harvest and storage

Osteochondral plugs were obtained from a middle-aged male within 48 hours after passing using the OATS (osteoarticular allograft transfer system) from Arthrex (Naples, Florida). Osteochondral plugs were sterilely obtained from the knee joint (to include distal femur and proximal tibia). Osteochondral plugs were visually confirmed to have intact articular surface; any areas with osteoarthritis (devoid of intact articular cartilage) were discarded. We obtained ~135 osteochondral plugs. The plugs were transferred into FBS solution, and then taken to the lab for PBS wash and rescue period.

Osteochondral plugs were washed with DPBS before being stored in standard 50/50 Dulbecco's Modified Eagle's Medium/F12 nutrient mixture with 10% fetal bovine serum (FBS), 1% penicillin/streptomycin (P/S), and 1% fungizone at 37° C for 2 hours prior to treatment.

5.2.3 Antiseptics/antibiotics biocompatibility test

Osteochondral plugs were randomized to the following treatments: 0.9% NS as the live control; chlorhexidine at 0.01%, and 0.5%; povidone-iodine (PI) at 0.25%, 0.50%, and 1.00%; bacitracin at 10K units/L, 50K units/L, and 100K units/L; and vancomycin at 4mg, 10mg, and 25mg (diluted in 25mL cell media) resulting in 160mg/L, 400mg/, and 1,000mg/L. Osteochondral plugs were exposed to treatment utilizing 1 of 2 techniques: a 1-minute lavage, or a 48-hour soak to simulate intra-wound application of vancomycin (i.e., the procedure previously described in **Figure 4.1**).

Treatments were made from stock solutions and diluted using DPBS. Bacitracin concentrations were determined and calculated using the international standard concentration for bacitracin of 51.2 units/mg as determined by Humphrey, et. al.¹³⁶

5.2.4 Live/dead Assay

The procedure for live/dead assay follows those previously completed by Cooperstein, et al.⁶⁶ Briefly, a combined live/dead solution such as those sold by ThermoScientific was made by adding 1µL of calcein AM (1mM stock solution), and 1 µL of ethidium homodimer-1 (2mM) to 1 mL of DPBS. Osteochondral plugs were maintained in cell media and removed for viability tests at specified times after exposure: day 0 (immediately after exposure), day 2 (2 days after exposure), day 4 (4 days after exposure), and day 6 (6 days after exposure). For bacitracin, viability tests were completed at day 0, day 3 (3 days after exposure), and day 6 (6

days after exposure). Plugs were then rinsed, dissected, and cell media was replaced with working live/dead solution. Cells were incubated at 37° C and 5% CO₂ with live/dead solution for 60 minutes and then rinsed with sterile DPBS prior to imaging. Fluorescent images were taken on a Nikon Eclipse TS200F inverted microscope at 10X with an epifluorescence attachment (Nikon Instruments, Melville, NY) and a SPOT Insight color mosaic digital camera (Diagnostic Instruments, Sterling Heights, MI). Acquired images were then enhanced using Fiji (Image J Software). Images of dead cells (red) were enhanced to increase brightness and contrast. This allows dead cells to show in merged images where they otherwise would be overshadowed by live cells stained in green. As a result, some of the merged images are oversaturated and appear to contain red hues.

After imaging, cells were analyzed and counted using Fiji (Image J Software), following a previously established protocol.¹²² In short, all images were converted from to color to an 8-bit grayscale image. Then, the “Find Maxima” function was used, and “noise tolerance” was set to 15.

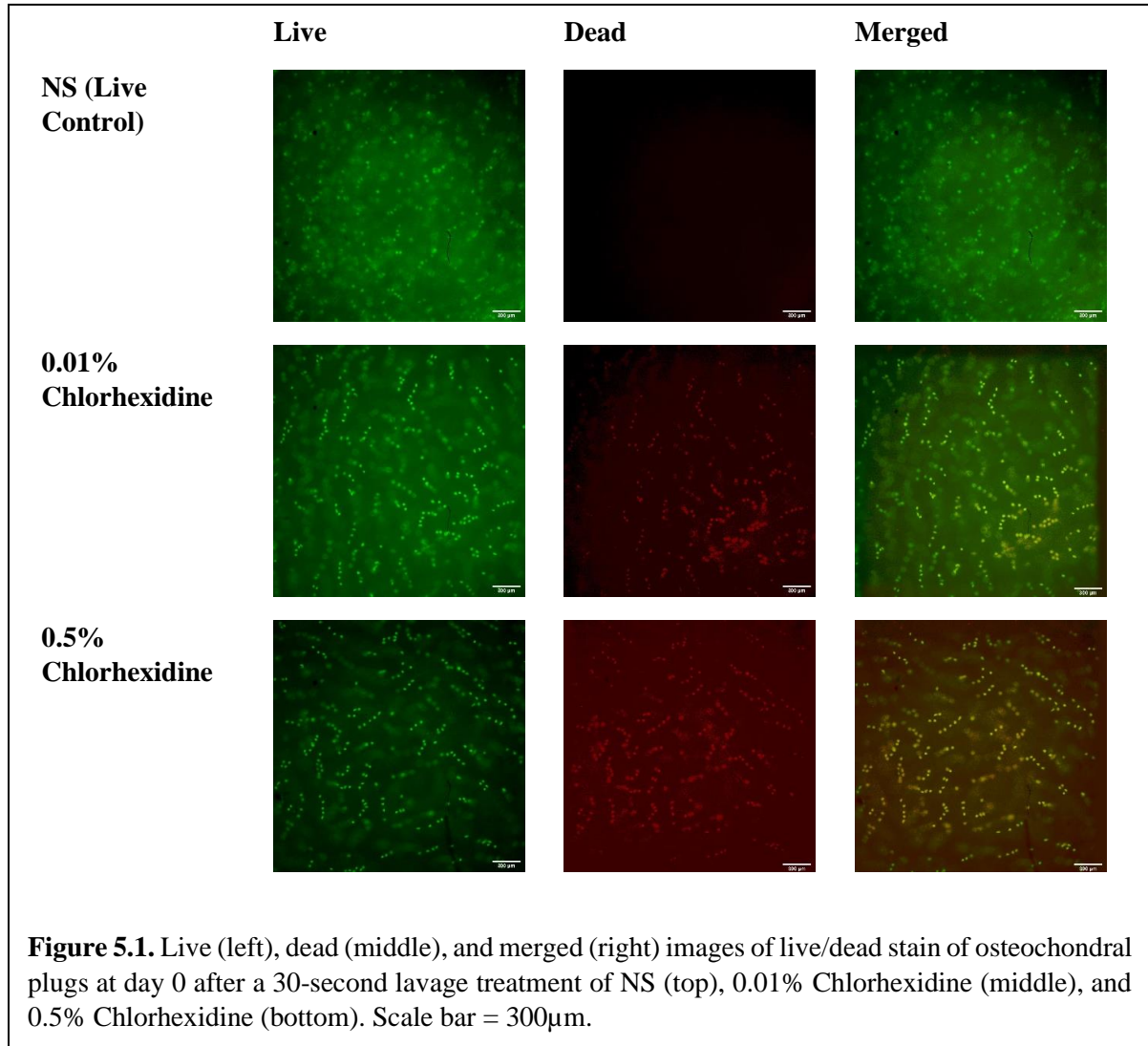
The formulas used for quantification were:

1. *Total cells = # of Live cells + # of Dead Cells*

2. *% Live cells = $\frac{\# \text{ of Live cells}}{\text{Total Cell Number}} * 100$*

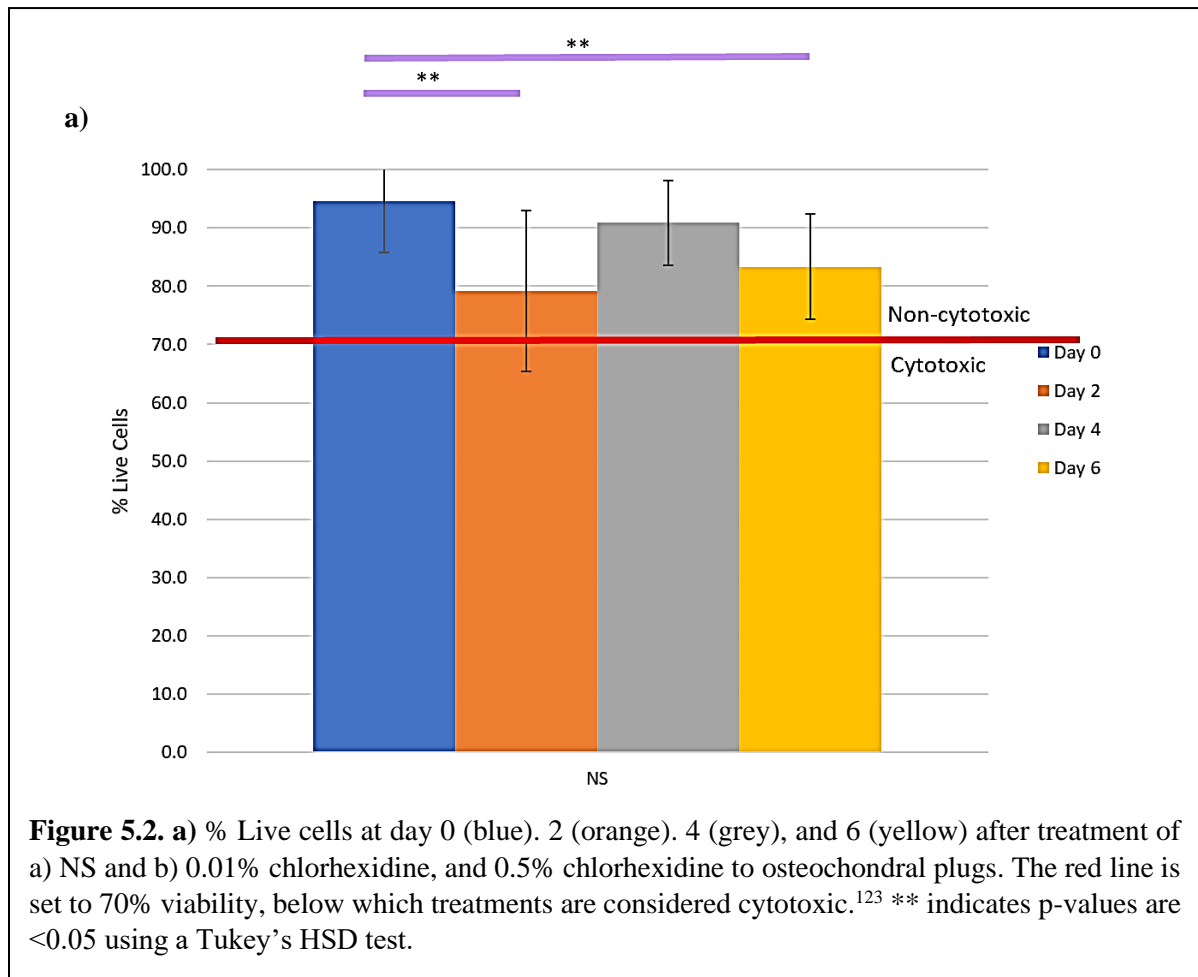
Following live/dead counts and evaluation of % live cells, ANOVA was completed at each day across all treatments. A post-hoc test of Tukey’s HSD was used to evaluate which treatments, in comparison to normal saline, were significantly different. Furthermore, an ANOVA was completed within each treatment comparing the differences over time, with a post-hoc test of Tukey’s HSD to evaluate which days, in comparison to day 0, were significantly different.

5.3 Results and Discussion



The live/dead viability assay was performed at days 0, 2, 4, and 6 (0, 3, and 6 for bacitracin) after osteochondral plug harvest and treatment of normal saline (NS), vancomycin, chlorhexidine, povidone-iodine (PI), and bacitracin. **Figure 5.1** shows representative images of live (left), dead (middle), and merged images (right) of osteochondral plugs at day 0 for NS, and chlorhexidine controls. After treatment with NS, the chondrocytes appear to be viable, with little cell death (see top row of **Figure 5.1**, which is primarily green, with very little red fluorescence). In comparison, both concentrations of chlorhexidine (0.01%, middle row; and 0.5%, bottom row of **Figure 5.1**), appear to induce cell death. The higher concentration (0.5%

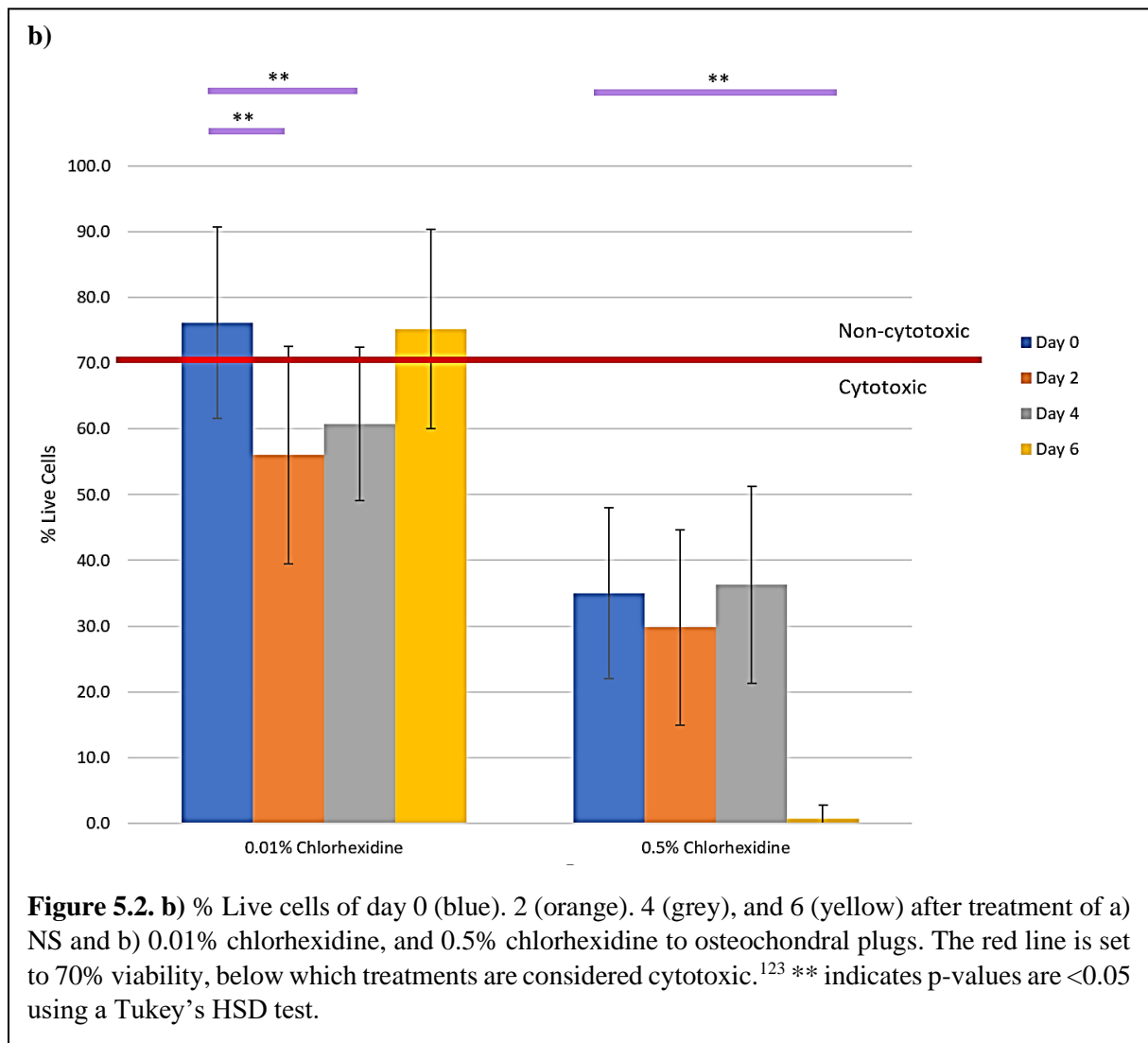
chlorhexidine, bottom row), appears more cytotoxic, as evidenced by the red fluorescence. These results shows that our treatment and staining was successful, with similar results to the one previous study published in the literature utilizing chlorhexidine at similar concentrations on salvaged contaminated grafts.⁴⁷



In **Figure 5.2**, a quantitative evaluation of the live/dead data was completed for NS and chlorhexidine conditions over days 0, 2, 4, and 6 using cell counting.¹²² The red line in **Figure 5.2** is set to 70% viability, which is the level at which treatments are considered to be cytotoxic toward cells by ISO-10993.¹²³ ** indicates p-values are <0.05 using Tukey's HSD in comparison to day 0. **Figure 5.2a** shows that osteochondral plugs are viable *ex vivo* following NS wash treatment even 6 days after treatment (cell viability >70% for all time points). **Figure**

5.2b shows that chlorhexidine at 0.01% is mildly toxic, with cell viabilities of 76.1% ± 23.9% (day 0), 56.1% ± 16.5% (day 2), 60.7% ± 11.7% (day 4), and 75.2% ± 15.1% (day 6). Cell viability drops significantly at two and four days after exposure. However, after day 4, there appears to be a trend towards recovery, possibly due to the doubling of healthy cells within the culture medium. This may explain our findings that by day 6, chondrocytes treated with 0.01% chlorhexidine are similar to those found at day 0 (no significant change observed).

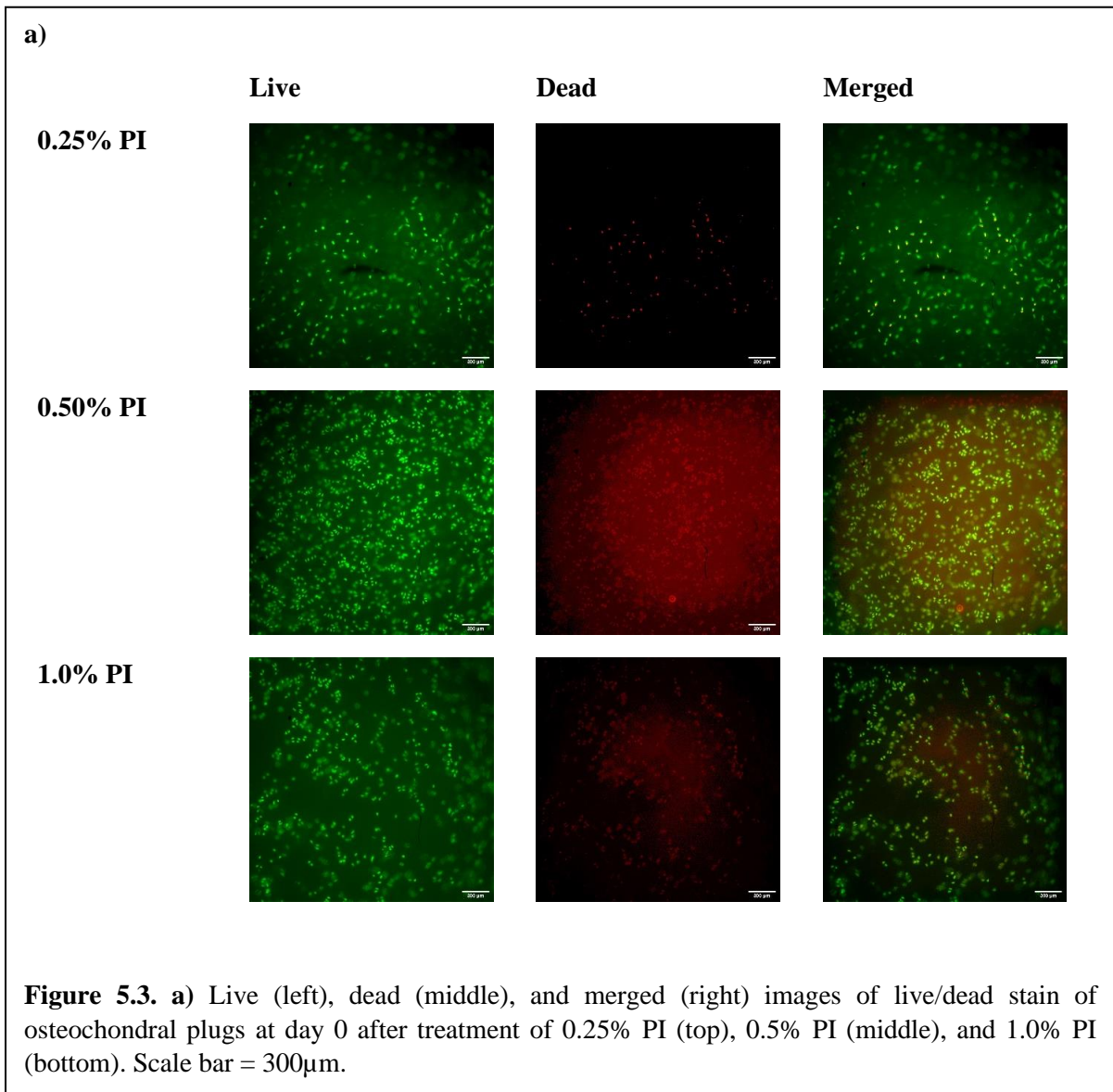
In contrast, at the higher concentration of chlorhexidine (0.5%), the chondrocytes at each time



point have cell viabilities below 50% (35.0% ± 13.0% (day 0), 29.8% ± 14.9% (day 2), 36.3%

$\pm 14.9\%$ (day 4)). By day 6, virtually all of the chondrocytes exposed to 0.5% chlorhexidine are dead ($0.7\% \pm 2.1\%$).

Figure 5.3a shows representative images of live (left), dead (middle), and merged images (right) of osteochondral plugs after exposure to povidone-iodine (PI) at increasing concentrations (0.25% PI, 0.50% PI, and 1.0% PI. 0.25% PI) at day 0. At the lowest concentration of PI, there appears to be little cell death; however, at medium and high dosages



(0.50% and 1.0%) of PI the larger number of red cells fluorescing indicates greater cytotoxicity.

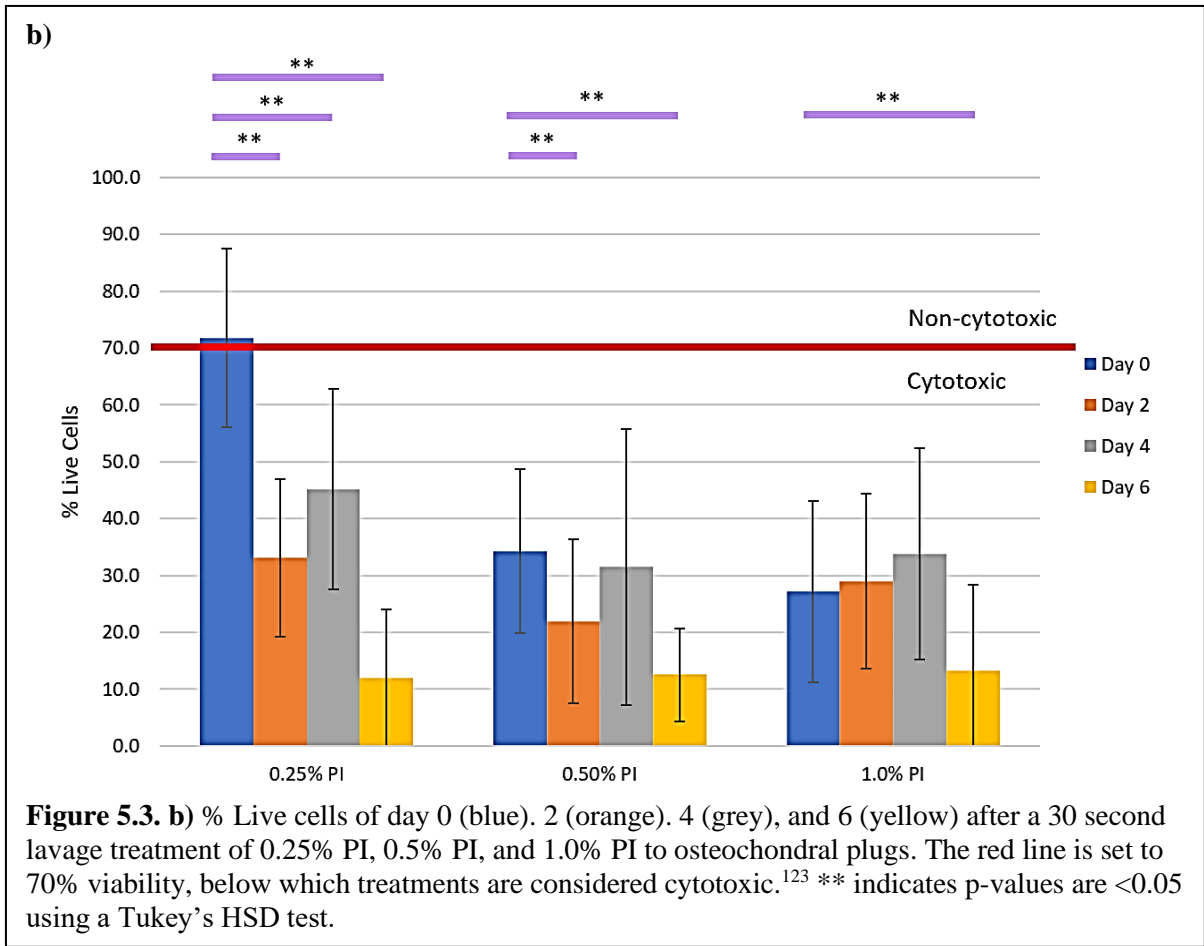


Figure 5.3b confirms these observations using a quantitative evaluation of the live/dead data for PI conditions over days 0, 2, 4, and 6 using cell counting.¹²² Similar to **Figure 5.2**, the red line on **Figure 5.3b** is set to 70% viability, which indicates the level below which treatments are considered to be cytotoxic toward cells by ISO-10993.¹²³ **Figure 5.3b** shows that—despite the appearance of viability in **Figure 5.3a**—even at the low concentrations of PI (0.25%), PI appears to already be borderline cytotoxic to chondrocytes at day 0 (71.8% ± 15.7%). Long-term evaluation of PI at 0.25% shows significant drop in cell viability to 33.1% ± 13.9% by day 2, 45.2% ± 17.7% by day 4, and 12.0 ± 12.0% by day 6.

Similar drops in viabilities are found at higher concentrations of PI. Higher concentrations of PI (0.5% and 1.0%) are considered toxic even at day 0 ($34.3\% \pm 14.4\%$ and $27.2\% \pm 15.9\%$ respectively), 0.50% PI continues to have cytotoxic effects at 2 days ($21.9\% \pm 14.4\%$), 4 days ($31.5\% \pm 24.2\%$), and 6 days ($12.6\% \pm 8.2\%$) after exposure. Similarly, 1.0% appears cytotoxic to osteochondral plugs 2 days ($29.0\% \pm 15.4\%$), 4 days ($33.8\% \pm 18.6\%$), and 6 days ($13.2\% \pm 15.2\%$) after exposure.

Figure 5.4 shows the results of live/dead imaging and cell counts after 0, 2, 4, and 6 days after treatment with vancomycin. Representative images stained with live (left) and dead staining (middle), and merged images (right) of osteochondral plugs are presented in **Figure 5.4a** at day 0 for 160mg/L, 400 mg/L and 1000 mg/L of vancomycin. Vancomycin appears to be cytotoxic toward the chondrocytes with toxicity increasing with higher concentration.

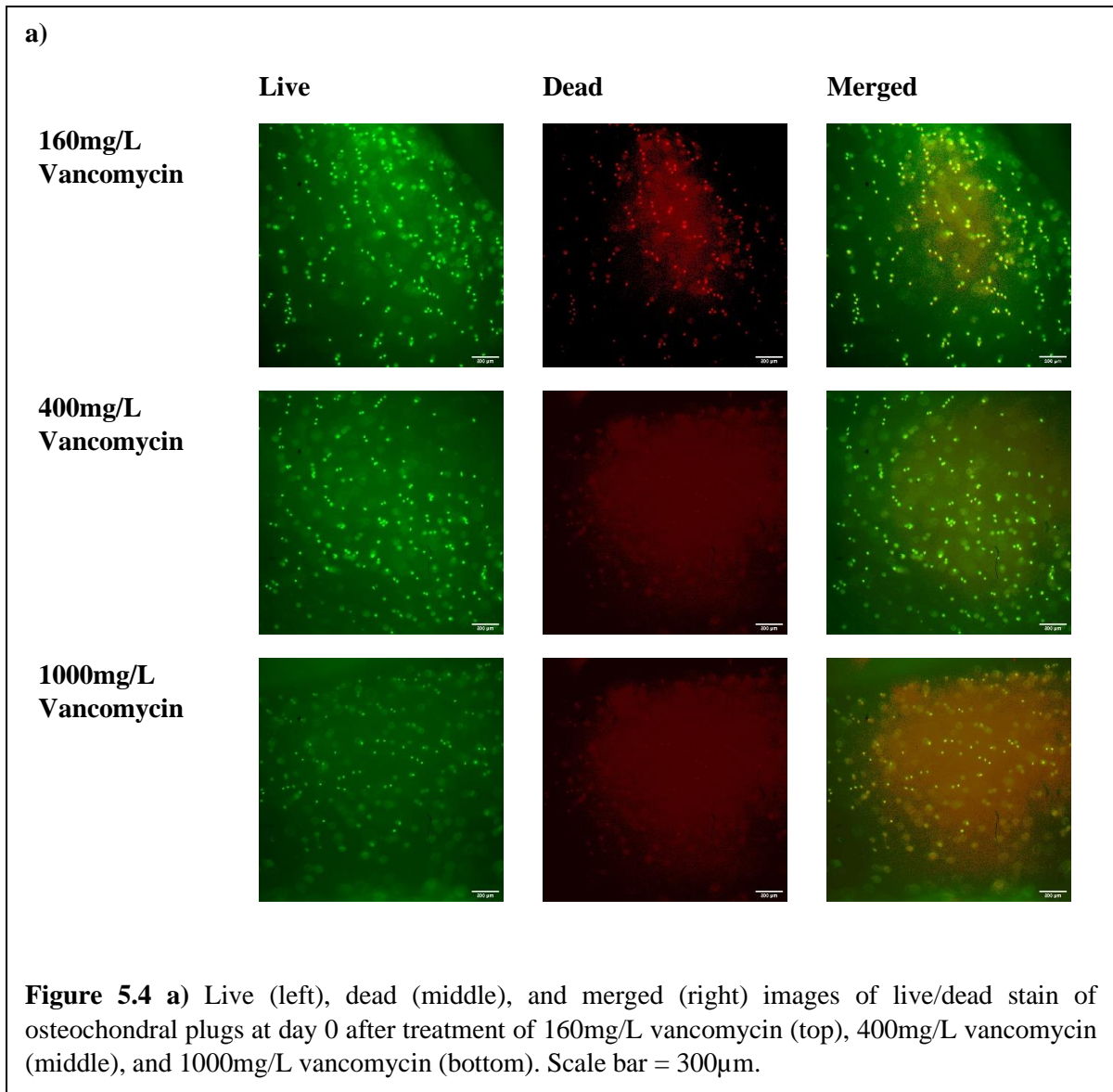


Figure 5.4b shows the quantitative results of live/dead counts over days 0, 2, 4, and 6 of vancomycin treatments. The red line on **Figure 5.4b** indicates 70% viability, below which treatments are considered cytotoxic to cells. **Figure 5.4b** confirms that all three concentrations (160mg/L, 400mg/, and 1,000mg/L g) of vancomycin concentrations are toxic to chondrocytes at all time points tested (days 0, 2, 4, and 6). Exposure to 160mg/L of vancomycin led to chondrocyte viabilities of 44.3% \pm 14.3% (day 0), 24.0% \pm 10.2% (day 2), 47.4% \pm 11.6% (day 4), and 30.2% \pm 21.0% (day 6). Drops in viabilities were statistically significant in

comparison to day 0 at day 2, and day 6. Treatment to 400mg/L of vancomycin had chondrocyte viabilities of 22.6% ± 12.1% (day 0), 30.1% ± 11.3% (day 2), 43.1% ± 17.5% (day 4), and 22.4% ± 13.5% (day 6). At 1,000mg/L, vancomycin led to chondrocyte viabilities of 27.3% ± 14.9% (day 0), 22.7% ± 16.7% (day 2), 3.7% ± 5.6% (day 4), and 7.8% ± 11.9% (day 6). At all concentrations, cell viability is low, with no significant recovery 6 days after treatment (unlike cells exposed to chlorhexidine).

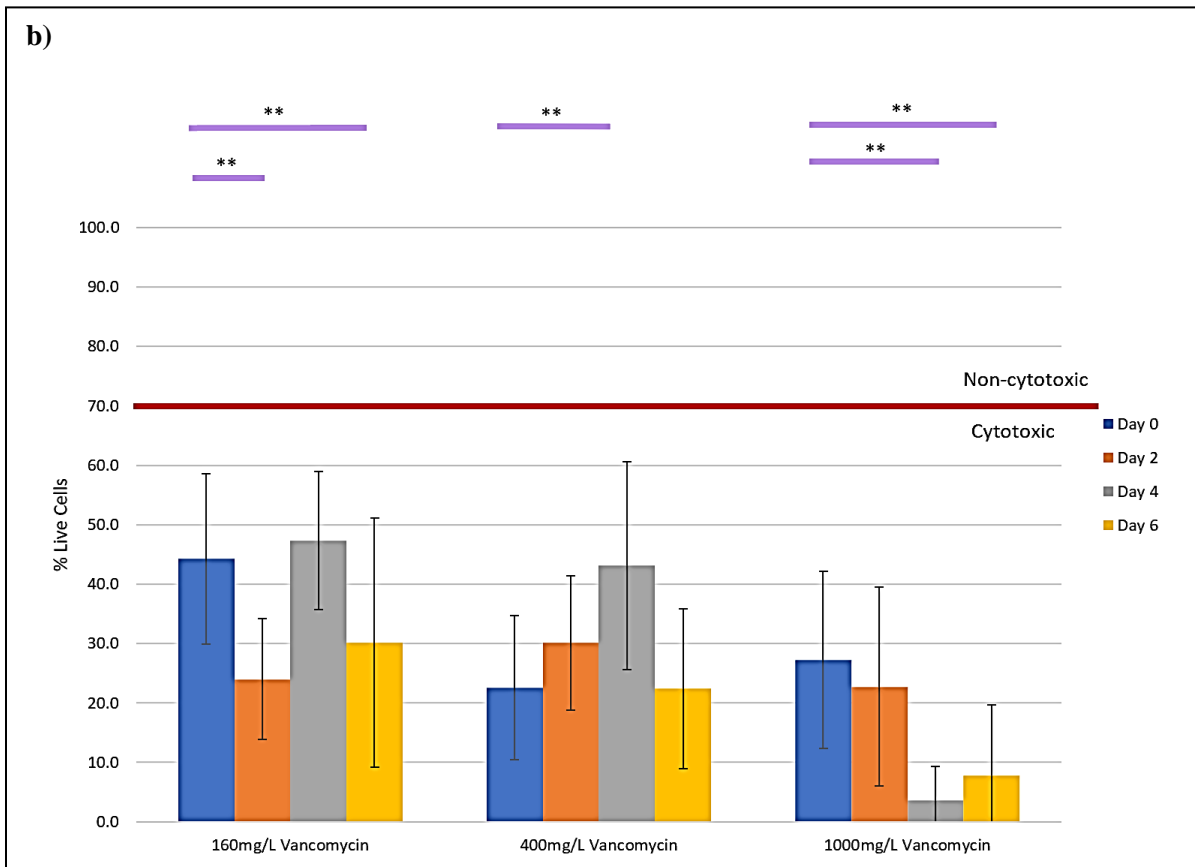


Figure 5.4. b) % Live cells of day 0 (blue). 2 (orange). 4 (grey), and 6 (yellow) after a 48-hour soak of 160mg/L, 400mg/L, and 1000mg/L vancomycin to osteochondral plugs. The red line is set to 70% viability, below which treatments are considered cytotoxic.¹²³ ** indicates p-values are <0.05 using a Tukey's HSD test.

Figure 5.5 shows the results of live/dead imaging and counts at days 0, 3, and 6 after exposure to bacitracin. **Figure 5.5a** are representative images live (left), dead (middle), and merged images (right) of osteochondral plugs at day 0 for 10K units/L 50K units/L, and 1000 units/L of bacitracin. At day 0, bacitracin appears to be the most biocompatible, with less cell death observed after exposure compared to the other antibiotics/antiseptics/treatments in this chapter and **Chapter 4**. Bacitracin also appears to have an optimal dosage, as more live cells are observed at 10K units/L and the most cell death is observed at 100K units/L.

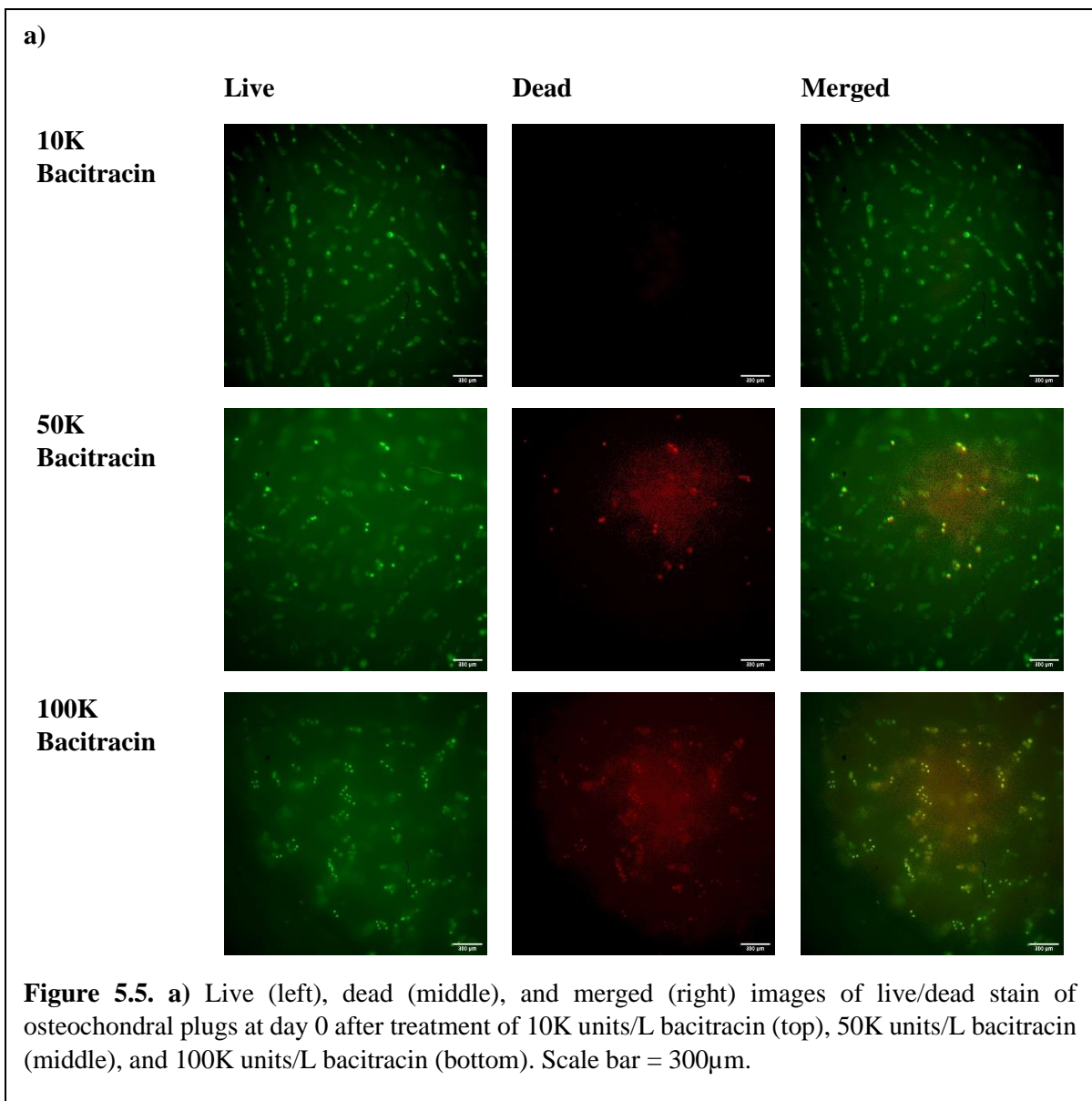
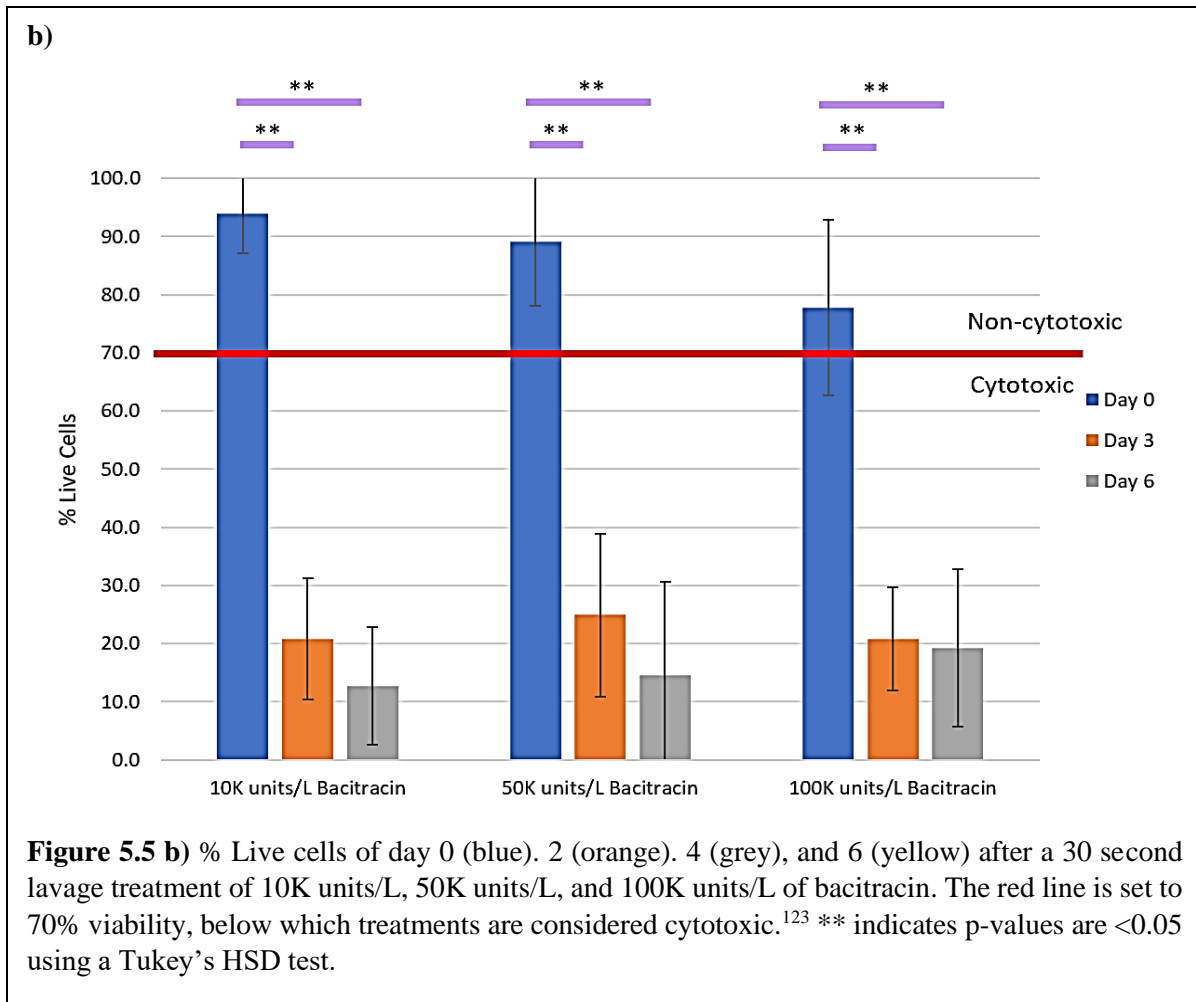


Figure 5.5b shows the results of live/dead counts over days 0, 3, and 6 of bacitracin treatments.

Figure 5.5b confirms the findings in **Figure 5.5a**. At day 0, all concentrations of bacitracin appear biocompatible, with cell viabilities >70% (10K/L bacitracin: 94.0% ± 6.0%, 50K/L bacitracin: 89.1 ± 10.9%, 100K/L bacitracin - 77.8% ± 15.1%). However, cell viability drops



dramatically at day 3 (~60% for all concentrations). In fact, viabilities for the 10K/L bacitracin drops to 20.8% ± 10.4% 3 days after exposure and continues to drop to 12.8% ± 10.1% 6 days after exposure. Similar trends are found in 50K/L bacitracin and 100K/L bacitracin with drops to 24.9% ± 14.0%, and 20.8% ± 8.9% 3 days after exposure; and 14.6% ± 16.0% and 19.3% ± 13.6% 6 days after exposure.

Based on ANOVA comparing the average % of live cells over time within each treatment group, all treatment groups were statistically significant. As a result, a Tukey's HSD post-hoc test was used to compare average % live cells between time points to determine which time points are statistically different.

ANOVA analysis of the data from day 0 shows that cell viability following the different treatments were statistically significant with a p-value of 1.22×10^{-68} . Analysis at day 0 using Tukey's HSD test (as seen in **Table 5.2**) shows that in comparison to normal saline, cell viability following treatment with almost all of the possible treatments (the highest dosage of bacitracin, 100K units/L; as well as all concentrations of vancomycin, chlorhexidine, and PI),

| <i>group 1</i> | <i>group 2</i> | <i>mean</i> | <i>q-stat</i> | <i>lower</i> | <i>upper</i> | <i>p-value</i> |
|----------------|-----------------------|-------------|---------------|--------------|--------------|----------------|
| Normal Saline | Vancomycin 160mg/L | 50.32 | 15.99 | 35.60 | 65.03 | 2.02E-14** |
| Normal Saline | Vancomycin 400mg/L | 72.00 | 22.89 | 57.29 | 86.72 | 2.02E-14** |
| Normal Saline | Vancomycin 1000mg/L | 67.31 | 21.39 | 52.60 | 82.02 | 2.02E-14** |
| Normal Saline | Bacitracin 10K | 0.64 | 0.20 | -14.08 | 15.35 | 1 |
| Normal Saline | Bacitracin 50K | 5.47 | 1.74 | -9.24 | 20.18 | 0.99 |
| Normal Saline | Bacitracin 100K | 16.83 | 5.35 | 2.12 | 31.54 | 0.01** |
| Normal Saline | Chlorhexidine 0.01% | 18.46 | 5.87 | 3.75 | 33.17 | 2.81E-3** |
| Normal Saline | Chlorhexidine 0.5% | 59.56 | 18.93 | 44.85 | 74.27 | 2.02E-14** |
| Normal Saline | Povidone Iodine 0.25% | 22.80 | 7.25 | 8.09 | 37.52 | 4.36E-05** |
| Normal Saline | Povidone Iodine 0.50% | 60.28 | 19.16 | 45.56 | 74.99 | 2.02E-14** |
| Normal Saline | Povidone Iodine 1.0% | 67.37 | 21.41 | 52.66 | 82.09 | 2.02E-14** |

Table 5.2. Tukey's HSD test results of day 0 comparing treatments to normal saline. Standard error = 3.15. ** indicates p-values are <0.05 using a Tukey's HSD test.

was significantly different than those exposed to normal saline. The high q-stat values (~1) and extremely high p-values (<0.05) for bacitracin at day 0 at low and medium dosage indicate that cell viability after treatment with bacitracin at these amounts does not significantly affect the viability of cells, and therefore, this antibiotic is biocompatible at these dosages.

Continued analysis on days 2, 4, and 6, showed similar results to day 0. ANOVA comparing the different treatments showed statistically significant results at all times. At day 2, the p-value was 3.12×10^{-29} . At day 4 and 6 the p-values were 4.97×10^{-35} , and 1.10×10^{-63} respectively. The post-hoc tests of days 2-6 can be seen in **Tables 5.3-5.5**. It should be noted that bacitracin was not part of the analysis for days 2, and 4 as bacitracin was not evaluated at these time periods but was evaluated at day 3 instead due to minimal availability of samples. At all time points, all treatment groups (excluding 0.01% chlorhexidine at day 6) were significantly

| <i>group 1</i> | <i>group 2</i> | <i>mean</i> | <i>q-stat</i> | <i>Lower</i> | <i>upper</i> | <i>p-value</i> |
|----------------|--------------------------|-------------|---------------|--------------|--------------|----------------|
| Normal Saline | Vancomycin 160mg/L | 55.23 | 16.42 | 40.26 | 70.20 | 2.02E-14** |
| Normal Saline | Vancomycin 400mg/L | 49.08 | 14.59 | 34.11 | 64.05 | 2.00E-14** |
| Normal Saline | Vancomycin 1000mg/L | 56.49 | 16.79 | 41.52 | 71.46 | 2.04E-14** |
| Normal Saline | Chlorhexidine 0.01% | 23.16 | 6.89 | 8.19 | 38.13 | 9.52E-05** |
| Normal Saline | Chlorhexidine 0.5% | 49.43 | 14.69 | 34.45 | 64.40 | 2.05E-14** |
| Normal Saline | Povidone Iodine 0.25% | 46.08 | 13.70 | 31.11 | 61.05 | 2.07E-14** |
| Normal Saline | Povidone Iodine 0.50% | 57.27 | 17.03 | 42.30 | 72.25 | 2.04E-14** |
| Normal Saline | Povidone Iodine 1.0% | 50.24 | 14.93 | 35.27 | 65.22 | 2.04E-14** |

Table 5.3. Tukey’s HSD test results of day 2 comparing treatments to normal saline. Standard error = 3.36. ** indicates p-values are <0.05 using a Tukey’s HSD test.

different from normal saline, indicating that our results seen in treatments are different from our negative control of normal saline.

| <i>group 1</i> | <i>group 2</i> | <i>mean</i> | <i>q-stat</i> | <i>lower</i> | <i>Upper</i> | <i>p-value</i> |
|----------------|--------------------------|-------------|---------------|--------------|--------------|----------------|
| Normal Saline | Vancomycin 160mg/L | 43.56 | 12.01 | 27.43 | 59.70 | 6.07E-13** |
| Normal Saline | Vancomycin 400mg/L | 47.82 | 13.19 | 31.68 | 63.96 | 2.48E-14** |
| Normal Saline | Vancomycin 1000mg/L | 87.28 | 24.07 | 71.14 | 103.41 | 2.04E-14** |
| Normal Saline | Chlorhexidine 0.01% | 30.21 | 8.33 | 14.08 | 46.35 | 8.34E-07** |
| Normal Saline | Chlorhexidine 0.5% | 54.62 | 15.06 | 38.49 | 70.76 | 2.02E-14** |
| Normal Saline | Povidone Iodine 0.25% | 45.73 | 12.61 | 29.60 | 61.87 | 6.88E-14** |
| Normal Saline | Povidone Iodine 0.50% | 59.45 | 16.40 | 43.31 | 75.59 | 2.04E-14** |
| Normal Saline | Povidone Iodine 1.0% | 57.17 | 15.77 | 41.03 | 73.31 | 2.02E-14** |

Table 5.4. Tukey’s HSD test results of day 4 comparing treatments to normal saline. Standard error = 3.63. ** indicates p-values are <0.05 using a Tukey’s HSD test.

From our initial evaluation of chondrocytes immediately after exposure to 0.25% PI, 0.01% chlorhexidine, and all concentrations of bacitracin, each of these antibiotics and antiseptics show promise as clinically effective and non-toxic antiseptics/antibiotics in orthopedic procedures. However, further evaluation at longer time periods shows that of all antiseptic/antibiotic treatments, only 0.01% chlorhexidine remains non-toxic to *ex vivo* osteochondral plugs. Other conditions, including all concentrations of vancomycin (160mg/L, 400mg/L, and 1000mg/L), and high concentrations of PI (0.50%, and 1.0%) are toxic to chondrocytes at all time points. As expected, osteochondral plugs that were exposed to normal saline remained alive with high viabilities even 6 days after exposure, indicating that our

method of maintenance was not the cause of cell death and the toxic effects seen in chondrocytes are likely a result of exposure to antiseptics and antibiotics.

| <i>group 1</i> | <i>group 2</i> | <i>mean</i> | <i>q-stat</i> | <i>lower</i> | <i>upper</i> | <i>p-value</i> |
|----------------|--------------------------|-------------|---------------|--------------|--------------|----------------|
| Normal Saline | Vancomycin 160mg/L | 53.95 | 17.51 | 39.54 | 68.37 | 3.77E-15** |
| Normal Saline | Vancomycin 400mg/L | 61.74 | 20.03 | 47.32 | 76.15 | 3.77E-15** |
| Normal Saline | Vancomycin 1000mg/L | 76.33 | 24.77 | 61.91 | 90.74 | 3.77E-15** |
| Normal Saline | Bacitracin 10K | 71.36 | 23.16 | 56.95 | 85.78 | 3.77E-15** |
| Normal Saline | Bacitracin 50K | 69.46 | 22.54 | 55.05 | 83.88 | 3.77E-15** |
| Normal Saline | Bacitracin 100K | 64.82 | 18.81 | 48.71 | 80.94 | 3.77E-15** |
| Normal Saline | Chlorhexidine 0.01% | 8.94 | 2.90 | -5.48 | 23.35 | 0.66 |
| Normal Saline | Chlorhexidine 0.5% | 83.37 | 27.05 | 68.95 | 97.78 | 3.77E-15** |
| Normal Saline | Povidone Iodine 0.25% | 72.09 | 23.39 | 57.68 | 86.51 | 3.77E-15** |
| Normal Saline | Povidone Iodine 0.50% | 71.53 | 23.21 | 57.12 | 85.95 | 3.77E-15** |
| Normal Saline | Povidone Iodine 1.0% | 70.86 | 22.99 | 56.45 | 85.28 | 3.77E-15** |

Table 5.5. Tukey’s HSD test results of day 6 comparing treatments to normal saline. Standard error = 3.08. ** indicates p-values are <0.05 using a Tukey’s HSD test.

5.4 Conclusions

In this work, the relative biocompatibility of several antibiotics (vancomycin, bacitracin) and antiseptics (povidone-iodine, chlorhexidine) toward chondrocytes harvested from human knees was evaluated using live/dead assays. These antibiotics and antiseptics were initially approved for use with humans by the FDA for either topical or oral usage and have more

recently been used in orthopedic procedures to prevent joint infection following hip and knee arthroplasty.

Our research shows that vancomycin, povidone-iodine, bacitracin, and chlorhexidine are cytotoxic toward human chondrocytes when used at (and even under) the concentrations currently recommended for surgical use. Therefore, their use under these conditions should be re-evaluated. Given the increasing numbers of joint replacement surgeries experienced by patients (at earlier ages), exposing sensitive cells such as osteochondrocytes' to cytotoxic agents could mean a faster return to osteoarthritis for patients, with a shorter time span between revisions. Lower concentrations should be evaluated for their safety and efficacy prior to continued use in the surgical arena.

Chapter 6: Investigation of the in-vitro cytotoxicity of PEG 3350 with human gastrointestinal cells.

Manuscript in preparation for publication by Nguyen, P.A.H.; Cuylear, D.; and Canavan, H.E.

Abstract

Colorectal cancer (CRC) is the fourth most common type of cancer and the fourth leading cause of cancer-related deaths in the United States, with an estimated 200,000 new cases each year. A method to reliably screen for and prevent CRCs exist, and it is known as a colonoscopy. A colonoscopy is a procedure that allows gastroenterologists to visualize and remove the polyps that lead to 75 to 80% of CRC. A colonoscopy is recommended every few years, beginning at the age of 50, dependent on your risk of CRC. Although individuals may be compliant to their first screening, as many as 40% will not return for any future screenings, dramatically increasing their risk for CRC. It is believed that low patient compliance is due to the preparation experienced by the patient prior to the exam. The preparation is a 4-L consisting of polyethylene glycol 3350 and other salts that help clear out the colon. PEG was initially developed in the mid-1800s by Laurencio and Wurtz through the polymerization of ethylene oxide with alkali metal hydroxide or zinc chloride. By the 1930s, PEG was commercialized; and PEG became used in a variety of areas including pharmaceuticals such as topical reagents, lubricants, cosmetics, and detergents. With limited additional *in vitro* studies on Chinese Hamster cells utilizing PEG with molecular weight of 6000-7000 and small *in vivo* studies on men, PEG 3350 became the primary colonoscopy preparation reagent. In this study, we investigate the relative cytotoxicity of primary human stomach cells (HSCs), human small intestine cells (HSIs), and human colon cells (HCCs) after exposure to increasing concentrations of PEG 3350 (1%, 5%, 10%, 15%, and 20%) over multiple time periods (2, 6,

12, 24, and 48 hours). Cell viability was investigated using cell morphology, live/dead assay, and XTT assay. Though long considered to be a biocompatible polymer due to its acceptance by the FDA, PEG 3350 *does* appear to negatively affect the morphology and viability of human stomach and intestinal cells. Exposure to 5% PEG 3350 and 10% PEG 3350 cannot be considered cytotoxic at relevant time frames to all cell lines within the human digestive system, cytotoxic effects are seen with small changes in cell morphology as well as a decrease in cell viability as measured by XTT in all cell types. Importantly, one of the primary complaints about the GI preparation method is that the solution can be improperly mixed due to its high viscosity. In such cases, it is possible that higher concentrations (up to 20%) could be experienced in the GI tract of a patient. These results indicate that, contrary to the belief on the safety of PEG 3350, cytotoxic effects may be experienced from the current preparation method.

6.1 Introduction

6.1.1 Colorectal Cancer (CRC) and Colonoscopy

Colorectal cancer (CRC) is the fourth most common type of cancer and the fourth leading cause of cancer-related deaths in the United States, with an estimated 200,000 new cases each year.¹³⁷ The rate at which people are diagnosed with colorectal cancer has dropped by 32% from 2000-2013.¹³⁸ Death rates have dropped by 34% over the same time period.¹³⁸ This positive improvement in health is seen to be a direct result of more individuals participating in a reliable screening and prevention method for CRC called a colonoscopy.¹³⁸ A colonoscopy is a procedure that allows gastroenterologists to visualize and remove the polyps that lead to 75 to 80% of CRC.¹³⁹ Colonoscopy has therefore become the screening test of choice, as it offers the advantage of simultaneously being a diagnostic *and* preventive tool by allowing immediate detection and removal of polyps.¹⁴⁰

Despite the proven efficacy of colonoscopy as a screening tool, CRC remains one of the leading causes of death in the USA and other developed nations. The persistence of deaths due to CRC is due, in part, to low patient compliance adhering to the screening tool. Although individuals may be compliant to their first screening, as many as 40% will not return for any future screenings, dramatically increasing their risk for CRC.^{141,142} In the case of colonoscopy, it is not the exam itself that causes issues, as the procedure is traditionally performed while the patient is under “twilight” (vs. general anesthesia) conditions that limit the awareness or discomfort experienced by the patient.

6.1.2 Patient Compliance and User Experience (UX)

It is believed that low patient compliance is due to the preparation experienced by the patient prior to the exam. The night prior to receiving the screening, patients must prepare their gastrointestinal (GI) tract by consuming the standard 4-liter poly(ethylene glycol)-electrolyte lavage solution (PEG-ELS) that has been approved and accepted for use by the Food & Drug Administration (FDA).

Approximately 34% of patients who undergo the procedure report moderate to significant discomfort with the preparation,^{143,144} with patients describing the preparation as foul tasting, with side effects including nausea, vomiting, abdominal bloating, abdominal pain, and rectal irritation. In addition, a small percentage of patients, particularly women, elderly persons, and physically smaller patients, experience more severe side effects, including dehydration, loss of consciousness, and nephrotoxicity (reversible kidney failure) due to this preparation.^{145,146} These effects are most likely compounded by the fact that the dosage is not optimized for individual patients (i.e., all patients receive the same dose, regardless of gender, mass, etc.). In addition, one of the complaints of the mixture noted above is that the PEG-ELS solutions tend

to not be homogenous, so the dosage experienced may vary greatly from the estimated ~5.2% (w/w).

As discussed in **Chapter 1**, the FDA approval process is both lengthy and expensive; therefore, it is unlikely that the key to improved patient compliance is through new materials. Instead, we chose to explore how the “user experience” (UX, in design language)/ patient and medical practitioner experience of products such as GoLytely™ and other PEG-ELS solutions might be improved by varying the dosage and/or delivery system used for PEG.

6.1.3 History of Colonoscopy

In the 1970s prior to the usage of PEG in colonoscopy preparation, clinical trials for colonoscopy screening method focused on using high concentrations of sodium chloride solutions. This method proved quite effective; however, it was shown to have significant side effects over longer periods of time, due to the negative effects it had on sodium/potassium transport in the ileum and colon.³⁰

6.1.4 History of PEG

PEG was initially developed in the mid-1800s by Laurencio and Wurtz through the polymerization of ethylene oxide with alkali metal hydroxide or zinc chloride.^{30,147} By the 1930s, PEG was commercialized; and PEG became used in a variety of areas including pharmaceuticals such as topical reagents, lubricants, cosmetics, and detergents.^{30,147}

While PEG was initially used as a biomaterial nearly 100 years ago, it was transitioned into the current FDA structure with minimal evaluation of its toxicity *in vitro* or *in vivo*. Shintani *et. al* showed that one specific strain of PEG, PEG86-1, is a biocompatible polymer *in vitro* at different molecular weights.¹⁴⁸ Pontecorvo showed PEG 6000-7750 promoted cell growth in

Chinese hamster hypoxanthine guanine phosphoribosyltransferase-deficient (HGPRT⁻), strain wg cells and mouse thymidine kinase-deficient (TK⁻), strain 3T3 cells¹⁴⁹. After these studies were completed, no other studies have fully examined the short and long-term effects of low and high concentrations of PEG, in particular PEG 3350, on human cell lines. To date, no research thoroughly determines the cytotoxic effects of PEG 3350 on cells pertinent to the human gastrointestinal tract.

6.1.5 Incorporation of PEG into Colonoscopy

In response to such limitations, Davis *et al.* conducted a study using PEG alongside other electrolytes to evaluate the effect PEG had on the water and electrolyte absorption and secretion in the gastrointestinal tract.¹⁵⁰ This method was deemed appropriate because it showed no evidence of volume overload or electrolyte imbalance in a human model. Thus, the preparation solution “GoLytely™” was created.¹⁵¹ Further research completed by Hammer *et al.* concluded that PEG 3350 was enough to increase the amount of stool a patient produces needed to perform the procedure and as such, PEG 3350 became the primary colonoscopy preparation reagent.¹⁵²

6.1.6 Current Work

In this study, we investigate the relative cytotoxicity of primary human stomach cells (HSCs), human small intestine cells (HSIs), and human colon cells (HCCs) after exposure to PEG 3350. The cells have been observed after exposure to increasing concentrations of PEG 3350 (1, 5, 10, 15, and 20% (w/w)) mixed with cells’ respective cell media, over multiple time periods (2, 6, 12, 24, and 48 hours). The cellular response of the three cells lines were analyzed by observing their cell morphology as well as through live/dead™ and XTT assays.

6.2 Materials and Methods

6.2.1 Materials

Over the counter poly(ethylene glycol), with a molecular weight of 3350 g/mol (PEG 3350), was purchased from EQUATE (Ahmadi, Kuwait).

Primary human (*Homo sapiens*) stomach (Hs.738/Int), small intestine (HIEC-6), and colon cells (CCD-18Co) were purchased from ATCC (Manassas, VA). Dulbecco's Modification of Eagle's Medium, 1X (DMEM) with 4.5 g/L glucose, L-glutamine and sodium pyruvate was purchased from Corning (Manassas, VA) for human stomach cells. Opti-MEM I (1X) reduced serum medium with HEPES, 2.4 g/L sodium bicarbonate, and L-Glutamine was purchased from Life Technologies Corporation (Grand Island, NY) for human small intestine cells. Eagle's Minimum Essential Medium (EMEM) with Earle's salt, L-Glutamine, and sodium bicarbonate was purchased from Sigma-Aldrich (St. Louis, MO) for human colon cells.

Fetal bovine serum (FBS), fungizone, and penicillin/streptomycin (P/S) were purchased from HyClone (Logan, UT). HEPES buffer (1M solution) was purchased from Mediatech, Inc. (Manassas, VA). GlutaMAX-I (100X) was purchased from Life Technologies Corporation (Grand Island, NY). Epidermal growth factor (Human, Recombinant) (EGF) was purchased from Discovery Labware, Inc. (Bedford, MA). A 0.25% trypsin/ethylenediamine tetra-acetic acid (EDTA) was purchased from Gibco (Grand Island, NY). Dulbecco's phosphate buffer solution (DPBS) was purchased from VWR Life Sciences (Sanburn, NY).

Ethidium Homodimer I (Eth-D) and was purchased from Invitrogen (Grand Island, NY) and calcein AM purchased from Biotium (Fremont, CA). XTT Cell Viability Assay Kit was purchased from Biotium (Fremont, CA). 200 proof ethanol and deuterated oxide were purchased from Burdick and Jackson (Deer Park, TX).

6.2.2 Cell culture

Cells were cultured according to manufacturer's suggestion with some adaptations made by our research group to optimize the cells' performance.¹⁵³⁻¹⁵⁵ Briefly, human stomach cells (HSCs) were cultured in DMEM, supplemented with 10% FBS, 1% P/S, and 1% fungizone. Human small intestine cells (HSIs) were cultured in Opti-MEM, supplemented with 30 ng/mL EGF, 10% FBS, 1% P/S, and 1% fungizone. Human colon cells (HCCs) were cultured with EMEM supplemented with 10% FBS, 1% P/S, and 1% fungizone. All cell lines were incubated at 37° C in an 80-100% humid atmosphere with 5% CO₂. When 80% confluent, the cells were detached from the cell culture flask using 0.25% trypsin/EDTA and redeposited into new flasks. Tests were conducted on cells from passage 2 up to 10.

6.2.3 Preparation of cell media/PEG 3350 solutions

PEG 3350 was weighed to make 1%, 5%, 10%, 15%, 20% (w/w) solutions for cell growth. Before adding the various weight volumes of PEG 3350 to the cell media, we exposed PEG 3350 to UV-light (~254nm) for five minutes to ensure the polymer continues to be sterile and cytotoxicity are not a result of bacterial contamination. After UV-light exposure, PEG 3350 was added to cell media (DMEM 1X, Opti-MEM, and EMEM) to make the 1%, 5%, 10%, 15%, and 20% (w/w) solutions.

6.2.4 PEG 3350 direct contact test

The cellular response to direct contact of PEG 3350 was evaluated by observing the cells' morphology. Cells were seeded at 1.0×10^5 cells per well in a 48-well plate then given 24 hours to adhere and grow prior to exposure to experimental protocol. At that time, the normal cell media were exchanged for cell media with PEG 3350 (1-20% w/w), negative (cell media

without PEG 3350), and positive controls (a 70% ethanol solution). Exposure times were 2, 6, 12, 24, and 48 hours.

6.2.5 Cell morphology

After exposure at specified time points, images for all the cell lines were obtained using 20x objective lens on a Nikon Eclipse TS200F inverted microscope (Nikon Instruments, Melville, NY) and a SPOT Insight color mosaic digital camera (Diagnostic Instruments, Sterling Heights, MI).

6.2.6 Live/dead assay

The procedure for live/dead assay follows those previously completed in our group and outlined by Cooperstein *et al.*⁶⁶ A combined solution similar to those produced by ThermoScientific was made by adding 1 μ L of 2 mM calcein AM, and 1 μ L of 2 mM ethidium homodimer to every 1 mL of DPBS. After exposure to experimental protocol, cells were removed from incubation and cell media, cell media with PEG 3350, and ethanol were replaced with working live/dead solution. Cells were incubated at 37° C and 5% CO₂ with live/dead solution for 45 minutes and then rinsed with sterile DPBS prior to imaging. Fluorescent images were taken on a Nikon Eclipse TS200F inverted microscope at 20X with an epifluorescence attachment (Nikon Instruments, Melville, NY) and a SPOT Insight color mosaic digital camera (Diagnostic Instruments, Sterling Heights, MI).

6.2.7 XTT metabolic assay

XTT cell viability was purchased from Biotium (Fremont, CA). The procedure for XTT was adapted from the procedures provided by the manufacturer.¹⁵⁶ A working solution of XTT was prepared by adding 50 μ L of activated XTT (Biotium solution + activation reagent) to every 10 mL of XTT solution. XTT solution and cell media were used at a 1:1 ratio. After cells were

exposed to PEG treatments, cells were removed from incubation, and cell media/ethanol/experimental conditions were replaced with working XTT solution. Cells were incubated for six hours with working XTT solution and then removed for absorbance measurements at 475 and 600 nm (background) with a SpectraMax M5 microplate reader (Molecular Devices, San Jose, CA). A blank control was included, in which XTT working solution was added to the column and incubated for six hours for sample background measurements.

Viability was calculated with this equation:

% Viable Cells

$$= \frac{\text{Sample Absorbance (475 nm)} - \text{Sample Background (660 nm)}}{\text{Negative Control Absorbance (475 nm)} - \text{Negative Control Background (660 nm)}} * 100$$

6.2.8 XTT data analysis

A one-way analysis of variance (ANOVA) was used to determine whether any statically significant differences occurred between treatments at each time point. Accompanied by ANOVA, a Levene's homogeneity of variances test, and a Kolmogorov-Smirnov were completed to ensure the assumptions of ANOVA were true. If the assumption of homogeneity could not be rejected, a follow up using the Welch test was completed. A Tukey's HSD test was used post-hoc following ANOVA to test the statistical significance between treatment groups at each time point. Statistical analysis was completed utilizing RealStats Excel-Add In.

6.3 Results and Discussion

6.3.1 Cell Morphology

The relative cytotoxicity of PEG 3350 toward mammalian gastrointestinal tract cells was examined via observation of cellular morphology after exposure to increasing concentrations

of PEG 3350 (1%, 5% [the current therapeutic dosage], 10%, 15% and 20%) at multiple time points (2, 6, 12, 24, and 48 hours exposure) using bright-field microscopy.

These time frames were chosen as they are the relative time points at which food travels through the different parts of the digestive system in a healthy human (see **Table 1**).¹⁵⁷⁻¹⁶¹

Specifically, solid and mixed foods are present in the stomach from 0-6 hours, the small intestine from 3-6 hours, and the colon from 4-72 hours (average times are 30-40 hours).¹⁵⁷⁻

161

Figure 6.1 shows human stomach cells (HSCs) exposed to 1%, 5%, 10%, 15%, and 20% PEG

| <i>Course of digestion</i> | <i>Time Elapsed</i> |
|---------------------------------------|---------------------|
| 50% of stomach contents emptied | 2.5-3 hours |
| Total emptying of the stomach | 4 to 6 hours |
| 50% emptying of the small intestine | 2.5 to 3 hours |
| Total emptying of the small intestine | 3 to 6 hours |
| Transit through the colon | 30 to 40 hours |

Table 6.1. Average transit times in healthy humans following the ingestion of a standard meal (i.e. solid, or mixed foods).¹⁵⁷⁻¹⁶¹

3350 at 2, 6, 12, 24, and 48 hours. The results of cellular response to PEG 3350 were compared to negative control (exposed to DMEM only, absent PEG 3350), as well as a positive control (a 70% ethanol solution). Examination of negative controls showed that the HSCs grew well at all time points, with spindle-shaped cells adhering to the culture substrate. Minimal cell detachment indicated by lighter, circular-shaped cells was observed in the negative control (DMEM) even at the longest time points.

In comparison, the positive control sample (far right column, 70% EtOH) had fewer adherent (spindle-shaped) cells, and more detached cells (circular shaped). The rounded cell shape indicated that the positive control (70% ethanol) was toxic toward the cells. In particular, short exposure time (2 hours) to the positive control showed a significant amount of cell death. Although the positive control surfaces did not appear (due to cell morphology) to completely kill the HSCs at all time points, they are likely dead, despite their spindle-shape. The lack of morphological changes seen after exposure to ethanol is due to EtOH's known capabilities and use as a fixative agent for mammalian cells.¹⁶²

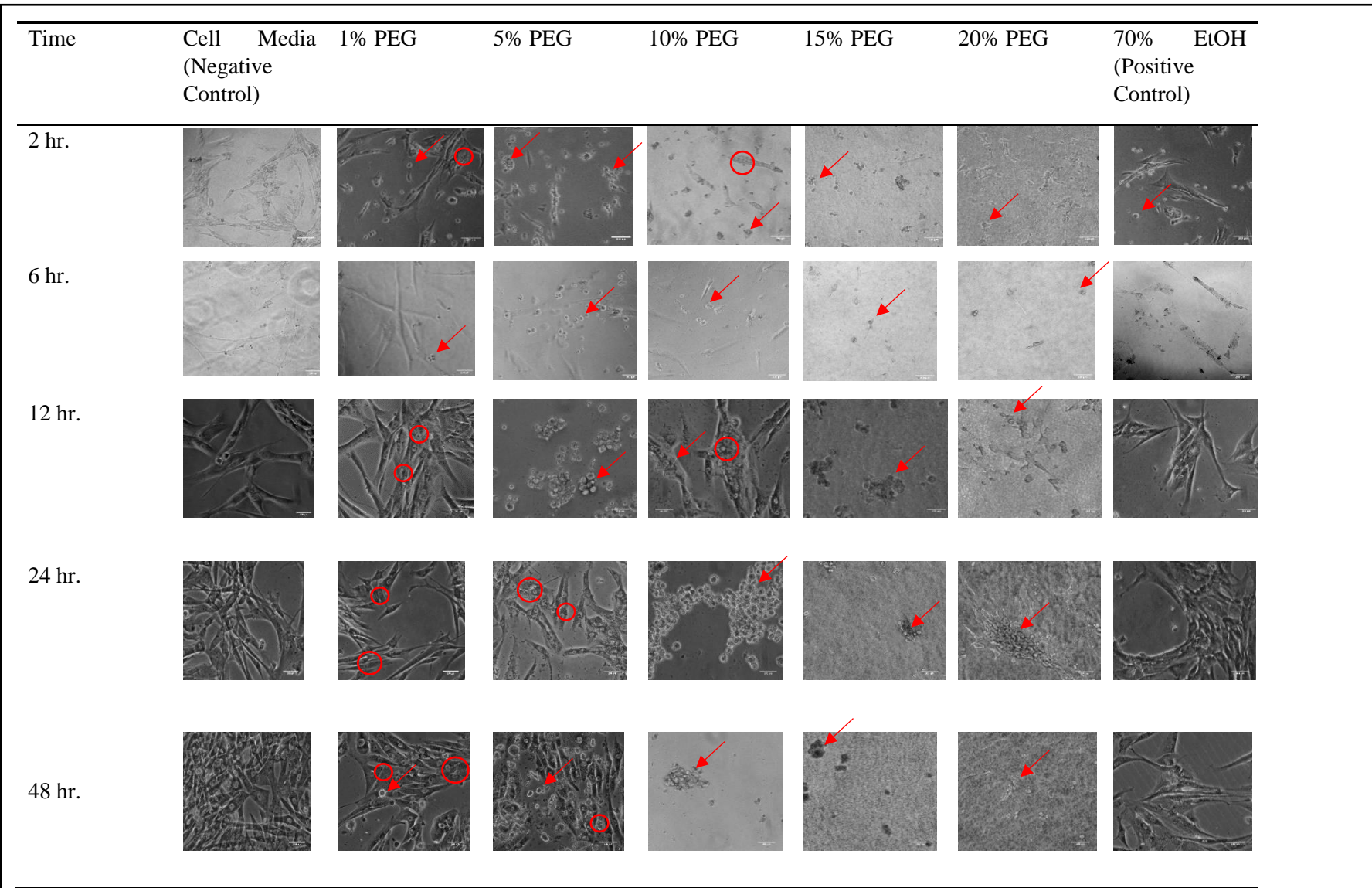


Figure 6.1. Cell morphology of human stomach cells. Bright field microscopy images of HSCs exposed to 1%, 5% 10%, 15%, and 20% PEG after 26, 12, 24, and 48 hours. From left to right, cell media control (negative), 1%, 5% 10%, 15%, and 20% PEG, and 70% EtOH (positive control). Red circles = intracellular bubbles. Red arrows = rounded cells, changed cell morphology. Scale bar = 200 μ m. N = 18.

HSCs exposed to 1% PEG 3350 (second column) continued to grow to confluency over time and did not appear to differ from their counterparts in the negative control (DMEM) from 2-24 hours. At 48 hours, HSCs grown in negative controls appear to be more rounded and less confluent than the negative control. At the therapeutic dosage of 5% PEG 3350, even more significant differences were observed. The cells' morphology at 5% PEG exposure was not the usual stellate shape (such as those in the negative controls at all time points). Instead, the cells in the "therapeutic dosage" of 5% PEG began to have a rounded appearance as early as 2 hours. After 24 hours, cells exposed to 5% PEG 3350 appeared to have intracellular "bubbles" or "holes" within the cell bodies (indicated by red circles). By 48 hours, the 5% PEG 3350 appeared to have more rounded cells (likely dead, indicated by red arrows) in comparison to the 1% solution, despite the 5% solution also continuing to grow spindle-shaped live cells. Furthermore, the remaining spindle-shaped live cells appear to contain intracellular "bubbles". These intracellular "bubbles" appear to be similar to those seen on fibroblasts exposed to cpNIPAM in **Chapter 2**. We believe that these "bubbles" are a result of cells forming vacuoles as it goes down the apoptotic pathway.

Cells exposed to 10% PEG 3350 had a decrease in number of cells as well as an increase in rounded shaped cells, indicative of death with similar formation of intracellular "bubbles". Observation of the cells exposed to 15% and 20% PEG 3350 (columns 5 and 6) appeared to have died within 2 hours of exposure and were detached from the cell culture plate. Later time points indicated similar results with no spindle-shaped cells seen. It appears that even at the current therapeutic dosage of ~5%, PEG 3350 can be cytotoxic to human stomach cells such as those in the human gastrointestinal system.

Figure 6.2 shows HSCs grown in different concentrations of PEG 3350 over increasing amounts of time. The cellular response to PEG 3350 was compared to the negative control (OPTI-MEM only, absent PEG 3350) and positive control (a 70% ethanol solution) similar to the analysis of HSCs. Examination of the response to the control samples indicated that the negative control grew accordingly with minimal cell death.

At low concentrations, cell morphology indicates that HSIIs are tolerating the 70% EtOH (positive controls, far right column) unfavorable conditions because the cells morphology was similar to those found in the cell media (negative control, far left column) from 2-12 hours. Beginning at 24 hours, the morphology of the positive control changed from the stellate shape to a rounded appearance. Again, this is expected due to EtOH's known capabilities as a fixative agent.¹⁶²

The cellular response to exposure to 1% PEG 3350 (second column) was similar to those found for the HSCs. The appearance of the cells did not differ from the negative control. From 2-48 hours at exposure to the therapeutic dosage at 5% PEG 3350, cells continued to appear healthy, with stellate formation similar to those found in the negative control.

Cell morphology changed dramatically after exposure to 10% PEG 3350. After 2 hours of exposure, the cells appeared to be less spindle shaped and more rounded (red arrows). As time increased, the cells became more circular and detached from the culture substrate. By 48 hours of exposure to 10% PEG 3350, no stellate-shaped cells were seen. Similar patterns of cell deaths were seen in HSIIs exposed to 15% PEG 3350. By 24 hours of exposure, no visible stellate-shaped cells were present. No changes to HSIIs viability were seen in 15% PEG 3350 exposure times of 48 hours. Exposure to 20% PEG 3350 appear to lead to cell death in HSIIs within 2 hours as no stellate-shaped cells were found at this time.

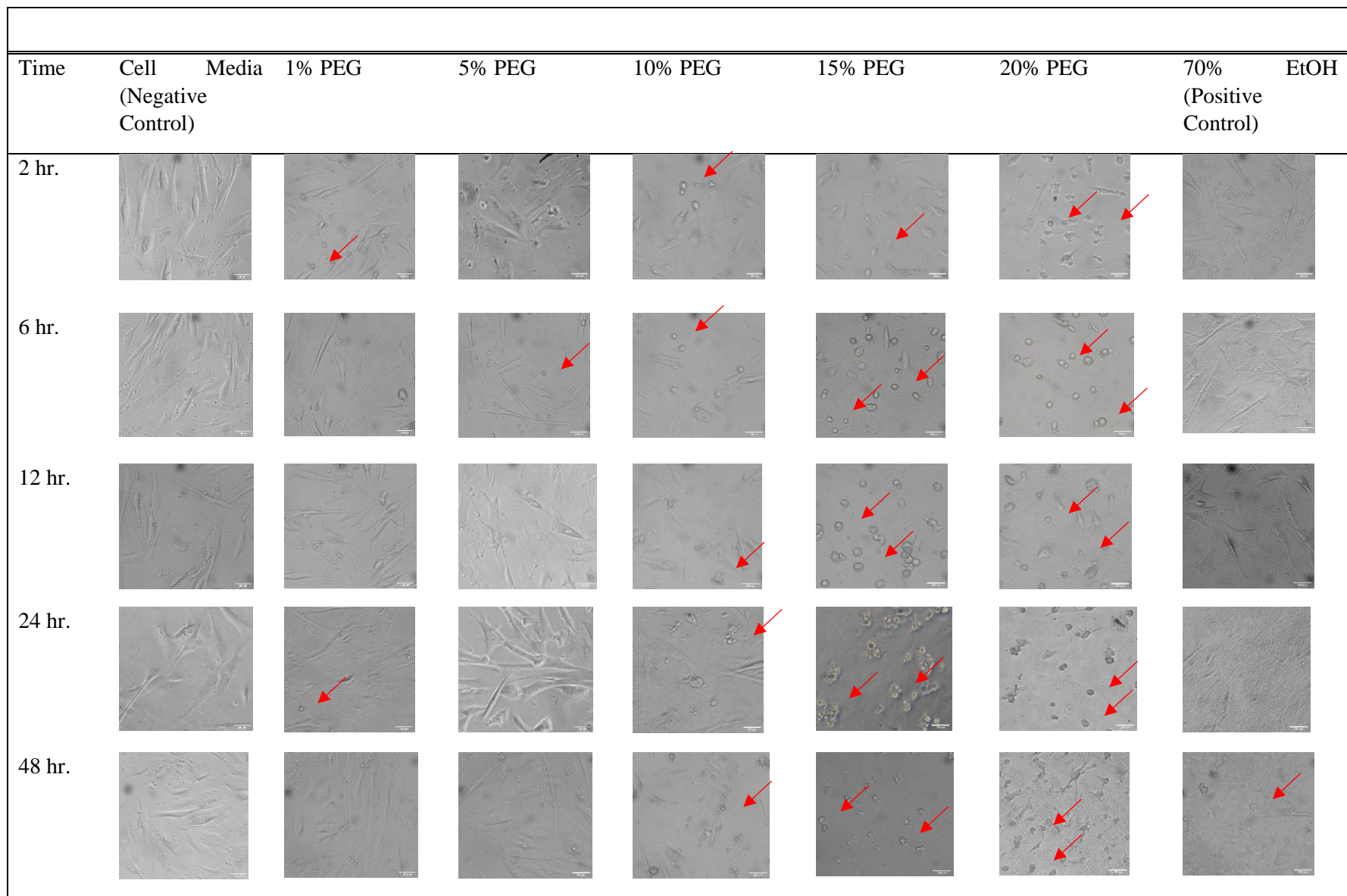


Figure 6.2. Cell morphology of human small intestine cells. Bright field microscopy images of HSIs exposed to 1%, 5% 10%, 15%, and 20% PEG after 26, 12, 24, and 48 hours. From left to right, cell media control (negative), 1%, 5% 10%, 15%, and 20% PEG, and 70% EtOH (positive control). Red arrows = rounded cells, changed cell morphology. No circles, as no intracellular bubbles were seen. Scale bar = 200 μ m.

Figure 6.3 shows the cell morphology of HCCs exposed to 1%, 5%, 10%, 15%, and 20% PEG 3350 over 2, 6, 12, 24, and 48 hours. The cellular response to PEG 3350 was compared to the negative control (EMEM only) and the positive control (a 70% ethanol solution). Examination of the response of the control samples indicated that the cells grown in EMEM with FBS (negative control) grew well at all time points, as expected. Similarly, the 70% EtOH (positive control) had few stellate-shaped cells, with large amounts of dead cells leading to blurriness at all time points.

The cellular response to exposure to 1% PEG 3350 exposure was similar to those found for HSCs and HSI, such that the appearance of cells did not differ from the negative control. After exposure to 5% PEG 3350, the cell morphology significantly changed through 2 to 12 hours. However, the live cells that were present recovered from the initial toxicity effects, grew to confluency, and appeared to be elongated and stellate like those found in the negative control by 24 hours of exposure. However, longer periods of exposure to 5% PEG 3350, such as 48 hours, saw a decrease in cell number and the remaining cells appeared to be more rounded with the appearance of some intracellular “bubbles” (as indicated by red circles).

After exposure to 10% PEG 3350, cells became more rounded and decreased in confluency even at the shortest exposure time of 2 hours. As exposure time increased, the negative effects increased with less stellate shaped cells, and more rounded shaped cells until 48 hours, where no stellate shaped cells were seen. Similar results were seen at exposure to 15% PEG 3350, however, no stellate shaped cells were seen, as early as 24 hours. Exposure to 20% PEG 3350 led to cell death as early 2 hours of exposure, with no stellate shaped cells found at this time. Cell detachment from the culture substrate occurred throughout the remaining time points.

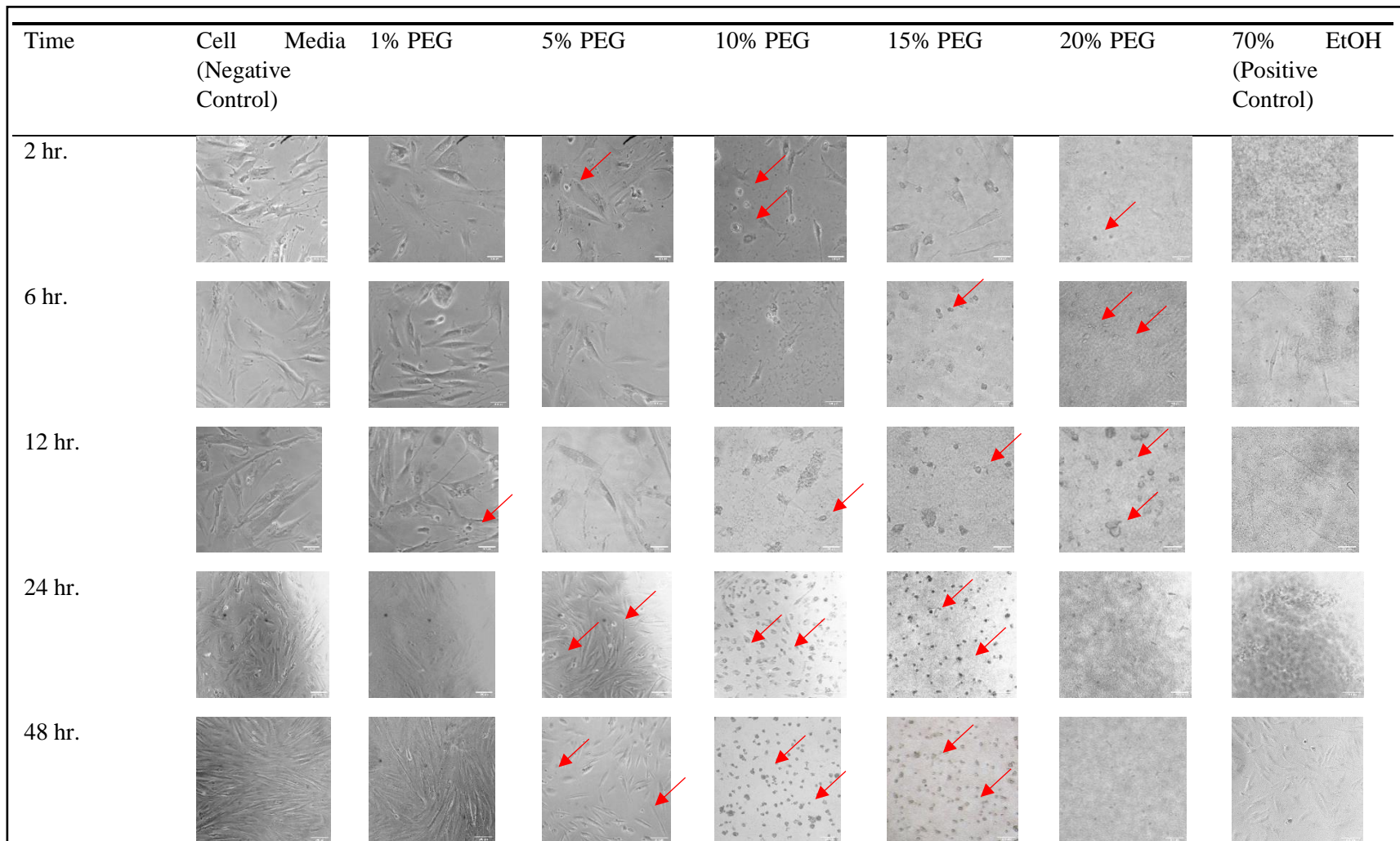


Figure 6.3. Cell morphology of human colon cells. Bright field microscopy images of HCCs exposed to 1%, 5% 10%, 15%, and 20% PEG after 26, 12, 24, and 48 hours. From left to right, cell media control (negative), 1%, 5% 10%, 15%, and 20% PEG, and 70% EtOH (positive control). Red arrows = rounded cells, changed cell morphology. No circles, as no intracellular bubbles were seen. Scale bar = 200 μ m. N = 18.

Overall, cell morphology showed that HCCs and HSCs were sensitive to PEG 3350 at therapeutic dosage (at 5% PEG 3350). HCCs' and HSCs' reactions were within physiologically relevant time frames, with HCCs' being affected as early as 24 hours, and HSCs' being affected as early as early as 2 hours. Intracellular "bubbles" were seen in HSCs and HSIIs at multiple time points and multiple concentrations, likely indicative of early cell death via apoptosis.

6.3.2 Live/dead assay

Figure 6.4 shows human stomach cells stained with calcein AM and Eth-D following exposure to 1%, 5%, 10%, 15%, and 20% PEG 3350 over 2, 6, 12, 24, and 48 hours. As with Figure 1, the negative control (DMEM only, absent PEG 3350) and positive control (a 70% ethanol solution) are presented at the far left and far right columns, respectively. Between, cells exposed to increasing concentrations of PEG from 1 to 20% are presented. Top to bottom are the time points from 2-48 hours.

Figure 6.4 shows that the cells exposed to minimal PEG 3350 (toward the left of the figure) for shorter time periods (toward the top of the figure) were the healthiest, as indicated by large amounts of green (live) cells. In addition, the cells' morphology appeared to be spindle-shaped, similarly to those exposed to cell media. Conversely, increasing concentrations of PEG 3350, and increasing exposure time resulted in more cell death, as shown by less green (live) fluorescence and more red (dead) fluorescence. The results of cellular response to PEG 3350 were compared to cell media (negative control) as well as to the 70% EtOH (positive control).

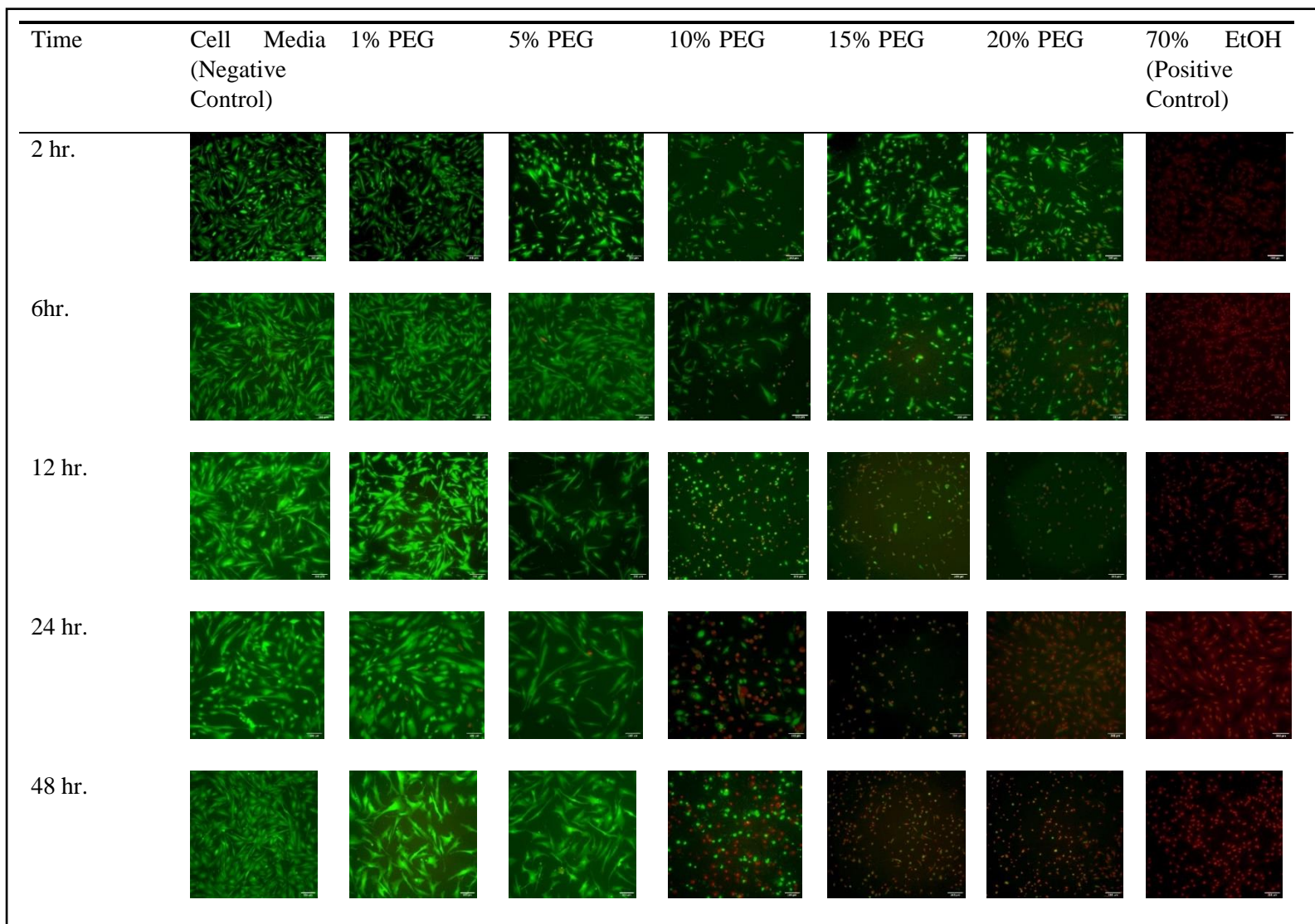
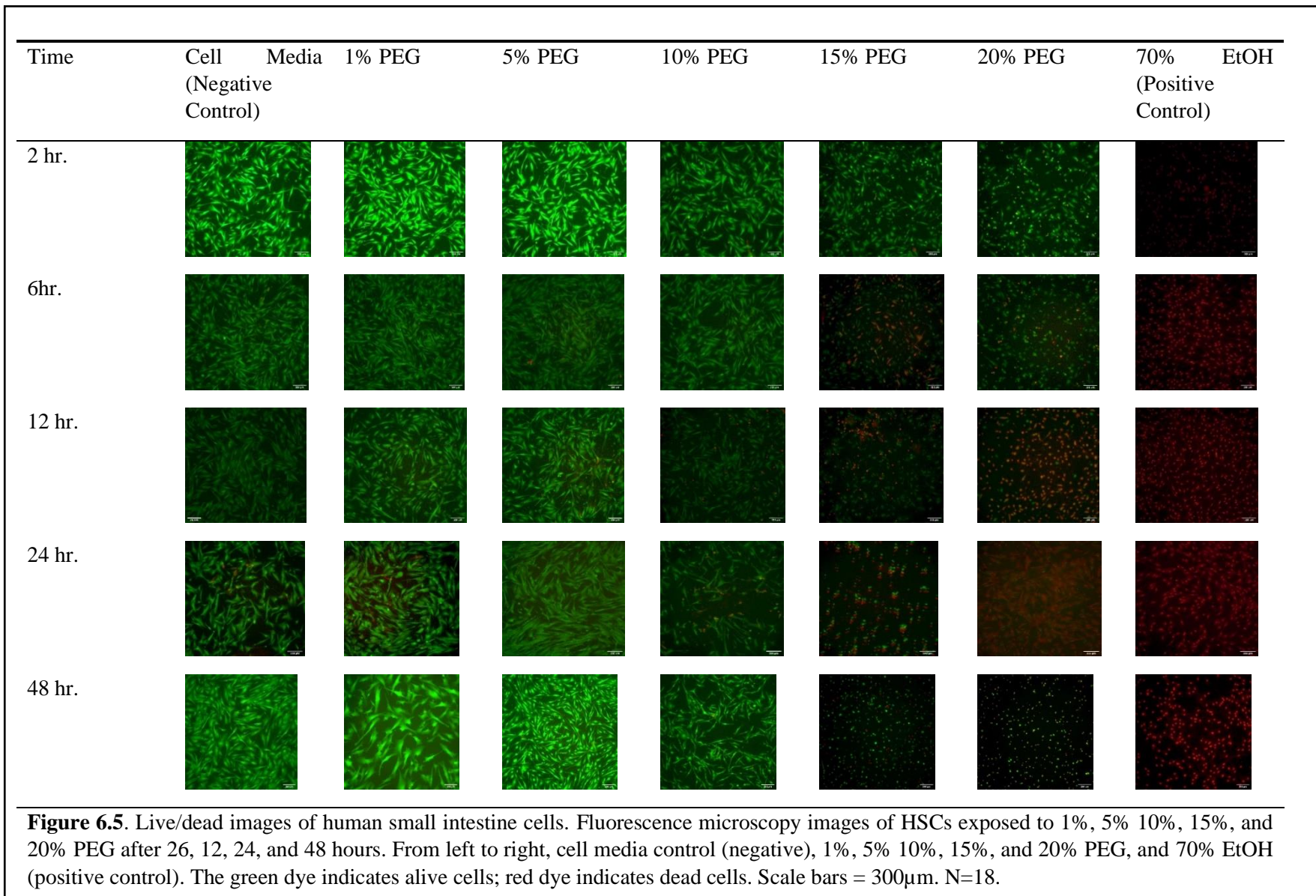


Figure 6.4. live/dead images of human stomach cells. Fluorescence microscopy images of HSCs exposed to 1%, 5% 10%, 15%, and 20% PEG after 26, 12, 24, and 48 hours. From left to right, cell media control (negative), 1%, 5% 10%, 15%, and 20% PEG, and 70% EtOH (positive control). The green dye indicates alive cells; red dye indicates dead cells. Scale bars = 300 μ m. N=18.

The results indicate that exposure to very low concentrations (1%) of PEG 3350 resulted in similar outcomes to the cell media (many live cells, with normal appearance), which is not indicative of cell death. However, after exposure to the therapeutic dosage (5%) PEG 3350 for 2 hours, the number of live cells decreased significantly, and the cells' morphology changed as well. Exposure to intermediate concentrations (10% and 15%) PEG 3350 resulted in similar outcomes with the exceptions that cell death (red dye) was apparent within 24 hours and that few live cells were visible. Complete cell death was seen after 48 hours of exposure to 10% and 15% PEG 3350. 20% PEG 3350 showed almost complete cell death at our shortest exposure time of 2 hours similar to those found in our positive controls.

The results from the live/dead assay indicate similar results found in our comparisons of cell morphology (**Figure 6.1**). Together with the previous results, this outcome indicates that very high concentrations of PEG 3350 resulted in extensive cell death within a physiologically relevant time range (2 hours). Furthermore, even lower concentrations of PEG (the therapeutic 5%) resulted in immediate changes to cell viability and morphology after 2 hours of exposure in HSCs.

Figure 6.5 shows human small intestine cells stained with calcein AM and Eth-D following exposure to 1%, 5%, 10%, 15%, and 20% PEG 3350 over 2, 6, 12, 24 and 48 hours. As with **Figure 6.4**, the negative control (Opti-MEM only, absent PEG 3350) and positive control (a 70% ethanol solution) are presented at the far left and far right columns, respectively. Between, cells exposed to increasing concentrations of PEG from 1 to 20% are presented. Top to bottom are the time points from 2-48 hours.



In comparison to the cell media (negative control), exposure to 1% PEG 3350 did not result in cell death. Even with exposure to the therapeutic (5%) concentration of PEG 3350, the cells appeared to grow similar to the negative control (confluent, alive). The differences in cellular response were not observed until exposure to 10% PEG 3350. At lower time points (2-12 hours), minimal cell death was seen. however, cell number is markedly decreased in comparison to those exposed to cell media control beginning at 24 hours. Exposure to 15% PEG 3350 had a dramatic decrease in confluency after 2 hours, with cell morphology less stellate, and rounder than those found in the cell media control. Cell death became apparent after 6 hours of exposure and on. Exposure to 20% PEG 3350 exposure produced the same results as seen for the cells exposed to 15% PEG 3350.

Figure 6.6 shows human colon cells stained with calcein AM and Eth-D following exposure to 1%, 5%, 10%, 15%, and 20% PEG 3350 over 2, 6, 12, 24, and 48 hours. As with **Figure 6.7**, the negative control (EMEM only, absent PEG 3350) and positive control (a 70% ethanol solution) are presented at the far left and far right columns, respectively. Between, cells exposed to increasing concentrations of PEG from 1 to 20% are presented. Top to bottom are the time points from 2-48 hours.

In comparison to the cell media (negative) control, exposure to 1% PEG lead to no obvious cytotoxicity effects observed in HCCs from the live/dead assay. The cells continue to grow to confluency, and cells remain stellate shaped and viable even after 48 hours of exposure to 1% PEG. However, beginning at the therapeutic dose of 5%, exposure to PEG 3350 leads to decrease in human colon cell number beginning at 12 hours. Even so, cells remain stellate shaped with no increase in dead cells as indicated by red stain at all time points until 48 hours (in which a small number of dead cells was observed).

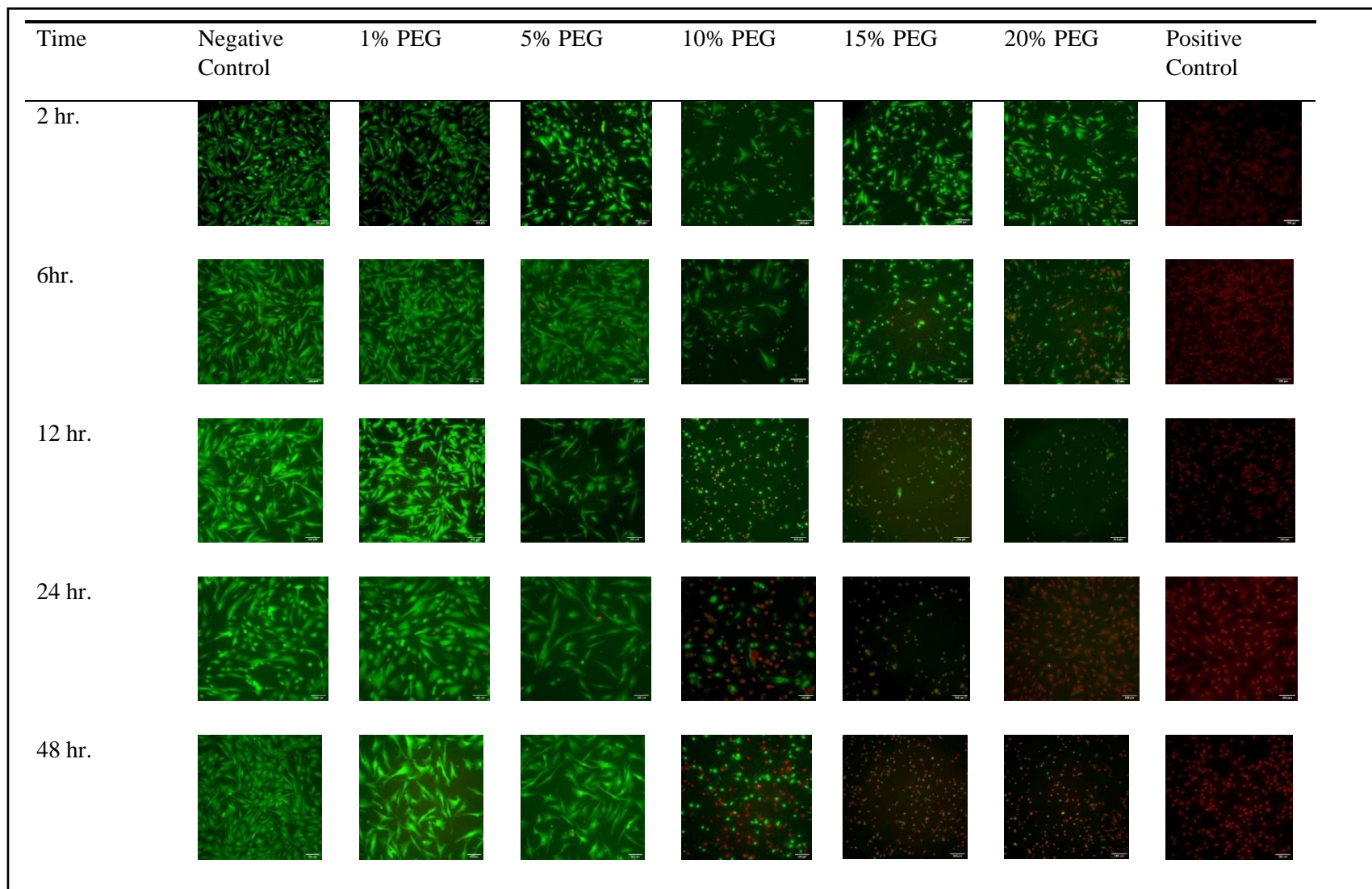


Figure 6.6. Live/dead images of human colon cells. Fluorescence microscopy images of HSCs exposed to 1%, 5% 10%, 15%, and 20% PEG after 26, 12, 24, and 48 hours. From left to right, cell media control (negative), 1%, 5% 10%, 15%, and 20% PEG, and 70% EtOH (positive control). The green dye indicates alive cells; red dye indicates dead cells. Scale bars = 300 μ m. N=18.

Exposure to higher concentrations of PEG 3350 such as 10% lead to an even bigger difference in comparison to the cell media (negative) control. There is a decrease in the number/confluency of HCCs' as early as after 2 hours of exposure. Not only that, a larger number of dead cells can be seen as soon as 12 hours, and this pattern continues until 48 hours. Similar patterns to exposure to 10% PEG 3350 are seen in HCCs exposed to 15% PEG 3350: there is a clear decrease in cell number/confluency. However, cells begin to die off at a shorter exposure time of 6 hours.

Unlike our findings utilizing cell morphology, it appears as if there are a number of live cells remaining after 2 hours of exposure to 20% PEG 3350. However, the total number of live cells is lower in comparison to the cell media (negative) control. By 6 hours, the majority of cells appear to die off and by 24 hours, the majority of cells are dead. No recovery is detected after 48 hours of exposure.

6.3.3 XTT metabolic assay

To confirm our findings, an XTT metabolic assay was performed on all the cell type from 2-48 hours to increasing concentrations of PEG 3350. **Figure 6.7** shows the results of HSCs exposed to increasing PEG concentrations at subsequent time points. The red bar in this figure marks 70% viability, below which solutions are considered to be cytotoxic toward cells.¹⁶³ ** indicates $p < 0.05$ between treatment condition vs positive control at every time point using Tukey's HSD.

Exposure to 1% PEG 3350 leads to a small decrease in cell viability at multiple time points, including at 12 and 48 hours. Even so, cell viability remains $>70\%$ at all time points (after 2 hours cell viability was $97.6 \pm 5.3\%$, after 6 hours cell viability was at $104.3 \pm 8.7\%$, after 12 hours cell viability was $82.6 \pm 7.2\%$, after 24 hours cell viability was $92.0 \pm 11.2\%$, and after 48

hours cell viability was $80.1 \pm 5.3\%$). Furthermore, these changes in cell viability are not statistically significant in comparison to the cell media (negative) control at all time points from 2-24 hours. At 48 hours, the difference was statistically significant, in which the p-value was 1.49×10^{-6} . However, viability is $>70\%$. As a result, exposure to 1% PEG 3350 can be

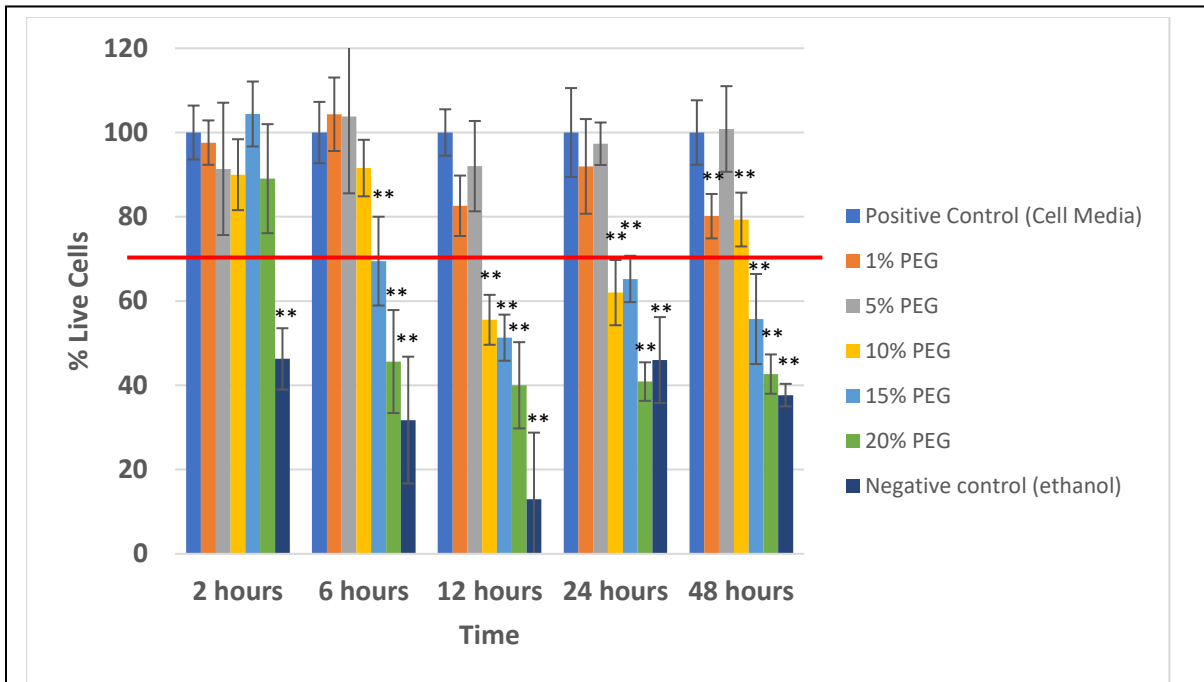


Figure 6.7. XTT metabolic assay of human stomach cells. XTT metabolic assay results from HSCs exposed to increasing concentrations of PEG 3350 over time. Red line indicates 70% cell viability, below which the solution is cytotoxic. ** indicates $p < 0.05$ between treatment condition vs positive control at every time point using Tukey's HSD. $N = 6$.

considered non cytotoxic to HSCs at all time points. This confirmed previous observations that exposure to 1% PEG 3350 is non-cytotoxic to HSCs as seen in from the cell morphology (**Figure 6.1**) and live/dead results (**Figure 6.2**).

Interestingly, similar cell viabilities were found in HSCs exposed to the current therapeutic dose at 5% PEG 3350. Cell viabilities were $>70\%$ at all time points, specifically they were $91.4 \pm 15.7\%$ after 2 hours, $103.8 \pm 18.2\%$ after 6 hours, $92.0 \pm 10.7\%$ after 12 hours, $97.3 \pm 5.0\%$ after 24 hours, and $100.8 \pm 10.1\%$ after 48 hours. Due to the cell high viabilities and standard

deviations, the differences between our cell media control and exposure to 5% PEG 3350 was not statistically significant at all time points. As such, based on XTT assay – exposure to 5% PEG 3350 is not considered to be cytotoxic to HSCs from 2-48 hours. This is similar to our findings utilizing cell morphology, but different from our findings using live/dead assay. This may be a result of differences in what the assays are measuring. As XTT assay rely on a mitochondrial reduction to convert the tetrazolium to formazan.^{94,156} If exposure to 5% PEG 3350 increases the enzymatic activity of the remaining cells, then the XTT assay will report a high cell viability even if there are less cells than those found in the media control.

By comparison, exposure to 10% PEG 3350 resulted in decreased cell viability within 12 hours of exposure. Specifically, exposure to 10% PEG 3350 lead to cell viabilities of 90.0±8.4% after 2 hours, 91.6±6.7% after 6 hours, 55.5±5.9% after 12 hours, 62.0±7.7% after 24 hours, and 79.3±6.8% after 48 hours. Changes in viability after exposure to 10% PEG 3350 was not statistically significant until 12 hours and beyond. Although there are drops in cell viability, the stronger cells appear to recover from the initial cell death. As such, exposure to 10% PEG 3350 can be considered borderline toxic to HSCs long term, although shorter exposure times lead to cytotoxic effects.

Exposures to 15% PEG 3350 is where clear cytotoxicity effects are seen, with cytotoxicity found as early as after 6 hours of exposure. Exposure to 15% PEG 3350 leads to HSC viabilities of 104.4±7.7% after 2 hours, 69.5±10.5% after 6 hours, 51.3±5.5% after 12 hours, 65.2±5.5% after 24 hours, and 55.7±10.7% after 48 hours. Decreases in cell viability do not recover and remain <70% at all time points after the first decrease after 6 hours of exposure. Furthermore, this decrease is statistically significant from the cell media (negative) control beginning at 6 hours, with p-values of 6.0×10^{-5} at 6 hours, 4.0×10^{-3} at 12 hours, 1.6×10^{-8} at 24 hours, and

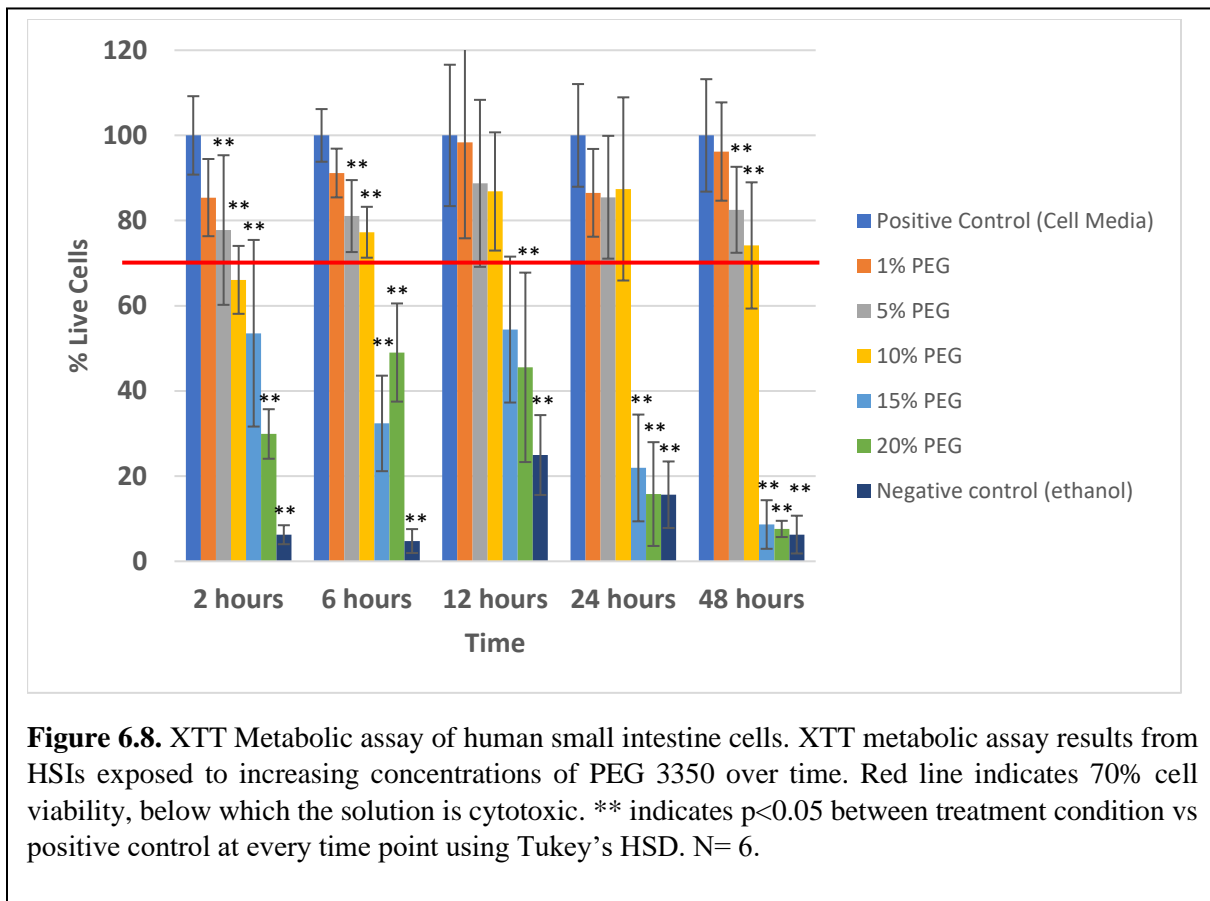
6.7×10^{-7} at 48 hours. 15% PEG 3350 is cytotoxic towards HSCs at exposure times of 6 hours and beyond.

XTT assay results of HSCs exposed to 20% PEG 3350 shows similar findings to those found at exposure to 15% PEG 3350 and previous findings about 20% PEG 3350 using cell morphology and live/dead assay. HSC has viabilities of $89.0 \pm 12.9\%$ after 2 hours, $45.6 \pm 12.2\%$ after 6 hours, $40.0 \pm 10.2\%$ after 12 hours, $40.9 \pm 4.6\%$ after 24 hours, and $42.7 \pm 4.7\%$ after 48 hours exposure to 20% PEG 3350. Again, decreases in cell viability do not recover and remain $<70\%$ at all time points after the first decrease after 6 hours of exposure. This decrease is statistically significant from the cell media (negative) control beginning at 6 hours, with p-values of 2.5×10^{-10} at 6 hours, 6.3×10^{-5} at 12 hours, 1.5×10^{-13} at 24 hours, and 2.0×10^{-14} at 48 hours. Exposure to 20% PEG 3350 is cytotoxic towards HSCs beginning at 6 hours and beyond.

The ethanol (positive) control confirms that the XTT assay is reliable as cell viabilities are $>70\%$ at all time points as expected. Exposure to ethanol leads to HSC viabilities of $46.3 \pm 12.9\%$ after 2 hours, $31.7 \pm 12.2\%$ after 6 hours, $13.0 \pm 10.2\%$ after 12 hours, $46.0 \pm 4.6\%$ after 24 hours, and $37.7 \pm 4.7\%$ after 48 hours exposure. This difference is statistically significant in comparison to the media (negative) control at all time points.

The XTT assay on HSCs show that, in general, although HSCs appear to experience some morphological differences at concentrations as low as 5% PEG 3350, metabolically, they do not behave differently and continue to metabolize ATP at a similar rate. In contrast, exposure to higher concentrations of PEG are statistically different from our negative control (DMEM) in a time period as short as 6 hours. ANOVA between the different treatment groups was significant at all time points.

The XTT metabolic assay was also performed on all HSI and HCCs. **Figure 6.8** shows the results of HSI exposed to increasing PEG concentrations for increasing time periods. The red bar in this figure marks 70% viability, below which solutions are considered to be cytotoxic toward cells.¹⁶³ ** indicates $p < 0.05$ between treatment condition vs positive control at every time point using Tukey's HSD.



Similar to the results found with HSCs, exposure to 1% PEG 3350 had no cytotoxic effects on HSI. Cell viabilities of HSI exposed to 1% PEG 3350 were $85.4 \pm 9.1\%$ after 2 hours, $91.2 \pm 5.7\%$ after 6 hours, $98.4 \pm 22.5\%$ after 12 hours, $86.5 \pm 10.3\%$ after 24 hours, and $96.2 \pm 11.5\%$ after 48 hours. The fluctuations in cell viability of HSI exposed to 1% PEG 3350 were not statistically different from those found in the cell media (negative) control at all time

points. 1% PEG 3350 can be considered non-cytotoxic to HSIs for exposure times up to 48 hours.

Exposure to 5% PEG 3350 leads to a decrease in metabolic activity in HSIs, though viability remains high, >70%. HSIs exposed to 5% PEG 3350 has viabilities of $77.8 \pm 17.6\%$ after 2 hours, $81.1 \pm 8.5\%$ after 6 hours, $88.7 \pm 19.6\%$ after 12 hours, $85.5 \pm 14.4\%$ after 24 hours, and $82.5 \pm 10.1\%$ after 48 hours. There is a small drop in viability initially, however, the remaining cells continue to grow and recover from the initial cytotoxic effects. This initial drop is statistically different from the cell media (negative) control indicating the effects are likely a result of exposure to PEG 3350. However, 5% PEG 3350 cannot be considered cytotoxic to HSIs as viability is >70% at all time points.

Similar results to 5% PEG 3350 are found with HSIs exposed to 10% PEG 3350. Exposure to 10% PEG 3350 leads to viabilities of $66.1 \pm 8.0\%$ after 2 hours, $77.3 \pm 6.0\%$ after 6 hours, $86.8 \pm 13.9\%$ after 12 hours, $87.4 \pm 21.5\%$ after 24 hours, and $74.2 \pm 14.8\%$ after 48 hours in HSIs. This initial drop is significant in comparison to the cell media control. As the cell viability is borderline 70%, exposure 10% PEG 3350 can only be considered borderline cytotoxic to HSIs.

Exposure to 15% PEG 3350 and 20% PEG 3350 causes clear cytotoxic effects in HSIs metabolism as soon as 2 hours, with cell viability <70%. HSIs exposed to 15% PEG 3350 has viabilities of $53.5 \pm 21.9\%$ after 2 hours, $32.4 \pm 11.2\%$ after 6 hours, $54.4 \pm 17.1\%$ after 12 hours, $21.9 \pm 12.5\%$ after 24 hours, and $8.6 \pm 5.7\%$ after 48 hours. HSIs exposed to 20% PEG 3350 has viabilities of $29.9 \pm 5.8\%$ after 2 hours, $49.0 \pm 11.5\%$ after 6 hours, $45.5 \pm 22.2\%$ after 12 hours, $15.8 \pm 12.2\%$ after 24 hours, and $7.6 \pm 1.9\%$ after 48 hours. At all time points, the difference in HSIs' viability after exposure to 15% PEG 3350 and 20% PEG 3350 is statistically different

from those found in the cell media (negative) control. Both concentrations of PEG 3350 are cytotoxic to HSI as early as 2 hours after exposure.

Figure 6.9 presents the % cell viability utilizing an XTT assay of HCCs after exposure to increasing concentrations of PEG 3350 at 2 hours, 6 hours, 12 hours, 24 hours, and 48 hours. As with **Figure 6.3 and 6.6**, the red line in **Figure 6.9** indicates 70% viability, below which solutions are cytotoxic toward cells. Similar to previous morphological and live/dead results, exposure to 1% PEG 3350 is non-cytotoxic towards HCCs at all time points. Cell viabilities were >70%, 116.5±14.7% after 2 hours, 82.3±13.3% after 6 hours, 88.8±6.8% after 12 hours, 93.4±6.2% after 24 hours, and 89.6±12.5% after 48 hours. Although cell viability decreases significantly at 6 hours, HCCs' viability remains above what is considered cytotoxic. At the

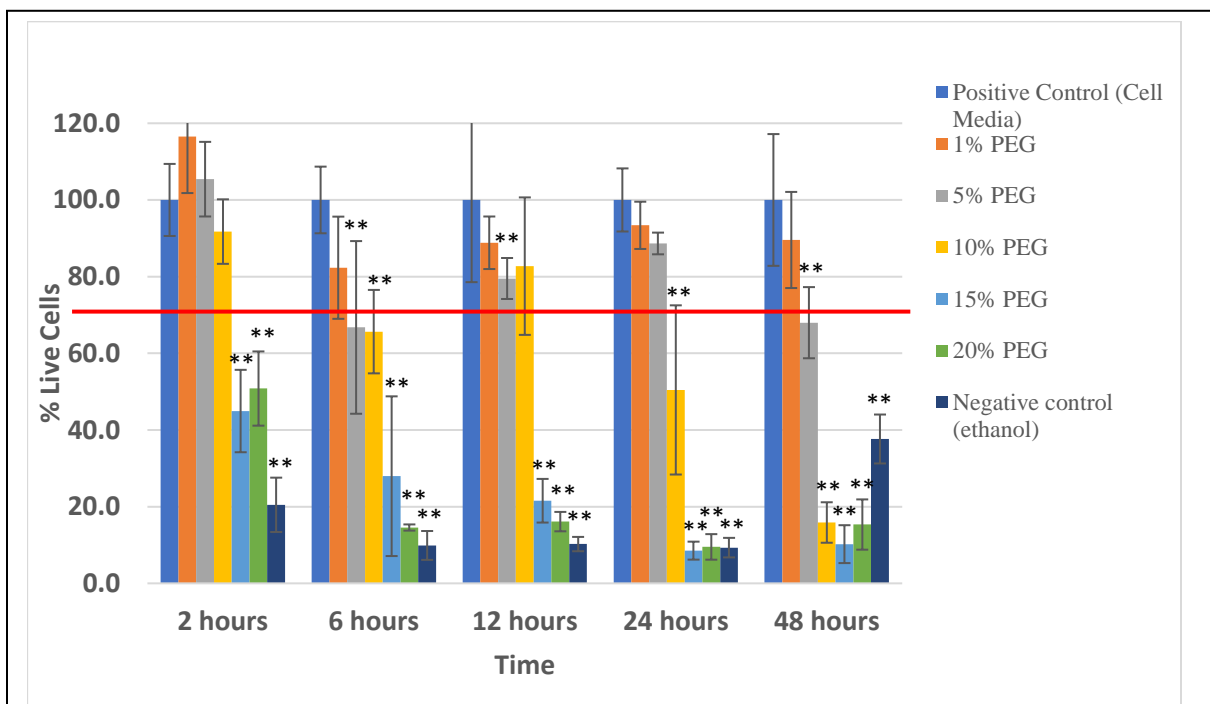


Figure 6.9. XTT Metabolic assay of human colon cells. XTT metabolic assay results from HCCs exposed to increasing concentrations of PEG 3350 over time. Red line indicates 70% cell viability, below which the solution is cytotoxic. ** indicates $p < 0.05$ between treatment condition vs positive control at every time point using Tukey's HSD. N= 6.

therapeutic dosage of 5% PEG, cells exposed to the shortest time period of 2 hours had a higher viability, but longer time periods of 6-48 hours show a significant decrease in viability that is at borderline toxicity at levels. HCCs exposed to 5% PEG 3350 has viabilities of $105.4 \pm 9.7\%$ after 2 hours, $66.8 \pm 22.5\%$ after 6 hours, $79.5 \pm 5.3\%$ after 12 hours, $88.6 \pm 2.8\%$ after 24 hours, and $68.0 \pm 9.3\%$ after 48 hours. The decrease in viability at 6 hours is significant with a p-value of 1.3×10^{-3} in comparison to the cell media (negative) control. Even so, cell viability of HCCs are ~70% or greater at all time points, which indicates that PEG 3350 is borderline cytotoxic in which some cytotoxic effects can be seen but is not deemed cytotoxic by the ISO-10993.

HCCs' exposure to higher concentrations of PEG 3350 leads to clearer signs of cytotoxicity. 10% PEG 3350 leads to HCCs' viability drop over time, with clear cytotoxicity seen beginning at 24 hours. Specifically, HCCs exposed to 10% PEG 3350 has viabilities of $91.7 \pm 8.4\%$ after 2 hours, $65.7 \pm 10.9\%$ after 6 hours, $82.7 \pm 17.9\%$ after 12 hours, $50.4 \pm 22.1\%$ after 24 hours, and $15.9 \pm 5.3\%$ after 48 hours. Tukey's HSD pairwise comparison shows that the difference between our cell media (negative) control and exposure to 10% PEG 3350 were significant at 6, 24, and 48 hours. This shows that there was a significant decrease in cell viability after initial exposure, but resilient cells were able to grow and withstand the initial cytotoxic effects. However, over time, even the resilient cells did not tolerate the growth conditions, and cytotoxic effects returned at longer term exposure times of 24 and 48 hours. Short term exposure of HCCs to 10% PEG 3350 leads to cytotoxic effects that can be overcome. Long term exposure (24 hours+) of HCCs to 10% PEG are cytotoxic.

Similar to results in cell morphology and live/dead, HCCs exposed to 15% PEG 3350 and 20% PEG 3350 are found to be cytotoxic utilizing the XTT assay. HCCs exposed to 15% PEG 3350 has viabilities of $44.9 \pm 10.7\%$ after 2 hours, $27.9 \pm 20.8\%$ after 6 hours, $21.6 \pm 5.7\%$ after 12

hours, $8.5 \pm 2.3\%$ after 24 hours, and $10.2 \pm 4.9\%$ after 48 hours. HCCs exposed to 20% PEG 3350 has viabilities of $50.8 \pm 9.7\%$ after 2 hours, $14.6 \pm 0.8\%$ after 6 hours, $16.1 \pm 2.5\%$ after 12 hours, $9.5 \pm 3.3\%$ after 24 hours, and $15.3 \pm 6.6\%$ after 48 hours. At all time points, the difference in HCCs' viability after exposure to 15% PEG 3350 and 20% PEG 3350 is statistically different from those found in the cell media (negative) control with viabilities of $<70\%$. Both concentrations of PEG 3350 are cytotoxic to HSCs as early as 2 hours after exposure.

In HSCs, XTT assay results indicate that cells remain viable until they are exposed to PEG3350 at concentrations of 10% or greater for long periods of time, often beyond the time it takes for foods to pass through the stomach. However, morphological changes, decrease in confluency, and the number of live cells could be seen at the therapeutic dosage of 5% as early as 2 hours and continue to 48 hours. Specifically, pore formation – or intracellular “bubble” formation can be seen in HSCs at the therapeutic dosage of 5% at 2 hours. As seen in **Chapter 2**, this is possibly apoptotic (programmed cell death) response of fibroblastic cell types to cytotoxic conditions.

HSCs exposed to XTT assay show no cytotoxicity following exposure to 1% PEG 3350. However, exposure to 5% and 10% PEG 3350 lead to borderline cytotoxic effects, in which viabilities' hover $\sim 70\%$. At concentrations of $>15\%$ PEG 3350, cell viability significantly decreases, and PEG 3350 is considered cytotoxic. Similar results are found using cell morphology and live/dead where some changes in cell morphology and cell viability is seen at the therapeutic dose of 5% and 10% PEG 3350. However, it isn't until 15% PEG 3350 and higher in which confluency, cell morphology, and live/dead assay clearly shows a cytotoxic effect. This shows that HSCs are more resistant to cytotoxic effects caused by exposure to PEG 3350 than HCCs.

Exposure of HCCS to increasing concentrations of PEG 3350 have similar outcomes to those found with HSIs. However, foods and drinks remain in the colon for much longer than HSIs. As a result, it is important to note that although viability hovers ~70% for the therapeutic dosage of 5% from 20-40 hours, going above it and exposing HCCs to 10% PEG 3350 or greater for 20-40 hours will cause cytotoxicity. Similar trends are found using cell morphology and live/dead assay where lower concentrations lead to cell death and morphological changes.

6.4 Conclusions

Though long considered to be a biocompatible polymer due to its acceptance by the FDA, PEG 3350 *does* appear to negatively affect the morphology and viability of human stomach and intestinal cells. Although exposure to 5% PEG 3350 and 10% PEG 3350 cannot be considered cytotoxic at relevant time frames to all cell lines within the human digestive system, cytotoxic effects are seen with small changes in cell morphology as well as a decrease in cell viability as measured by XTT in all cell types.

The cytotoxic effects were observed at the current therapeutic dosage of an assumed perfectly mixed solution of 5%. Importantly, one of the primary complaints about the GI preparation method is that the solution can be improperly mixed due to its high viscosity. In such cases, it is possible that higher concentrations (up to 20%) could be experienced in the GI tract of a patient.

These results indicate that, contrary to the belief on the safety of PEG 3350, cytotoxic effects may be experienced from the current preparation method. Furthermore, these results may explain why some patients (especially women, children, the elderly, and others with low body mass) experience more negative symptoms from GI preparation than healthy adult men. To prevent such negative outcomes, the current dosage should be re-evaluated, and ensured to

always be less than 5%. It will be essential to develop a method for providing accurate dosage utilizing height, weight, and other physical characteristics related to the patient and correlate it with the data of PEG 3350 to improve patient compliance and outcomes following a colonoscopy preparation.

Chapter 7: Developing a pH responsive hydrogel for the delivery of PEG 3350 within the human gastrointestinal tract

Manuscript in preparation for publication by Nguyen, P.A.H.*; Cuylear, D.*; Mounho, S.; and Canavan, H.E.

*indicates equal author contribution

Abstract

Oral administration of drugs is the most ideal choice of drug delivery due to its simplicity, convenience, and high rate of patient acceptance. However, orally delivered drugs are exposed to a relatively inhospitable environment that can affect pharmaceutical absorption. Furthermore, drugs travelling through the gastrointestinal tract will experience different transit times and environmental conditions leading to early breakdown. Many drugs such as PEG 3350 (discussed in **Chapter 6**) used for osmotic laxatives are often described as “foul tasting,” making them difficult to ingest. These factors frequently lead to reduction in patient compliance. Hydrogels are ideal as drug delivery systems due to their ability to protect drugs, proteins, and peptides from the environment – preventing drugs from being degraded prior to delivery at their ideal site. Natural polymers are optimal candidates for hydrogels as they are known to be non-toxic and are currently already FDA approved for use in food products. Hydrogels have been fabricated out of these known natural polymers such as alginate, and chitosan. In this work, we use chitosan, and sodium alginate using a one-step procedure to create a system that will allow for the delivery of PEG 3350 into the stomach. We confirmed that elemental composition of the hydrogels via XPS. Hydrogel networks’ stability following exposure to solutions of physiologically relevant pH, as well as gastric simulation fluid were confirmed via rheology. Hydrogels are pH-responsiveness and PEG release at physiologically

relevant conditions (as evidenced by weight change, spectrometry of rhodamine-labelled PEG). We showed that the leachate from the hydrogels contains only PEG (not any other component of the hydrogel, or contaminants) using NMR. Finally, we showed that the optimal concentration of PEG to be loaded hydrogels for drug delivery is 15% PEG (w/w).

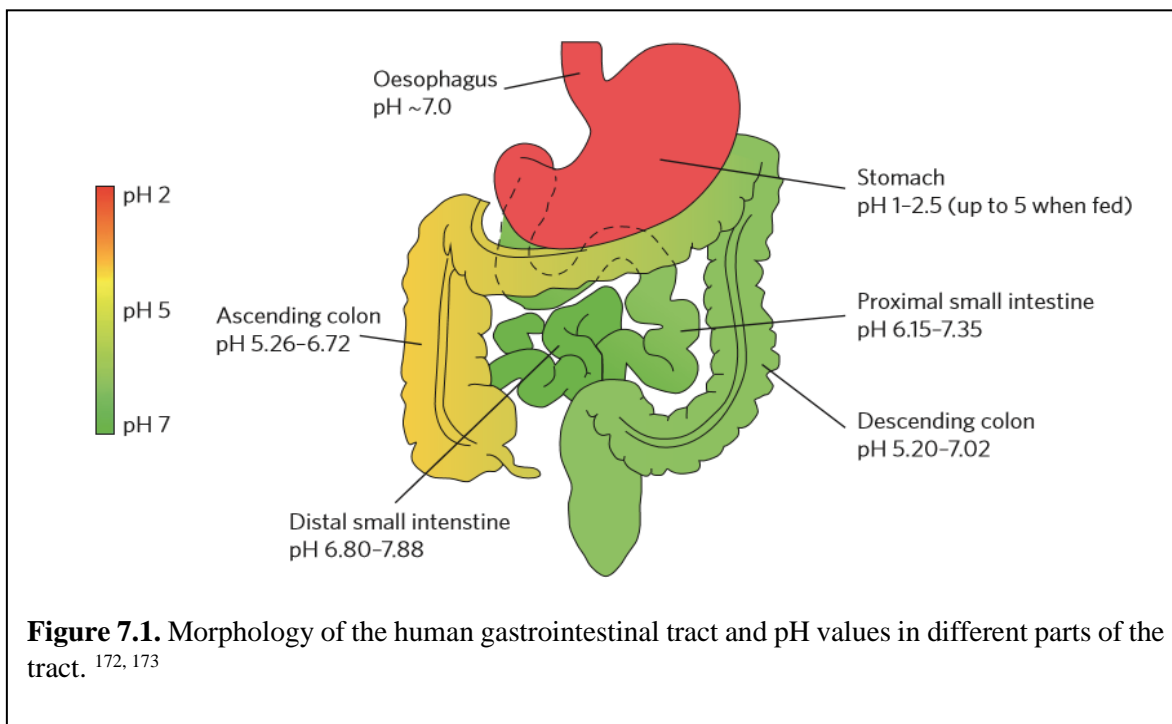
When compared to the traditional technique for GI prep (GoLyteLy™), this technique affords several distinct advantages, such as the ability to precisely and predictably tailor the dosage of PEG to the needs of the patient, preventing the potentially cytotoxic effects seen in **Chapter 6**.

7.1 Introduction

Oral administration of drugs is the most ideal choice of drug delivery due to its simplicity, convenience, and high rate of patient acceptance.¹⁶⁴ Patient non-compliance is often associated with injections of protein and peptide molecules, whereas oral administration improves the bioavailability of poorly water soluble drugs and reduces adverse effects associated with chemotherapy.^{165,166} Furthermore, oral drug formulations have benefits both for the physician and the industry, including flexible dosing schedules, reduced demands on staff, reduced costs through fewer hospital or clinic visits, and less expensive production.¹⁶⁶⁻¹⁶⁸

However, orally delivered drugs are exposed to a relatively inhospitable environment that can affect pharmaceutical absorption. Drugs travelling through the gastrointestinal tract will experience different transit times and environmental conditions (determined by the pH, the water content, and the presence of enzymes and live bacteria, **see Figure 7.1.**)^{169,170} Exposure to these conditions can result in deactivation of protein medications and cell death of probiotics – decreasing the bioavailability of drugs in the GI tract.^{166,171,172} In addition, many drugs such as PEG 3350 (discussed in **Chapter 6**) used for osmotic laxatives are often described as “foul

tasting,” making them difficult to ingest. This frequently leads to reduction in patient compliance.

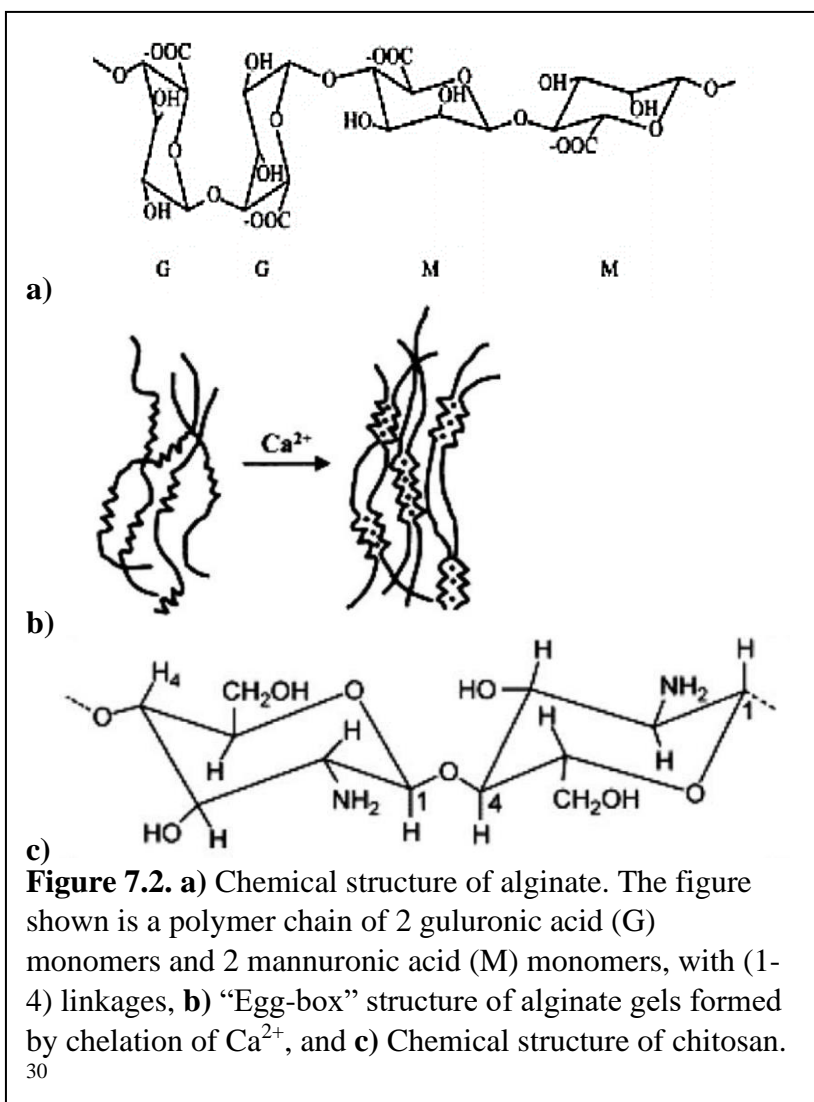


To overcome these problems, researchers have been focusing on stimulus-responsive hydrogels that are capable of responding to pH,¹⁷³⁻¹⁷⁶ ionization,^{171,177-179} temperature,^{180,181} glucose,^{182,183}, etc. Hydrogels are three-dimensional hydrophilic networks composed of homopolymers or copolymers absorbing large quantities of water without dissolution. Hydrogels have attracted much attention in recent years for drug delivery due to their softness, hydrophilicity, superabsorbancy, viscoelasticity, biodegradability, biocompatibility and their similarity with extracellular matrix.¹⁷⁶ Furthermore, hydrogels are ideal as drug delivery systems due to their ability to protect drugs, proteins, and peptides from the environment – preventing drugs from being degraded prior to delivery at their ideal site.¹⁸²

However, current formulations capable of producing great site-specificity have depended on the use of synthetic molecules that are toxic at high concentrations.^{182,184,185} Other systems

depend on nanomaterials that have been found to be digested prior to arrival at the site.¹⁸⁶ Natural polymers are ideal candidates for hydrogels as they are known to be non-toxic and are currently already FDA approved for use in food products. Hydrogels have been fabricated out of these known natural polymers such as alginate,¹⁸⁷⁻¹⁹⁰ and chitosan.^{187,191,192}

Alginate is a water-soluble natural biopolymer extracted from brown algae and composed of alternating blocks of 1-4 α -L-guluronic and β -D-mannuronic acid residues (see **Figure 7.2a**). This polymer forms hydrogels in presence of divalent cations like Ca^{2+} , Ba^{2+} , Sr^{2+} , and Zn^{2+} and this characteristic allows preparing drug loaded beads.^{193,194} The mechanism of this gelation



process involves the exchange of sodium ions from the guluronic acids with the divalent cations, stacking these guluronic groups to form an "egg box structure" as seen in **Figure 7.2b**.¹⁹³ Chitosan is a linear polysaccharide composed of D-glucosamine and N-acetyl-D-glucosamine units linked by β -(1-4) glycosidic linkages (see **Figure 7.2c**).^{189,191} Chitosan is

commonly found in chitin shell of crustaceans such as crab and shrimp. To obtain chitosan, ground shells are deproteinated and demineralized by sequential treatment with alkali and acid, after which the extracted chitin is deacetylated to chitosan by alkaline hydrolysis at high temperatures. Production of chitosan from these sources is inexpensive and easy.¹⁹³ Furthermore, chitosan is a biocompatible, biodegradable, and nontoxic that is already commonly used in food and is approved by the FDA.¹⁹³ All of these properties make it an ideal candidate as a natural polymer for use in hydrogels and other materials.

Alginate shrinks in low pH (<3) systems and is soluble at higher pH (>6), making this polymer ideal for targeted small intestine delivery. This effect is a result of alginate's carboxyl group's pK_a which is 3.5. This allows the carboxyl to become less viscous as pH increases. Chitosan exhibits a pH-sensitive behavior as a weak poly-base and dissolves easily at low pH (<3) while it is insoluble at higher pH ranges. Together, they create a more stable system at pH ranges of 4-6, that is pH responsive at low pH such as those found in the stomach yet dissolves at higher pH such as those found in the small intestine.¹⁹⁵ Cross-linking of alginate and chitosan in a hydrogel provide materials useful for medical and pharmaceutical applications as the obtained system is characterized by enhanced stability compared to those obtained with a single polymer.¹⁹⁵ The two polymers form the polyelectrolyte complex via the ionic interaction between the carboxyl residues of alginate and the amino residues of chitosan.¹⁹⁵

Hydrogels can be produced by two different methods: utilizing a two-step procedure or a one-step procedure.¹⁹⁶ In the two-step method, calcium alginate hydrogel beads are produced by dropping a solution of alginate into a gelling bath containing calcium ions. The beads are then transferred into a chitosan solution to form a membrane on the surface of the hydrogels. In the

one-step procedure, droplets of alginate solution fall into an aqueous solution containing both the gelling agent for alginate (e.g., calcium ions) and chitosan.¹⁹⁷

In this work, we use chitosan, and sodium alginate using the one-step procedure to create a system that will allow for the delivery of PEG 3350 into the stomach. Our approach is to make a set of hydrogels that are palatable, safe, and can encapsulate poly(ethylene glycol) (PEG) 3350 and deliver them to the stomach and small intestine within the gastrointestinal system to achieve its function as an osmotic laxative while reducing commonly found side effects in current preparations.

7.2 Materials and Methods

7.2.1 Materials

Poly(ethylene glycol), with a molecular weight of 3350 g/mol (PEG 3350), was purchased from EQUATE (Ahmadi, Kuwait). Sodium alginate from cultivated sea kelp was purchased from Cape Crystal (Far Hills, NJ). Chitosan was purchased from BulkSupplements.Com (Henderson, NV). Calcium Chloride was purchased from Will Powder (Miami Beach, FL). Acetic Acid – 100% was purchased from KMG Electronic Chemicals Inc. (Fort Worth, TX). 10.0 N Sodium hydroxide and 1.0 N Hydrochloric acid were purchased from Millipore Sigma (Burlington, MA). Deuterated acetic acid (Acetic acid-d₄) was purchased from Sigma-Aldrich (St. Louis, MO). 100 ml Burette was purchased from VWR (Radnor, PA). Sodium taurocholate, Pepsin (1:10,000), lecithin and sodium chloride were purchased from VWR (Radnor, PA). Rhodamine labeled-PEG 3350 was purchased from Creative PEGWorks (Durham, NC). NMR tubes were purchased from Wilmad Labglass (Vineland, NJ)

7.2.2 Sodium alginate and PEG 3350 solution

Sodium alginate was weighed to 1% (w/v) and added to milli-q water. The alginate solution was given time (~one night) to dissolve. After the alginate solution dissolved, PEG 3350 was weighed to make 1%, 5%, 10%, 15%, and 20% (w/w) and added to the 1% (w/v) alginate solution, independently.

7.2.2 Chitosan purification

Chitosan was purified from a previous protocol with some adaptations made by our research group.¹⁹⁸ Briefly, chitosan was dissolved with 0.1M acetic acid, then precipitated using sodium hydroxide, then rinsed with Millipore water. This process is repeated 3x to create purified chitosan. Purified chitosan was weighed out to make a 0.1% (w/v) and added to milli-q water. Calcium chloride was weighed out to make a 3% (w/v) solution and was added to the chitosan/milli-q water solution. Acetic acid was added to the solution and adjusted to make a 0.005 M solution.

7.2.3 Hydrogel formation

50 mL of the purified chitosan solution was added to a beaker. ~15-20 mL of the sodium alginate/PEG 3350 solution was added to a 100 mL burette. The sodium alginate/PEG 3350 solution stayed in the burette for ~15 minutes to allow the air bubbles to rise out of the solution. The sodium alginate/PEG 3350 solution was titrated into the chitosan solution. The formed hydrogel complex stayed in solution for 30 minutes to ensure full cross-linking of the components. After 30 minutes, the hydrogels were taken from the solution and rinsed in milli-q water three times before taken for XPS, rheology, and other experiments.

7.2.4 X-ray photoelectron spectroscopy (XPS)

Hydrogels were lyophilized with Labconco's 2.5 Plus Freezone lyophilizer (Kansas City, MO) for 24 hours prior for use in XPS. Survey spectra of the lyophilized hydrogels were taken at

the Department of Chemistry and Biotechnology at Swinburne University of Technology using a Kratos Axis Nova instrument (Kratos, UK). This instrument has a monochromatized Al X-ray source (source energy of 1486.69 eV) at a power of 150W. All samples were run as insulators meaning the electron flood gun was used. Pass energy for survey spectra (composition) was 160 eV with a step size of 1eV. High resolution spectra were collected at a pass energy of 20eV and a step size of 0.1eV. For the high-resolution Cls spectra all binding energies were referenced to the Cls C-C bonds at 285.0 eV. A detail scan was run for N, C, and O to improve quantification. Data analysis was carried out using Casa XPS. A number of constraints were placed due to high resolution Cls spectra between sample differences. Constraints of FWHM for C-C was 0.5, 13, C-N/C-O was 0.5, 13.5, and for O-C-O/C=O was 0.3, 8.5

7.2.5 Rheology

All rheological studies were conducted using a rotational stress rheometer MCR 300 (Paar Physica) by parallel plate geometry with 1 mm gap. The experiments were carried out mainly in the two following modes:

Amplitude sweep oscillations in the range of strains from 0.01% to 200% at the constant angular frequency of 10.0 rad/s (~1.59 Hz). The deviation from linear viscoelastic behavior in this experiment is named the large-amplitude-oscillation-shear regime of deformations determining the strain for the frequency sweep measurements.

Frequency sweep measurements were taken from 600 rad/s to 0.5 rad/s at 2.0% strain of hydrogels. Hydrogels were exposed pH = 1, pH = 4, pH = 7, or GSF for 30 minutes prior to each run. 3 runs were completed per hydrogel type and pH/GSF condition.

7.2.6 Degradation of hydrogels

In order to test the degradation stability, the hydrogels were placed in individual wells containing 500 μL of pH solutions 1-8, fasted state gastric simulation fluid (GSF), and small intestine simulation fluid (SISF). These solutions were chosen to simulate the variety of conditions that hydrogels could be exposed to in drinks as well as those found in the stomach, and small intestine. At the time of the experiment, the well-plates containing the hydrogels were at room temperature, and weight was measured in 30-minute intervals until reaching 60 minutes (GSF and SISF) or 120 minutes (pH = 1-8). The degradation of the hydrogels was then investigated measuring the weight change in % using Equation (7.1) where W_f and W_i are the final weight and initial weight respectively.

$$\text{Weight change (\%)} = 100 + \left(\frac{W_f - W_i}{W_i} * 100 \right) \text{ (Equation 7.1)}$$

Acidic pH solutions were made by adding hydrochloric acid to milli-q water (pH 1-4). Basic pH solutions were made by adding sodium hydroxide to milli-q water (pH 5-8). After making the pH solutions.

7.2.7 Simulated gastric and small intestine fluids

Fasted-state gastric simulation fluid (GSF) and small intestinal simulation fluid (SISF) were made according to a previous protocol.¹⁹⁹ Briefly, fasted-state GSF was made by supplementing milli-q water with 80 μM sodium taurocholate, 20 μM lecithin, 34.2 mM sodium chloride, and 0.1 mg/mL of pepsin. The pH of solution was adjusted to 1.6 with hydrochloric acid. Fasted-state intestinal fluid was made by supplementing milli-q water with 3 mM sodium taurocholate, 0.2 mM lecithin, 19.12 mM maleic acid, 34.8 mM sodium hydroxide, 68.62 mM sodium chloride. The pH was adjusted to 6.5 by adding sodium hydroxide.

7.2.8 Release of PEG functionalized with Rhodamine

PEG-functionalize with rhodamine 6G were encapsulated in increasing concentrations of 1%, 5%, 10%, 15%, and 20% (w/w) using alginate/chitosan and CaCl₂. The PEG-rhodamine hydrogels were then placed into the fasted-state gastric and intestinal simulation fluids (GSF and SISF) for 120 minutes. At 30-minute intervals, the hydrogels were taken out and the solution was read using a plate reader with emission set at 450, excitation at 500, and readings were taken every 10 nm until 700 nm was reached. After the plate reading, the hydrogels were replaced back into solution for continued analysis. Readings were taken in three conditions, experimental conditions (exposure to GSF or SISF), control conditions (no hydrogels, blank), and maximal conditions (hydrogels crushed in GSF and SISF to ensure maximal release). To determine the amount of % PEG released, Equation (7.2) was used where λ_E , λ_C , and λ_{max} represents the wavelengths found in the experimental conditions (exposure to GSF, or SISF), control conditions (no hydrogels, blank), and maximal conditions (hydrogels crushed) respectively.

$$W\% \text{ PEG Released} = \frac{\lambda_E(580) - \lambda_C(580)}{\lambda_{max}(580) - \lambda_C(580)} * 100 \text{ (Equation 7.2)}$$

7.2.9 PEG 3350 release in gastric and small intestine simulation fluid

A single hydrogel containing different concentrations of PEG 3350 (1,5,10,15, and 20% [w/w]) were placed in 1 mL of each simulation fluid for 60 minutes. Every 10 minutes the hydrogel was taken from the simulation fluid and weighed. After being weighed, the single hydrogel was replaced back into its respective simulation fluid.

7.2.10 NMR characterization of leachate

Single hydrogels of each concentration of PEG 3350 (1,5,10,15,20% [w/w]) were placed in deuterated acetic acid (pH 2.14) for 120 minutes. Every 30 minutes the hydrogel was taken out

and placed in new deuterated acetic acid solutions. The leachate (old solution) was transferred to NMR tubes for analyzation.

NMR was used to confirm release of only PEG 3350 in solution. The NMR spectra of the leachate were taken at the University of New Mexico (UNM) Nuclear Magnetic Resonance facility with an Advance III NMR spectrometer (Bruker, Billerica, MA). It is a 300 MHz, standard bore, nanobay instrument. Spectra were obtained on a 5 mm broadband/proton probe, at room temperature, using deuterated acetic acid as a solvent.

7.3 Results and Discussion

In the previous chapter, we demonstrated that PEG 3350 at higher concentrations is toxic to human gut cells at short-term and long-term exposure. Furthermore, we explored the consequences this has in clinical use. As mentioned, PEG 3350 is commonly used as an osmotic laxative that is a one-size-fits all solution for many patients who undergo a colonoscopy preparation. However, patients who are elderly, female, or generally smaller in stature tend to experience more significant side effects associated with the preparation including palatability as well as nausea, vomiting, abdominal pain, etc. We hypothesize these smaller and/or more sensitive individuals are not able to withstand the higher concentration of PEG 3350 than their gastrointestinal system permits.

In this work, we evaluate a potential solution to the problem by creating and testing pH responsive hydrogels that can deliver PEG 3350 to the stomach. As the PEG 3350 is encapsulated in the hydrogel, patients do not have to taste the preparation. Furthermore, this method allows for the opportunity to search for a weight appropriate dose, in which patients can get different numbers of hydrogels, based on their weight and height. The hydrogels were created with increasing concentrations of PEG to identify the ideal amount of PEG that could

be encapsulated using this method (the concentration of alginate and chitosan were kept constant). After they were created, the hydrogels were first evaluated using XPS to ensure that there were no contaminants in our process. Rheological measurements of the hydrogels following exposure to GSF, pH = 1, 4, and 7 solutions to test its physiological response in comparison to previous studies. Weight loss measurements of hydrogels were taken to evaluate drug release following exposure to acidic and basic solutions over 2 hours. This series of experiments were then followed by weight loss measurements of hydrogels following exposure to GSF and SISF over 2 hours. Additional studies of drug release were completed with PEG functionalized with rhodamine to determine the percentage of drug released. Finally, to confirm that the hydrogel is releasing only PEG, hydrogel leachates were taken following exposure to deuterated acetic acid and evaluated using NMR.

7.3.1. X-ray photoelectron spectroscopy (XPS)

| | 1% PEG | 5% PEG | 10% PEG | 15% PEG | 20% PEG |
|-----------|-----------|-----------|-----------|-----------|-----------|
| C | 73.5±3.4% | 71.9±3.2% | 72.2±2.1% | 75.8±2.2% | 72.3±2.4% |
| O | 15.0±2.2% | 18.3±1.0% | 19.2±1.4% | 20.3±1.9% | 21.4±1.3% |
| Si | 4.8±0.6% | 0.5±0.4% | 0.7±0.2% | 1.0±0.2% | 0.3±0.5% |
| Ca | 2.5±0.5% | 2.8±0.3% | 3.1±0.2% | 1.7±0.1% | 2.7±0.7% |
| Cl | 4.2±1.2% | 6.0±3.2% | 4.8±0.6% | 2.7±0.7% | 3.4±1.8% |

Table 7.1. XPS survey spectra results of hydrogels loaded increasing concentrations of PEG 1%-20% (w/w).

The surface chemistry of these hydrogels was accessed by X-ray photoelectron spectroscopy (XPS). **Figure 7.3a and 7.3b** show the results of preliminary data of survey and high resolution C1s spectra for all five types of hydrogels as the concentration of PEG increases, as well as the composition of the hydrogels as predicted from the stoichiometry of the outer shell of the hydrogels.

Figure 7.3a indicates that our hydrogels loaded with 1% PEG (w/w) contains less O and more Si than is expected. [Note: as this anomaly is only present in the 1% PEG sample, this is likely the result of an attempt to crush the lyophilized hydrogels using a mortar and pestle; contamination of the pestle by silicone and/or PDMS may have led to contamination of these samples.] As visual inspection of the 1% samples that had been crushed in this manner also had anomalous appearance, following this initial attempt, all of the remaining hydrogel samples were not crushed prior to XPS.

The hydrogels loaded with 5% PEG have elemental composition of 71.9% C, 18.3% O, 0.5% Si, 2.8% Ca, and 6.0% Cl. 10% PEG loaded hydrogels have elemental composition of 72.2% C, 19.2% O, 0.7% Si, 3.1% Ca, and 4.8% Cl. Hydrogels loaded with 15% PEG and 20% PEG have elemental compositions of 75.8% C, 20.3% O, 1.0% Si, 1.7% Ca, and 1.3% Cl; and 72.3% C, 21.4% O, 0.3% Si, 2.7% Ca, and 3.4% Cl respectively. The elemental composition of these samples are consistent despite increasing PEG concentration, as is evident in **Figure 7.3** and **Table 7.1**. The only difference that is statistically significant is that of the atomic percentage of oxygen for the 5% vs. 20% PEG ($p = 0.03$ when subjected to student t-test); this result is of interest, as the lower dose (5%) was shown to be tolerated by all cell types in **Chapter 6**, whereas the higher dose (20%) was not. Furthermore, the results of all PEG %s are relatively consistent with that predicted from the stoichiometry of the copolymer (alginate and chitosan) combination (51.6% C, 0.8% N, 43.7% O, and 4.0% Ca). The difference is likely due to the presence of adventitious carbon, as well as salt ions introduced during the production process of the hydrogels. Nitrogen was expected at only trace concentrations ($<1.0\%$), which is at the detection limit of the instrument for Nitrogen (0.5-1.0%).⁴⁸

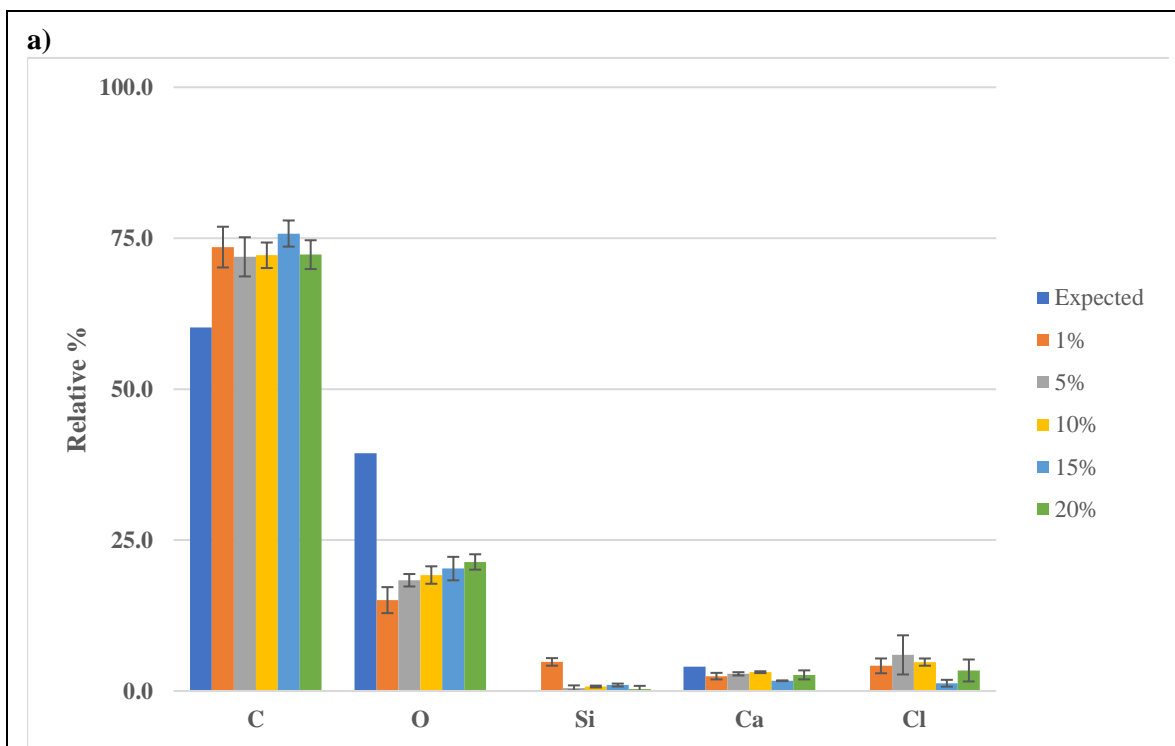


Figure 7.3. a) Surface chemistry of alginate-chitosan hydrogels loaded with PEG by XPS. In part a), the atomic % of carbon, oxygen, silicon, calcium and chlorine are shown for hydrogels loaded with 1% PEG (orange), 5% PEG (grey), 10% PEG (yellow), 15% PEG (light blue), and 20% PEG (green). The theoretical composition of alginate-chitosan hydrogels as calculated from the chitosan-alginate outer shell is shown for comparison. N = 3.

Figure 7.3b shows the high resolution C1s spectra for hydrogels loaded with 1% PEG, 5% PEG, 10% PEG, 15% PEG and 20% PEG. The high-res spectra show that the carbon-carbon peaks are difficult to deconvolute with large deviations within samples as well as between samples. Hydrogels loaded with 1% PEG show the carbon species consist of 39.5% C-C, 43.8% C-O/C-N, and 16.8% O-C-O/C=O. Hydrogels loaded with 5% PEG, 10% PEG, 15% PEG, and 20% PEG show the carbon species breakdown to be 30% C-C, 35% C-O/C-N, and 36% O-C-O/C=O; 33% C-C, 39% C-O/C-N, and 29% O-C-O/C=O; 27% C-C, 49% C-O/C-N, and 24% O-C-O/C=O; and 42% C-C, 43% C-O/C-N, and 14% O-C-O/C=O respectively. Statistically, there is no difference between the molecular environment of carbon for any of the samples. The C1s carbon environment of the PEG samples differ from the expected theoretical

values of 83.3% C-O/C-N and 16.7% O-C-O/C=O. This is most likely due to the low sample number (n) as well as the extremely low %N (<1.0%) mentioned previously that overemphasize the error computed. It should also be noted that the peak envelope observed for the C1s data varied widely between samples (see **Figure 7.4**). These results could be due to either: a) the dehydration required to achieve high vacuum to perform XPS, or b) the insulating nature of polymers. (Explained below)

Biological and other samples are known to deform due to dehydration when placed under high

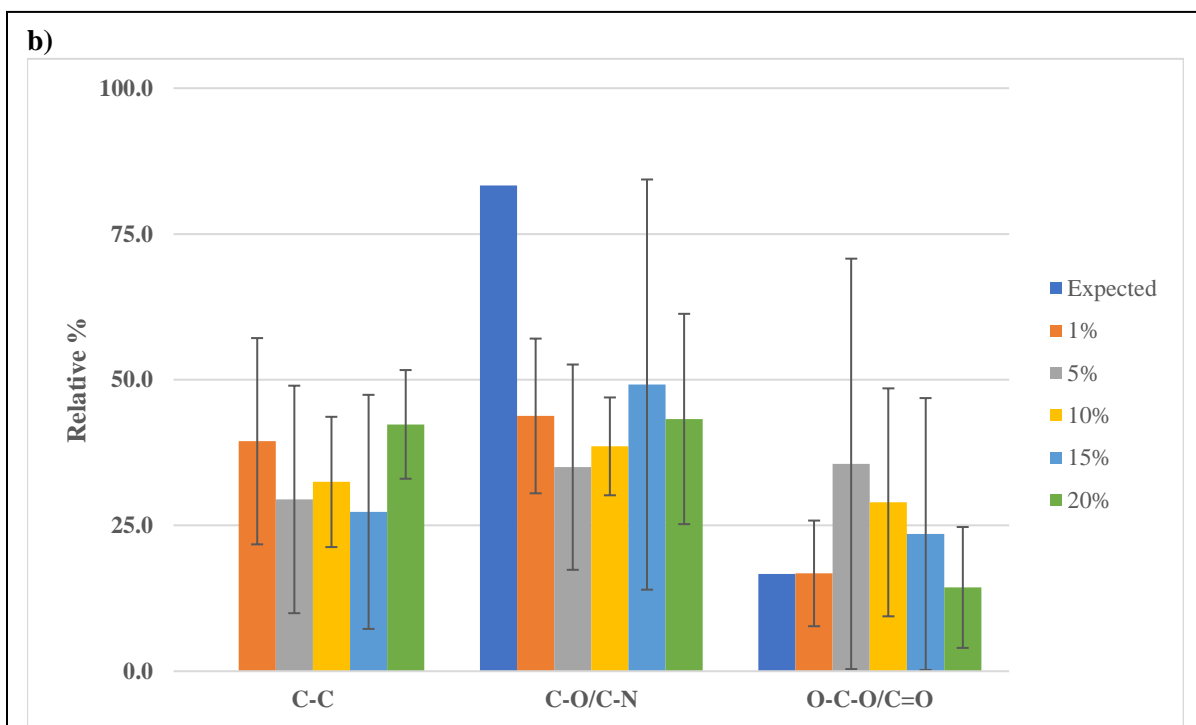
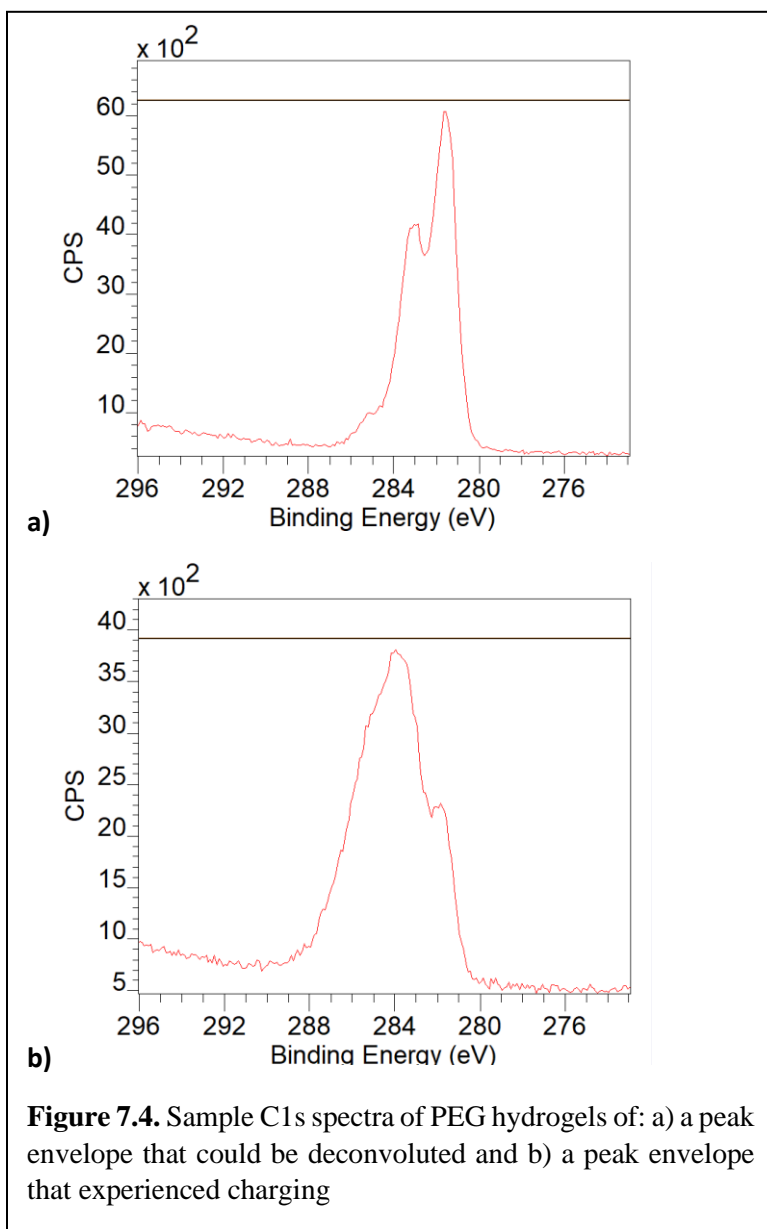


Figure 7.3. b), the high resolution carbon species (C-C/C-H, C-OH/C-N, and N-C=O) are shown shown for hydrogels loaded with 1% PEG (orange), 5% PEG (grey), 10% PEG (yellow), 15% PEG (light blue), and 20% PEG (green). The theoretical composition of alginate-chitosan hydrogels as calculated from the chitosan-alginate outer shell is shown for comparison. N = 3.

vacuum can be seen in **Figure 7.5**. Lyophilization (freeze-drying) was used to prepare the hydrogels for analysis in the high vacuum environment. As a result of the rapid dehydration, the structure of the hydrogel may simply collapse (Figure 7.5, left side), or a fracture may be introduced (Figure 7.5, right side). The event experienced by the hydrogel (collapse vs.

fracture) will cause different regions of the hydrogels to be available for sample analysis (as the escape depth for XPS is ~50-100 Angstroms). In this case there is spillage/leakage of the encapsulated PEG and, as a result, the PEG core is analyzed. For a collapsed (or non-fractured hydrogel), the chitosan/alginate shell will be analyzed, resulting in increased %N, C-N, and



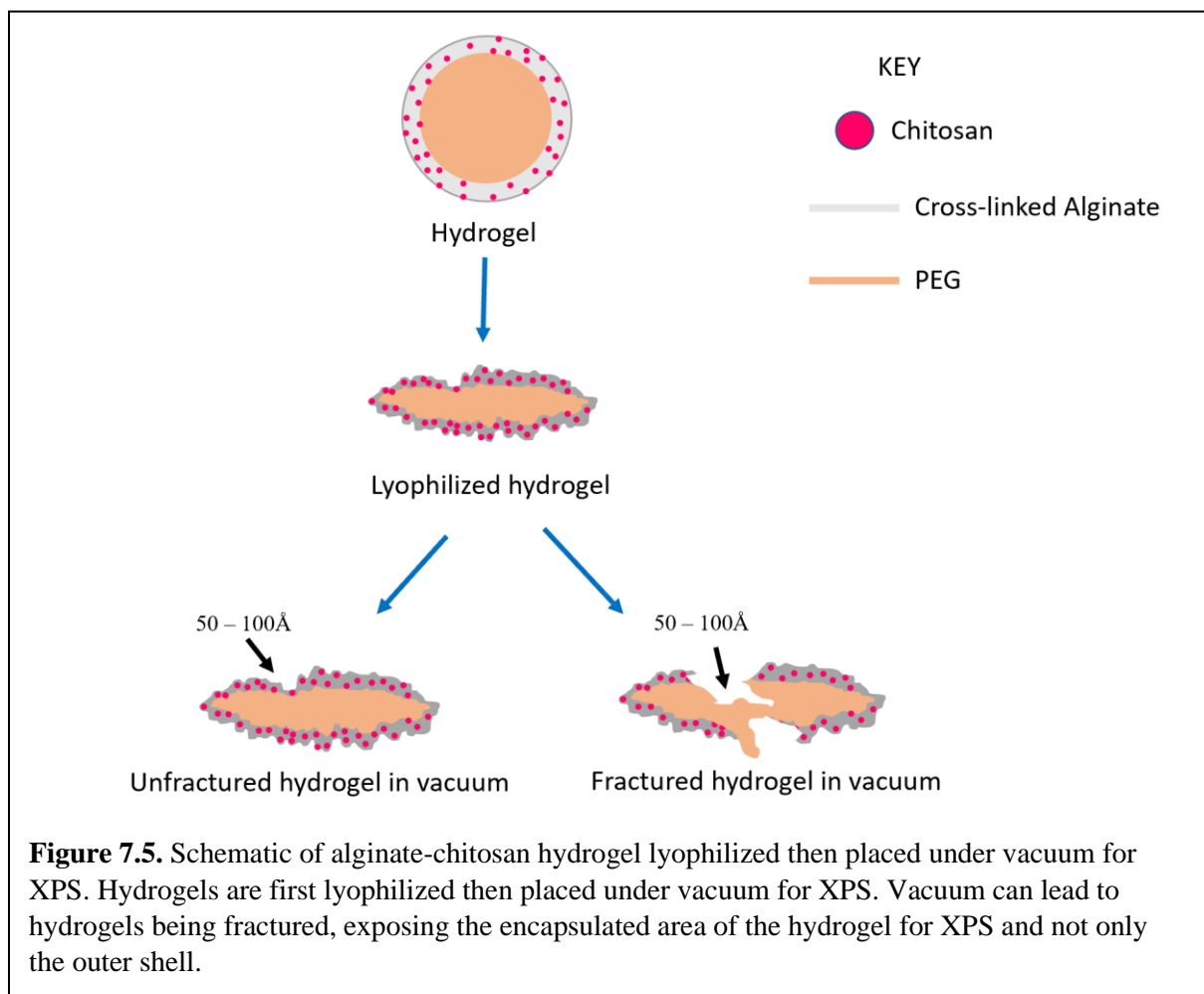
C=O detected. For a fractured hydrogel, the PEG core will be analyzed, instead, resulting in increased C-O detected. We believe that this is the origin of spot-to-spot variation within the samples. [Note: due to the large deviations between samples and within samples of the high-resolution spectra, these results should be considered preliminary data, and additional experiments may be required prior to publication.]

The second source of abnormal C1s peak envelope appearance

is most likely due to charging of the samples. “Charging” occurs when the rate of electrons being ejected from the sample surface is higher than the rate of electrons diffusing through the

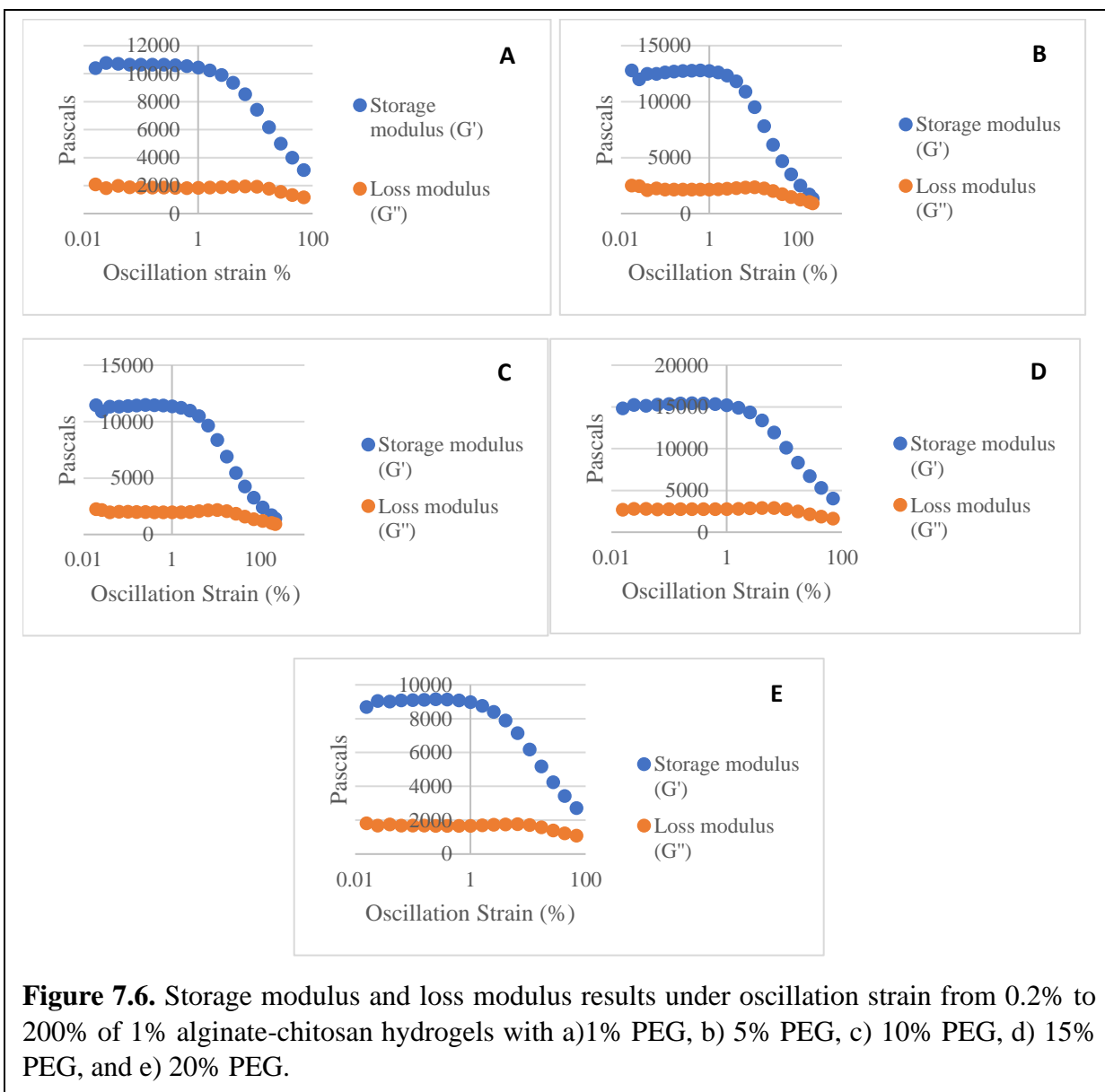
material (often insulators such as PEG) and the charge is not compensated.²⁰⁰ As a result, the ejected photoelectron will feel an electrostatic attraction due to positive charge accumulation at the specimen's surface, resulting in a photoelectron slow down and loss of kinetic energy before being detected by the energy analyzer. Charging leads to the loss of information of the photoelectron initial state and affects the photoemission spectrum by shifting all the feature to higher kinetic/binding energies.²⁰⁰ As a result, the C1s peak envelope becomes an unresolved “hump” which is difficult to deconvolute.

Overall, XPS survey spectra of elemental composition shows no unexpected contamination in the fabrication process.



7.3.2 Rheology

To determine hydrogel network stability, the hydrogels' viscoelastic behavior following a 30-minute exposure to different pH solutions (1, 4, and 7) and GSF were analyzed. Frequency sweeps are needed to observe this behavior as it could better explain hydrogels' network stability. However, frequency sweeps generally are observed the behavior of a sample in the non-destructive deformation range, an amplitude sweep was necessary to determine a non-destructive strain. A amplitude sweep of strain from 0.02% to 200% strain was completed, and a 2% strain was determined to be ideal, as this was prior to the large-amplitude-oscillation-shear regime deformations region for all concentrations (e.g. constant chitosan and alginate with increasing concentrations of PEG 3350, see **Figure 7.6**).



Frequency sweep experiments were then completed with a 2% strain to determine the stability of the hydrogel networks following exposure to different conditions pH conditions (pH = 1, 4, and 7) as well as GSF. The $\tan(\delta)$ (G''/G') for hydrogels loaded with increasing concentrations of PEG (1% PEG, 10% and 20% PEG) following a 30-minute exposure to GSF, pH = 1, 4, and 7 with varying frequency are shown in **Figure 7.7**.

Each of the hydrogel networks remain stable (i.e., $G''/G' < 1.0$) following exposure to all experimental conditions. Closer observation of Figure 7.6 shows that, following a 30-minute exposure to pH 4 or 7, the G''/G' results for all hydrogel concentrations are similar to those found in the control (exposure to air). Exposure to lower pH conditions (i.e., pH = 1 and GSF) does affect hydrogels, with the material becoming less stiff, as indicated by the increased G''/G' values. This shows that there is some change to the hydrogel networks following exposure to low pH conditions, although the gel remains in a gel-like state, and no dissolution occurs. At the highest concentration of PEG loaded into the hydrogel, the pH response seems to decrease with G''/G' following exposure to GSF and pH = 1, more similar to those found in samples controls.

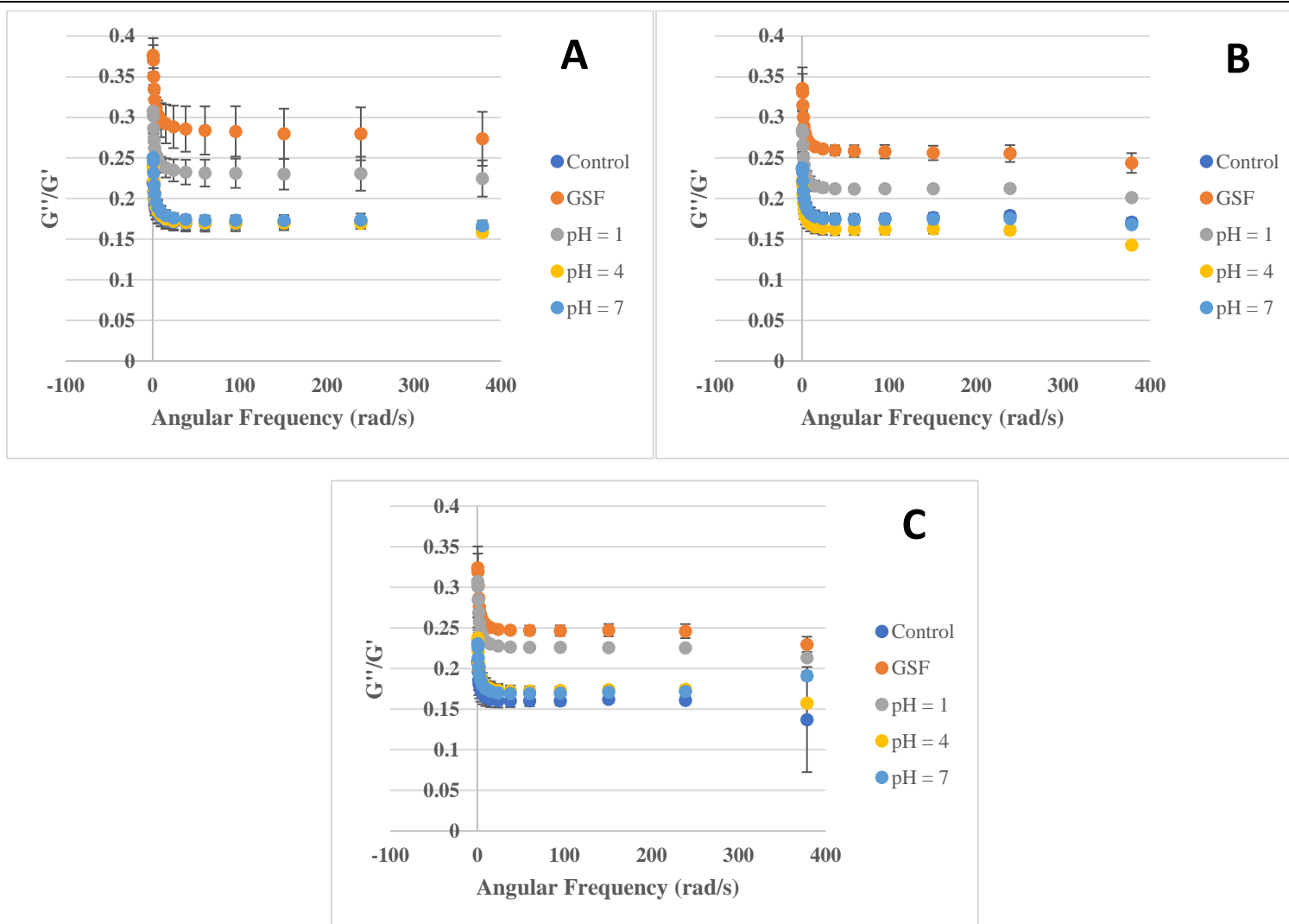


Figure 7.7. $\tan(\delta)$ (G''/G') vs angular frequency results of hydrogels loaded with increasing concentrations of a) PEG: 1%, b) 5%, and c) 10% following a 30-minute exposure to varying pH solutions of 1, 4, and 7 as well as GSF. Rheological results indicate that hydrogel networks are stable following exposure to different pH conditions, but is also pH responsive, with an increase in G''/G' following exposure to GSF and pH = 1. $N = 3$.

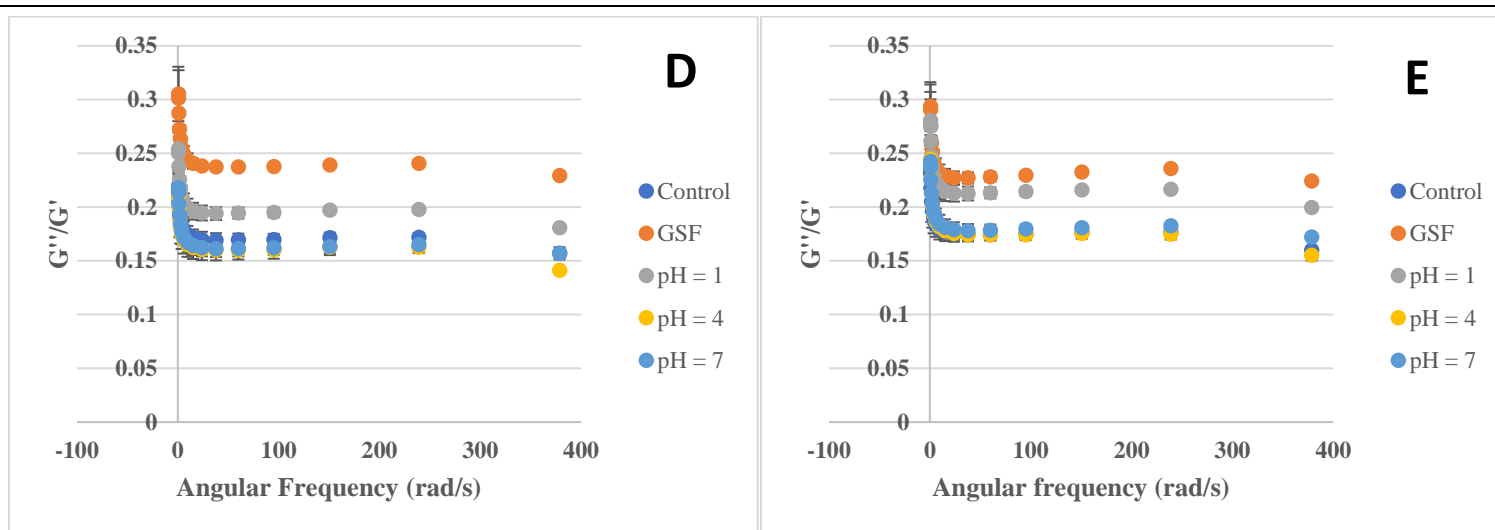


Figure 7.7 $\tan(\delta)$ (G''/G') vs angular frequency results of hydrogels loaded with **d**) 15%, and **e**) 20% PEG concentrations of following a 30-minute exposure to varying pH solutions of 1, 4, and 7 as well as GSF. Rheological results indicate that hydrogel networks are stable following exposure to different pH conditions, but is also pH responsive, with an increase in G''/G' following exposure to GSF and pH = 1. $N = 3$.

7.3.3 Weight change of hydrogels in acidic and basic solutions

As the results from rheology indicate that the hydrogels are stable at all concentrations at all pHs, we then measured the extent to which a weight change was observed for the hydrogels in acidic and basic conditions. In this way, we could determine whether the hydrogel structures were intact, but releasing their internal cargo (preferred outcome), or not.

Figure 7.8 charts the degradation results (% of weight change) of 1%, 5%, 10%, 15% and 20% PEG-loaded hydrogels following placement in pH = 1-8 over the course of 120 minutes.

Overall, the hydrogels were pH-responsive in acidic solutions, with the largest amount of weight change in acidic pH solutions of 1 and 2. The lower PEG concentration hydrogels (1-15% PEG) were the most responsive, with the greatest weight change. At pH 1 and pH 2, hydrogels loaded with 1% PEG 3350 lost ~45% and ~44% of its original weight respectively. Similar losses were found in 5% PEG 3350, at which hydrogels lost ~47% and ~44% of its weight in pH 1 and 2, respectively. Higher concentrations of PEG-loaded hydrogels at 10% and 15% lost 52% and 48% of their weight in pH 1 and 2, and 53% and 51% of its weight in pH 1 and 2, respectively. In comparison, at the highest PEG concentration (20%), the lowest % weight loss was detected at pH 1 and 2, where only ~28%, and ~19% loss was detected. At higher pH of 3-8, <25% of weight loss was detected across all time periods and concentrations. From these results, it is apparent that although the hydrogel structure remains intact (from rheology results), for physiological applications, hydrogel complexes loaded with 1-15% would be most suitable, as they lose ~ 50% of their cargo within the first 60 minutes (relevant time frame) after being placed in the low pH solution.

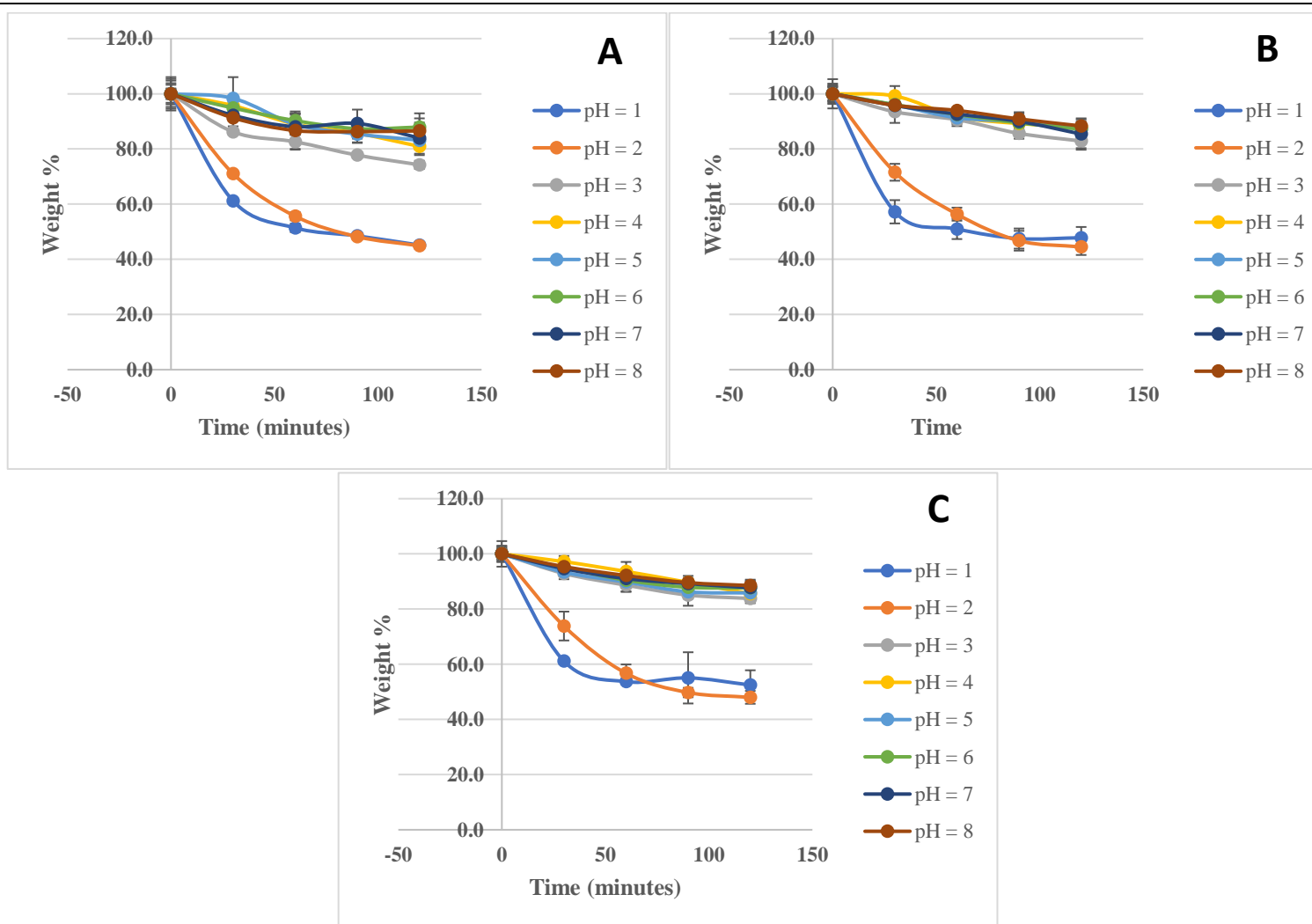


Figure 7.8. Change in weight % of hydrogels loaded with increasing concentrations of a) PEG: 1%, b) 5%, and c) 10% following a 30-minute exposure to varying pH solutions of 1 (blue), 2 (orange), 3 (grey) 4 (yellow), 5 (light blue), 6 (green), 7 (dark blue), and 8 (brown). Hydrogels in low pH solutions (1 and 2) display high amounts of weight loss while little weight changes higher pH solutions (pH 4 – 8). N=6.

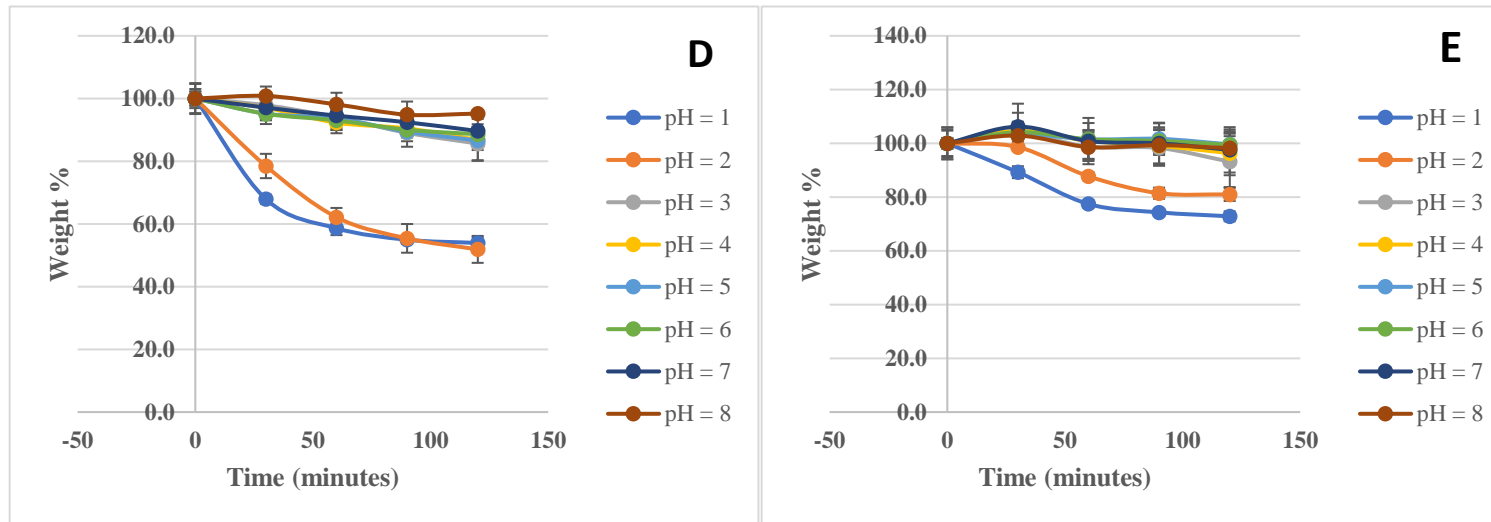


Figure 7.8 continued. Change in weight % of hydrogels loaded with increasing concentrations **d**) 15%, and **e**) 20% following a 30-minute exposure to varying pH solutions of 1 (blue), 2 (orange), 3 (grey) 4 (yellow), 5 (light blue), 6 (green), 7 (dark blue), and 8 (brown). Hydrogels in low pH solutions (1 and 2) display high amounts of weight loss while little weight changes higher pH solutions (pH 4 – 8). N=6.

7.3.4 Hydrogel weight gain/loss in gastric simulation fluid and small intestine simulation fluid

Next, the hydrogels were exposed to gastric and small intestine simulation fluids in order to mimic the more complicated physiological milieu. **Figure 7.9a** shows the amount of PEG 3350 (in %) weight change in hydrogels loaded with PEG (1-20%) following exposure to fasted-stated gastric simulation fluid (GSF) over 60 minutes, in 10-minute intervals. A shorter time interval was chosen due to observations in previous studies where the greatest weight change was found within the first 60 minutes of exposure to low pH conditions. The GSF, which has a pH of 1.6, was made and implemented in this experiment to ensure that this hydrogel system could release the cargo in our intended target – the stomach.

All of the hydrogel systems used in the experiment were responsive to the GSF. The amount of weight loss decreased as the concentration of PEG-loaded into the hydrogels increased. Hydrogels loaded with 1% and 5% PEG 3350 performed similarly, losing ~50% of its weight by 30 minutes with ~60% weight lost by 60 minutes. Hydrogels loaded with 10% PEG 3350 were slightly less responsive, with ~50% of the weight loss reached at 40. By 60 minutes, 54% of the weight was lost. 15% PEG 3350 loaded hydrogels were unable to lose 50% of its weight until the 60-minute mark. Finally, 20% PEG loaded hydrogels had the least change in weight, with only ~30% of its original weight lost. Furthermore, the standard deviations within samples were largest in 20% PEG loaded hydrogels. These hydrogels did not lose 50% of their weight by the 60-minute mark. This is indicative that there may be a loading limitation in these hydrogels, in which 20% PEG decreases efficiency in response, as the hydrogel networks may not be as tightly cross-linked. Overall, the hydrogels were responsive to the FaGSF and are promising vessels for drug release in a stomach-like environment.

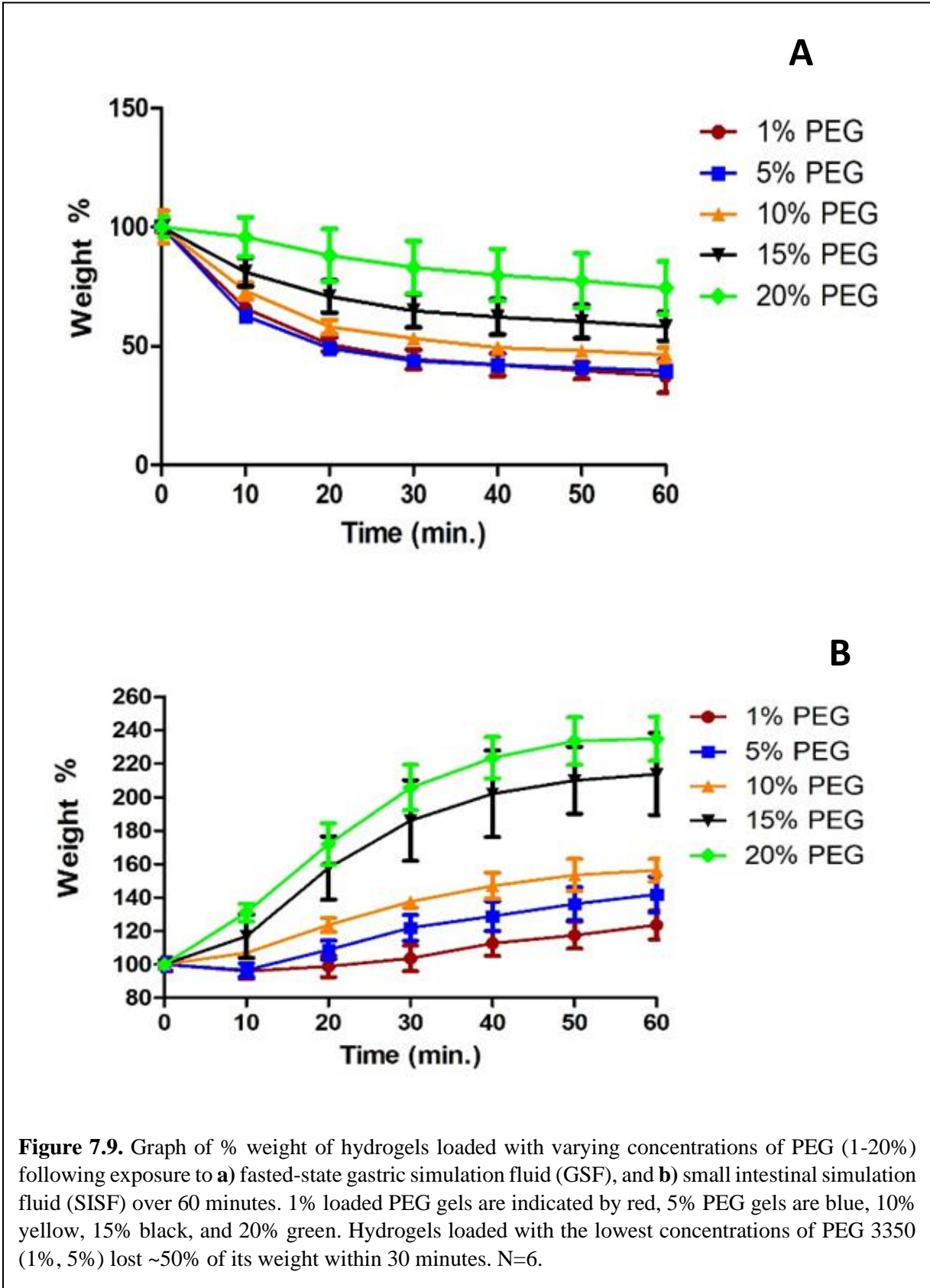


Figure 7.9b shows the amount of PEG 3350 that was released into fasted-state intestinal simulation fluid (SISF). SISF was used for this part of the experiment to evaluate the hydrogels' stability within the small intestine (which has a pH of 6.3). The results obtained in from hydrogels exposed to SISF were significantly different from the previous section, which were exposed to pH = 1-8 or GSF; instead of *losing* weight, the hydrogels at all concentrations of PEG *gained* a significant amount of weight after being placed in the SISF. Furthermore, as the concentration of PEG 3350 loaded into the hydrogels increased, the amount of weight gained by the hydrogels increased.

The hydrogels loaded with lower concentrations of PEG (1 and 5% PEG 3350) gained 23% and 41% weight over 60 minutes, respectively. At 10%, there was ~56% increase in weight over 60 minutes. The largest amount of weight gained was found in hydrogels loaded with 15% and 20% PEG 3350, with a weight increase of 113% and 134%, respectively. We hypothesize that this opposite result is due to a number of causes: 1) compared to GSF, SISF contains far more sodium, as well as maleic acid, and does not contain pepsin; 2) alginate is known to shrink at low pH (such as in GSF) and swells at higher pH (such as SISF); 3) chitosan is soluble at low pH (such as in GSF) and is insoluble at higher pH (such as SISF). It is unclear which of these differences is the driving factor behind the rapid swelling and weight gain, and it is most likely that it is a combination of the swelling of alginate, and its interactions with the other components of SISF. Overall, these results confirm that the hydrogels respond to changes in pH in physiologically-relevant conditions (such as GSF and SISF), and therefore have great potential for drug release in the stomach.

7.3.5 Rhodamine-PEG release

| Time (minutes) | 1% PEG | 5% PEG | 10% PEG | 15% PEG | 20% PEG |
|-----------------------|---------------|---------------|----------------|----------------|----------------|
| 0 | 0±10.3 | 0±1.5 | 0±1.2 | 0±0.1 | 0±0.9 |
| 30 | 13.0±1.9 | 41.2±1.8 | 50.6±6.6 | 54.8±2.5 | 46.0±6.2 |
| 60 | 17.7±1.2 | 49.3±3.1 | 67.5±5.6 | 69.7±2.1 | 62.5±12.1 |
| 90 | 18.6±1.4 | 48.8±3.9 | 68.9±9.4 | 72.6±2.2 | 66.4±12.8 |
| 120 | 19.2±1.2 | 47.5±4.7 | 69.0±9.0 | 70.8±2.7 | 67.3±14.0 |

Table 7.2. Percentage of PEG-labeled with rhodamine 6G released following exposure to gastric simulation fluid over 120 minutes, with 30-minute intervals.

Having demonstrated that the PEG hydrogels are pH-responsive in physiologically relevant conditions, we obtained PEG that was functionalized with rhodamine 6G so that we could ensure that PEG is released as a result of the pH change. Rhodamine is an inexpensive dye that fluoresces red and is easily tracked via spectroscopy.

Tables 7.2 and 7.3 chart the amount of rhodamine labeled-PEG 3350 that was released into fasted-stated gastric simulation fluid (GSF) and small intestine simulation fluid (SISF), respectively. **Table 7.2** indicates that hydrogels loaded with 1% PEG 3350 released the least PEG 3350 following exposure to GSF. Hydrogels loaded with 15% PEG 3350 released the most PEG (70%) following exposure to GSF. Furthermore, the 15% loaded PEG hydrogels released PEG the fastest, as well (within 30 minutes). However, when the concentration of PEG was raised to 20%, the hydrogels' response worsened: they did not release more than 50% in solution after 30 minutes, and only had 67% in solution after 120 minutes. Therefore, there appears to be a limitation in how much PEG can be loaded and released into the hydrogels.

From these results, it appears that 15% PEG loaded hydrogel is ideal in gastric simulation fluid, delivering the most PEG in the shortest amount of time. In addition, creating hydrogels with a high concentration of PEG (15% vs. 1%) will reduce the total amount of drug that will need to be ingested to deliver the optimal dosage of PEG. For the current size of the hydrogels being studied, this translates to a reduction of the dosage by 15x.

Table 7.3 shows the performance of hydrogels loaded with 1%-20% PEG following exposure to SISF over 120 minutes. Although the results from the previous section's weight change data indicates that the hydrogels swell in SISF, the PEG itself is not retained; it appears that PEG is released into the SISF solution over time. Similarly to the results in GSF, there is a dosage effect at work for hydrogels in SISF, with increased PEG concentration yielding increased release of PEG into SISF. Also similar to results in GSF, 15% PEG hydrogels released the largest amount of PEG (~70%) in SISF in the shortest time frame (120 minutes). Finally, as with the results in GSF, 20% loaded PEG hydrogels perform worse than the 15% PEG hydrogels, releasing only ~50% in 120 minutes.

From these results, it appears that 15% PEG loaded hydrogel is ideal also for small intestine simulation fluid, delivering the most PEG in the shortest amount of time. However, these results should be considered preliminary, for several reasons. For example, instead of testing duplicate PEG-loaded hydrogels to the GSF and SISF solutions *in parallel*, a more physiologically relevant test would be to expose them *sequentially* to GSF followed by SISF over physiologically-relevant time frames. In this way, the amount of PEG released in the small intestine following digestion in the stomach could be truly determined.

In addition, results from the hydrogels exposed to SISF have large standard deviations within samples. This is likely a result of spectrometer difficulties that occurred within the lab while this study was completed. Therefore, replicate studies should be performed prior to publication.

| Time (minutes) | 1% PEG | 5% PEG | 10% PEG | 15% PEG | 20% PEG |
|-----------------------|---------------|---------------|----------------|----------------|----------------|
| 0 | 0±2.8 | 0±5.1 | 0±10.5 | 0±10.7 | 0±5.1 |
| 30 | 6.4±1.6 | -9.4±19.5 | 37.2±22.8 | 34.4±20.9 | 34.5±16.2 |
| 60 | 24.6±4.2 | 6.0±20.7 | 47.8±3.8 | 49.9±16.9 | 43.8±12.1 |
| 90 | 16.2±9.6 | 4.3±21.1 | 59.9±25.1 | 59.2±15.5 | 49.2±14.6 |
| 120 | 15.6±11.2 | 29.1±30.6 | 63.2±31.1 | 69.0±22.5 | 54.3±15.7 |

Table 7.3. Percentage of PEG-labeled with rhodamine 6G released following exposure to small intestine simulation fluid over 120 minutes, with 30-minute intervals. N = 6.

7.3.6 Nuclear Magnetic Resonance of hydrogel leachate

The results from the previous sections indicate that the hydrogels respond to change in pH by releasing PEG. In this section, we studied the leachate from the hydrogels to determine whether other components are being released into solution, as well.

This was achieved by performing a study in which 1% PEG-loaded hydrogels were exposed to deuterated acetic acid over a time period of 120 minutes, with ¹H NMR data collection of the solution performed every 30 minutes.

Figure 7.10 shows the expected peaks if alginate²⁰¹ (top) and/or chitosan²⁰² (middle) was present. The bottom spectra on **Figure 7.10** shows the deuterated acetic acid solution following exposure to PEG-loaded hydrogels after 120 minutes. The bottom spectra on **Figure 7.10** shows peaks at ~3.8 ppm indicative of CH₂CH₂O-, and ~4.6 ppm indicative of -OH both of which are indicative of PEG.²⁰³ No peaks are observed that would indicate the presence of

chitosan or alginate in the leachate, however are seen. Similar NMR spectra were obtained after 30 minutes, 60 minutes, and 90 minutes (data not shown, as they are identical).

This NMR data indicates that only PEG is being released from the hydrogels, and no other contaminants (including alginate or chitosan), are released following exposure to acidic conditions such as those found in the stomach.

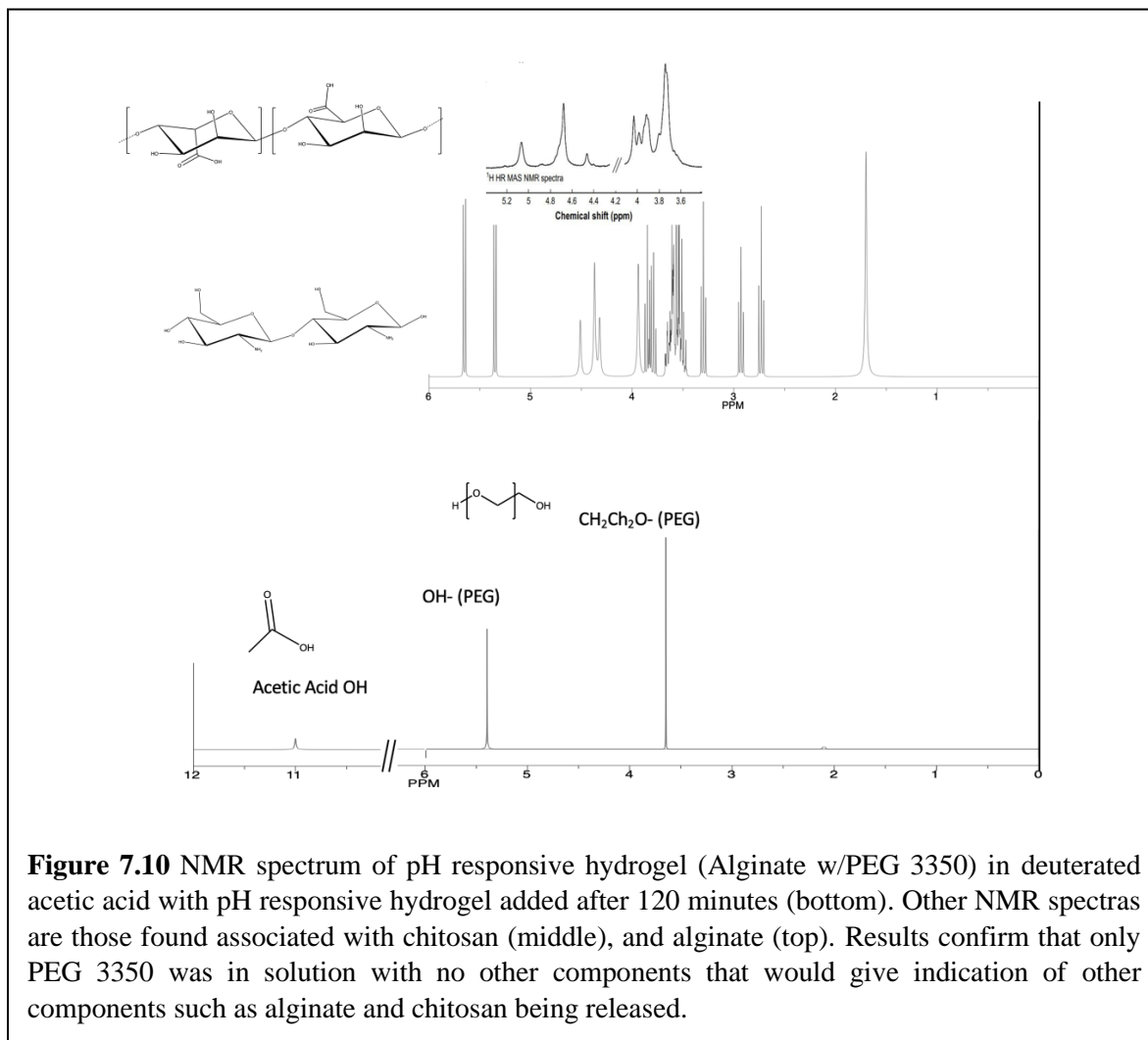


Figure 7.10 NMR spectrum of pH responsive hydrogel (Alginate w/PEG 3350) in deuterated acetic acid with pH responsive hydrogel added after 120 minutes (bottom). Other NMR spectra are those found associated with chitosan (middle), and alginate (top). Results confirm that only PEG 3350 was in solution with no other components that would give indication of other components such as alginate and chitosan being released.

7.4 Conclusions

The softness, hydrophilicity, superabsorbancy, viscoelasticity, biodegradability, biocompatibility, and other properties of hydrogels have led to their extensive use as potential drug delivering agents.¹⁷⁶ However, most studies have not sought to improve on the use of

hydrogels for the delivery of low compliance drugs such as GoLytely™ that are currently used in colonoscopy preparation.

In our study, we evaluated the use of chitosan-alginate hydrogels as a pH-responsive hydrogel system to deliver PEG 3350 into the stomach and small intestine. We confirmed that the elemental composition of the hydrogels is consistent with what was expected from the mixture using XPS. We also showed that the hydrogel networks are stable following exposure to solutions of physiologically relevant pH, as well as gastric simulation fluid via rheology. Furthermore, the hydrogels are pH-responsive and release PEG at physiologically relevant conditions (as evidenced by weight change, spectrometry of rhodamine-labelled PEG). As importantly, we showed that the leachate from the hydrogels contains only PEG (not any other component of the hydrogel, or contaminants) using NMR. Finally, we showed that the optimal concentration of PEG to be loaded hydrogels for drug delivery is 15% PEG (w/w).

When compared to the traditional technique for GI prep (GoLytely™), this technique affords several distinct advantages, such as the ability to precisely and predictably tailor the dosage of PEG to the needs of the patient, preventing the potentially cytotoxic effects seen in **Chapter 6**. In addition, the ability to create capsules that are stable in neutral pH solutions such as water means that the technique may prevent the unpredictable viscosity and unpleasant taste that many patients find unbearable. Finally, all of these components have previously been approved for use in humans by the FDA and are therefore suitable for use in this system. These results therefore indicate that this method for delivering PEG 3350 via encapsulation within chitosan/alginate hydrogels has great potential as an osmotic laxative alternative for those struggling with the palatability and side effects of the current prep technique.

Chapter 8: Conclusions and Future Directions

8.1 Conclusions

8.1.1 Unanticipated sources of toxicity within existing protocols

The cytotoxicity of reagents (NIPAM) used in current experimental protocols were investigated as described in **Chapter 3**. This work examined the cytotoxic effects of using pre-polymerized NIPAM on mammalian cells and evaluated whether its continued use without purification is beneficial. Although other forms of polymerized NIPAM are non-toxic to cells, cpNIPAM purchased from retailers should be purified prior to use to prevent unintended cytotoxic effects. Furthermore, any biomedical devices, and technologies that utilize cpNIPAM without purification can lead to unexpected cytotoxicity response in tissue culture.

Cytotoxicity was not only found in experimental protocols, but also in medical protocols, as well. It is often assumed that the use of topical and oral antibiotics and antiseptics is safe, and that the application of these items directly to wounds will have few side effects during surgery. As a result, current surgical procedures often encourage the use of antibiotics (e.g., bacitracin, tranexamic acid, and vancomycin), and antiseptics (e.g., chlorhexidine, and povidone iodine) to prevent infection (**Chapter 5**), or as part of the antifibrinolytic process (**Chapter 4**). However, in this work, it was demonstrated that each of the antibiotics, antiseptics, and antifibrinolytic tested are detrimental to chondrocytes (knee joint cells). As these cells are poorly vascularized, they are less likely to recover as compared to other more vascularized cell types. In turn, this could lead to more difficult recovery periods following knee surgical procedures, and over time, osteoarthritis for patients who have had these materials applied during joint replacement and other surgeries.

8.1.2 Cytotoxicity despite FDA approval

Although the FDA evaluates the safety of drugs and medical devices prior to their release in the market, many are used for purposes other than they were originally intended, and often with unanticipated consequences. In 2003, the Centers for Medicare and Medicaid Services collaborated with the CDC and 10 other national organizations to develop the Surgical Infection Prevention Project. This effort resulted in recommendations of prophylactic antibiotic usage for patients undergoing clean-contaminated surgeries to prevent surgical site infections.²⁰⁴ Since, antibiotics have become the standard of care and are widely used in a range of surgeries.

A number of studies were performed to determine the effectiveness of antibiotics for the prevention of surgical site infections.^{132,204–206} **Chapter 5** showed that this assumption may be incorrect as even rapid washing (30 seconds) with antibiotics including bacitracin and vancomycin lead to delayed cytotoxicity seen in chondritic knee cartilage. Similar assumptions on the safety of tranexamic acid in surgeries and PEG 3350 were made based on their FDA approval. **Chapter 4** showed that tranexamic acid exposure may not be appropriate as current recommended concentrations are cytotoxic to knee chondrocytes, delaying healing post-surgery. **Chapter 6** showed that PEG 3350 at current therapeutic concentrations changes the behavior of gut cells including stomach, small intestine, and colon cells. Taken together, these chapters emphasize the need for careful evaluation of the possible cytotoxic effects of antibiotics in surgical applications prior to their use.

8.1.3 Biocompatible devices

Chapter 7 outlines the development of a new biocompatible method to deliver colonoscopy preparations with more control and precision using well known polymers such as sodium

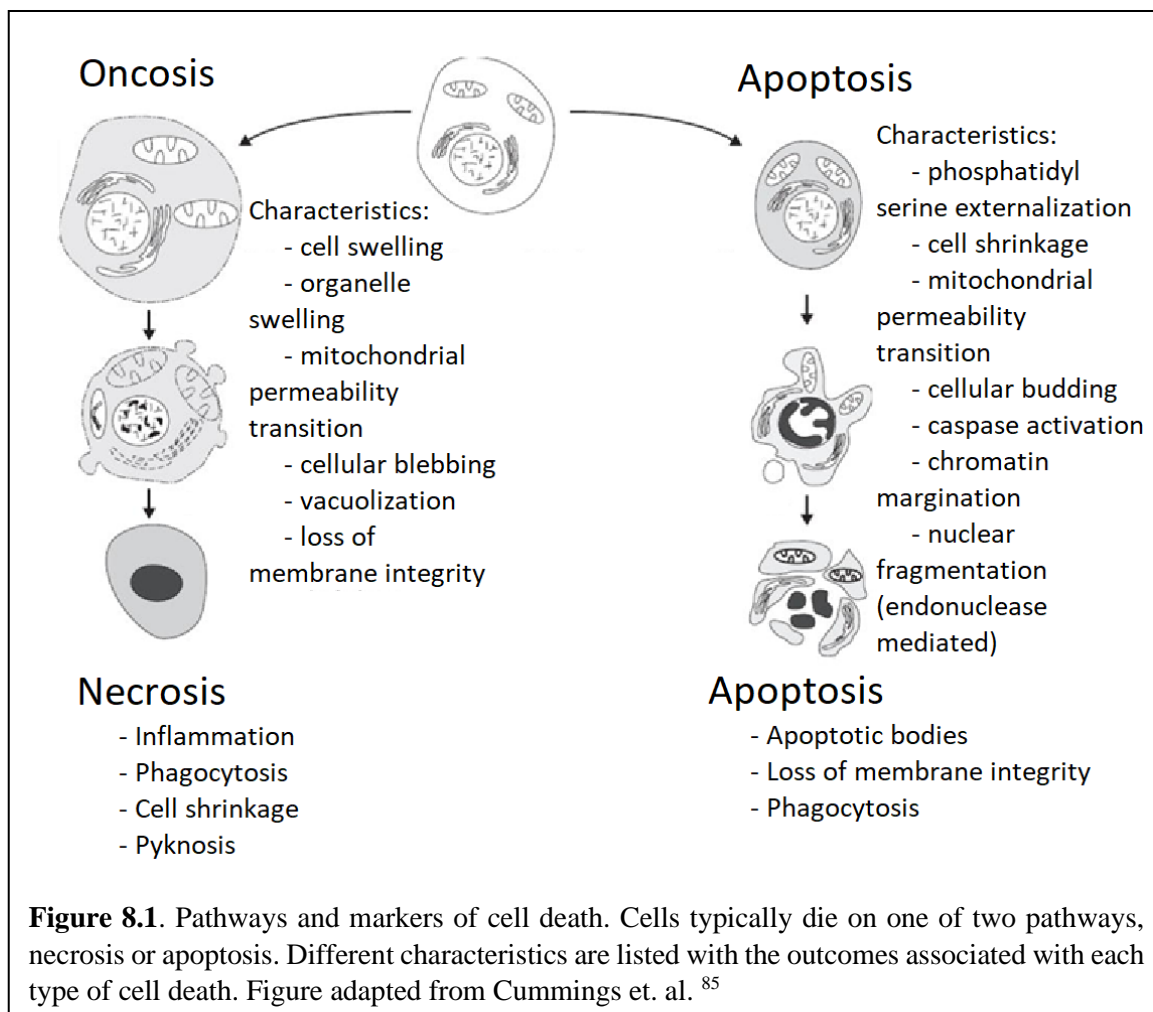
alginate. Sodium alginate and chitosan have been previously used in food,¹⁹³ and many studies have shown their safety to the human gastrointestinal system.^{207,208} This makes them ideal candidates as part of a pH-responsive drug delivery hydrogel system.

Chapter 7 characterizes the ideal concentrations and their effectiveness as a potential delivery vehicle for PEG 3350 and identifies the ideal concentration of PEG 3350 versus sodium alginate and chitosan to deliver the maximum amount of drug. Studies were completed evaluating the hydrogels' pH responsiveness utilizing simple pH solutions as well as simulated gastrointestinal and small intestinal simulation fluids.

8.2 Future Directions

8.2.1 Assessing the mechanism of death

Cell death typically occurs by necrosis or apoptosis (see **Figure 8.1**).⁸⁵ Following injury, a series of cellular mechanisms called oncosis takes place and eventually lead to necrosis. Necrosis is characterized by cell and organelle swelling, pyknosis, loss of ion gradients, increased permeability, loss of cell membrane integrity, and the release of intracellular contents.⁸⁵ Apoptosis, on the other hand, is ATP-dependent and characterized by cell shrinkage, maintenance of plasma membrane integrity, chromatin condensation, and nuclear



fragmentation.²⁰⁹ It has been shown that the type of death greatly affects response *in vivo*. Necrotic cell death typically induces inflammation, while apoptotic death does not. Inflammation is essential in efficient tissue repair, but large amounts of inflammation has been shown to delay healing and results in increased scarring. Furthermore, chronic inflammation is a hallmark of non-healing injuries and wounds, predisposing the tissue to cancer development.²¹⁰

It was shown in **Chapter 2** that cpNIPAM is cytotoxic and detrimental to cells with cell morphology differences, specifically the formation of intracellular pores in 3T3 cells. As mentioned above, necrotic vs apoptotic cell deaths lead to different responses *in vivo*. These

differences can significantly affect their uses. For example, if cpNIPAM leads to necrotic cell death in BAECs and VEROs then its use as a polymer in the medical setting will likely be limited to materials that are not implanted into humans or taken to be implanted into humans. Not only that, this may delay NIPAM's approval in the FDA process as controlling mechanism of deposition and polymer formation greatly affects cell behavior. Future studies should be repeated on these cell lines to assess and better understand their mechanism of death as this could affect their use *in vivo* changing the current standards of care.

Multiple methods could be used to evaluate the mechanism of death. Many previous studies rely on the use of the Comet assay, an assay that looks at fragmented DNA stained with a fluorescent dye, such ethidium bromide, and the length of the tail of DNA from the cell corresponds to the degree of apoptosis.²¹¹ Caspase assays that detect for apoptosis by the presence of caspases 2, 3, 6, 7, 8, 9, and 10 are another effective method. These are fluorescent assays that will fluoresce or chemically luminesce under the presence of caspases.²¹¹ Luciferase, an ATP detecting assay could also be used to assist in differentiating the type of cell death. Here, presence of ATP will cause Luciferase to luminesce. High levels of luminescence are indicative of cells undergoing apoptotic death following exposure to a cytotoxic polymer.¹⁰⁰ Annexin V, an apoptosis detecting assay, could also be used in combination with other assays. Healthy cells contain phosphatidylserine, a phospholipid, within their membranes. Annexin V is a protein that binds to phosphatidylserine but is not cell permeable. Thereby, cells that are alive are not affected by Annexin V. However, during apoptosis, cell membranes will lose asymmetry and phosphatidylserine will be exposed to the surface, allowing Annexin V to bind.

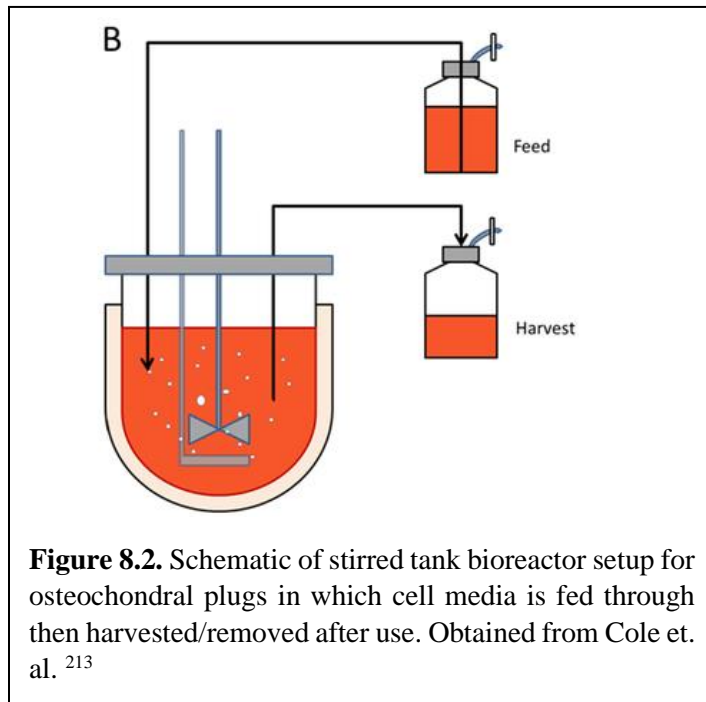
Using these assays in combination such as using both Luciferase and Annexin V on BAECs, 3T3s, and VEROs following exposure to cpNIPAM substrates and leachates will allow us to determine the mechanism of cell death and understand the mechanism in which NIPAM monomers and short chain polymers cause cytotoxicity in multiple cell types thereby improving the fundamental understanding of pNIPAM.

Similar follow up studies using these assays could be completed with PEG 3350 as pore formation was also found in HSCs following exposure to PEG 3350 in **Chapter 6**. Understanding the mechanism of death of PEG 3350 in HSCs vs HSI and HCCs will help explain why PEG 3350 causes more severe side effects in groups with generally smaller statures such as women and elderly individuals.²¹² This will help improve the current understanding regarding PEG's cytotoxicity and can lead to an improvement in the standard of care, allowing physicians to further study on an effective, but non-toxic dose for these populations that require PEG 3350 in their medical care.

Follow ups on the mechanism in which antifibrinolytics such as TXA (in **Chapter 4**) are leading to cytotoxic effects seen on chondrocytes is also necessary. Current evaluations without pH measurements showed a change in media pH from red to yellow indicative of an acidic environment (pH <6.8) after 24 hours of exposure to TXA. Although it was not explored, and media was changed every 24 hours, the reaction continued even after TXA was removed and cells were maintained in a media environment.

It is known that environmental changes greatly affect cell viability,⁶² and it is possible that the acidic conditions are toxic to chondrocytes found in the osteochondral plugs. To better understand if the observed cytotoxic effects are caused by environmental changes or due to exposure to TXA, a study could be completed using a bioreactor in which fresh media is fed

through and waste media is emptied out automatically (see **Figure 8.2**).²¹³ This will allow clinicians to better understand the effects TXA has on chondrocytes viability and aid clinicians



in their non-approved use of previously approved FDA drugs.

8.2.2 Search for a potential “safe” and effective concentration of antibiotics and antiseptics

Antibiotics and antiseptics have become an essential part of surgical procedures including knee arthroplasties. However, it has not been established whether a specific

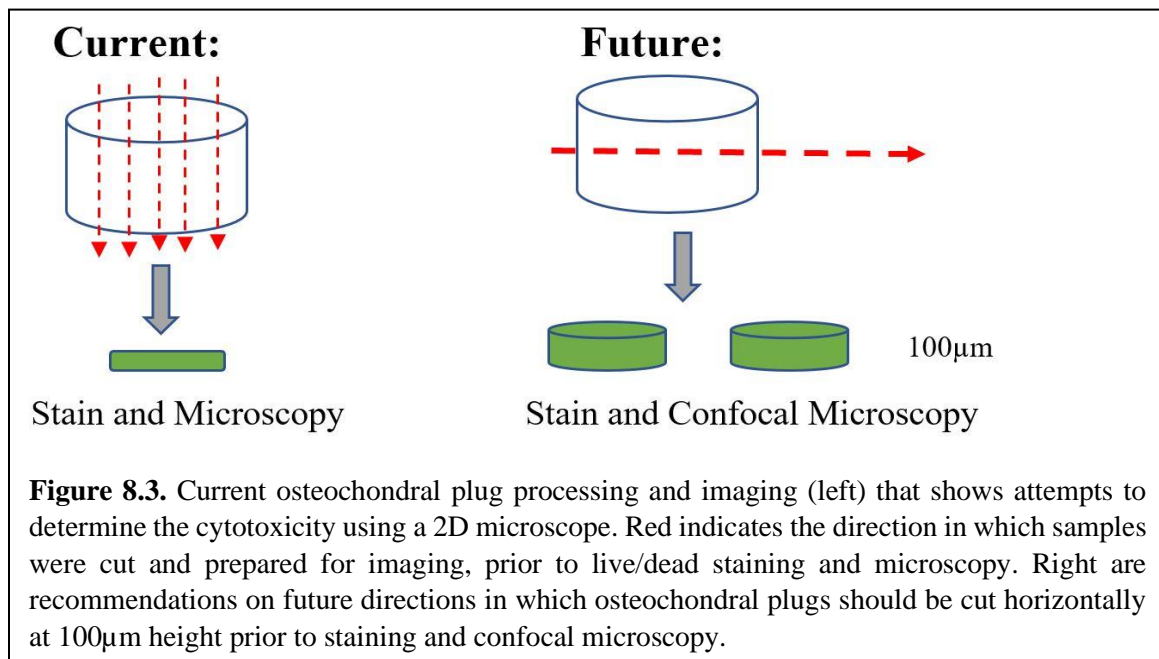
antiseptic, a combination of agents, etc. are better suited to prevent the formation of biofilms or other infections.⁴³ To further complicate the matter, although the WHO and CDC recommend the use of dilute betadine for irrigation of wounds during orthopedic procedures, the optimal volume, frequency, and duration is unknown. Other antiseptics and antibiotics along with saline and ringers lactate solutions have also been proposed as potential irrigation solutions but a “gold standard” does not exist due to a lack of clinical studies.⁴³

Further studies on ideal concentration, volume, and frequency of antibiotics and antiseptic use in surgeries should be completed. Evaluation of the effective concentration and assessing cytotoxicity with chondrocytes should be completed, allowing us to determine a safe and effective surgical dosage.

8.2.3 Depth of penetration of antibiotics, antiseptics, and antifibrinolytics and additional techniques to evaluate cytotoxicity

A study evaluating the depth of penetration of the antibiotics, antiseptics, and antifibrinolytics will allow for better understanding of how deep these reagents are able to penetrate into the chondrocytes.

Our current study evaluates the plugs in a 2-dimensional environment utilizing a fluorescent microscope, dependent on creating small slices of osteochondral plugs for fluorescent imaging. Future studies could use a confocal microscope to evaluate the depth at which these reagents are able to penetrate into chondrocytes by cutting the osteochondral plug in 100 μm dimensions horizontally. Subsequent staining utilizing a live/dead assay could be carried out followed by visualization under a confocal microscope (see **Figure 8.3**). This will allow the confocal microscope to image the plug in a 3D format and give a clearer picture.



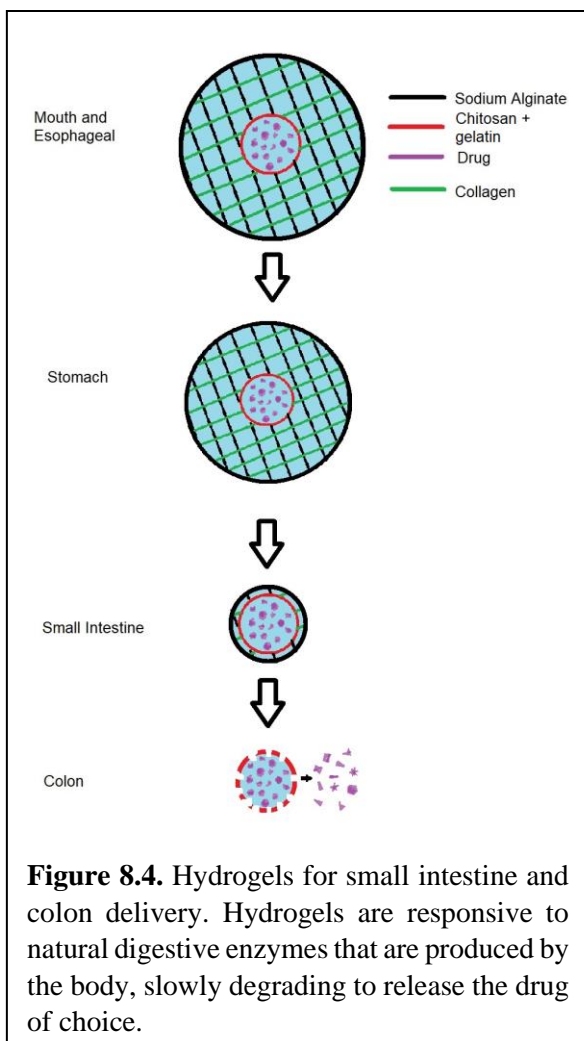
Furthermore, confirmation of cytotoxicity should be completed with another assay such as an XTT assay to evaluate its metabolic activity to ensure that the visual live/dead images and

counts correlate with true cytotoxicity effects seen as a result of osteochondral plug exposure to antibiotics, antiseptics, and antifibrinolytics. Osteochondral plugs could be exposed to antibiotics, antiseptics, and antifibrinolytics for similar time frames prior to being placed in cell media with XTT assay and incubated. Plugs would then be removed prior to readings being taken for evaluation of metabolic activity – which often correlates directly with cell viability.

8.2.4 Encapsulation of PEG with electrolytes

Hydrogel studies have focused on encapsulation and release of PEG 3350 for delivery of colonoscopy preparations. However, GoLytely™ does not *only* contain PEG 3350. Along with 227.1g of PEG 3350, GoLytely™ also contains 21.5g sodium sulfate, 6.36g sodium bicarbonate, 5.53g sodium chloride, and 2.82g potassium chloride all mixed with 4L of water. The additional salts are electrolytes to help prevent osmotic imbalances as one prepares for a colonoscopy.

To improve our hydrogel system, we must also test the ideal concentration of PEG 3350, sodium alginate, along with these electrolytes. It appears as if 10 wt% PEG and 15 wt% PEG have the most ideal drug release time frame. As such, it would be best to test these concentrations and 5wt% PEG3350 solutions along with their respective electrolytes to ensure that PEG 3350 is still being released in gastrointestinal simulation fluid with a similar drug release profile.



8.2.5 Encapsulation of bacteria and other materials using stimulus-responsive polymers for targeted drug delivery

The hydrogel system that we developed in **Chapter 7** to deliver GI preparation drugs to the stomach utilizes a pH-responsive system to deliver drugs to the stomach as a bolus dose. However, it would be useful to be able to deliver drugs or other cargo to distinct areas of the GI tract, such as the small intestine or the colon. It is known that each of these areas of the gut commonly function in slightly different pH environments (e.g., the pH of the small intestine is ~6-8, in the colon it is 5-7).

Therefore, in the future, we envision that the

“Bubblyte™” system could be adapted to create a multi-layered hydrogel that is capable of delivering other health promotive cargo (e.g., probiotics, vitamins, and healthy gut bacteria) by creating sequentially digested layers of the gel core.

Multi-layered hydrogels will be fabricated for site-specific drug delivery (**Figure 8.4**) to the end of the small intestine and the colon. The outer shell of the hydrogel will consist of sodium alginate and collagen which will promote stability in the acidic environment of the stomach. Sodium alginate and collagen are both fibrous materials that are known to be difficult to digest by the small intestine. Consequently, release of drugs will be delayed until the hydrogel reaches

the desired location. The inner shell will consist of gelatin and chitosan. Gelatin will be digested by natural enzymes in the small intestine, leaving chitosan with a specific cell-binding sequence and the drug.

Hydrogel properties will be characterized by (i) determination of rheological properties using a rheometer, (ii) visualization using confocal microscopy and scanning electron microscopy, and (iii) testing its capability to release drugs. Hydrogels can be exposed to gastric simulation fluid initially followed by small intestine fluid to determine vitamin release of the hydrogel where NMR is taken to determine if the correct drug is being released at the correct time. Similar studies using a fluorescently labeled vitamin model could also allow for mathematical calculations of the amount of drug being released over time.

The test material for this system will be probiotics or vitamins to demonstrate the small intestine delivery capabilities of this system. In the case of bacteria-based systems, release of the bacteria will be tracked *in situ* by placing hydrogels into GSF for 3 hours followed by exposure to small intestine simulation fluid (SISF) for 5 hours. Hydrogels will be monitored and weighed every 30 minutes to determine degradation. Live/dead and other viability assays can be performed with both fluid types using a flow cytometer to evaluate bacterial viability and release from the hydrogel.

References

1. History of FDA's Internal Organization. FDA. <https://www.fda.gov/about-fda/history-fdas-fight-consumer-protection-and-public-health/history-fdas-internal-organization>. Published 2018.
2. Junod S. *FDA and Clinical Drug Trials: A Short History*.; 2008. <https://www.fda.gov/downloads/AboutFDA/WhatWeDo/History/ProductRegulation/UCM593494.pdf>http://www.bioplanassociates.com/quickguides/qg_clinicalTrials.pdf.
3. Gieringer DH. The Safety and Efficacy of New Drug Approval. In: *5 Cato J*. Vol 177. ; 1985.
4. Food and Drug Administration. *A History of the FDA and Drug Regulation in the United States*.; 2006. <http://www.fda.gov/centennial/history/history.html>.
5. Kelsey FO, Dakota S, Company WSM. Frances Oldham Kelsey, Who Saved U.S. Babies from Thalidomide, Dies at 101. *The New York Times*. August 7, 2015.
6. Zuckerman DM, Brown P, Nissen SE. Medical device recalls and the FDA approval process. *Arch Intern Med*. 2011;171(11):1006-1011. doi:10.1001/archinternmed.2011.30
7. Lipsky MS, Sharp LK. From idea to market: the drug approval process. *J Am Board Fam Pract*. 2001;14(5):362-367. <http://www.ncbi.nlm.nih.gov/pubmed/11572541>.
8. US Food and Drug Administration. FDA Basics - What is FDA's budget and what is its impact?
9. Van Norman GA. Drugs, Devices, and the FDA: Part 1: An Overview of Approval Processes for Drugs. *JACC Basic to Transl Sci*. 2016;1(3):170-179. doi:10.1016/j.jacbts.2016.03.002
10. Purohit-sheth CDRT. *Food and Drug Administration (FDA): FDA Overview and Bioresearch Monitoring*. United States of America; 2017. <https://slideplayer.com/slide/10850015/>.
11. Petro J. Drugs and Devices. *Am J Cosmet Surg*. 2016;33(3):109-111. doi:10.1177/0748806816663916
12. Sertkaya, Aylin; Birkenbach A. *Examination of Clinical Trial Costs and Barriers for Drug Development*. Washington, D.C.; 2014. <https://aspe.hhs.gov/report/examination-clinical-trial-costs-and-barriers-drug-development>.
13. Wood AJJ. A Proposal for Radical Changes in the Drug-Approval Process. *N Engl J Med*. 2006;355(6):618-623. doi:10.1056/nejmsb055203
14. Light DW. The Food and Drug Administration: Inadequate Protection from Serious Risks. In: Light DW, ed. *The Risks of Prescription Drugs*. New York: Columbia University Press; 2010:40-69. doi:10.7312/ligh14692-002

15. Richards-Kortum R. Emerging Medical Technologies : High Stakes Science and The Need for Technology Assessment. In: *Biomedical Engineering for Global Health.* ; 2009.
16. Mello MM, Brennan TA. A cautionary tale about allowing politics and legal pressures to overwhelm science in evaluating new therapies. *Health Aff.* 2001;20(5).
17. Antman K, Hortobagyi G. Is More Better? ASCO Plenary Session Opens Debate on High Dose Chemotherapy. *Oncologist.* 1999;4(3):269-274.
18. Bezwoda WR, Seymour L, Dansey RD. High-Dose Chemotherapy With Hematopoietic Rescue as Primary Treatment for Metastatic Breast Cancer : A Randomized Trial. This article was retracted in June 2001 . *J Clin Oncol.* 1995;10:2483-2489.
19. BEZWODA WR. High-dose chemotherapy with heamatopoietic rescue: application to primary management of metastatic breast cancer. *Eur J Cancer Care (Engl).* 1997;6(s1):10-15. doi:10.1111/j.1365-2354.1997.tb00319.x
20. Grady D. Breast Cancer Researcher Admits Falsifying Data. *The New York Times.* <http://www.nytimes.com/2000/02/05/us/breast-cancer-researcher-admits-falsifying-data.html>. Published February 5, 2000.
21. McGreal C. Top researcher falsified breast cancer results. *The Guardian.* <https://www.theguardian.com/world/2000/feb/19/chrismcgreal>. Published February 19, 2000.
22. DiMasi JA, Grabowski HG, Hansen RW. Innovation in the pharmaceutical industry: New estimates of R&D costs. *J Health Econ.* 2016;47:20-33. doi:10.1016/j.jhealeco.2016.01.012
23. Light DW. Bearing the Risks of Prescription Drugs. In: Light DW, ed. *The Risks of Prescription Drugs.* New York: Columbia University Press; 2010:1-39.
24. Emnueal E. Big Pharma’s Go-To Defense of Soaring Drug Prices Doesn’t Add-Up. *The Atlantic.* <https://www.theatlantic.com/health/archive/2019/03/drug-prices-high-cost-research-and-development/585253/>. Published March 23, 2019.
25. Light DW. Serious Risks And Few New Benefits From FDA-Approved Drugs. *HealthAffairs.* <https://www.healthaffairs.org/doi/10.1377/hblog20150706.049097/full/>. Published 2015.
26. Nasr A, Lauterio TJ, Davis MW. Unapproved drugs in the united states and the food and drug administration. *Adv Ther.* 2011;28(10):842-856. doi:10.1007/s12325-011-0059-4
27. Stafford RS. Regulating Off-Label Drug Use — Rethinking the Role of the FDA. *N Engl J Med.* 2008;358(14):1427-1429. doi:10.1056/nejmp0802107
28. US food and drug administration. Understanding Unapproved Use of Approved Drugs “Off Label.” FDA U.S. Food and Drug Administration. <https://www.fda.gov/patients/learn-about-expanded-access-and-other-treatment->

- options/understanding-unapproved-use-approved-drugs-label. Published 2018.
29. Policies MOF, Evaluation D. *Manual of Policies and Procedures.*; 2015.
 30. Fordtran J, Hofmann A. Seventy Years of Polyethylene Glycols in Gastroenterology: The Journey of PEG 4000 and PEG 3500 From Nonabsorbable Marker to Colonoscopy Preparation to Osmotic Laxative. *Gastroenterology*. 2017;152(4):675-680. doi:10.1053/j.gastro.2017.01.027
 31. Reed JA, Lucero AE, Hu S, et al. A low-cost, rapid deposition method for smart films: Applications in mammalian cell release. *ACS Appl Mater Interfaces*. 2010;2(4):1048-1051. doi:10.1021/am900821t
 32. Bluestein BM, Reed JA, Canavan HE. Effect of substrate storage conditions on the stability of “Smart” films used for mammalian cell applications. *Appl Surf Sci*. 2017;392:950-959. doi:10.1016/j.apsusc.2016.07.004
 33. Fukumori K, Akiyama Y, Kumashiro Y, et al. Characterization of Ultra-Thin Temperature-Responsive Polymer Layer and Its Polymer Thickness Dependency on Cell Attachment/Detachment Properties. *Macromol Biosci*. 2010;10(10):1117-1129. doi:10.1002/mabi.201000043
 34. Yang J, Yamato M, Nishida K, et al. Cell delivery in regenerative medicine: The cell sheet engineering approach. *J Control Release*. 2006;116(2 SPEC. ISS.):193-203. doi:10.1016/j.jconrel.2006.06.022
 35. Kushida A, Yamato M, Konno C, Kikuchi A, Sakurai Y, Okano T. Temperature-responsive culture dishes allow nonenzymatic harvest of differentiated Madin-Darby canine kidney (MDCK) cell sheets. *J Biomed Mater Res*. 2000;51(2):216-223. doi:10.1002/(SICI)1097-4636(200008)51:2<216::AID-JBM10>3.0.CO;2-K
 36. Mortisen D, Peroglio M, Alini M, Eglin D. Tailoring thermoreversible hyaluronan hydrogels by “click” chemistry and RAFT polymerization for cell and drug therapy. *Biomacromolecules*. 2010;11(5):1261-1272. doi:10.1021/bm100046n
 37. Abdul M, Su Y, Wang D. Mechanical properties of PNIPAM based hydrogels : A review. *Mater Sci Eng C*. 2017;70:842-855. doi:10.1016/j.msec.2016.09.081
 38. Ashraf S, Park HK, Park H, Lee SH. Snapshot of phase transition in thermoresponsive hydrogel PNIPAM: Role in drug delivery and tissue engineering. *Macromol Res*. 2016;24(4):297-304. doi:10.1007/s13233-016-4052-2
 39. Chen S, Shi J, Xu X, et al. Study of stiffness effects of poly(amidoamine)-poly(n-isopropyl acrylamide) hydrogel on wound healing. *Colloids Surfaces B Biointerfaces*. 2016;140:574-582. doi:10.1016/j.colsurfb.2015.08.041
 40. Lima LH, Morales Y, Cabral T. Poly-N-isopropylacrylamide (pNIPAM): A reversible bioadhesive for sclerotomy closure. *Int J Retin Vitr*. 2016;2(1):1-7. doi:10.1186/s40942-016-0048-5
 41. Kim H, Kim K, Lee SJ. Nature-inspired thermo-responsive multifunctional membrane adaptively hybridized with PNIPAM and PPy. *Nat Publ Gr*. 2017;(March).

doi:10.1038/am.2017.168

42. Lima LH, Morales Y, Cabral T. Ocular Biocompatibility of Poly-N-Isopropylacrylamide (pNIPAM). *J Ophthalmol*. 2016;2016:1-6. doi:10.1155/2016/5356371
43. Blom A, Cho JE, Fleischman A, et al. General Assembly, Prevention, Antiseptic Irrigation Solution: Proceedings of International Consensus on Orthopedic Infections. *J Arthroplasty*. 2019;34(2):S131-S138. doi:10.1016/j.arth.2018.09.063
44. Schmidt K, Estes C, McLaren A, Spangehl MJ. Chlorhexidine Antiseptic Irrigation Eradicates Staphylococcus epidermidis From Biofilm: An in vitro study. *Clin Orthop Relat Res*. 2018;476(3):648-653. doi:10.1007/s11999.00000000000000052
45. Lobdell KW, Stamou S, Sanchez JA. Hospital-Acquired Infections. *Surg Clin North Am*. 2012;92(1):65-77. doi:10.1016/j.suc.2011.11.003
46. Petrisor B, Jeray K, Schemitsch E, et al. Fluid lavage in patients with open fracture wounds (FLOW): An international survey of 984 surgeons. *BMC Musculoskeletal Disord*. 2008;9:1-9. doi:10.1186/1471-2474-9-7
47. Campbell J, Filardo G, Bruce B, et al. Salvage of contaminated osteochondral allografts: The effects of chlorhexidine on human articular chondrocyte viability. *Am J Sports Med*. 2014;42(4):973-978. doi:10.1177/0363546513519950
48. Hoflund GARB. Spectroscopic Techniques : X-ray Photoelectron Spectroscopy (XPS), Auger Electron Spectroscopy (AES), and Ion Scattering Spectroscopy (ISS). In: Riviere JC, Myhra S, eds. *Handbook of Surface and Interface Analysis: Methods for Problem-Solving*. New York: Marcel Dekker; 1998:57-86.
49. X-ray photoelectron spectroscopy. https://en.wikipedia.org/wiki/X-ray_photoelectron_spectroscopy. Published 2005.
50. Escamilla R, Huerta L, Morales F, Akachi T. Valence band XPS and UPS studies of non-stoichiometric superconducting NbB_{2+x}. *Supercond Sci Technol*. 2012;25(1):15002. doi:10.1088/0953-2048/25/1/015002
51. Hesse R, Chassé T, Streubel P, Szargan R. Error estimation in peak-shape analysis of XFS core-level spectra using UNIFIT 2003: How significant are the results of peak fits? *Surf Interface Anal*. 2004;36(10):1373-1383. doi:10.1002/sia.1925
52. Wagner MS, Horbett TA, Castner DG. Characterizing multicomponent adsorbed protein films using electron spectroscopy for chemical analysis, time-of-flight secondary ion mass spectrometry, and radiolabeling: Capabilities and limitations. *Biomaterials*. 2003;24(11):1897-1908. doi:10.1016/S0142-9612(02)00612-9
53. Canavan HE, Graham DJ, Cheng X, Ratner BD, Castner DG. Comparison of native extracellular matrix with adsorbed protein films using secondary ion mass spectrometry. *Langmuir*. 2007;23(1):50-56. doi:10.1021/la062330o
54. Andrade JD. X-ray Photoelectron Spectroscopy. In: Andrade J, ed. *Surface and Interfacial Aspects of Biomedical Polymers*. Boston, MA: Springer; 1985:105-106.

55. Korin E, Froumin N, Cohen S. Surface Analysis of Nanocomplexes by X-ray Photoelectron Spectroscopy (XPS). *ACS Biomater Sci Eng.* 2017;3(6):882-889. doi:10.1021/acsbiomaterials.7b00040
56. Contact Angle Goniometer / Tensiometer Instruments ramé-hart Product Matrix. Rame-hart. <http://www.ramehart.com/goniometer.htm>. Published 2018.
57. Canavan HE, Cheng X, Graham DJ, Ratner BD, Castner DG. A plasma-deposited surface for cell sheet engineering: Advantages over mechanical dissociation of cells. *Plasma Process Polym.* 2006;3(6-7):516-523. doi:10.1002/ppap.200600017
58. Reed JA. Assessment of the biocompatibility, stability, and suitability of novel thermoresponsive films for the rapid generation of cellular constructs. 2011.
59. Schuh JR, Chan SI. *Nuclear Magnetic Resonance.* Vol 20.; 1982. doi:10.1016/S0076-695X(08)60150-7
60. Spinney R. 5.3 Nuclear Magnetic Resonance (NMR) Spectroscopy. LibreTexts. [https://chem.libretexts.org/Courses/Purdue/Purdue%3A_Chem_26505%3A_Organic_Chemistry_I_\(Lipton\)/Chapter_5._Spectroscopy/5.3_Nuclear_Magnetic_Resonance_\(NMR\)_Spectroscopy](https://chem.libretexts.org/Courses/Purdue/Purdue%3A_Chem_26505%3A_Organic_Chemistry_I_(Lipton)/Chapter_5._Spectroscopy/5.3_Nuclear_Magnetic_Resonance_(NMR)_Spectroscopy).
61. Basics of rheology. Anton Paar. <https://wiki.anton-paar.com/en/basics-of-rheology/#oscillation-tests-and-viscoelasticity>. Published 2019.
62. Invitrogen. *Cell Culture Basics Handbook.*; 2010. doi:10.1093/chemse/bjt099
63. Cell Types & Culture Characteristics. In: *Fundamental Techniques in Cell Culture Laboratory Handbook.* Vol 12. Sigma Aldrich; 2010:3-6. <http://www.sigmaaldrich.com/content/dam/sigma-aldrich/articles/protocols/biology/volume12-Cell-Types-and-Culture-Characteristics/Cell-Types-and-Culture-Characteristics.pdf>.
64. Reed JA, Lucero AE, Cooperstein MA, Canavan HE. The effects of cell culture parameters on cell release kinetics from thermoresponsive surfaces. *J Appl Biomater Biomech.* 2013;6(2):81-88. doi:10.1016/j.biotechadv.2011.08.021
65. Cooperstein MA, Nguyen PAH, Canavan HE. Poly(*N*-isopropyl acrylamide)-coated surfaces: Investigation of the mechanism of cell detachment. *Biointerphases.* 2017;12(2):02C401. doi:10.1116/1.4979920
66. Cooperstein MA, Canavan HE. Assessment of cytotoxicity of (N-isopropyl acrylamide) and poly(N-isopropyl acrylamide)-coated surfaces. *Biointerphases.* 2013;8(1):19. doi:10.1186/1559-4106-8-19
67. Szymonowicz M, Korczynski M, Dobrzynski M, et al. Cytotoxicity evaluation of high-temperature annealed nanohydroxyapatite in contact with fibroblast cells. *Materials (Basel).* 2017;10(6):1-13. doi:10.3390/ma10060590
68. Uzunoglu S, Karaca B, Atmaca H, et al. Comparison of XTT and Alamar blue assays in the assessment of the viability of various human cancer cell lines by AT-101 (-/-gossypol). *Toxicol Mech Methods.* 2010;20(8):482-486.

doi:10.3109/15376516.2010.508080

69. Imajoh M, Sugiura H, Oshima SI. Morphological changes contribute to apoptotic cell death and are affected by caspase-3 and caspase-6 inhibitors during red sea bream iridovirus permissive replication. *Virology*. 2004;322(2):220-230. doi:10.1016/j.virol.2004.02.006
70. Lestari F, Hayes AJ, Green AR, Chattopadhyay G. In vitro cytotoxicity and morphological assessment of smoke from polymer combustion in human lung derived cells (A549). *Int J Hyg Environ Health*. 2012;215(3):320-332. doi:10.1016/j.ijheh.2011.12.006
71. Saraste A, Pulkki K. Morphologic and biochemical hallmarks of apoptosis. *Cardiovasc Res*. 2000;45(3):528-537. doi:10.1016/S0008-6363(99)00384-3
72. Wallig MA, Janovitz EB. Morphologic Manifestations of Toxic Cell Injury. In: *Haschek and Rousseaux's Handbook of Toxicologic Pathology*. 3rd ed. London: Academic Press; 2013:77-105.
73. Invitrogen Molecular Probes. *LIVE/DEAD Viability/Cytotoxicity Kit for Mammalian Cells*.; 2005. <https://tools.lifetechnologies.com/content/sfs/manuals/mp03224.pdf>.
74. *Ethidium Homodimer III SDS*. Fremont, CA; 2013.
75. *Increase Accuracy and Efficiency of Cytotoxicity Assessment Using the EarlyTox Live / Dead Assay Kit and High-Content Imaging*.; 2017.
76. Chen CC, Chang JH, Lee JB, Javier J, Azar DT. Human corneal epithelial cell viability and morphology after dilute alcohol exposure. *Invest OphthalmolVisSci*. 2002;43(8):2593-2602. <http://www.ncbi.nlm.nih.gov/pubmed/12147590>.
77. Altman SA, Randers L, Rao G. Comparison of Trypan Blue Dye Exclusion and Fluorometric Assays for Mammalian Cell Viability Determinations. *Biotechnol Prog*. 1993;9(6):671-674. doi:10.1021/bp00024a017
78. Monteiro-Riviere NA, Inman AO, Zhang LW. Limitations and relative utility of screening assays to assess engineered nanoparticle toxicity in a human cell line. *Toxicol Appl Pharmacol*. 2009;234(2):222-235. doi:10.1016/j.taap.2008.09.030
79. Lévesque a, Paquet a, Pagé M. Measurement of tumor necrosis factor activity by flow cytometry. *Cytometry*. 1995;20(2):181-184. doi:10.1002/cyto.990200211
80. Pike CJ, Overman MJ, Cotman CW. Beta-Amyloid Peptides in Vitro. *Biochemistry*. 1995;23895-23898.
81. Kirshenbaum LA, Schneider MD. Adenovirus E1A represses cardiac gene transcription and reactivates DNA synthesis in ventricular myocytes, via alternative pocket protein- and p300-binding domains. *J Biol Chem*. 1995;270(14):7791-7794. doi:10.1074/jbc.270.14.7791
82. Weil M, Jacobson MD, Coles HS, et al. Constitutive expression of the machinery for programmed cell death. *J Cell Biol*. 1996;133(5):1053-1059.

doi:10.1083/jcb.133.5.1053

83. Xiu Ming Wang, Terasaki PI, Rankin GW, Chia D, Hui Ping Zhong, Hardy S. A new microcellular cytotoxicity test based on calcein AM release. *Hum Immunol*. 1993;37(4):264-270. doi:10.1016/0198-8859(93)90510-8
84. Scientific TF. USER GUIDE LIVE / DEAD™ Fixable Dead Cell Stain Kits. *LIVE/DEAD™ Fixable Dead Cell Stain Kits*. 2016;0002416:1-10. https://tools.thermofisher.com/content/sfs/manuals/live_dead_fixable_dead_cell_stains_man.pdf.
85. Cummings BS, Wills LP, Schnellmann RG. Measurement of Cell Death in Mammalian Cells. *Curr Protoc Pharmacol*. 2004;1(Lemasters 1999):1-30. doi:10.1002/0471141755.ph1208s25.Measurement
86. Proskuryakov S, Gabai V. Mechanisms of Tumor Cell Necrosis. *Curr Pharm Des*. 2010;16(1):56-68. doi:10.2174/138161210789941793
87. Stockert JC, Horobin RW, Colombo LL, Blázquez-Castro A. Tetrazolium salts and formazan products in Cell Biology: Viability assessment, fluorescence imaging, and labeling perspectives. *Acta Histochem*. 2018;120(3):159-167. doi:10.1016/j.acthis.2018.02.005
88. Riss TL, Moravec RA, Niles AL, et al. Cell Viability Assays. In: Sittampalam GS, Coussens NP, eds. *Assay Guidance Manual*. Bethesda, MD: Eli Lilly & Company and the National Center for Advancing Translational Sciences; 2004:1-31. <http://www.ncbi.nlm.nih.gov/pubmed/23805433>.
89. Abel SDA, Baird SK. Honey is cytotoxic towards prostate cancer cells but interacts with the MTT reagent: Considerations for the choice of cell viability assay. *Food Chem*. 2018;241(July 2017):70-78. doi:10.1016/j.foodchem.2017.08.083
90. Scherließ R. The MTT assay as tool to evaluate and compare excipient toxicity in vitro on respiratory epithelial cells. *Int J Pharm*. 2011;411(1-2):98-105. doi:10.1016/j.ijpharm.2011.03.053
91. Smith SM, Wunder MB, Norris DA, Shellman YG. A simple protocol for using a LDH-Based cytotoxicity assay to assess the effects of death and growth inhibition at the same time. *PLoS One*. 2011;6(11). doi:10.1371/journal.pone.0026908
92. Pokrywczynska M, Balcerczyk D, Jundzill A, et al. Isolation, expansion and characterization of porcine urinary bladder smooth muscle cells for tissue engineering. *Biol Proced Online*. 2016;18(1):1-15. doi:10.1186/s12575-016-0047-9
93. Fotakis G, Timbrell JA. In vitro cytotoxicity assays: Comparison of LDH, neutral red, MTT and protein assay in hepatoma cell lines following exposure to cadmium chloride. *Toxicol Lett*. 2006;160(2):171-177. doi:10.1016/j.toxlet.2005.07.001
94. Stepanenko AA, Dmitrenko V V. Pitfalls of the MTT assay: Direct and off-target effects of inhibitors can result in over/underestimation of cell viability. *Gene*. 2015;574(2):193-203. doi:10.1016/j.gene.2015.08.009

95. Wang S, Yu H, Wickliffe JK. Limitation of the MTT and XTT assays for measuring cell viability due to superoxide formation induced by nano-scale TiO₂. *Toxicol Vitro*. 2011;25(8):2147-2151. doi:10.1016/j.tiv.2011.07.007
96. Ulukaya E, Ozdikicioglu F, Oral AY, Demirci M. The MTT assay yields a relatively lower result of growth inhibition than the ATP assay depending on the chemotherapeutic drugs tested. *Toxicol Vitro*. 2008;22(1):232-239. doi:10.1016/j.tiv.2007.08.006
97. Biotium. *XTT Cell Viability Kit Product Information*. Fremont, CA
98. Wilde KN. In Vitro cytotoxicity and skin irritation testing of antimicrobial conjugated electrolytes: interactions with Mammalian Cells. 2012.
99. Canavan HE. The effects of cell culture parameters on cell release kinetics from thermoresponsive surfaces. *J Appl Biomater Biomech*. 2013;6(2):81-88. doi:10.1016/j.biotechadv.2011.08.021
100. Riss TL, Moravec RA, Niles AL, et al. Cell Viability Assays. In: *Assay Guidance Manual [Internet]*. Vol 114. Updated 20. Bethesda (MD): Eli Lilly & Company and the National Center for Advancing Translational Sciences; 2013:785-796. doi:10.1016/j.acthis.2012.01.006
101. Tenopoulou M, Kurz T, Doulias P, Galaris D, Brunk UT. Does the calcein-AM method assay the total cellular 'labile iron pool' or only a fraction of it? *Biochem K*. 2007;266:261-266. doi:10.1042/BJ20061840
102. Chauncey J, Wieters J. Tranexamic Acid. In: *StatPearls [Internet]*. Treasure Island, Florida: StatPearls Publishing; 2018. <https://www.ncbi.nlm.nih.gov/books/NBK532909/>.
103. Dunn CJ, Goa KL. Tranexamic Acid: A Review of its Use in Surgery and Other Indications. *Adis Drug Eval*. 1999;57(6):1005-1032. doi:10.2165/00003495-199957060-00017
104. Melvin JS, Stryker LS, Sierra RJ. Tranexamic Acid in Hip and Knee Arthroplasty. *J Am Acad Orthop Surg*. 2015;23(12):732-740.
105. Cheriyan T, Maier SP, Bianco K, et al. Efficacy of tranexamic acid on surgical bleeding in spine surgery: A meta-analysis. *Spine J*. 2015;15(4):752-761. doi:10.1016/j.spinee.2015.01.013
106. Amer KM, Rehman S, Amer K, Haydel C. Efficacy and Safety of Tranexamic Acid in Orthopaedic Fracture Surgery. *J Orthop Trauma*. 2017;31(10):520-525. doi:10.1097/bot.0000000000000919
107. Yang Z-G, Chen W-P, Wu L-D. Effectiveness and Safety of Tranexamic Acid in Reducing Blood Loss in Total Knee Arthroplasty: A Meta-Analysis. *J Bone Jt Surg*. 2012;94:1153-1159.
108. Georgiadis AG, Muh SJ, Silverton CD, Weir RM, Laker MW. A Prospective double-blind placebo controlled trial of topical tranexamic acid in total knee arthroplasty. *J*

- Arthroplasty*. 2013;28(8 SUPPL):78-82. doi:10.1016/j.arth.2013.03.038
109. Panteli M, Papakostidis C, Dahabreh Z, Giannoudis P V. Topical tranexamic acid in total knee replacement: A systematic review and meta-analysis. *Knee*. 2013;20(5):300-309. doi:10.1016/j.knee.2013.05.014
 110. MacGillivray RG, Tarabichi SB, Hawari MF, Raoof NT. Tranexamic Acid to Reduce Blood Loss After Bilateral Total Knee Arthroplasty. A Prospective, Randomized Double Blind Study. *J Arthroplasty*. 2011;26(1):24-28. doi:10.1016/j.arth.2009.11.013
 111. Tanaka N, Sakahashi H, Sato E, Hirose K, Ishima T, Ishii S. Timing of the administration of tranexamic acid for maximum reduction in blood loss in arthroplasty of the knee. *J Bone Joint Surg Br*. 2001;83(5):702-705. <http://www.ncbi.nlm.nih.gov/pubmed/11476309>.
 112. Benoni G, Fredin H. Fibrinolytic Inhibition With Tranexamic Acid Reduces Blood Loss and Blood Transfusion After Knee Arthroplasty. *J Bone Joint Surg Br*. 2018;78-B(3):434-440. doi:10.1302/0301-620x.78b3.0780434
 113. Zhou XD, Tao LJ, Li J, Wu LD. Do we really need tranexamic acid in total hip arthroplasty? A meta-analysis of nineteen randomized controlled trials. *Arch Orthop Trauma Surg*. 2013;133(7):1017-1027. doi:10.1007/s00402-013-1761-2
 114. Yue C, Kang P, Yang P, Xie J, Pei F. Topical application of tranexamic acid in primary total hip arthroplasty: A randomized double-blind controlled trial. *J Arthroplasty*. 2014;29(12):2452-2456. doi:10.1016/j.arth.2014.03.032
 115. Johansson T, Pettersson LG, Lisander B. Tranexamic acid in total hip arthroplasty saves blood and money: A randomized, double-blind study in 100 patients. *Acta Orthop*. 2005;76(3):314-319. doi:10.1080/00016470510030751
 116. Phillips SJ, Chavan R, Porter ML, et al. Does salvage and tranexamic acid reduce the need for blood transfusion in revision hip surgery? *J Bone Joint Surg Br*. 2006;88-B(9):1141-1142. doi:10.1302/0301-620x.88b9.17605
 117. Smit KM, Naudie DDR, Ralley FE, Berta DM, Howard JL. One dose of tranexamic acid is safe and effective in revision knee arthroplasty. *J Arthroplasty*. 2013;28(8 SUPPL):112-115. doi:10.1016/j.arth.2013.05.036
 118. Noordin S, Waters TS, Garbuz DS, Duncan CP, Masri BA. Tranexamic acid reduces allogenic transfusion in revision hip arthroplasty. *Clin Orthop Relat Res*. 2011;469(2):541-546. doi:10.1007/s11999-010-1441-2
 119. Poeran J, Rasul R, Suzuki S, et al. Tranexamic acid use and postoperative outcomes in patients undergoing total hip or knee arthroplasty in the United States: Retrospective analysis of effectiveness and safety. *BMJ*. 2014;349(May 2019). doi:10.1136/bmj.g4829
 120. Wind T, Barfield W, Moskal J. The Effect of Tranexamic Acid on Blood Loss and Transfusion Rate in Primary Total Knee Arthroplasty. *J Arthroplasty*. 2013;28(7):1080-1083. doi:10.1302/2046-3758.58.bjr-2016-0001.r2

121. New Mexico Donor Services. <https://donatelifenm.org/>.
122. BTRI Life Sciences. *Quantification of Live/Dead Staining Using Fiji Software Analyze.*; 2015. [https://brtilifesciences.com/PDF/Quantification of Live_Dead Staining Using Fiji software.pdf](https://brtilifesciences.com/PDF/Quantification%20of%20Live_Dead%20Staining%20Using%20Fiji%20software.pdf).
123. Goode J. Use of International Standard ISO 10993-1, “Biological evaluation of medical devices - Part 1: Evaluation and testing within a risk management process.” *Dep Heal Hum Serv Food Drug Adm.* 2016:68. doi:<http://www.fda.gov/downloads/medicaldevices/deviceregulationandguidance/guidancedocuments/ucm348890.pdf>
124. Tuttle J, Feltman P, Ritterman S, Ehrlich M. Effects of Tranexamic Acid Cytotoxicity on In Vitro Chondrocytes. *Am J Orthop.* 2015;44(12):E497-502.
125. Parker JD, Lim KS, Kieser DC, Woodfield TBF, Hooper GJ. Is tranexamic acid toxic to articular cartilage when administered topically? *Bone Jt J.* 2018;100B(3):404-412. doi:10.1302/0301-620X.100B3.BJJ-2017-1135.R1
126. Ahlberg A, Eriksson O, Kjellman H. Diffusion of tranexamic acid to the joint. *Acta Orthop.* 1976;47(5):486-488. doi:10.3109/17453677608988725
127. Wallis WJ, Simkin PA, Nelp WB, Foster DM. Intraarticular volume and clearance in human synovial effusions. *Arthritis Rheum.* 1985;28(4):441-449. doi:10.1002/art.1780280413
128. Sa-ngasoongsong P, Chanplakorn P, Wongsak S, et al. An In Vivo Study of Low-Dose Intra-Articular Tranexamic Acid Application with Prolonged Clamping Drain Method in Total Knee Replacement: Clinical Efficacy and Safety. *Biomed Res Int.* 2015;2015:1-6. doi:10.1155/2015/164206
129. Picetti R. What concentration of tranexamic acid is needed to inhibit fibrinolysis? A systematic review of pharmacodynamics studies. *Blood Coagul Fibrinolysis.* 2019;30(1):1-10.
130. Gao F, Sun W, Guo W, Li Z, Wang W, Cheng L. Topical Administration of Tranexamic Acid Plus Diluted-Epinephrine in Primary Total Knee Arthroplasty: A Randomized Double-Blinded Controlled Trial. *J Arthroplasty.* 2015;30(8):1354-1358. doi:10.1016/j.arth.2015.03.003
131. Zimlichman E, Henderson D, Tamir O, et al. Health Care–Associated Infections. *JAMA Intern Med.* 2013;173(22):2039. doi:10.1001/jamainternmed.2013.9763
132. Spiegel DA, Baldwin KD, Flynn JM, Dormans JP, Kanj WW. Vancomycin Prophylaxis of Surgical Site Infection in Clean Orthopedic Surgery. *Orthopedics.* 2013;36(2):138-146. doi:10.3928/01477447-20130122-10
133. Brown NM, Cipriano CA, Moric M, Sporer SM, Della Valle CJ. Dilute Betadine Lavage Before Closure for the Prevention of Acute Postoperative Deep Periprosthetic Joint Infection. *J Arthroplasty.* 2012;27(1):27-30. doi:10.1016/j.arth.2011.03.034
134. Ruder JA, Springer BD. Treatment of Periprosthetic Joint Infection Using

- Antimicrobials: Dilute Povidone-Iodine Lavage. *J Bone Jt Infect.* 2016;2(1):10-14. doi:10.7150/jbji.16448
135. Blom A, Cho JE, Fleischman A, et al. General Assembly, Prevention, Antiseptic Irrigation Solution: Proceedings of International Consensus on Orthopedic Infections. *J Arthroplasty.* 2019;34(2):S131-S138. doi:10.1016/j.arth.2018.09.063
 136. Humphrey J., Lightbrown JW, Mussett MV, Perry WLM. The international standard for bacitracin. *Bull World Health Organ.* 1953;9:861-869. doi:10.1016/0022-1759(93)90172-4
 137. Institute NNC. Cancer Stat Facts: Cancer of the Colon and Rectum. NIH. <https://seer.cancer.gov/statfacts/html/colorect.html>.
 138. Simon S. Report : Colon and Rectal Cancer Rates Continue to Drop Among Older Americans. *American Cancer Society.* March 1, 2017.
 139. Tsai M-H, Xirasagar S, Li Y-J, de Groen PC. Colonoscopy screening among US adults aged 40 or older with a family history of colorectal cancer. *Prev Chronic Dis.* 2015;12:E80. doi:10.5888/pcd12.140533
 140. Bechtold ML, Mir F, Puli SR, Nguyen DL. Optimizing bowel preparation for colonoscopy: A guide to enhance quality of visualization. *Ann Gastroenterol.* 2016;29(2):137-146. doi:10.20524/aog.2016.0005
 141. Thomas D, Trisha M, John C, et al. Predictor of nonadherence to screening colonoscopy. *J Gen Intern Med.* 2005;20(11):989. doi:10.1111/j.1525-1497.2005.0164.x
 142. Malhotra A, Aziz K, Freston JW. Colorectal cancer screening: A retrospective study of compliance with guidelines in a university-based primary care practice. *Qual Prim Care.* 2007;15(3):151-155.
 143. The prep is worse than the procedure. *Harvard Lett.* 2010;(January):6-8.
 144. Komaroff A. Colonoscopy prep worse than the test. *The Times.* <http://thetimes-tribune.com/news/health-science/colonoscopy-prep-worse-than-the-test-1.1454340>. Published March 6, 2013.
 145. Florentin M, Liamis G, Elisaf MS. Colonoscopy preparation-induced disorders in renal function and electrolytes. *World J Gastrointest Pharmacol Ther.* 2017;5(2):50. doi:10.4292/wjgpt.v5.i2.50
 146. Rees CJ, Bevan R, Zimmermann-Fraedrich K, et al. Expert opinions and scientific evidence for colonoscopy key performance indicators. *Gut.* 2016;65(12):2045-2060. doi:10.1136/gutjnl-2016-312043
 147. Herzberger J, Niederer K, Pohlit H, et al. Polymerization of ethylene oxide, propylene oxide, and other alkylene oxides: Synthesis, novel polymer architectures, and bioconjugation. *Chem Rev.* 2016;116(4):2170-2243. doi:10.1021/acs.chemrev.5b00441

148. Shintani Y, Iwamoto K, Kitano K. Applied Microbiology Biotechnology Polyethylene glycols for promoting the growth of mammalian cells. 1988:24-25.
149. Pontecorvo G. Production of mammalian somatic cell hybrids by means of polyethylene glycol treatment. *Somatic Cell Genet.* 1975;1(4):397-400. doi:10.1007/BF01538671
150. Davis GR, Santa Ana CA, Morawski SG, Fordtran JS. Development of a lavage solution associated with minimal water and electrolyte absorption or secretion. *Gastroenterology.* 1980;78(5):991-995. doi:10.1016/0016-5085(80)90781-7
151. Administration F and D. *Reference ID: 3377625.*; 2013.
152. Hammer HF, Santa Ana CA, Schiller LR, Fordtran JS. Studies of osmotic diarrhea induced in normal subjects by ingestion of polyethylene glycol and lactulose. *J Clin Invest.* 1989;84(4):1056-1062. doi:10.1172/JCI114267
153. ATCC. *Hs 738.St/Int (ATCC CRL-7869).* Manassas; 2019.
154. ATCC. *HIEC-6 (ATCC CRL-3266).*; 2007.
155. ATCC. Human Colon Cells. CCD-18Co (ATCC® CRL-1459™).
156. Biotium. XTT Assay Product Information. :30007.
157. Bowen R. Gastrointestinal Transit : How Long Does It Take ? Colorado State University.
<http://www.vivo.colostate.edu/hbooks/pathphys/digestion/basics/transit.html>.
Published 2006.
158. Metcalf AM, Phillips SF, Zinsmeister AR, MacCarty RL, Beart RW, Wolff BG. Simplified assessment of segmental colonic transit. *Gastroenterology.* 1987;92(1):40-47. doi:10.1016/0016-5085(87)90837-7
159. Degen LP, Phillips SF. Variability of gastrointestinal transit in healthy women and men. *Gut.* 1996;39:299-305. doi:10.1017/CCO9780511777714.035
160. Proano M, Camilleri M, Phillips SF, Brown ML, Thomforde GM. Transit of solids through the human colon: regional quantification in the unprepared bowel. *Am J Physiol Liver Physiol.* 1990;258(6):G856-G862. doi:10.1152/ajpgi.1990.258.6.g856
161. Maurer A, Krevsky B. Whole-gut transit scintigraphy in the evaluation of small-bowel and colon transit disorders. *Semin Nucl Med.* 1995;25(4):326-338.
162. Hobro AJ, Smith NI. An evaluation of fixation methods: Spatial and compositional cellular changes observed by Raman imaging. *Vib Spectrosc.* 2017;91:31-45. doi:10.1016/j.vibspec.2016.10.012
163. International Organization for Standardization. ISO 10993-1 : Biological evaluation of medical devices — Part 1: Evaluation and testing within a risk management process. *Int Stand.* 2009;(Part 1):1-28. doi:10.1109/IEEESTD.2007.4288250
164. Xu W, Ling P, Zhang T. Polymeric micelles, a promising drug delivery system to

- enhance bioavailability of poorly water-soluble drugs. *J Drug Deliv.* 2013;2013(1). doi:10.1155/2013/340315
165. Pfeiffer P, Mortensen JP, Bjerregaard B, et al. Patient preference for oral or intravenous chemotherapy: A randomised cross-over trial comparing capecitabine and Nordic fluorouracil/leucovorin in patients with colorectal cancer. *Eur J Cancer.* 2006;42(16):2738-2743. doi:10.1016/j.ejca.2006.06.027
 166. Liu L, Yao WD, Rao YF, Lu XY, Gao JQ. pH-Responsive carriers for oral drug delivery: challenges and opportunities of current platforms. *Drug Deliv.* 2017;24(1):569-581. doi:10.1080/10717544.2017.1279238
 167. De Portu S, Mantovani LG, Ravaioli A, et al. Cost analysis of capecitabine vs 5-fluorouracil-based treatment for metastatic colorectal cancer patients. *J Chemother.* 2010;22(2):125-128. doi:10.1179/joc.2010.22.2.125
 168. Cardoso F, Colleoni M, Di Leo A, et al. Oral chemotherapy in advanced breast cancer: expert perspectives on its role in clinical practice. *Cancer Treat Commun.* 2016;6(September 2015):S1-S10. doi:10.1016/S2213-0896(16)06001-1
 169. Khutoryanskiy V V. Supramolecular materials: Longer and safer gastric residence. *Nat Mater.* 2015;14(10):963-964. doi:10.1038/nmat4432
 170. Evans DF, Pye G, Bramley R, Clark AG, Dyson TJ, Hardcastle JD. Measurement of gastrointestinal pH profiles in normal ambulant human subjects. *Gut.* 1988;29(8):1035-1041. doi:10.1136/gut.29.8.1035
 171. Yoshida T, Lai T, Kwon G, Sako K. pH- and ion-sensitive polymers for drug delivery. *Expert Opin Drug Deliv.* 2013;10(11):1497-1513. doi:10.1021/mp300595a.Development
 172. Yin ZC, Wang YL, Wang K. A pH-responsive composite hydrogel beads based on agar and alginate for oral drug delivery. *J Drug Deliv Sci Technol.* 2018;43:12-18. doi:10.1016/j.jddst.2017.09.009
 173. Ng WL, Yeong WY, Naing MW. Development of Polyelectrolyte Chitosan-gelatin Hydrogels for Skin Bioprinting. *Procedia CIRP.* 2016;49:105-112. doi:10.1016/j.procir.2015.09.002
 174. Treenate P, Monvisade P. In vitro drug release profiles of pH-sensitive hydroxyethylacryl chitosan/sodium alginate hydrogels using paracetamol as a soluble model drug. *Int J Biol Macromol.* 2017;99:71-78. doi:10.1016/j.ijbiomac.2017.02.061
 175. Jabeen S, Maswal M, Chat OA, Rather GM, Dar AA. Rheological behavior and Ibuprofen delivery applications of pH responsive composite alginate hydrogels. *Colloids Surfaces B Biointerfaces.* 2016;139:211-218. doi:10.1016/j.colsurfb.2015.12.013
 176. Rizwan M, Yahya R, Hassan A, et al. pH sensitive hydrogels in drug delivery: Brief history, properties, swelling, and release mechanism, material selection and applications. *Polymers (Basel).* 2017;9(4). doi:10.3390/polym9040137

177. Terefe NS, Glagovskaia O, De Silva K, Stockmann R. Application of stimuli responsive polymers for sustainable ion exchange chromatography. *Food Bioprod Process*. 2014;92(2):208-225. doi:10.1016/j.fbp.2014.02.003
178. Le Garrec D, Taillefer J, Van Lier JE, Lenaerts V, Leroux JC. Optimizing pH-responsive polymeric micelles for drug delivery in a cancer photodynamic therapy model. *J Drug Target*. 2002;10(5):429-437. doi:10.1080/1061186021000001887
179. Deen G, Loh X. Stimuli-Responsive Cationic Hydrogels in Drug Delivery Applications. *Gels*. 2018;4(1):13. doi:10.3390/gels4010013
180. Cicotte K, Reed JA, Nguyen PAH, De Lora J, Hedberg-Dirk EL, Canavan HE. Optimization of electrospun poly(N-isopropyl acrylamide) mats for the rapid reversible adhesion of mammalian cells. *Biointerphases*. 2017;12(2). doi:10.116/1.4984933
181. Ng WL, Yeong WY, Naing MW. Polyelectrolyte gelatin-chitosan hydrogel optimized for 3D bioprinting in skin tissue engineering. *Int J Bioprinting*. 2016;2(0). doi:10.18063/IJB.2016.01.009
182. Sood N, Bhardwaj A, Mehta S, Mehta A. Stimuli-responsive hydrogels in drug delivery and tissue engineering. *Drug Deliv*. 2016;23(3):758-780. doi:10.3109/10717544.2014.940091
183. Wang C, Yu B, Knudsen B, Harmon J, Moussy F, Moussy Y. Synthesis and performance of novel hydrogels coatings for implantable glucose sensors. *Biomacromolecules*. 2008;9(2):561-567. doi:10.1021/bm701102y
184. Schwall CT, Banerjee IA. *Micro- and Nanoscale Hydrogel Systems for Drug Delivery and Tissue Engineering*. Vol 2.; 2009. doi:10.3390/ma2020577
185. Naha PC, Bhattacharya K, Tenuta T, et al. Intracellular localisation, geno- and cytotoxic response of polyN-isopropylacrylamide (PNIPAM) nanoparticles to human keratinocyte (HaCaT) and colon cells (SW 480). *Toxicol Lett*. 2010;198(2):134-143. doi:10.1016/j.toxlet.2010.06.011
186. Park K. Facing the truth about nanotechnology in drug delivery. *ACS Nano*. 2013;7(9):7442-7447. doi:10.1021/nn404501g
187. Dai YN, Li P, Zhang JP, Wang AQ, Wei Q. Swelling characteristics and drug delivery properties of nifedipine-loaded pH sensitive alginate-chitosan hydrogel beads. *J Biomed Mater Res - Part B Appl Biomater*. 2008;86(2):493-500. doi:10.1002/jbm.b.31046
188. Mary CS, Swamiappan S. Sodium alginate with PEG/PEO blends as a floating drug delivery carrier - In vitro evaluation. *Adv Pharm Bull*. 2016;6(3):435-442. doi:10.15171/apb.2016.056
189. Meng X, Li P, Wei Q, Zhang H-X. pH sensitive alginate-chitosan hydrogel beads for carvedilol delivery. *Pharm Dev Technol*. 2011;16(1):22-28. doi:10.3109/10837450903479947

190. Lee KY, Rowley JA, Eiselt P, Moy EM, Bouhadir KH, Mooney DJ. Controlling mechanical and swelling properties of alginate hydrogels independently by cross-linker type and cross-linking density. *Macromolecules*. 2000;33(11):4291-4294. doi:10.1021/ma9921347
191. Mohy Eldin MS, Omer AM, Wassel MA, Tamer TM, Abd Elmonem MS, Ibrahim SA. Novel smart pH sensitive chitosan grafted alginate hydrogel microcapsules for oral protein delivery: I. preparation and characterization. *Int J Pharm Pharm Sci*. 2015;7(10):320-326.
192. Wong YY, Yuan S, Choong C. Degradation of PEG and non-PEG alginate-chitosan microcapsules in different pH environments. *Polym Degrad Stab*. 2011;96(12):2189-2197. doi:10.1016/j.polymdegradstab.2011.09.009
193. George M, Abraham TE. Polyionic hydrocolloids for the intestinal delivery of protein drugs: Alginate and chitosan - a review. *J Control Release*. 2006;114(1):1-14. doi:10.1016/j.jconrel.2006.04.017
194. Ouwerx C, Veilings N, Mestdagh M, Axelos M. Physico-chemical properties and rheology of alginate gel beads formed with various divalent cations. *Polym Gels Networks*. 1998;6(5):393-408.
195. Afzal S, Maswal M, Dar AA. Rheological behavior of pH responsive composite hydrogels of chitosan and alginate: Characterization and its use in encapsulation of citral. *Colloids Surfaces B Biointerfaces*. 2018;169:99-106. doi:10.1016/j.colsurfb.2018.05.002
196. Pasparakis G, Bouropoulos N. Swelling studies and in vitro release of verapamil from calcium alginate and calcium alginate-chitosan beads. *Int J Pharm*. 2006;323(1-2):34-42. doi:10.1016/j.ijpharm.2006.05.054
197. Huguet M, Dellacherie E. Calcium alginate beads coated with chitosan: Effect of the structure of encapsulated materials on their release. *Process Biochem*. 1996;31(8):745-751. doi:10.1016/S0032-9592(96)00032-5
198. Qaqish RB, Amiji MM. Synthesis of a fluorescent chitosan derivative and its application for the study of chitosan – mucin interactions Synthesis of a fluorescent chitosan derivative and its application for the study of chitosan ± mucin interactions. 2018;8617(May):98-107. doi:10.1016/S0144-8617(98)00109-X
199. Marques MRC, Loebenberg R, Almukainzi M. Simulated Biological Fluids with Possible Application in Dissolution Testing. 2011;(August):15-28.
200. Coln Santana JA. *Quantitative Core Level Photoelectron Spectroscopy*. (Claypool M&, ed.). San Rafael, CA; 2015. doi:10.1088/978-1-6270-5306-8
201. Salomonsen T, Jensen HM, Larsen FH, Steuernagel S, Engelsen SB. Alginate monomer composition studied by solution- and solid-state NMR - A comparative chemometric study. *Food Hydrocoll*. 2009;23(6):1579-1586. doi:10.1016/j.foodhyd.2008.11.009
202. Knight DK, Shapka SN, Amsden BG. Structure, depolymerization, and

- cytocompatibility evaluation of glycol chitosan. *J Biomed Mater Res - Part A*. 2007;83(3):787-798. doi:10.1002/jbm.a.31430
203. Dust JM, Fang ZH, Harris JM. Proton NMR Characterization of Poly(ethylene Glycols) and Derivatives. *Macromolecules*. 1990;23(16):3742-3746. doi:10.1021/ma00218a005
204. Salkind AR, Rao KC. Antibiotic Prophylaxis to Prevent Surgical Site Infections. *Am Fam Physician*. 2011;83(5):585-590.
205. Sewick A, Makani A, Wu C, O'Donnell J, Baldwin KD, Lee GC. Does dual antibiotic prophylaxis better prevent surgical site infections in total joint arthroplasty? infection. *Clin Orthop Relat Res*. 2012;470(10):2702-2707. doi:10.1007/s11999-012-2255-1
206. Wyatt RWB, Maletis GB, Lyon LL, Schwalbe J, Avins AL. Efficacy of Prophylactic Antibiotics in Simple Knee Arthroscopy. *Arthrosc - J Arthrosc Relat Surg*. 2017;33(1):157-162. doi:10.1016/j.arthro.2016.05.020
207. Mahou R, Meier RRH, Bühler LH, Wandrey C. Alginate-poly(ethylene glycol) hybrid microspheres for primary cell microencapsulation. *Materials (Basel)*. 2014;7(1):275-286. doi:10.3390/ma7010275
208. Jabeen S, Chat OA, Maswal M, Ashraf U, Rather GM, Dar AA. Hydrogels of sodium alginate in cationic surfactants: Surfactant dependent modulation of encapsulation/release toward Ibuprofen. *Carbohydr Polym*. 2015;133:144-153. doi:10.1016/j.carbpol.2015.06.111
209. Lemasters JJ, Qian T, Bradham CA, et al. Mitochondrial dysfunction in the pathogenesis of necrotic and apoptotic cell death. *J Bioenerg Biomembr*. 1999;31(4):305-319. doi:10.1023/A:1005419617371
210. Eming SA, Krieg T, Davidson JM. Inflammation in wound repair: Molecular and cellular mechanisms. *J Invest Dermatol*. 2007;127(3):514-525. doi:10.1038/sj.jid.5700701
211. Coleman J, Liu R, Wang K, Kumar A. Detecting Apoptosis, Autophagy, and Necrosis. In: Muganda P, ed. *Apoptosis Methods in Toxicology*. New York: Humana Press; 2016:77-92. doi:10.1007/978-1-4939-3588-8
212. Gonzales M, Nelson H, Rhyne RL, Stone SN, Hoffman RM. Surveillance of colorectal cancer screening in New Mexico Hispanics and non-hispanic whites. *J Community Health*. 2012;37(6):1279-1288. doi:10.1007/s10900-012-9568-6
213. Cole H, Demont A, Marison I. The Application of Dielectric Spectroscopy and Biocalorimetry for the Monitoring of Biomass in Immobilized Mammalian Cell Cultures. *Processes*. 2015;3(2):384-405. doi:10.3390/pr3020384